

ISSN (1230-0322)
2024, Vol. 74, No. 1

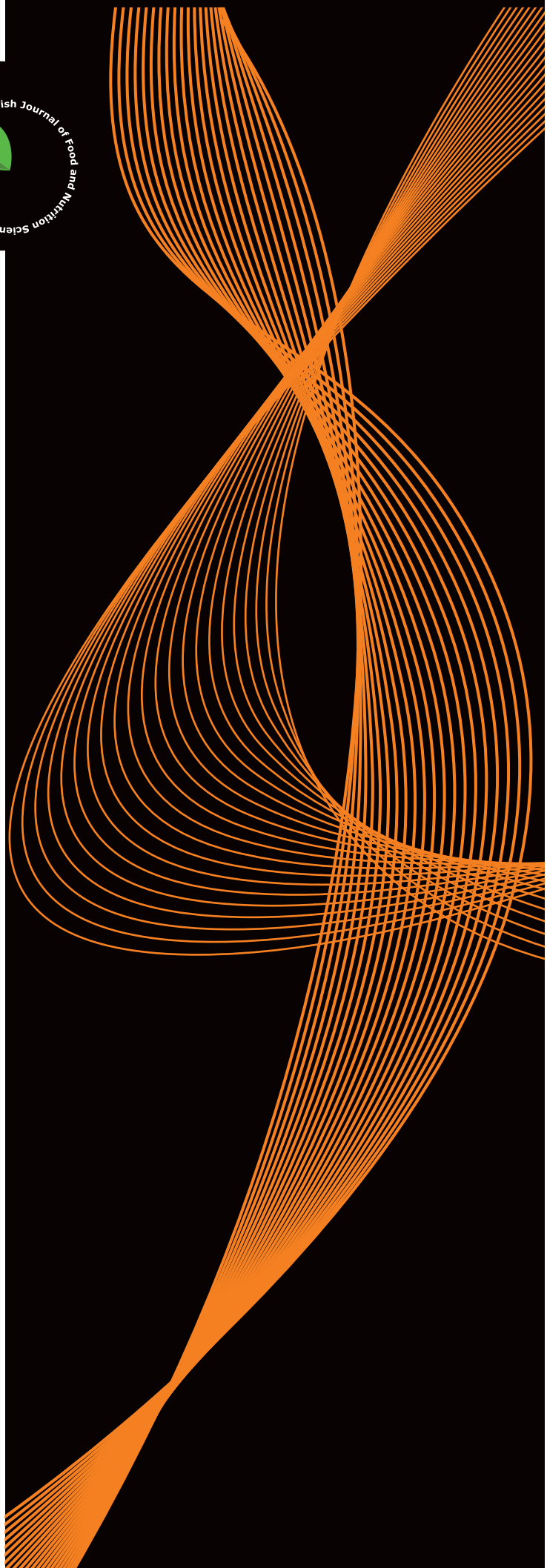
Food

Published

by Institute of Animal
Reproduction and Food
Research of the Polish
Academy of Sciences,



Polish Journal of Food and Nutrition Sciences
formerly Acta Alimentaria Polonica



Published since 1957 as
Roczniki Chemii i Technologii Żywności and Acta Alimentaria Polonica (1975–1991)

EDITOR-IN-CHIEF

Magdalena Karamać, Department of Chemical and Physical Properties of Food, Institute of Animal Reproduction and Food Research of the Polish Academy of Sciences, Olsztyn, Poland

SECTION EDITORS

Food Technology Section

Prof. Zeb Pietrasik, Meat, Food and Bio Processing Branch, Alberta Agriculture and Forestry, Leduc, Canada

Prof. Alberto Schiraldi, DISTAM, University of Milan, Italy

Food Chemistry Section

Prof. Ryszard Amarowicz, Department of Chemical and Physical Properties of Food, Institute of Animal Reproduction and Food Research of the Polish Academy of Sciences, Olsztyn, Poland

Food Quality and Functionality Section

Prof. Vural Gökmen, Hacettepe University, Ankara, Turkey

Prof. Piotr Minkiewicz, Department of Food Biochemistry, University of Warmia and Mazury in Olsztyn, Poland

Nutritional Research Section

Prof. Jerzy Juśkiewicz, Department of Biological Function of Food, Institute of Animal Reproduction and Food Research of the Polish Academy of Sciences, Olsztyn, Poland

Dr. Luisa Pozzo, Institute of Agricultural Biology and Biotechnology, CNR, Pisa, Italy

LANGUAGE EDITOR

Prof. Ron Pegg, University of Georgia, Athens, USA

STATISTICAL EDITOR

Dr. Magdalena Karamać, Institute of Animal Reproduction and Food Research of the Polish Academy of Sciences, Olsztyn, Poland

EXECUTIVE EDITOR, NEWS AND MISCELLANEA SECTION

Joanna Molga, Institute of Animal Reproduction and Food Research of the Polish Academy of Sciences, Olsztyn, Poland;
E-mail: pjfns@pan.olsztyn.pl

SCOPE: The Journal covers fundamental and applied research in food area and nutrition sciences with a stress on interdisciplinary studies in the areas of food, nutrition and related subjects.

POLICY: Editors select submitted manuscripts in relation to their relevance to the scope. Reviewers are selected from the Advisory Board and from Polish and international scientific centres. Identity of reviewers is kept confidential.

AUTHORSHIP FORMS referring to Authorship Responsibility, Conflict of Interest and Financial Disclosure, Copyright Transfer and Acknowledgement, and Ethical Approval of Studies are required for all authors.

FREQUENCY: Quarterly – one volume in four issues (March, June, September, December).

COVERED by Web of Science, Current Contents/Agriculture, Biology & Environmental Sciences, Journal Citation Reports and Science Citation Index Expanded, BIOSIS (Biological Abstracts), SCOPUS, FSTA (formerly: Food Science and Technology Abstracts), CAS (Chemical Abstracts), AGRICOLA, AGRO-LIBREX data base, EBSCO, FOODLINE, Leatherhead FOOD RA data base FROSTI, AGRIS and Index Copernicus data bases, Biblioteka Nauki ICM, Biblioteka Narodowa – POLONA, and any www browser; ProQuest: The Summon, Bacteriology Abstracts, Immunology Abstracts.

EDITORIAL AND BUSINESS CORRESPONDENCE: Submit contributions (see Instructions to Authors) and address all communications regarding subscriptions, changes of address, etc. to:

CORRESPONDENCE TO: Ms. Joanna Molga
Polish Journal of Food and Nutrition Sciences
Institute of Animal Reproduction and Food Research
of Polish Academy of Sciences
ul. Tuwima 10, 10-747 Olsztyn, Poland
e-mail: pjfns@pan.olsztyn.pl; <http://journal.pan.olsztyn.pl>

ADVISORY BOARD OF PJFNS 2023–2026

Wilfried Andlauer

University of Applied Sciences and Arts Western Switzerland Valais, Sion, Switzerland

Vita di Stefano

University of Palermo, Italy

Maria Juana Frias Arevalillo

Institute of Food Science, Technology and Nutrition ICTAN, Madrid, Spain

Francesco Gai

National Research Council, Institute of Sciences of Food Production, 10095 Grugliasco, Italy

Nicole R. Giuggioli

Department of Agricultural, Forest and Food Sciences (DISAFA), University of Turin, Italy

Adriano Gomes da Cruz

Department of Food, Federal Institute of Education, Science and Technology of Rio de Janeiro (IFRJ), Brazil

Henryk Jeleń

Poznań University of Life Sciences, Poland

Andrzej Lenart

Warsaw University of Life Sciences, Poland

Adolfo J. Martínez-Rodríguez

CSIC-UAM, Madrid, Spain

Andre Mazur

INRA, Clermont, France

Francisco J. Morales

CSIC, Madrid, Spain

Fatih Öz

Ataturk University, Erzurum, Turkey

Ron B. Pegg

University of Georgia, Athens, USA

Mariusz K. Piskula

Institute of Animal Reproduction and Food Research of the Polish Academy of Sciences in Olsztyn, Poland

Da-Wen Sun

National University of Ireland, Dublin, Ireland

Lida Wądołowska

Warmia and Mazury University, Olsztyn, Poland

Wiesław Wiczkowski

Institute of Animal Reproduction and Food Research of the Polish Academy of Sciences in Olsztyn, Poland

Henryk Zieliński

Institute of Animal Reproduction and Food Research of the Polish Academy of Sciences in Olsztyn, Poland

Contents

ORIGINAL PAPERS

| | |
|------------------------------------------------------------------------------------------------------------------------------------------------------------------------------------|-----|
| Antioxidant, Anti-Tyrosinase, and Wound-Healing Capacities of Soy Protein Hydrolysates Obtained by Hydrolysis with Papaya and Cantaloupe Juices Showing Proteolytic Activity | 5 |
| <i>T.-P. Nguyen, Q.T. Le, M.L.T. Tran, K.N. Ta, K.T. Nguyen</i> | |
| Variation in the Lipid Profile of Pacific Oyster (<i>Crassostrea gigas</i>) Cultured in Khanh Hoa Coast, Vietnam, Based on Location and Harvest Period..... | 16 |
| <i>M.V. Nguyen, D. Kakooza, A.P.T. Tran, V.T.T. Tran</i> | |
| Effects of Stewing Modes on Physicochemical Quality and Formation of Flavour Compounds of Chinese Dagu Chicken Soup | 26 |
| <i>H. Guan, X. Xu, Ch. Feng, Y. Tian, D. Liu, X. Diao</i> | |
| Effects of Freeze-Thaw Cycles on the Flavor of Nanguo Pear | 41 |
| <i>G. Bai, Y. Wang, J. Zheng, X. Zhang, Z. Zhuang, D. Zhu, X. Cao</i> | |
| Recovery of Proteins from Sweet Potato Cell Liquid by Acidification via Inoculation-Enhanced Fermentation and Determination of Functional Properties of Protein Products | 49 |
| <i>Q. Li, L. Liu, Y. Han, X. Zhao, M. Yao, J. Ma, M. Han, J. Zhang</i> | |
| Curcumin Prevents Free Fatty Acid-Induced Lipid Accumulation via Targeting the miR-22-3p/ <i>CRLS1</i> Pathway in HepG2 Cells | 59 |
| <i>Y. Mei, X. Sun, S.-Y. Huang, X. Wu, K.-T. Ho, L. Lu, Ch. Chen, J. Li, J. Liu, G. Li</i> | |
| Effect of Infrared Drying on the Drying Kinetics and the Quality of Mango (<i>Mangifera indica</i>) Powder | 69 |
| <i>P.B.D. Nguyen, T.V.L. Nguyen, T.T.D. Nguyen</i> | |
| High-Fiber Extruded Purple Sweet Potato (<i>Ipomoea batatas</i>) and Kidney Bean (<i>Phaseolus vulgaris</i>) Extends the Feeling of Fullness | 82 |
| <i>E. Palupi, N. M. Nurdin, G. Mufida, F.N. Valentine, R. Pangestika, R. Rimbawan, A. Sulaeman, D. Briawan, F. Filianty</i> | |
| REVIEW | |
| Current Perspective About the Effect of a Ketogenic Diet on Oxidative Stress – a Review..... | 92 |
| <i>N. Drabińska</i> | |
| Volume 73's Reviewers' Index | 106 |
| Instructions for Authors | 108 |



Ministerstwo Edukacji i Nauki

W latach 2022–2024 kwartalnik naukowy *Polish Journal of Food and Nutrition Sciences* realizuje projekt nr RCN/SP/0520/2021/1 finansowany ze środków budżetu państwa – Ministerstwo Edukacji i Nauki w ramach programu „Rozwój czasopism naukowych”. Dofinansowanie wynosi 120 000 zł. W ramach projektu podejmowane są działania zmierzające do podniesienia poziomu praktyk wydawniczych i edytorskich, zwiększenia wpływu czasopism na rozwój nauki oraz utrzymania się czasopism w międzynarodowym obiegu naukowym.



Ministry of Education and Science Republic of Poland

In the years 2022–2024, the scientific quarterly *Polish Journal of Food and Nutrition Sciences* accomplishes a project no. RCN/SP/0520/2021/1 financed from the state budget – Ministry of Education and Science Republic of Poland in the framework of a program “Development of scientific journals”. The financing amounts to 120,000 PLN. The program aims at improving the level of publishing and editing practices, increasing the impact of scientific journals on science development, and extending the international range of scientific journals.

Subscription

2024 – One volume, four issues per volume. Annual subscription rates are: Poland 150 PLN, all other countries 80 EUR.

Prices are subject to exchange rate fluctuation. Subscription payments should be made by direct bank transfer to Bank Gospodarki Żywnościowej, Olsztyn, Poland, account No 1720300045111000000452110 SWIFT code: GOPZPLWOLA with corresponding banks preferably. Subscription and advertising offices at the Institute of Animal Reproduction and Food Research of Polish Academy of Sciences, ul. J. Tuwima 10, 10-747 Olsztyn, Poland, tel./fax (48 89) 5234670, fax (48 89) 5240124, e-mail: pjfns@pan.olsztyn.pl; <http://journal.pan.olsztyn.pl>

Zamówienia prenumeraty: Joanna Molga (e-mail: pjfns@pan.olsztyn.pl)

Wersja pierwotna (referencyjna) kwartalnika PJFNS: wersja papierowa (ISSN 1230–0322)

Nakład: 70 egz.; Ark. wyd. 16,7; Ark. druk. 14

Skład i druk: ITEM

Antioxidant, Anti-Tyrosinase, and Wound-Healing Capacities of Soy Protein Hydrolysates Obtained by Hydrolysis with Papaya and Cantaloupe Juices Showing Proteolytic Activity

Thi-Phuong Nguyen¹ , Quang Thai Le¹, Mai Linh Thi Tran², Kim Nhung Ta³ , Khoa Thi Nguyen^{1,*} 

¹NTT Hi-Tech Institute, Nguyen Tat Thanh University, Ho Chi Minh City 700000, Vietnam

²Department of Biotechnology, Ho Chi Minh City University of Science, Ho Chi Minh City 700000, Vietnam

³Faculty of Advanced Technologies and Engineering, VNU Vietnam Japan University, Hanoi 100000, Vietnam

Purified and crude proteases have been broadly applied to obtain hydrolysates from soy protein isolate (SPI) with the improved functional and biological properties. However, the use of fruit juices containing native proteases to produce SPI hydrolysates with better bioactivities receives less attention. The present study attempted to investigate the ability of papaya (*Carica papaya*) and cantaloupe (*Cucumis melo*) juices in the hydrolysis of SPI and assess the antioxidant, anti-tyrosinase, and wound-healing activities of obtained hydrolysates. Our analysis showed that SPI was hydrolysed by papaya juice, at the juice to substrate ratio of 2.5:2 (v/w), with a degree of hydrolysis (DH) of approximately 11% after 4 h of treatment at 55°C. A higher DH (about 26%) was obtained by the hydrolysis with cantaloupe juice at the same juice to substrate ratio and treatment conditions. Papain used at the enzyme to substrate ratio of 0.625:2 (w/w) broke down SPI in a similar DH as papaya juice at the juice to substrate ratio of 2.5:2 (v/w). The ABTS^{•+}-scavenging, [•]OH-scavenging and tyrosinase inhibitory capacities of SPI were lower than those of hydrolysates obtained by the treatment with papaya juice (IC₅₀ of 2.39, 7.17, and 32.07 µg/mL, respectively) and cantaloupe juice (IC₅₀ of 2.46, 6.93, and 30.49 µg/mL, respectively). An enhancement in ABTS^{•+}-scavenging, [•]OH-scavenging and anti-tyrosinase activities was also observed in the hydrolysate obtained by papain (IC₅₀ of 2.75, 17.85, and 117.80 µg/mL, respectively) compared to SPI. However, the increased level of the [•]OH-scavenging capacity of the hydrolysate obtained by papain was lower than that of the fruit juice-treated samples. Remarkably, the hydrolysates prepared from the hydrolysis with fruit juices accelerated the wound closure in human fibroblasts by estimate 1.5 times after 24 h of treatment while this property was not observed in the hydrolysate by papain. Our study data suggest the potential of SPI hydrolysates obtained by papaya and cantaloupe juices in the preparation of healthy food products.

Key words: antiradical activity, cantaloupe fruit, fibroblast model, degree of hydrolysis, papain, papaya fruit, soy protein isolate, tyrosinase inhibition

INTRODUCTION

Soy protein isolate (SPI), together with soy protein concentrate (SPC) and soy flour, is a renowned commercial product of processed soybean (*Glycine max*) [Qin *et al.*, 2022]. Containing a minimum of 90 g of protein in 100 g with two major water-insoluble

globulins (glycinin or 11S and β-conglycinin or 7S), SPI is commonly used in nutritional drinks, protein bars, and infant formula products [Paulsen, 2009; Qin *et al.*, 2022]. Health benefits of soy protein consumption, including prevention of cancer, reduction of cardiovascular disease-associated risks and complications,

*Corresponding Author:

e-mail: khoant@ntt.edu.vn (K.T. Nguyen)

Submitted: 16 July 2023

Accepted: 13 December 2023

Published on-line: 22 January 2024



© Copyright by Institute of Animal Reproduction and Food Research of the Polish Academy of Sciences
© 2024 Author(s). This is an open access article licensed under the Creative Commons Attribution-NonCommercial-NoDerivs License (<http://creativecommons.org/licenses/by-nc-nd/4.0/>).

lowering low-density lipoprotein cholesterol, and improvement of postmenopausal symptoms in women have been reported in a number of studies [Lima *et al.*, 2017; Messina, 2014; Qin *et al.*, 2022; Sirtori *et al.*, 2009]. However, the digestibility of soy protein is lower than that of other protein sources; its *in vitro* digestibility value is often less than 80%. This is due to the presence of antinutritional factors, such as lipooxygenase, urease, and trypsin inhibitors [Vagadia *et al.*, 2017]. In order to increase the protein digestibility, enzymatic hydrolysis has been widely implemented as small peptides in the protein hydrolysates can be rapidly absorbed by small intestine [Webb Jr, 1990]. Enzymatic hydrolysis is also more desirable than chemical hydrolysis due to its advantages in reducing side chemical reactions and unwanted products [Campbell *et al.*, 1996]. SPI hydrolysates were proven to have higher bioactivities compared to SPI, including anti-adipogenic, anti-angiotensin, anti-inflammatory, anticancer, antioxidant, and antibacterial effects [Hsieh *et al.*, 2022; Joo *et al.*, 2004; Lee *et al.*, 2008; Tsou *et al.*, 2010; Zhang *et al.*, 2020b]. In addition, enzymatic protein treatment also fosters great potential in decreasing soy protein-related allergenicity while improving emulsifying capacity, foaming property, solubility, water- and oil-binding capacity, and sensory profile of SPI hydrolysates relative to the parent proteins [Meinlschmidt *et al.*, 2016].

Commercial enzymes used in SPI hydrolysis are isolated from fungal, bacterial, animal, and plant sources. Since the peptide diversity and consequent bioactivities of hydrolysed products can be restricted with the application of a single type of enzyme, enzyme combination has been considered as a means to obtain SPI hydrolysates with appealing properties, such as antioxidant capacity [Chen *et al.*, 2020]. The use of more than two enzymes or a mixture of native proteases from fruit juices in SPI hydrolysis has not been intensively studied, although it was described for soy proteins and other protein sources [Tovar-Jiménez *et al.*, 2021; Utami *et al.*, 2019]. In one study, soy proteins digested by pineapple juice produced a hydrolysate as a complex nitrogen source for the growth of lactic acid bacteria [Utami *et al.*, 2019]. In another study, a hydrolysate of whey protein concentrate produced by a combination of purified *Sporisorium reilianum* aspartyl protease (Eap1), chymotrypsin (C), and trypsin (T) (Eap1-C-T) showed antihypertensive activity; however, its capacity was weaker than of that produced by single enzymes (Eap1, C, and T) and combinations of two enzymes (Eap1-C, Eap1-T, and C-T) [Tovar-Jiménez *et al.*, 2021].

Papaya (*Carica papaya*) and cantaloupe (*Cucumis melo*) are promising sources of proteolytic enzymes [Kaneda *et al.*, 1997; Pendzhiev, 2002]. The crude papaya extract contains numerous proteases in which a well-known enzyme, papain (EC 3.4.22.2), can be used to generate protein hydrolysates with less pronounced bitterness [Humiski & Aluko, 2007; Meinlschmidt *et al.*, 2016]. Recently, papaya juice has been employed to hydrolyse edible bird's nest and the achieved hydrolysate has been shown to inhibit α -glucosidase, a hyperglycemia-associated enzyme, whereas the hydrolysates obtained with two commercial enzymes, Alcalase and papain, did not exhibit this ability [Zulkifli *et al.*, 2019]. This suggests the improvement of antihyperglycemic activity in edible bird's nest hydrolysed by papaya juice as

compared to the tested enzymes. Similar to papaya fruit, high amounts of proteases, including a renowned serine protease, cucumisin (EC 3.4.21.25), are present in melon fruit [Yamagata *et al.*, 1989]. A crude melon extract was also reported to produce kila fish protein hydrolysate with higher antioxidant activity than Alcalase [Alavi *et al.*, 2019].

Due to the proteolytic potentials of papaya and cantaloupe, this study aimed to exploit the ability of two fruit juices in SPI hydrolysis. The bioactivities of the obtained hydrolysates, including *in vitro* antioxidant, anti-tyrosinase, and wound-healing abilities on fibroblast model, were also compared to those of unhydrolysed SPI and the hydrolysate obtained using the commercial enzyme – papain. The antioxidant capacity was selected for the assessment as this property has been investigated for SPI hydrolysates in various studies [Chen *et al.*, 2020; Knežević-Jugović *et al.*, 2023; Lee *et al.*, 2008; Peña-Ramos & Xiong, 2002]. Moreover, antioxidant peptides derived from the protein hydrolysates have captured great attention for their effects against oxidative stress-related diseases [Zhu *et al.*, 2022]. Recently, researchers have shown interests on the anti-tyrosinase and wound-healing activities of the protein hydrolysates due to their potential application in health and beauty products [Chotphruethipong *et al.*, 2021; Wong *et al.*, 2018]. As a result, the present study evaluated these bioactivities in SPI hydrolysates obtained by fruit juices although they have not been previously recorded for SPI hydrolysates.

MATERIALS AND METHODS

■ Materials

SPI powder (90 g of protein/100 g of SPI) and papain enzyme (50 USP/mg) were purchased from Shiv Health Foods LLP (Kota, India) and Biogreen BPC., JSC (Hanoi, Vietnam), respectively. Fresh ripe papaya and cantaloupe fruits used in this study were harvested during the wet and dry seasons in Southern Vietnam. Human fibroblast cells were a kind gift from Dr. Tran Le Bao Ha, Laboratory of Tissue Engineering and Biomedical Materials, University of Science, HCMC National University (Ho Chi Minh, Vietnam).

■ Preparation of papaya and cantaloupe fruit juices and determination of their proteolytic activity

Papaya and cantaloupe were peeled and squeezed; the resultant juices were then centrifuged at $4,951\times g$ for 10 min at 10°C . The supernatants, designated here as papaya juice (PJ) and cantaloupe juice (CJ), were used in the subsequent experiments.

The analysis of the proteolytic activity of PJ and CJ was conducted according to the protocol for the Sigma's non-specific protease activity assay [Cupp-Enyard, 2008]. Free tyrosinases produced by the proteases of PJ and CJ on the casein substrate were reacted with Folin-Ciocalteu phenol reagent to form blue chromophores, which absorbance was measured by a spectrophotometer (Genway Biotech, San Diego, CA, USA). A standard curve plotted for tyrosine was used to express the protease activity of PJ and CJ in terms of unit, which was defined as the μmol of tyrosine equivalents released from casein *per min*. The results were calculated by the Equation (1):

$$\text{Protease activity (U/mL)} = (\mu\text{mol tyrosine eq} \times a) / (b \times c \times d) \quad (1)$$

where: a is total volume of assay (11 mL), b is time of assay (10 min), c is volume of PJ or CJ (1 mL), and d is volume used in spectrophotometric measurement (2 mL).

■ Preparation of soy protein hydrolysates by papaya and cantaloupe fruit juices, and papain

The SPI slurry (~20 mg/mL) was prepared by mixing 2.0 g of SPI with 100 mL of distilled water. To obtain SPI hydrolysates, a volume of 2.5 mL of PJ or CJ was added to the SPI slurry containing 2.0 g of SPI (juice to substrate ratio of 2.5:2, v/w). The temperature was set at 55°C and the pH was about 6.5 for PJ and 8.5 for CJ during the hydrolysis. The hydrolysed samples after 1, 2, and 4 h of treatment were heated at 90°C for 20 min to terminate the reaction and then centrifuged at 8,801×g for 10 min at 10°C. The obtained supernatants (hydrolysates) were collected for sodium dodecyl-sulfate polyacrylamide gel electrophoresis (SDS-PAGE) analysis and further experiments. The hydrolysates of SPI by PJ and CJ were hereafter designated as HPJ and HCJ, respectively. Mixtures of SPI with papaya and cantaloupe juices were considered as HPJ 0 h and HCJ 0 h, respectively.

The hydrolyses of SPI by papain were carried out at different papain to substrate ratios (0.3125:2, 0.625:2, and 1.25:2, w/w) and the conditions of 55°C, 4 h, and pH 6.5. Subsequent steps were performed similarly to those mentioned above for the SPI hydrolysis with PJ and CJ. The hydrolysate of SPI with papain was hereafter designated as Hpapain. A mixture of SPI and papain was considered as Hpapain 0 h.

■ Sodium dodecyl-sulfate polyacrylamide gel electrophoresis analysis

Samples including SPI, HPJ 0 h, HCJ 0 h, HPJ and HCJ after 1–4 h of hydrolysis, and Hpapain obtained using different papain to substrate ratios, were mixed with sodium dodecyl-sulfate (SDS) protein loading buffer, boiled for 5 min and loaded on SDS-polyacrylamide gel electrophoresis (SDS-PAGE) separating gels (12.5% of acrylamide, w/v). Color pre-stained protein ladder (New England Biolabs, Ipswich, MA, USA) was used as a molecular weight standard. After running in an electrophoresis apparatus (Bio-Rad Laboratories, Hercules, CA, USA), the gels were stained with Coomassie blue dye to observe protein bands. The SDS-PAGE profile of SPI was analysed according to a previous report [Xia *et al.*, 2020]. The amount of degraded β-conglycinin subunits (α, α') (in the molecular weight range of 70–100 kDa) was calculated based on the intensity of protein bands using Image J software (version 1.45, National Institutes of Health, Bethesda, MD, USA) in order to relatively compare the hydrolysis of SPI by PJ and papain.

■ Determination of degree of hydrolysis

The degree of hydrolysis (DH) was determined using o-phthalaldehyde (OPA) reagent according to the previous description [Nielsen *et al.*, 2001]. In brief, aliquots of 25 μL of the samples (SPI, HPJ 0 h, HCJ 0 h, HPJ and HCJ after 1–4 h of hydrolysis, and Hpapain obtained using different papain to substrate ratios)

and serine as a standard (0.9516 meqv/L) were pipetted into a 96-well Optiplate (PerkinElmer, Waltham, MA, USA). A volume of 200 μL of freshly prepared OPA reagent was pipetted into each well. The plate was incubated in the dark at room temperature for 5 min and absorbance readings were taken at 340 nm. MilliQ water was used as the blank.

The DH was calculated using Equation (2):

$$\text{DH (\%)} = (H/H_{\text{tot}}) \times 100\% \quad (2)$$

where: H is the number of cleaved peptide bonds during hydrolysis and H_{tot} is the total number of substrate peptide bonds (for soy protein products, $H_{\text{tot}} = 7.8$ meqv/g protein) [Nielsen *et al.*, 2001].

The H was calculated based on absorbance of reaction mixture with sample (A_{sample}), serine (A_{standard}), and blank (A_{blank}) using Equations (3) and (4) [Nielsen *et al.*, 2001]:

$$H \text{ (meqv/g protein)} = \frac{(\text{SerineNH}_2 - \beta)}{\alpha} \quad (3)$$

$$\text{SerineNH}_2 \text{ (meqv/g protein)} = \frac{(A_{\text{sample}} - A_{\text{blank}}) \times 0.9516}{(A_{\text{standard}} - A_{\text{blank}}) \times C} \quad (4)$$

where: α and β are constant values (0.97 and 0.342 for soy proteins, respectively), C is protein concentration in sample solution (18 g/L), and 0.9516 (meqv/L) corresponds to equivalent weight of the serine standard.

■ Determination of 2,2'-azino-bis(3-ethylbenzothiazoline-6-sulfonic acid) radical cation scavenging capacity

The antiradical capacity of SPI, HPJ, HCJ, and Hpapain (enzyme to substrate ratio of 0.625:2, w/w) from the hydrolysis at 0 and 4 h was performed using 2,2'-azino-bis(3-ethylbenzothiazoline-6-sulfonic acid), ABTS (Sigma-Aldrich Pte. Ltd., Singapore) as previously described [Re *et al.*, 1999]. A volume of 100 μL of diluted SPI (0.625, 1.25, 2.5, 5, 10, and 20 μg/mL) was mixed with 900 μL of ABTS^{•+} solution and incubated for 15 min. Similar steps were also performed with 100 μL of diluted HPJ, HCJ, and Hpapain 0 h and 4 h containing 0.625, 1.25, 2.5, 5, 10, and 20 μg/mL of initial SPI. The absorbance was measured at 734 nm in a UV spectrophotometer (Genway Biotech, USA). The ABTS^{•+}-scavenging capacity was calculated by the Equation (5):

$$\text{ABTS}^{\bullet+}\text{-scavenging capacity (\%)} = 100 - \frac{100 \times (A_2 - A_3)}{A_1} \quad (5)$$

where: A_1 is absorbance of negative control (ABTS^{•+} solution only), A_2 is absorbance of the sample after reacting with ABTS^{•+}, and A_3 is absorbance of the blank (the sample without ABTS^{•+}).

The concentration of sample which inhibits 50% of the ABTS^{•+} (IC_{50}) was calculated by GraphPad Prism software (version 5.0, Insightful Science LLC, San Diego, CA, USA).

■ Determination of hydroxyl radical-scavenging capacity

The assay with hydroxyl radical ([•]OH) generated in Fenton reaction was carried out following a previous study with slight

modifications [Chong *et al.*, 2022]. The initial solution was prepared by mixing 0.5 mL of 9 mM iron (II) sulphate (FeSO₄) in 10 mM of ethylenediaminetetraacetic acid, disodium salt (Na₂EDTA) and 1.0 mL of 8 mM hydrogen peroxide (H₂O₂). Then, a volume of 1.0 mL of the diluted SPI, HPJ, HCl, and Hpapain (enzyme to substrate ratio of 0.625:2, *w/w*) from the hydrolysis at 0 and 4 h containing 0.125, 0.25, 0.5, 1.0, 2.0, 4.0, 8.0 and 16.0 µg/mL of initial SPI was added into the mixture. Milli-Q water was used as a negative control. Subsequently, 0.2 mL of 9 mM of salicylic acid was added. All test tubes were incubated at 37°C for 30 min and absorbance was read at 510 nm using a microplate spectrophotometer (VICTOR Nivo 3F, PerkinElmer, USA). *OH-scavenging capacity was calculated using the Equation (6):

$$\text{*OH-scavenging capacity (\%)} = 100 - \frac{100 \times (A_2 - A_3)}{A_1} \quad (6)$$

where: A₁ is absorbance of negative control, A₂ is absorbance of the sample after reacting with salicylic acid and A₃ is absorbance of the blank (the sample without salicylic acid).

The IC₅₀ values were calculated by GraphPad Prism software (version 5.0, Insightful Science LLC, USA).

■ Determination of *in vitro* wound-healing activity

The *in vitro* wound-healing assay on the fibroblast model was conducted following the previous report [Nguyen *et al.*, 2023]. In brief, fibroblast cells were cultured in high-glucose Dulbecco's Modified Eagle Medium (DMEM) (HyClone, Cytiva, Marlborough, MA, USA) supplemented with fetal bovine serum (FBS, 0.1 g/mL) (HyClone, USA) for 24 h at 37°C with CO₂ (50 mL/L). After making a wound by a 10 µL pipette tip, the old medium was replaced with high-glucose DMEM medium and test samples (5 mL of sample in 100 mL of medium) including SPI, HPJ, HCl, and Hpapain (enzyme to substrate ratio of 0.625:2, *w/w*) from the hydrolysis at 0 and 4 h. Distilled water was used as a negative control. Wound images at 0, 12, and 24 h of treatment were taken in a light microscope (Euromex, Arnhem, Netherlands). The wound areas were quantified using ImageJ software (version 1.45, National Institutes of Health, USA). The wound-healing activity of the samples was calculated by the Equation (7):

$$\text{Wound closure (\%)} = \frac{100 \times (C_1 - C_2)}{C_1} \quad (7)$$

where: C₁ is the wound area of the sample at 0 h and C₂ is the wound area of the sample after 12 and 24 h of treatment.

■ Determination of mushroom tyrosinase inhibitory capacity

The anti-tyrosinase assay using mushroom tyrosinase and L-tyrosine (substrate) (Sigma-Aldrich Pte. Ltd., Singapore) was performed as previously described with small modifications [Tomita *et al.*, 1990]. A volume of 10 µL of tyrosinase (250 U/mL) was added to 60 µL of diluted SPI, HPJ, HCl, and Hpapain (enzyme to substrate ratio of 0.625:2, *w/w*) from the hydrolysis at 0 and 4 h containing 1.9, 3.8, 7.5, 15, 30, and 60 µg/mL of initial SPI in a 96-well plate. The plate was incubated at room

temperature for 20 min. Then, 140 µL of a reaction medium consisting of L-tyrosine (0.3 mg/mL) in phosphate buffer (pH 6.8) was added to the wells. The formation of L-dopachrome was monitored by measuring the absorbance at 480 nm in a microplate reader (VICTOR Nivo Filter, PerkinElmer, USA). The tyrosinase inhibitory capacity of the samples was calculated using the Equation (8):

$$\text{Tyrosinase inhibitory capacity (\%)} = \frac{100 \times [(B_1 - B_3) - (B_2 - B_4)]}{B_1 - B_3} \quad (8)$$

where: B₁ is absorbance of negative control, B₂ is absorbance of the sample after reacting with tyrosinase, B₃ and B₄ are absorbances of the blank for the negative control and sample, respectively (the reaction without L-tyrosine substrate).

GraphPad Prism software (version 5.0, Insightful Science LLC, USA) was used to calculate the IC₅₀ values.

■ Statistical analysis

Three independent hydrolysates of each type were obtained and analysed for bioactivities. To compare statistical differences among samples, one-way analysis of variance (ANOVA) with Tukey's post-hoc test was employed. Differences were considered significant at $p \leq 0.05$.

RESULTS AND DISCUSSION

■ The hydrolysis of soy protein isolate by papaya and cantaloupe juice proteases, and papain

Proteolytic enzymes are present in papaya and cantaloupe [Kaneda *et al.*, 1997; Pendzhiev, 2002]. In order to confirm our obtained juices contained these enzymes, the non-specific protease activity of PJ and CJ was determined by using casein as a substrate. The activity of total proteases in PJ and CJ was 0.87±0.04 U/mL and 2.66±0.02 U/mL, respectively, indicating that proteases were extracted into the juices and might be responsible for the proteolytic activity of the juices.

The SDS-PAGE separations of SPI and hydrolysates are shown in Figure 1. Proteins with molecular weights in the range of 25 kDa to 100 kDa predominated in the SPI profile. Major bands corresponded to subunits of β-conglycinin (α, α', and β): 70–100 kDa for the α, α' subunits and approximately 55 kDa for the β subunit. The bands in the range of 25–55 kDa were identified as acidic subunits of glycinin (A1–A4) while the basic subunit had a molecular weight of 25 kDa [Xia *et al.*, 2020]. This SDS-PAGE profile of SPI was consistent with that reported by Xia *et al.* [2020], although there was a small difference in the distribution of bands resulting in a slight difference in the estimation of protein molecular weight.

The SDS-PAGE profiles of hydrolysates obtained by PJ showed that after 1 h of SPI treatment with PJ at the juice to substrate ratio of 2.5:2 (*v/w*), band distribution was comparable to that for unhydrolysed soy proteins (Figure 1A). The proteins began to be significantly degraded after 2 h; however, they were not fully hydrolysed even after 4 h of treatment. This trend in the extent of SPI hydrolysis by PJ was confirmed by determining the degree of hydrolysis. The DH was 5% after 1 h of hydrolysis whereas

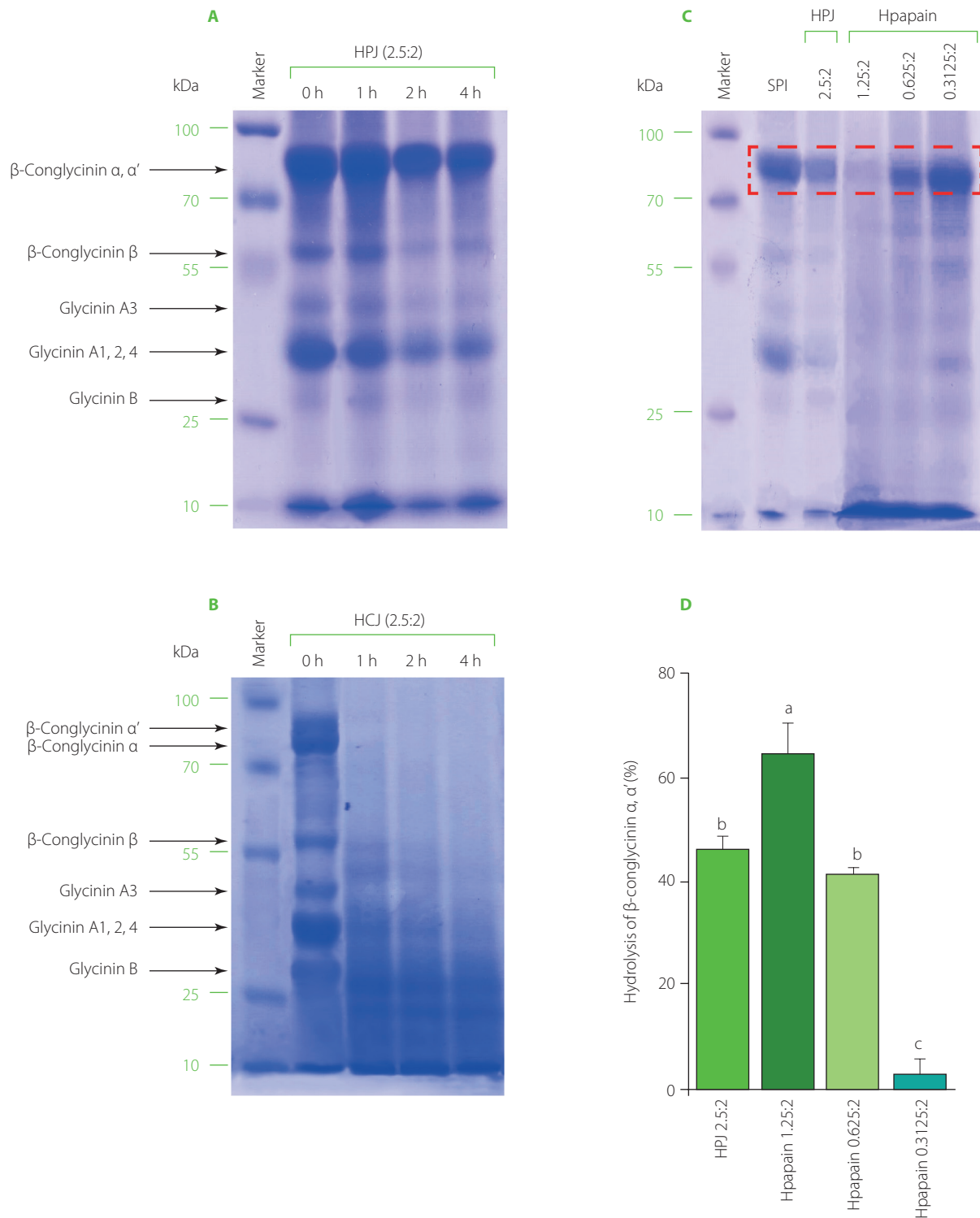


Figure 1. SDS-PAGE separation of soy protein isolate (SPI) hydrolysed by papaya juice (PJ), cantaloupe juice (CJ), and papain. (A) and (B) SPI hydrolysed by PJ and CJ at the juice to substrate ratio of 2.5:2 (v/w), temperature of 55°C, and reaction time of 0, 1, 2, and 4 h. (C) SPI hydrolysed by PJ (juice to substrate ratio of 2.5:2, v/w) and papain (enzyme to substrate ratio of 0.3125:2, 0.625:2, and 1.25:2, w/w) at a temperature of 55°C and reaction time of 4 h. (D) Quantification of β -conglycinin subunit (α, α') degradation (in the red-dashed box in C graph). Each data bar is presented as mean and standard deviation of three independent experiments. Different letters above bars indicate significant differences among samples ($p \leq 0.05$).

values reached nearly 10 and 11% after 2 and 4 h of hydrolysis, respectively (Figure 2A).

Meanwhile, as seen in the electrophoregrams of SPI hydrolysates obtained by CJ, at the juice to substrate ratio of 2.5:2 (v/w),

most of the bands corresponding to high molecular weights disappeared after 1–2 h of hydrolysis indicating that substantial amount of proteins was hydrolysed (Figure 1B). Protein degradation was even more extensive after 4 h of CJ treatment.

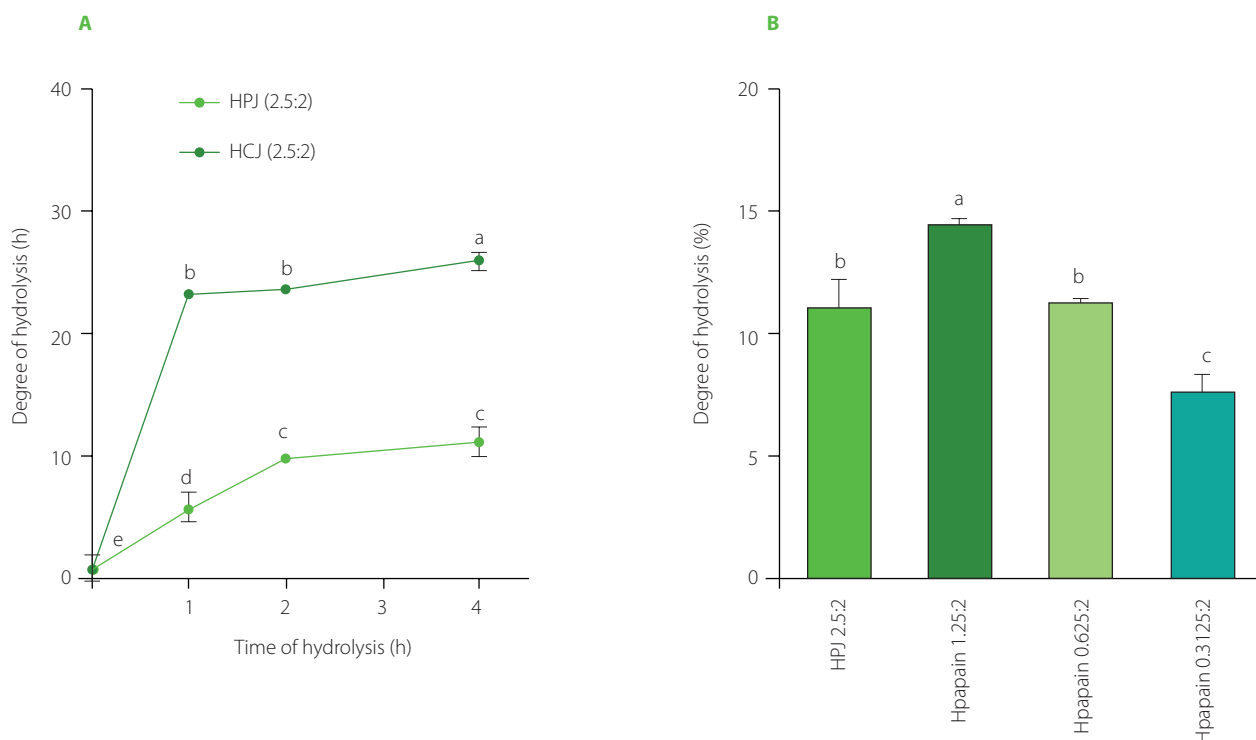


Figure 2. The degree of hydrolysis of soy protein isolate (SPI) hydrolysed by papaya juice (PJ), cantaloupe juice (CJ), and papain. **(A)** SPI hydrolysed by PJ and CJ at the juice to substrate ratio of 2.5:2 (v/w), temperature of 55°C, and reaction time of 0, 1, 2, and 4 h. **(B)** SPI hydrolysed by PJ (juice to substrate ratio of 2.5:2, v/w) and papain (enzyme to substrate ratio of 0.3125:2, 0.625:2, and 1.25:2, w/w) at a temperature of 55°C and reaction time of 4 h. Each data bar is presented as mean and standard deviation of three independent experiments. Different letters above bars indicate significant differences among samples ($p \leq 0.05$).

Consistently, 1 and 2 h of SPI hydrolysis with CJ resulted in a DH of about 23%, while a DH of 26% was obtained after 4 h of hydrolysis (Figure 2B). A crude melon extract produced at the juice to substrate ratio of 2:100 (w/v) was also reported to provoke an extensive hydrolysis on kilka fish protein [Alavi *et al.*, 2019]. This property of melon is attributed to cucumisin (about 10 g in 100 g of crude proteins) and other proteases detected in the fruit juice [Yamagata *et al.*, 1994].

The SDS-PAGE separations (Figure 1) and DH values (Figure 2) showed that the SPI hydrolysis performed by CJ was more extensive than that by PJ at the same juice to substrate ratio of 2.5:2 (v/w). This might be due to the difference in proteolytic activity of these two fruit juices, which was approximately 3-fold higher for CJ than PJ.

In order to compare bioactivities of SPI hydrolysates produced using fruit juices and a commercial enzyme, papain was selected as it is a well-characterised enzyme found naturally in raw papaya fruit [Mamboya & Amri, 2012]. Papain was also employed to produce SPI hydrolysate with better foaming properties and a less bitter taste than Alcalase, Corolase, Neutrase, Protamex, and pepsin [Meinlschmidt *et al.*, 2016]. We hither attempted to find the ratio of papain to substrate which allows for obtaining a relatively similar degree of SPI hydrolysis as when using PJ in the ratio of 2.5:2 (v/w). According to the pattern on the SDS-PAGE gel (Figure 1C) and the DH values (Figure 2B), SPI was the most extensively hydrolysed by papain at the enzyme to substrate ratio of 1.25:2, w/w (DH of nearly 15%). The effective

hydrolysis of soy proteins was also observed in a former study using papain at the enzyme to substrate ratio of 1:100 (w/v) [Peña-Ramos & Xiong, 2002]. The hydrolysis of SPI by papain at the enzyme to substrate ratio of 0.625:2 (w/w) approximately corresponded to that by PJ at juice to substrate ratio of 2.5:2 (v/w), as indicated by the decrease of intensity of the major protein band with the molecular weight in the range of 70–100 kDa (α , α' subunits of β -conglycinin) and the DH value (approximately 11%) (Figure 1C, 1D, and 2C). The band in the range of 70–100 kDa was selected for quantification since its high molecular weight prevented the overlap with bands of hydrolysis products.

As observed on the SDS-PAGE gel, the profile of hydrolysis products in the PJ-treated sample was dissimilar from that in the papain-treated one (Figure 1C). This is possibly related to the different substrate specificity of native proteases in PJ, resulting in the degradation of proteins at various positions and eventually generating products of hydrolysis with lower molecular weights. The different profiles between two hydrolysates by PJ and papain might contribute to differences in their bioactivities.

■ Antioxidant capacity of soy protein hydrolysates

Soy protein hydrolysates obtained by protease treatment can possess promising antioxidant property [Chen *et al.*, 2020; Knežević-Jugović *et al.*, 2023; Lee *et al.*, 2008; Peña-Ramos & Xiong, 2002]. Therefore, our study investigated if the SPI hydrolysates obtained by PJ, CJ, and papain also exhibited antioxidant capacity.

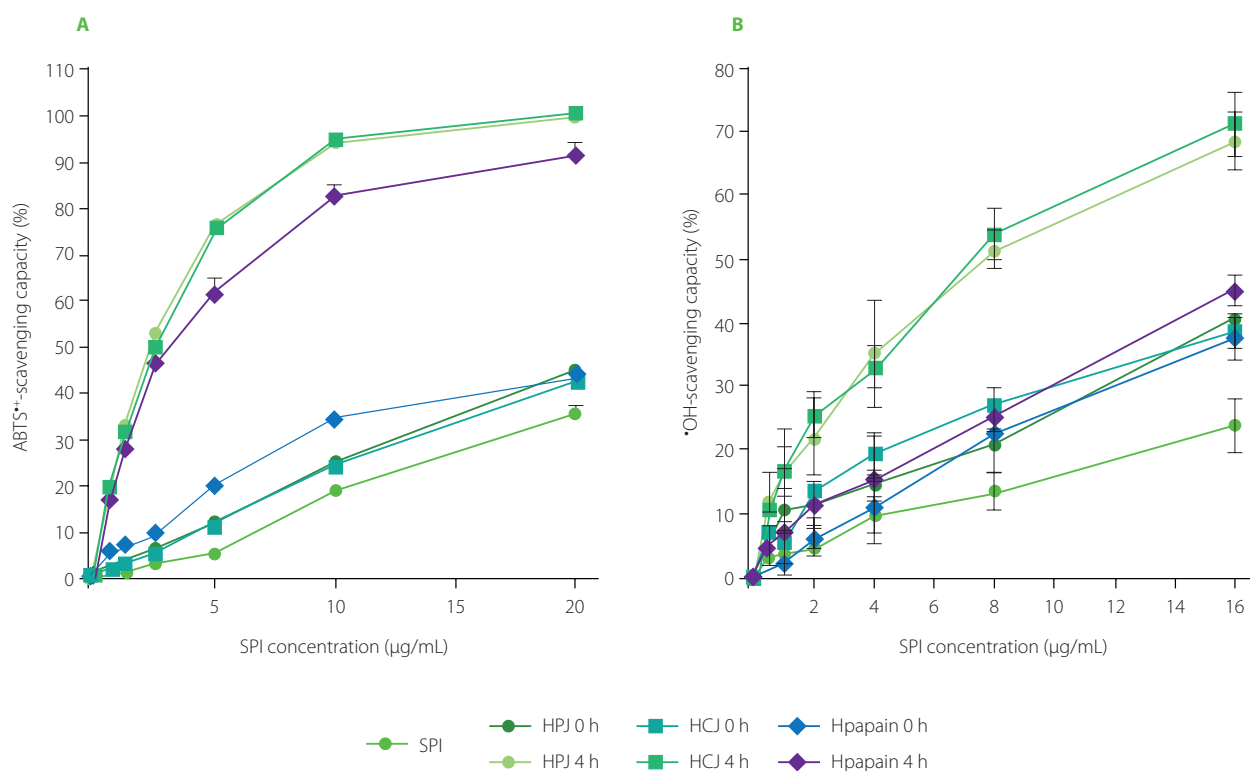


Figure 3. (A) ABTS^{•+}-scavenging capacity and (B) •OH-scavenging capacity of soy protein isolate (SPI), hydrolysates obtained by papaya juice (HPJ 4 h), cantaloupe juice (HCJ 4 h), and papain (Hpapain 4 h) and unhydrolysed mixture of SPI with papaya juice (HPJ 0 h), cantaloupe juice (HCJ 0 h), and papain (Hpapain 0 h). SPI hydrolysates were prepared at the juice to substrate ratio of 2.5:2 (*v/w*) or the papain to substrate ratio of 0.625:2 (*w/w*), temperature of 55°C, and reaction time of 4 h. Each data bar is shown as mean and standard deviation of three independent experiments.

The results of ABTS assay showed that at the initial SPI concentration of 10 µg/mL, SPI hydrolysates obtained by PJ and CJ after 4 h hydrolysis (HPJ 4 h and HCJ 4 h) were able to scavenge about 95% of ABTS^{•+} radicals whereas it was only 20% for unhydrolysed SPI and 25% for mixtures of SPI and fruit juices (HPJ 0 h and HCJ 0 h) (Figure 3A). At the same concentration, the ABTS^{•+}-scavenging capacity of hydrolysate obtained by papain after 4 h of hydrolysis (Hpapain 4 h) was approximately 80% higher than that of unhydrolysed SPI (20%) and a mixture of SPI and papain (Hpapain 0 h) (35%). In the •OH-scavenging

capacity analysis, HPJ 4 h and HCJ 4 h inhibited about 75% of the •OH, which are more effective than unhydrolysed SPI (nearly 17%), HPJ 0 h, and HCJ 0 h (nearly 40%) at the initial SPI concentration of 16 µg/mL (Figure 3B). At this initial concentration of SPI, the hydrolysate obtained by papain also had higher •OH-scavenging capacity (45%) than Hpapain 0 h (35%).

In general, the ABTS^{•+} and •OH-scavenging capacities of HPJ 4 h (IC₅₀ of 2.39 and 7.17 µg/mL, respectively), HCJ 4 h (IC₅₀ of 2.46 and 6.93 µg/mL, respectively), and Hpapain 4 h (IC₅₀ of 2.75 and 17.85 µg/mL, respectively) were significantly

Table 1. IC₅₀ values (µg/mL) of soy protein isolate (SPI), hydrolysates obtained by papaya juice (HPJ 4 h), cantaloupe juice (HCJ 4 h), and papain (Hpapain 4 h), and unhydrolysed mixture of SPI with papaya juice (HPJ 0 h), cantaloupe juice (HCJ 0 h), and papain (Hpapain 0 h) for the ABTS^{•+}-scavenging, •OH-scavenging, and tyrosinase inhibitory capacities.

| Sample | ABTS ^{•+} -scavenging capacity | •OH-scavenging capacity | Tyrosinase inhibitory capacity |
|-------------|-----------------------------------------|--------------------------|--------------------------------|
| SPI | 24.93±0.93 ^a | 42.82±4.09 ^a | > 300 ^a |
| HPJ 0 h | 22.38±1.35 ^a | 19.59±1.28 ^c | 116.40±7.00 ^c |
| HPJ 4 h | 2.39±0.11 ^b | 7.17±1.29 ^d | 32.07±2.20 ^d |
| HCJ 0 h | 20.60±6.10 ^a | 24.40±0.01 ^{bc} | 150.31±1.40 ^b |
| HCJ 4 h | 2.46±0.11 ^b | 6.93±1.14 ^d | 30.49±1.43 ^d |
| Hpapain 0 h | 21.15±3.02 ^a | 29.14±5.39 ^b | > 300 ^a |
| Hpapain 4 h | 2.75±0.02 ^b | 17.85±1.20 ^c | 117.80±5.60 ^c |

Each data value was presented as mean ± standard deviation of three independent experiments. Different letters (in superscripts) indicated significant differences among samples in each column (*p*≤0.05).

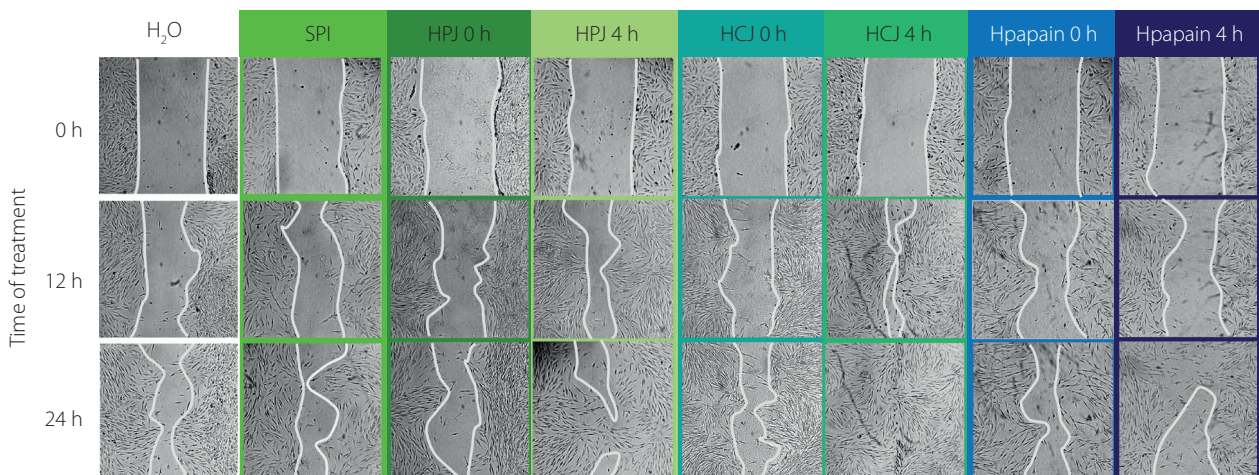
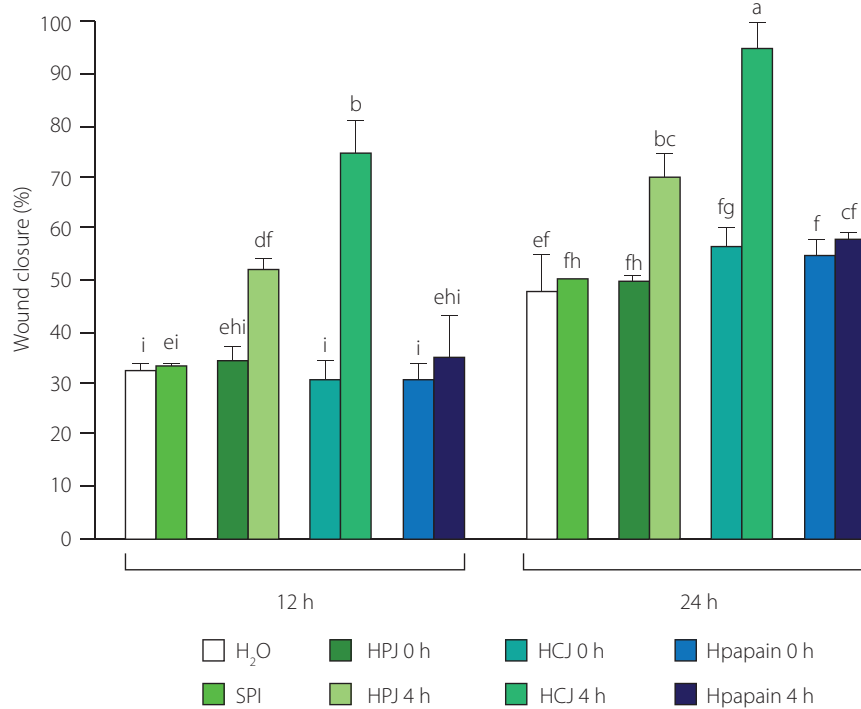
A**B**

Figure 4. *In vitro* wound-healing activity of soy protein isolate (SPI), hydrolysates obtained by papaya juice (HPJ 4 h), cantaloupe juice (HCJ 4 h), and papain (Hpapain 4 h), and unhydrolysed mixture of SPI with papaya juice (HPJ 0 h), cantaloupe juice (HCJ 0 h), and papain (Hpapain 0 h). (A) Images of wound closure in human dermal fibroblasts treated with water (H₂O, negative control) and samples at 0, 12, and 24 h. SPI hydrolysates were prepared at the juice to substrate ratio of 2.5:2 (v/w) or the papain to substrate ratio of 0.625:2 (w/w), temperature of 55°C, and reaction time of 4 h. (B) Quantification of wound closure (%) at 12 and 24 h. Each data bar is presented as mean and standard deviation of three independent experiments. Different letters above bars indicated significant differences among samples ($p \leq 0.05$).

higher in comparison to those of unhydrolysed SPI (IC₅₀ of 24.93 and 42.82 µg/mL, respectively). Our data also revealed a slightly stronger •OH-scavenging capacity of HPJ 4 h than Hpapain 4 h, despite both hydrolysates showed relatively similar DH. This might be rooted from the varying specificity of native proteases in the PJ which released a higher amount of peptides with •OH-scavenging activity or more active peptides. It should be noted that IC₅₀ values of HPJ 0 h, HCJ 0 h, and Hpapain 0 h for

the •OH-scavenging activity were slightly lower than that of SPI (Table 1). This higher radical scavenging capacity might be explained by the antioxidant activity of polyphenols of the papaya, carotenoids and vitamin C in the cantaloupe, or papain itself [Fundo *et al.*, 2018; Insanu *et al.*, 2022; Manosroi *et al.*, 2014].

SPI hydrolysates by PJ, CJ, and papain in our study displayed more effective free radical-scavenging capacity than unprocessed SPI, which was similar to a previous study using papain

and bromelain [Xu *et al.*, 2023]. The improved antioxidant potential of hydrolysates can be attributed to the release of bioactive peptides during hydrolysis. The structural characteristics of these peptides, such as their molecular weight, amino acid composition, sequence, hydrophobicity, and secondary structure, determine their antioxidant potential [Zou *et al.*, 2016]. For instance, C terminal Trp or Tyr-containing tripeptides from two libraries generated based on the sequence of the antioxidant peptides in the soy protein hydrolysates were found to exert strong radical-scavenging activities [Saito *et al.*, 2003]. In another study, low molecular-weight fractions of soy protein hydrolysate had stronger radical scavenging effects than the higher molecular-weight fractions [Abu-Salem *et al.*, 2013].

■ Wound-healing capacity of soy protein hydrolysates

The wound-healing property of peptides isolated from protein hydrolysates in previous studies [Gomes *et al.*, 2017; Song *et al.*, 2019], inspired us to examine this activity of the SPI hydrolysates obtained by PJ, CJ, and papain. Here, *in vitro* scratch assays on human fibroblasts were employed for the assessment of wound-healing property. Wound recovery was about 30% after 12 h and 50% after 24 h of treatment in the water-treated control, indicating the occurrence of self-wound-healing activity (Figure 4). SPI and Hpapain did not accelerate the healing process after 12 and 24 h, since similar percentages of wound closure were observed in the samples treated with SPI, Hpapain and water control. The same effects were also observed with HPJ 0 h and HCJ 0 h. On the contrary, HPJ 4 h and HCJ 4 h significantly ameliorated wound recovery in comparison with the other samples. Noticeably, at 24 h, wounds supplemented with HPJ 4 h and HCJ 4 h were closed by more than 70 and 90%, respectively. These results suggested that the wound-healing efficiency of SPI in the human fibroblast model was improved by the treatment with PJ and CJ but not with papain.

The distinctive composition of bioactive peptides in the SPI hydrolysates by fruit juices and papain might cause the difference in their wound-healing properties as peptides are capable of recovering wounds by influencing the inflammation, epithelialization, tissue granulation and remodeling steps [Gomes *et al.*, 2017; Wang *et al.*, 2022]. A recent study has shown that peptides prepared from the hydrolysis of soy protein with four commercial proteases promoted skin repair in rats through suppressing the excessive levels of factors in the inflammation step [Zhang *et al.*, 2020a]. It would be interesting to investigate if peptides generated by the hydrolysis by PJ and CJ act *via* the inflammatory pathway or other mechanisms in a further study.

■ Tyrosinase inhibitory activity of soy protein hydrolysates

Natural anti-tyrosinase agents are of great interests in recent years as they can be excellent sources for skin whitening [Zhao *et al.*, 2023]. Protein hydrolysates containing bioactive peptides have been shown to display outstanding anti-tyrosinase activities, implying their potential in the whitening area [Hu *et al.*, 2022; Upata *et al.*, 2022; Zhao *et al.*, 2023]. Therefore, our study

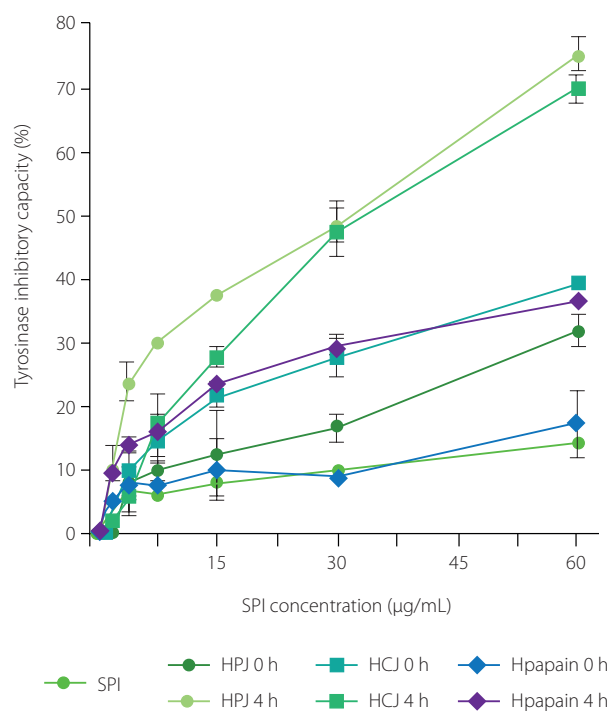


Figure 5. Tyrosinase inhibitory capacity of soy protein isolate (SPI), hydrolysates obtained by papaya juice (HPJ 4 h), cantaloupe juice (HCJ 4 h), and papain (Hpapain 4 h), and unhydrolysed mixture of SPI with papaya juice (HPJ 0 h), cantaloupe juice (HCJ 0 h), and papain (Hpapain 0 h). SPI hydrolysates were prepared at the juice to substrate ratio of 2.5:2 (*v/w*) or the papain to substrate ratio of 0.625:2 (*w/w*), temperature of 55°C, and reaction time of 4 h. Each data bar is presented as mean and standard deviation of three independent experiments.

assessed this property in SPI hydrolysates obtained by PJ, CJ, and papain although it has not been described for soy protein hydrolysates so far.

Our data showed that HPJ 4 h, HCJ 4 h, and Hpapain 4 h inhibited the activity of tyrosinase more strongly than unhydrolysed SPI and respective HPJ 0 h, HCJ 0 h, and Hpapain 0 h (Figure 5). At the SPI concentration of 60 µg/mL, unhydrolysed SPI and Hpapain 0 h displayed about 15% of inhibition of tyrosinase activity whereas the percentages of inhibition were nearly 30 and 35% for HPJ 0 h and HCJ 0 h, respectively. The inhibitory effect on enzyme activity was remarkably increased in HPJ 4 h and HCJ 4 h (75% of inhibition) and moderately improved in Hpapain 4 h (35% of inhibition, respectively). Consistently, the IC_{50} values of HPJ 4 h (32.07 µg/mL), HCJ 4 h (30.49 µg/mL), and Hpapain 4 h (117.80 µg/mL) were lower than those of unhydrolysed SPI (>300 µg/mL), respective HPJ 0 h (116.40 µg/mL), HCJ 0 h (150.31 µg/mL), and Hpapain 0 h (>300 µg/mL) (Table 1). It is also worth mentioning that HPJ 0 h and HCJ 0 h showed stronger tyrosinase inhibitory activity than unhydrolysed SPI, suggesting that papaya and cantaloupe juices possessed the ability to inhibit tyrosinase. These results are consistent with the anti-tyrosinase property of the extracts from papaya and cantaloupe fruits [Le *et al.*, 2023; Shin *et al.*, 2008]. Protein hydrolysates obtained by enzymes of plant origin have been analysed for their inhibition of tyrosinase activity. For example, the hydrolysates of calf fleshing by-products obtained by papain and bromelain exhibited inhibitory effects on tyrosinase

activity [Tedeschi *et al.*, 2021]. The improvement of anti-tyrosinase activity in the protein hydrolysates is possibly contributed by peptides as products of the hydrolysis process [Hu *et al.*, 2022]. As SPI hydrolysates achieved by PJ and CJ in our study revealed strong tyrosinase inhibitory abilities, it is of importance to isolate bioactive peptides or peptide fractions from these hydrolysates and examine their skin-whitening activity in *in vivo* models.

CONCLUSIONS

The present study results demonstrated the possibility of obtaining soy protein hydrolysates using papaya and cantaloupe juices with significantly higher ABTS^{•+} and •OH-scavenging, wound-healing, and anti-tyrosinase capacities compared to SPI. The commercial enzyme, papain, hydrolysing SPI at a relatively similar DH (about 11%) as PJ produced the hydrolysate with enhanced tyrosinase inhibitory and ABTS^{•+}-scavenging capacities but insignificant wound-healing effect. The •OH-scavenging capacity of the hydrolysate obtained by papain was also improved to a lesser extent as compared to that of the hydrolysates produced with papaya and cantaloupe juices. Based on these results, papaya and cantaloupe juices offer great opportunities to produce SPI hydrolysates with perspective applications in healthcare foods, such as supplementary drinks.

RESEARCH FUNDING

This research did not receive any specific grant from funding agencies in the public, commercial, or not-for-profit sectors.

CONFLICT OF INTERESTS

The authors declare that there is no conflict of interest.

ORCID IDs

K.T. Nguyen <https://orcid.org/0000-0001-8055-5636>
T.-P. Nguyen <https://orcid.org/0000-0002-6406-1406>
K.N. Ta <https://orcid.org/0000-0002-1915-1832>

REFERENCES

- Abu-Salem, F.M., Mahmoud, M.H., El-Kalyoub, M., Gibriel, A., Abou-Arab, A. (2013). Characterization of antioxidant peptides of soybean protein hydrolysate. *World Academy of Science, Engineering and Technology*, 79(7), 249-253.
- Alavi, F., Jamshidian, M., Rezaei, K. (2019). Applying native proteases from melon to hydrolyze tilapia fish proteins (*Clupeonella cultriventris caspia*) compared to commercial enzyme Alcalase. *Food Chemistry*, 277, 314-322. <https://doi.org/10.1016/j.foodchem.2018.10.122>
- Campbell, N.F., Shih, F.F., Hamada, J.S., Marshall, W.E. (1996). Effect of limited proteolysis on the enzymatic phosphorylation of soy protein. *Journal of Agricultural and Food Chemistry*, 44(3), 759-762. <https://doi.org/10.1021/jf950390m>
- Chen, C., Sun-Waterhouse, D., Zhang, Y., Zhao, M., Sun, W. (2020). The chemistry behind the antioxidant actions of soy protein isolate hydrolysates in a liposomal system: Their performance in aqueous solutions and liposomes. *Food Chemistry*, 323, art. no. 126789. <https://doi.org/10.1016/j.foodchem.2020.126789>
- Chong, P.K., Mun, S.L., Chang, L.S., Babji, A.S., Lim, S.J. (2022). Fractionation of edible bird's nest glycoprotein hydrolysates: characterisation and antioxidative activities of the fractions. *Food Science and Human Wellness*, 11(4), 886-894. <https://doi.org/10.1016/j.fshw.2022.03.015>
- Chotphruethipong, L., Binlath, T., Hutamekalin, P., Sukketsiri, W., Aluko, R.E., Benjakul, S. (2021). *In vitro* antioxidant and wound-healing activities of hydrolyzed collagen from defatted Asian sea bass skin as influenced by different enzyme types and hydrolysis processes. *RSC Advances*, 11(30), 18144-18151. <https://doi.org/10.1039/D1RA03131G>
- Cupp-Enyard, C. (2008). Sigma's non-specific protease activity assay-casein as a substrate. *JoVE*, 17(19), art. no. e899. <https://doi.org/10.3791/899>
- Fundo, J.F., Miller, F.A., Garcia, E., Santos, J.R., Silva, C.L., Brandão, T.R. (2018). Physicochemical characteristics, bioactive compounds and antioxidant activity in juice, pulp, peel and seeds of *Cantaloupe* melon. *Journal of Food Measurement and Characterization*, 12, 292-300. <https://doi.org/10.1007/s11694-017-9640-0>
- Gomes, A., Teixeira, C., Ferraz, R., Prudêncio, C., Gomes, P. (2017). Wound-healing peptides for treatment of chronic diabetic foot ulcers and other infected skin injuries. *Molecules*, 22(10), art. no. 1743. <https://doi.org/10.3390/molecules22092839>
- Hsieh, C.-H., Wang, T.-Y., Tung, B.-C., Liu, H.-P., Yeh, L.-T., Hsu, K.-C. (2022). The hydrolytic peptides of soybean protein induce cell cycle arrest and apoptosis on human oral cancer cell line HSC-3. *Molecules*, 27(9), art. no. 2839. <https://doi.org/10.3390/molecules27092839>
- Hu, Z.-Z., Ma, T.-X., Sha, X.-M., Zhang, L., Tu, Z.-C. (2022). Improving tyrosinase inhibitory activity of grass carp fish scale gelatin hydrolysate by gastrointestinal digestion: Purification, identification and action mechanism. *LWT – Food Science and Technology*, 159, art. no. 113205. <https://doi.org/10.1016/j.lwt.2022.113205>
- Humiski, L., Aluko, R. (2007). Physicochemical and bitterness properties of enzymatic pea protein hydrolysates. *Journal of Food Science*, 72(8), S605-S611. <https://doi.org/10.1111/j.1750-3841.2007.00475.x>
- Insanu, M., Nayaka, N.M.D.M.W., Solihin, L., Wirasutisna, K.R., Pramastya, H., Fidrianny, I. (2022). Antioxidant activities and phytochemicals of polar, semi-polar, and nonpolar extracts of used and unused parts of *Carica papaya* fruit. *Biotransformation and Agricultural Biotechnology*, 39, art. no. 102270. <https://doi.org/10.1016/j.bcab.2021.102270>
- Joo, J.-H., Yi, S.D., Lee, G.-H., Lee, K.-T., Oh, M.J. (2004). Antimicrobial activity of soy protein hydrolysate with *Asp. saitoi* protease. *Journal of the Korean Society of Food Science and Nutrition*, 33(2), 229-235. <https://doi.org/10.3746/jkfn.2004.33.2.229>
- Kaneda, M., Yonezawa, H., Uchikoba, T. (1997). Purification and some properties of a protease from the sarcocarp of musk melon fruit. *Bioscience, Biotechnology, and Biochemistry*, 61(12), 2100-2102. <https://doi.org/10.1271/bbb.61.2100>
- Knežević-Jugović, Z., Culetu, A., Mijalković, J., Duta, D., Stefanović, A., Šekuljica, N., Đorđević, V., Antov, M. (2023). Impact of different enzymatic processes on antioxidant, nutritional and functional properties of soy protein hydrolysates incorporated into novel cookies. *Foods*, 12(1), art. no. 24. <https://doi.org/10.3390/foods12010024>
- Le, X.-T., Nguyen, B.-T., Dang, Y.-P., Tran-Nguyen, K.-U., Le-Dang, T.-D., Pham, C.-D., Pham-Vu, M.-C. (2023). Screening of herbal plants for inhibitory activity and extracting skin-whitening active ingredients from papaya fruit. In *IOP Conference Series: Earth and Environmental Science*, 1226, art. no. 012020. <https://doi.org/10.1088/1755-1315/1226/1/012020>
- Lee, J.-S., Yoo, M., Koo, S.-H., Baek, H.-H., Lee, H.-G. (2008). Antioxidant and ACE inhibitory activities of soybean hydrolysates: Effect of enzyme and degree of hydrolysis. *Food Science and Biotechnology*, 17(4), 873-877.
- Lima, A., Oliveira, J., Mota, J., Ferreira, R.B. (2017). Proteins in soy might have a higher role in cancer prevention than previously expected: Soybean protein fractions are more effective MMP-9 inhibitors than non-protein fractions, even in cooked seeds. *Nutrients*, 9(3), art. no. 201. <https://doi.org/10.3390/nu9030201>
- Mamboya, E.A.F., Amri, E. (2012). Papain, a plant enzyme of biological importance: A review. *American Journal of Biochemistry and Biotechnology*, 8(2), 99-104. <https://doi.org/10.3844/ajbb.2012.99.104>
- Manosroi, A., Chankhampan, C., Pattamapun, K., Manosroi, W., Manosroi, J. (2014). Antioxidant and gelatinolytic activities of papain from papaya latex and bromelain from pineapple fruits. *Chiang Mai Journal of Science*, 41(3), 635-648.
- Meinlschmidt, P., Sussmann, D., Schweiggert-Weisz, U., Eisner, P. (2016). Enzymatic treatment of soy protein isolates: Effects on the potential allergenicity, technofunctionality, and sensory properties. *Food Science & Nutrition*, 4(1), 11-23. <https://doi.org/10.1002/fsn3.253>
- Messina, M. (2014). Soy foods, isoflavones, and the health of postmenopausal women. *The American Journal of Clinical Nutrition*, 100(suppl_1), 423S-430S. <https://doi.org/10.3945/ajcn.113.071464>
- Nguyen, T.-P., Phan, H.N., Do, T.D., Do, G.D., Ngo, L.H., Do, H.D.K., Nguyen, K.T. (2023). Polysaccharide and ethanol extracts of *Anoectochilus formosanus* Hayata: Antioxidant, wound-healing, antibacterial, and cytotoxic activities. *Heliyon*, 9(3), art. no. e13559. <https://doi.org/10.1016/j.heliyon.2023.e13559>
- Nielsen, P., Petersen, D., Dambmann, C. (2001). Improved method for determining food protein degree of hydrolysis. *Journal of Food Science*, 66(5), 642-646. <https://doi.org/10.1111/j.1365-2621.2001.tb04614.x>
- Paulsen, P. (2009). Chapter 13 – Isolated soy protein usage in beverages. In *Functional and Speciality Beverage Technology*, Woodhead Publishing Series in Food Science, Technology and Nutrition, pp. 318-345. <https://doi.org/10.1533/9781845695569.318>

27. Pendzhiev, A. (2002). Proteolytic enzymes of papaya: Medicinal applications. *Pharmaceutical Chemistry Journal*, 36(6), 315-317. <https://doi.org/10.1023/A:1020832807958>
28. Peña-Ramos, E., Xiong, Y. (2002). Antioxidant activity of soy protein hydrolysates in a liposomal system. *Food Science*, 67(8), 2952-2956. <https://doi.org/10.1111/j.1365-2621.2002.tb08844.x>
29. Qin, P., Wang, T., Luo, Y. (2022). A review on plant-based proteins from soybean: Health benefits and soy product development. *Journal of Agriculture Food Research*, 7, art. no. 100265. <https://doi.org/10.1016/j.jafr.2021.100265>
30. Re, R., Pellegrini, N., Proteggente, A., Pannala, A., Yang, M., Rice-Evans, C. (1999). Antioxidant activity applying an improved ABTS radical cation decolorization assay. *Free Radical Biology and Medicine*, 26(9-10), 1231-1237. [https://doi.org/10.1016/S0891-5849\(98\)00315-3](https://doi.org/10.1016/S0891-5849(98)00315-3)
31. Saito, K., Jin, D.-H., Ogawa, T., Muramoto, K., Hatakeyama, E., Yasuhara, T., Nokihara, K. (2003). Antioxidative properties of tripeptide libraries prepared by the combinatorial chemistry. *Journal of Agricultural and Food Chemistry*, 51(12), 3668-3674. <https://doi.org/10.1021/jf021191n>
32. Shin, Y.-S., Lee, J.-E., Yeon, I.-K., Do, H.-W., Cheung, J.-D., Kang, C.-K., Choi, S.-Y., Youn, S.-J., Cho, J.-G., Kwoen, D.-J. (2008). Antioxidant effects and tyrosinase inhibition activity of oriental melon (*Cucumis melo* L. var makuwa Makino) extracts. *Journal of Life Science*, 18(7), 963-967. <https://doi.org/10.5352/JLS.2008.18.7.963>
33. Sirtori, C.R., Galli, C., Anderson, J.W., Sirtori, E., Arnoldi, A. (2009). Functional foods for dyslipidaemia and cardiovascular risk prevention. *Nutrition Research Reviews*, 22(2), 244-261. <https://doi.org/10.1017/S0954422409990187>
34. Song, Y., Wu, C., Zhang, X., Bian, W., Liu, N., Yin, S., Yang, M., Luo, M., Tang, J., Yang, X. (2019). A short peptide potentially promotes the healing of skin wound. *Bioscience Reports*, 39(3), art. no. BSR20181734. <https://doi.org/10.1042/BSR20181734>
35. Tedeschi, T., Anzani, C., Ferri, M., Marzocchi, S., Caboni, M.F., Monari, S., Tassoni, A. (2021). Enzymatic digestion of calf fleshing meat by-products: Antioxidant and anti-tyrosinase activity of protein hydrolysates, and identification of fatty acids. *Foods*, 10(4), art. no. 755. <https://doi.org/10.3390/foods10040755>
36. Tomita, K., Oda, N., Ohbayashi, M., Kamei, H., Miyaki, T., Oki, T. (1990). A new screening method for melanin biosynthesis inhibitors using *Streptomyces bikiniensis*. *The Journal of Antibiotics*, 43(12), 1601-1605. <https://doi.org/10.7164/antibiotics.43.1601>
37. Tovar-Jiménez, X., Téllez-Jurado, A., Gómez-Aldapa, C.A., Mercado-Flores, Y., Arana-Cuenca, A. (2021). Antioxidant and antihypertensive activity of bovine whey protein concentrate enzymatic hydrolysates. *Biotechnia*, 23(1), 161-169. <https://doi.org/10.18633/biotechnia.v23i1.1321>
38. Tsou, M.-J., Kao, F.-J., Tseng, C.-K., Chiang, W.-D. (2010). Enhancing the anti-adipogenic activity of soy protein by limited hydrolysis with Flavourzyme and ultrafiltration. *Food Chemistry*, 122(1), 243-248. <https://doi.org/10.1016/j.foodchem.2010.02.070>
39. Upata, M., Siriwoharn, T., Makkhun, S., Yarnpakdee, S., Regenstein, J.M., Wang-tueai, S. (2022). Tyrosinase inhibitory and antioxidant activity of enzymatic protein hydrolysate from jellyfish (*Lobonema smithii*). *Foods*, 11(4), art. no 615. <https://doi.org/10.3390/foods11040615>
40. Utami, T., Kusuma, E., Satiti, R., Rahayu, E., Cahyanto, M. (2019). Hydrolyses of meat and soybean proteins using crude bromelain to produce halal peptone as a complex nitrogen source for the growth of lactic acid bacteria. *International Food Research Journal*, 26(1), 117-122.
41. Vagadia, B.H., Vanga, S.K., Raghavan, V. (2017). Inactivation methods of soybean trypsin inhibitor – A review. *Trends in Food Science & Technology*, 64, 115-125. <https://doi.org/10.1016/j.tifs.2017.02.003>
42. Wang, G., Chen, Z., Tian, P., Han, Q., Zhang, J., Zhang, A.-M., Song, Y. (2022). Wound healing mechanism of antimicrobial peptide cathelicidin-DM. *Frontiers in Bioengineering and Biotechnology*, 10, art. no. 977159. <https://doi.org/10.3389/fbioe.2022.977159>
43. Webb Jr, K. (1990). Intestinal absorption of protein hydrolysis products: a review. *Journal of Animal Science*, 68(9), 3011-3022. <https://doi.org/10.2527/1990.6893011x>
44. Wong, Z.C.F., Chan, G.K.L., Wu, K.Q.Y., Poon, K.K.M., Chen, Y., Dong, T.T.X., Tsim, K.W.K. (2018). Complete digestion of edible bird's nest releases free N-acetylneuraminic acid and small peptides: an efficient method to improve functional properties. *Food & Function*, 9(10), 5139-5149. <https://doi.org/10.1039/C8FO00991K>
45. Xia, W., Pan, S., Cheng, Z., Tian, Y., Huang, X. (2020). High-intensity ultrasound treatment on soy protein after selectively proteolyzing glycinin component: Physical, structural, and aggregation properties. *Foods*, 9(6), art. no. 839. <https://doi.org/10.3390/foods9060839>
46. Xu, Y., Yang, Y., Ma, C.-m., Bian, X., Liu, X.-f., Wang, Y., Chen, F.-l., Wang, B., Zhang, G., Zhang, N. (2023). Characterization of the structure, antioxidant activity and hypoglycemic activity of soy (*Glycine max* L.) protein hydrolysates. *Food Research International*, 173, Part 2, art. no. 113473. <https://doi.org/10.1016/j.foodres.2023.113473>
47. Yamagata, H., Masuzawa, T., Nagaoka, Y., Ohnishi, T., Iwasaki, T. (1994). Cucumisin, a serine protease from melon fruits, shares structural homology with subtilisin and is generated from a large precursor. *Journal of Biological Chemistry*, 269(52), 32725-32731. [https://doi.org/10.1016/S0021-9258\(20\)30051-X](https://doi.org/10.1016/S0021-9258(20)30051-X)
48. Yamagata, H., Ueno, S., Iwasaki, T. (1989). Isolation and characterization of a possible native cucumisin from developing melon fruits and its limited autolysis to cucumisin. *Agricultural and Biological Chemistry*, 53(4), 1009-1017. <https://doi.org/10.1080/00021369.1989.10869404>
49. Zhang, J., Fu, X., Li, W., Li, H., Ying, Z., Liu, X., Yin, L. (2020a). Enhancement of nutritional soy protein and peptide supplementation on skin repair in rats. *Journal of Functional Foods*, 75(9), art. no. 104231. <https://doi.org/10.1016/j.jff.2020.104231>
50. Zhang, J., Li, W., Ying, Z., Zhao, D., Yi, G., Li, H., Liu, X. (2020b). Soybean protein-derived peptide nutrition increases negative nitrogen balance in burn injury-induced inflammatory stress response in aged rats through the modulation of white blood cells and immune factors. *Food & Nutrition Research*, 64, art. no. 3677. <https://doi.org/10.29219/fnr.v64.3677>
51. Zhao, Y., Zhang, T., Ning, Y., Wang, D., Li, F., Fan, Y., Yao, J., Ren, G., Zhang, B. (2023). Identification and molecular mechanism of novel tyrosinase inhibitory peptides from the hydrolysate of Fengdan'peony (*Paeonia ostii*) seed meal proteins: Peptidomics and *in silico* analysis. *LWT – Food Science and Technology*, 180, art. no. 114695. <https://doi.org/10.1016/j.lwt.2023.114695>
52. Zhu, Y., Lao, F., Pan, X., Wu, J. (2022). Food protein-derived antioxidant peptides: Molecular mechanism, stability and bioavailability. *Biomolecules*, 12(11), art. no. 1622. <https://doi.org/10.3390/biom12111622>
53. Zou, T.-B., He, T.-P., Li, H.-B., Tang, H.-W., Xia, E.-Q. (2016). The structure-activity relationship of the antioxidant peptides from natural proteins. *Molecules*, 21(1), art. no. 72. <https://doi.org/10.3390/molecules21010072>
54. Zulkifli, A.S., Babji, A.S., Lim, J.S., Teh, A.H., Daud, N.M., Rhanman, H.A. (2019). Effect of different hydrolysis time and enzymes on chemical properties, antioxidant and antihyperglycemic activities of edible bird nest hydrolysate. *Malaysian Applied Biology*, 48(2), 149-156.

Variation in the Lipid Profile of Pacific Oyster (*Crassostrea gigas*) Cultured in Khanh Hoa Coast, Vietnam, Based on Location and Harvest Period

Minh Van Nguyen^{1*} , Derrick Kakooza¹ , Anh Phuong Thi Tran¹ , Vy Thao Thi Tran¹ 

¹Faculty of Food Technology, Nha Trang University, 02 Nguyen Dinh Chieu, Nha Trang, Vietnam

The lipid profiles of the oyster *Crassostrea gigas* cultured in Khanh Hoa coast at three locations and harvested in different months throughout the year were compared. Seasonal and locational changes in total lipid (TL) content, phospholipid content, free fatty acid content, fatty acid (FA) composition, and thrombogenicity index were found. The total lipid content and *n*-3/*n*-6 ratio in oysters from Ninh Hoa were higher compared to those from Cam Lam and Van Ninh. For oyster from all three farming areas, the total lipid content was the lowest during the two spawning seasons (May and September). Lipids from *C. gigas* were separated into neutral and polar lipid fractions using silica gel column chromatography. The amount of neutral lipids recovered from the oyster muscle was significantly higher than that of the polar lipids. The FA composition showed that *C. gigas* was abundant in saturated fatty acids (30.89–39.16 g/100 g TL), followed by polyunsaturated fatty acids (28.13–35.88 g/100 g TL), and monounsaturated fatty acids (19.32–23.75 g/100 g TL). The dominant polyunsaturated fatty acids of oysters from the three farming areas were eicosapentaenoic acid (9.09–13.77 g/100 g TL) and docosahexaenoic acid (6.71–16.47 g/100 g TL). Based on the present findings, it can be concluded that the Pacific oyster *C. gigas* cultured in Khanh Hoa, Vietnam is a promising source of highly nutritious exploitable lipids.

Key words: fatty acids, farming location, harvest season, lipid profile, phospholipids, thrombogenicity index

INTRODUCTION

Global aquaculture has increased in recent years and currently provides 50% of the world's food fish supply [Botta *et al.*, 2020]. In 2020, global mollusc production was over 17.7 million tons of which 6.06 million tons were oysters [FAO, 2022]. In 2018, commercial oyster production in Vietnam was at 15,000 tons from the coastal areas with *Crassostrea angulata* as the main farmed species [Ugalde *et al.*, 2023]. Oyster production relies on spat collection from the wild but the increasing demand for juveniles has led to the use of hatcheries [Rato *et al.*, 2019]. The contents of lipids, carbohydrates and protein of bivalves are influenced by the dietary nutritional profile [Anjos *et al.*, 2017].

The oyster's chemical composition varies between species due to factors like season, habitat, sexual maturity, age, and sexual cycle, with season being the most important factor among them [Hurtado *et al.*, 2012]. Lipid reserves in bivalves are an important energy source used in gonad maturation being utilized for energy during gametogenesis and a constituent in larvae and eggs [Rato *et al.*, 2019]. Neutral lipids are the major energy reserve in most marine animals, and their composition depends on the diet source [De La Parra *et al.*, 2005]. Diet (microalgae) has been shown to influence the polyunsaturated fatty acid (PUFA) profile of oysters as most bivalves have limited ability to produce long-chain fatty acids from short-chain precursors [Chu

*Corresponding Author:

tel: + 84 918 010 755; fax: +84 2583 831147; e-mail: minhvn@ntu.edu.vn (M.V. Nguyen)

Submitted: 10 October 2024

Accepted: 8 January 2024

Published on-line: 26 January 2024



© Copyright by Institute of Animal Reproduction and Food Research of the Polish Academy of Sciences
© 2024 Author(s). This is an open access article licensed under the Creative Commons Attribution-NonCommercial-NoDeriv License (<http://creativecommons.org/licenses/by-nc-nd/4.0/>).

& Greaves, 1991]. Lipids found in the oyster muscle contain high levels of phospholipids with important PUFAs such as eicosapentaenoic acid (EPA) and docosahexaenoic acid (DHA). The lipid content and composition of the fish and mollusc muscle vary depending on the fish species, season, sex, sexual maturation, and geographical variations [Kandemir & Polat, 2007]. In oysters, reproductive cycles affect the lipid profile more than the diet. Liu *et al.* [2020] showed seasonal variations in the lipid profile of the oyster, *Crassostrea talienwhanensis*, from the Yellow Sea area, with samples harvested in February having higher levels of PUFAs (48.77% of total lipids) and phospholipids (52.12% of total lipids). In turn, the oysters *Crassostrea rhizophorae* cultivated in the winter had a higher level of PUFAs, particularly the eicosapentaenoic-docosahexaenoic acid combination, and lower levels of saturated fatty acids [Lira *et al.*, 2013].

Pacific oyster *Crassostrea gigas* is widely cultured in Khanh Hoa province, Vietnam, at three different coastal areas: (1) Thuy Trieu lagoon – Cam Lam district, (2) Nha Phu lagoon – Ninh Hoa district, and (3) Mon lagoon – Van Ninh district. The climatic and environmental characteristics, as well as food system of these coastal areas, are different from each other. This is believed to have an effect on the lipid composition and, consequently, the nutritional value of Pacific oyster muscle. A previous study by Tung & Son [2019] reported that sea surface temperature of central Vietnam exhibited an average value of 23°C from January to February and 32°C in July to August, accompanied by a relatively stable salinity ranging from 31‰ to 34‰. In the mangrove ecosystem of Khanh Hoa province, a study by Lan *et al.* [2021] revealed a high diversity of phytoplankton, particularly silica algae, with water temperatures ranging from 29.4°C to 30.1°C. Truong *et al.* [2014] identified 185 zooplankton species in the Nha Phu estuary, with seasonal temperature variations ranging from 25.5°C in the wet season to 32.7°C in the dry season. The objective of this study was to understand the seasonal and locational variations in the lipid profile, including lipid classes, and fatty acid (FA) composition, of *C. gigas* harvested from Khanh Hoa coast. Results of this study will provide information on when to harvest *C. gigas* oyster for the highest lipid and the health indices of the lipids, which can be used in dietary recommendations.

MATERIALS AND METHODS

Materials and reagents

Oysters (*Crassostrea gigas*) were harvested from three Vietnamese farming regions; Thuy Trieu lagoon – Cam Lam, Nha Phu lagoon – Ninh Hoa, and Dam Mon lagoon – Van Ninh at the same location, on the 23rd and 24th of each month for 12 months from January 2021 to December 2021. The samples were commercial quality oysters (after 7–8 months of stocking) with an average size of 65–75 mm in length, and a weight of 70–80 g/oyster. After harvesting, the oysters were washed in seawater, placed in styrofoam boxes with ice, and transported to the laboratories of the Nha Trang University, Vietnam. Oyster muscle was manually separated from the shells, vacuum packed in polyamide bags and frozen at $-35\pm 2^\circ\text{C}$ in an air-blast freezer (Seatecco Corporation, Da Nang,

Vietnam). Frozen samples were stored at -80°C and analyzed within 2 weeks. Before analysis, the samples were completely thawed in a refrigerator at a temperature of 2°C.

The analytical materials and analytical grade reagents included *n*-hexane, chloroform, methanol, L-ascorbic acid, thin layer chromatography (TLC) plates (TLC silica gel 60 F₂₅₄), silica gel 60 (0.040–0.063 mm), diethyl ether, potassium chloride, sodium sulphate, and ninhydrin, and were purchased from Sigma-Aldrich (Burlington, MA, USA). All other reagents were also of analytical grade and were obtained from Merck (Darmstadt, Germany).

Determination of total lipid content

Oysters were extracted to obtain total lipid content according to the method of Bligh & Dyer [1959]. Briefly, 25 g of thawed oyster muscle was mixed with 25 mL of chloroform and 50 mL of methanol and homogenized in an Ultra-Turrax homogenizer (T25 basic, Ika Labor Technik, Staufen, Germany) for 2 min. To this end, 25 mL of chloroform was added, and the mixture was homogenized for 1 min. Then, 25 mL of 0.88% KCl was added to induce phase separation, and the mixture was homogenized for 1 min. After another 1 min of homogenization, the mixture was centrifuged at 1,942×g (Hermle Z326K universal refrigerated centrifuge, Wehingen, Germany) for 20 min at 4°C. The chloroform phase was collected and filtered through Whatman GF/C filters (Cytiva, Buckinghamshire, UK) filled with anhydrous sodium sulphate (Na₂SO₄) to remove traces of methanol and water. The total lipid content was determined by weighing after evaporation of chloroform to dryness at 40°C in a water bath, using a liquid nitrogen stream. The results were expressed as g per 100 g of the wet weight of oyster muscle.

Phospholipid content determination

Phospholipid (PL) content of the oyster muscle was determined according to the method of Stewart [1980], based on the complex formation of phospholipids with ammonium ferrothiocyanate. Briefly, a 100 µL of an aliquot of the chloroform phase containing lipids, extracted using the Bligh & Dyer method [1959], was added to 2 mL of chloroform. Subsequently, 1 mL of a thiocyanate reagent was added, and the mixture was vortexed for 1 min and centrifuged at 2,000×g (Hermle Z326K centrifuge) for 5 min at 4°C. The absorbance of the lower layer was measured at 488 nm using a Libra S50 UV/VIS spectrophotometer (Biochrom, Cambridge, UK). The results were expressed as g per 100 g of the total lipid and calculated using a standard curve prepared from phosphatidylcholine.

Free fatty acid content determination

Free fatty acid (FFA) content was determined according to the method of Bernárdez *et al.* [2005], based on complex formation of fatty acids with cupric acetate-pyridine. Briefly, 3 mL of an aliquot of the chloroform phase containing lipids, extracted using the Bligh & Dyer method [1959], was evaporated to dryness at 40°C in a water bath, using a liquid nitrogen stream. Subsequently, 3 mL of cyclohexane and 1 mL of cupric acetate-pyridine reagent were added, and the mixture was vortexed for 1 min

and then centrifuged at 2,000 \times g (Hermle Z326K centrifuge) for 10 min at 4°C. The absorbance of the upper layer was measured at 715 nm using a Libra S50 UV/VIS spectrophotometer (Biochrom). The results were expressed as g FFA per 100 g of the total lipid using a standard curve prepared from oleic acid.

■ Neutral and polar lipid separation

Total lipids recovered from *C. gigas* for the months of January, May, September, and November of each location were separated into neutral lipid and polar lipid fractions using column chromatography on silica gel according to the method described by Pernet *et al.* [2006] with some modifications. A glass column with an inner diameter of 180 mm, a length of 330 mm, and silica gel 60 (0.040–0.060 mm) were used. A lipid to sorbent ratio of 1:50 (w/v) was used, and the column was pre-conditioned with methanol and chloroform. A solution of 0.8 g of the lipid sample in 1 mL of chloroform was loaded onto the column and eluted at a rate of 1 mL/min with chloroform (100%) for 10 min followed by chloroform-methanol (95:5, v/v) for 20 min and then with chloroform-methanol (90:10, v/v) for 30 min to obtain the neutral lipid fraction. The elution was stopped when all the neutral lipids had been collected as confirmed using thin layer chromatography (TLC). Polar lipids were recovered by elution with methanol and complete recovery of the polar lipids was confirmed by performing TLC.

TLC was performed following the method described by Deranieh *et al.* [2013] with some modifications. TLC silica gel 60 F₂₅₄ plates were used as the stationary phase. The mobile phase for developing and separating neutral lipids consisted of a mixture of *n*-hexane/diethyl ether/acetic acid in a ratio of 70:30:2 (v/v/v). Another mobile phase composed of chloroform/methanol/water at a ratio of 65:25:4 (v/v/v) was used for developing and separating polar lipids. After TLC separation, the localization of the neutral lipids was visualized using iodine vapors, while the visualization of polar lipids was achieved using ninhydrin and 10% H₂SO₄ in MeOH.

The eluents of each fraction were evaporated using a rotary evaporator under vacuum at 40°C (Yamato RE-801-AW2 rotary evaporator, Yamato, Japan) and further under a gentle stream of nitrogen at 35°C. The weight of neutral and polar lipids was recorded, and the fractions were stored at –20°C in the dark until further analysis. The results were expressed as g neutral lipids or g polar lipids per 100 g of the total lipids.

■ Fatty acid profile analysis

Fatty acids of total lipids extracted were transesterified to methyl esters using base-catalysed esterification according to the American Oil Chemists' Society (AOCS) official method (Ce 1b-89, 2017) [AOCS, 2017]. The fatty acid methyl esters (FAMES) were dissolved in iso-octane and injected into a model GC 17A gas chromatograph (Shimadzu Corp., Kyoto, Japan) equipped with a Zebron ZB-wax fused silica wall-coated open tubular column (0.25 mm i.d. \times 30 m, 0.25 μ m in film thickness; Torrance, CA, USA) and a flame-ionization detector. The column oven and injection port temperature were held initially at 170°C for 2 min, then programmed to 240°C at a rate of 5°C/min, from 240°C to 250°C at

a rate of 1.6°C/min, and finally held at 250°C for 10 min. Nitrogen was used as a carrier gas with an inlet pressure of 2.0 kg/cm². Results were expressed as g per 100 g of the total lipids, and C23:0 (tricosanoic acid) was used as an internal standard.

■ Thrombogenicity index calculation

Thrombogenicity index (TI) was calculated according to Equation (1) by Ulbricht & Southgate [1991]. TI is the relationship between the pro-thrombogenic saturated fatty acids and the anti-thrombogenic monounsaturated fatty acids (MUFAs) and polyunsaturated fatty acids (PUFAs) that indicates the tendency to form clots in the blood vessels.

$$TI = \frac{(C14:0 + C16:0 + C18:0)}{(0.5 \times PUFA_{n-6}) + (3 \times PUFA_{n-3}) + (0.5 \times MUFA) + \frac{PUFA_{n-3}}{PUFA_{n-6}}} \quad (1)$$

■ Statistical analysis

All experiments were conducted in triplicate. The results were presented as means and standard deviations (SD). All the statistical analyses were carried out using the SPSS (version 26) software (SPSS Inc., Chicago, Illinois). The results were analyzed using one-way analysis of variance (ANOVA). Differences between samples were tested for significance by Student-Newman-Keuls post-hoc test at the 5% level of significance.

RESULTS AND DISCUSSION

■ Total lipid content

The total lipid content of the muscle of *C. gigas* from the three locations ranged between 2.64 and 3.15 g/100 g wet weight (Figure 1). The total lipid content of oysters significantly ($p < 0.05$) varied across harvest seasons and farming locations. Within the year, it was the lowest in the months of May and September. The content of total lipids recovered from Ninh Hoa oysters was slightly higher than that for Cam Lam and Van Ninh, which can be related to better food availability and quality and environmental conditions in Ninh Hoa compared to the other two areas. Lipid accumulation and depletion in molluscs depend on the stage of gonad maturation, food quality and supply, and the influence of environmental conditions on metabolic activity [Su *et al.*, 2006]. Lipids in oysters play an important role in gametogenesis and act as an energy source [De La Parra *et al.*, 2005]. They are accumulated when food is available, and during gonad maturation when there is conversion of glycogen into lipids. The low lipid content in oysters harvested in May and September in our study corresponded to the spawning period, an energy-intensive process. Post spawning, oysters accumulate storage lipids, especially triacylglycerols, in the resting phase [Napolitano & Ackman, 1992; De La Parra *et al.*, 2005]. Sterols are accumulated during gonad development in preparation for the reproductive processes [Pazos *et al.*, 1996]. Phytoplankton blooms during the rainy season in November and December probably were responsible for the increased lipid content of oysters (Figure 1). Previous studies have indicated seasonal and locational variations in the lipid content of *C. gigas* [Dridi *et al.*, 2007; Linehan *et al.*, 1999; Pazos *et al.*, 1996]. Linehan *et al.* [1999] observed that the highest total lipid content of *C. gigas* was in December (8.7% dry weight)

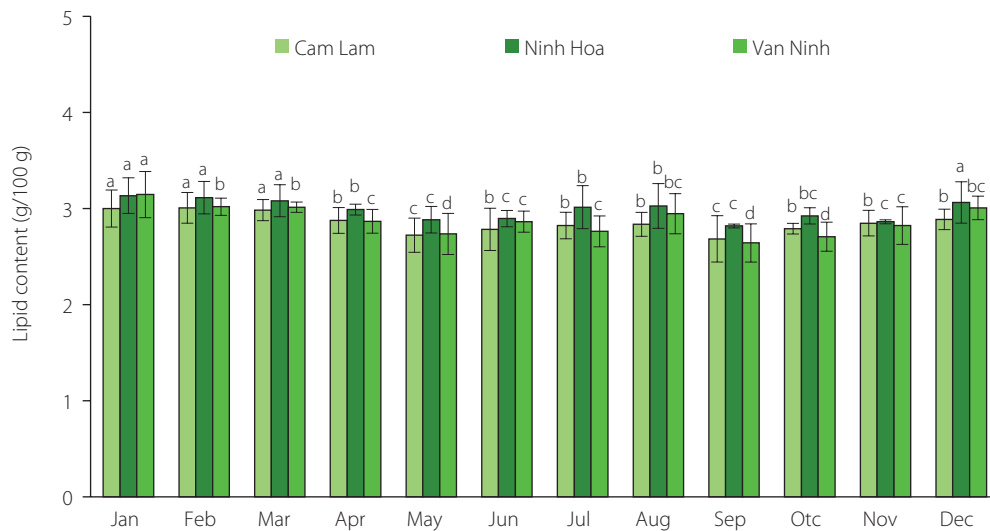


Figure 1. Total lipid content of *Crassostrea gigas* oysters cultured in Khanh Hoa coast at three locations and harvested in different months. Different letters above bars separately for each farming location indicate significant differences ($p < 0.05$).

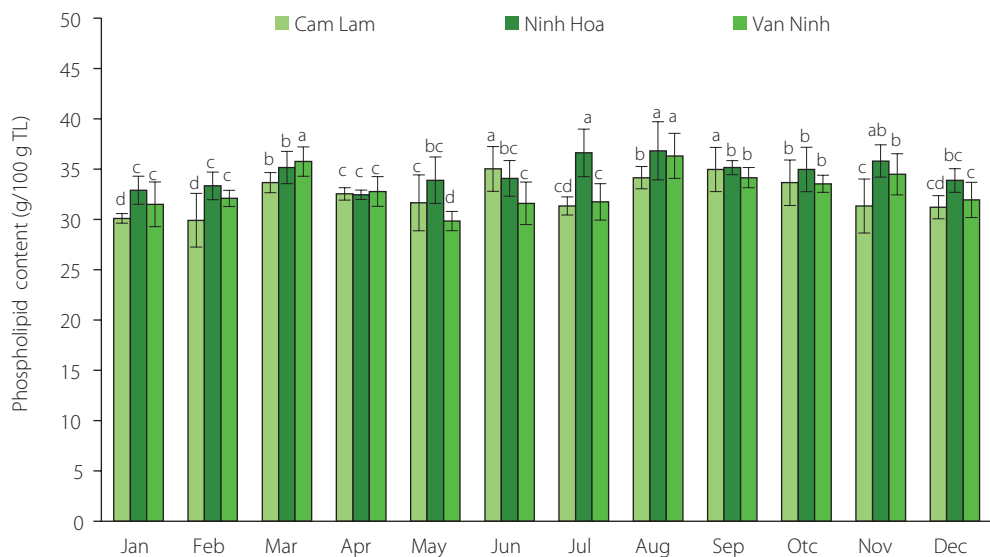


Figure 2. Phospholipid content of *Crassostrea gigas* oysters cultured in Khanh Hoa coast at three locations and harvested in different months. Different letters above bars separately for each farming location indicate significant differences ($p < 0.05$). TL, total lipids.

and the lowest in September (7.8% dry weight). Dagorn *et al.* [2016] reported the maximum total lipid content of the invasive *C. gigas* in April (8.6% dry weight) and the minimum in January (7.1% dry weight). In a study by Asha *et al.* [2014] on *Crassostrea madrasensis*, the average total lipid content on a wet weight basis was 3.25%. In the present study, the range of total lipid content for the *C. gigas* from the three locations was higher than that reported by Martino & Cruz [2004] for mangrove oyster *Crassostrea rhizophorae* (1.5–2.0 g per 100 g of the wet weight) collected at the mangrove of “Barra de Guaratiba” district, Brazil. These differences may be due to the location, environmental conditions, species, and food availability.

■ Phospholipid content

Phospholipids accounted for 29.84–36.82 g/100 g TL recovered from *C. gigas* and their content significantly ($p < 0.05$) varied with

oyster harvest season and farming location (Figure 2). The slightly higher phospholipid content was determined in the oysters from Ninh Hoa when compared to the other two locations (*i.e.*, Cam Lam and Van Ninh). In general, the phospholipid content increased from January to March, started to decrease in April and May, then increased from June and peaked in August. High phospholipid contents in January to March and in August can indicate increased formation of germinal cells (in males) during spermatogenesis. Phospholipid content increases during gonadal maturation as they form part of the structural membrane lipids and as lipovitellins that accumulate oocytes as a reserve for the cellular dividing process following fertilization [De La Parra *et al.*, 2005]. Phospholipid accumulation also increases during the period of maturity preceding spawning. Previous studies have indicated seasonal and locational variation in the phospholipid content of oysters [Dagorn *et al.*, 2016; Liu *et al.*, 2020;

De La Parra *et al.*, 2005; Saito & Marty, 2010]. A study by Dagorn *et al.* [2016] showed seasonal variation in the phospholipid content of *Crassostrea gigas* on the French Atlantic coast with 50.4% and 28.1% phospholipids (% of the total lipid) determined in winter and spring, respectively. Pogoda *et al.* [2013] found that the phospholipid content of the off-shore cultivated *C. gigas* ranged between 39.6–61.8% of the total lipid while that for the species *Ostrea edulis* was in the range of 42.6–55.5% of the total lipids. In a study by Liu *et al.* [2020], the phospholipid content of the oyster *C. talienwhanensis* from the Yellow Sea area was in the range of 11.46–52.12% of the total lipids. The highest phospholipid content in this study from the three areas was lower than the maximum reported in other studies [Dagorn *et al.*, 2016; Liu *et al.*, 2020; Pogoda *et al.*, 2013]. Phospholipids are synthesized and accumulated as a response to low water salinity and freezing temperatures [Fokina *et al.*, 2018]. This might explain the low phospholipid values in this study in comparison to other areas. However, the seasonal variation in the phospholipid content was minimal when compared to that reported in other studies [Dagorn *et al.*, 2016; Liu *et al.*, 2020; Pogoda *et al.*, 2013].

■ Free fatty acid content

The free fatty acid (FFA) content of the lipids recovered from *C. gigas* for the three locations ranged between 5.07 and 6.70 g/100 g TL (Figure 3). At the $p \geq 0.05$, there were no significant differences in the FFA content of the lipids of oysters from the three farming areas across the harvest season. However, the FFA content of oysters from each farming location varied significantly ($p < 0.05$) across the 12 months. The highest FFA content was observed in oysters harvested in April and October which corresponded to the two spawning seasons. Free fatty acids are generated after the degradation of the lipids by enzymes in dead cells [Saito & Marty, 2010]. They also represent an immediate energy source with their content being proportional to the metabolic demand [Viladrich *et al.*, 2016]. Stress conditions like thermal

stress and starvation can increase the FFA content. Increased FFA content has been reported in gorgonians after spawning as a mechanism to overcome reproductive stress [Viladrich *et al.*, 2016]. The increase in FFA content of *C. gigas* recorded in our study in April was probably a way for the oysters to meet the metabolic demands for the spawning period as FFAs were obtained from lipid reserves. It could also be a mechanism to overcome thermal stress as temperatures increase. Several studies have also reported low FFA levels in oysters harvested from different areas. Pogoda *et al.* [2013] reported low levels of free fatty acids in *Ostrea edulis* and *C. gigas* of 0.5–2.8% and 0.4–3.5% of the total lipids, respectively. Similar to this study, the highest values of FFA were recorded in April. FFA content determined for *C. talienwhanensis* from the Yellow Sea area was in the range of 0.65–7.88% of the total lipids [Liu *et al.*, 2020]. Saito & Marty [2010] reported high levels of FFA for the oyster *C. gigas* (2.7–8.1% of the total lipid).

■ Neutral and polar lipid contents

Total lipids recovered from *C. gigas* were fractionated into neutral lipids (38.75–69.68 g/100 g TL) and polar lipids (32.86–61.25 g/100 g TL) using column chromatography (Figure 4). A clear correlation was found – the higher the neutral lipid content, the lower the polar lipid content and *vice-versa*. Neutral lipids constituted a major portion of the lipids in the oysters from the three locations. Their content was higher in the oysters harvested in September (56.19–69.68 g/100 g TL) from the three locations and lower in January (38.75–56.99 g/100 g TL). For oysters farmed in Cam Lam, the content of polar lipids recovered in January and November was higher than that of the neutral lipids. Also, in January, the content of polar lipids recovered from oysters in Van Ninh was higher compared to the neutral lipid content. There was an equal distribution between neutral and polar lipids recovered in May for the oysters farmed in Ninh Hoa and Van Ninh at 50 g/100 g TL. Neutral lipids recovered from

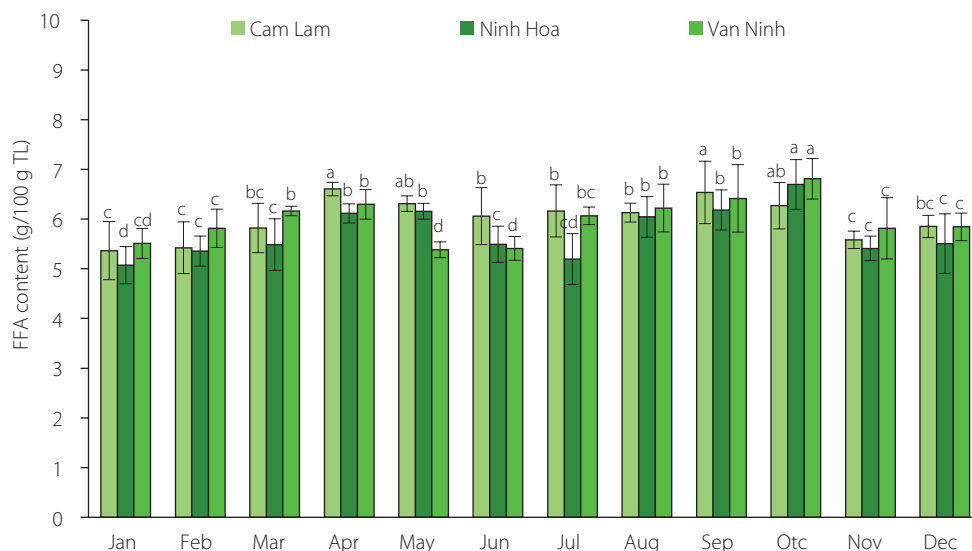


Figure 3. Free fatty acid (FFA) content of *Crassostrea gigas* oysters cultured in Khanh Hoa coast at three locations and harvested in different months. Different letters above bars separately for each farming location indicate significant differences ($p < 0.05$). TL, total lipids.

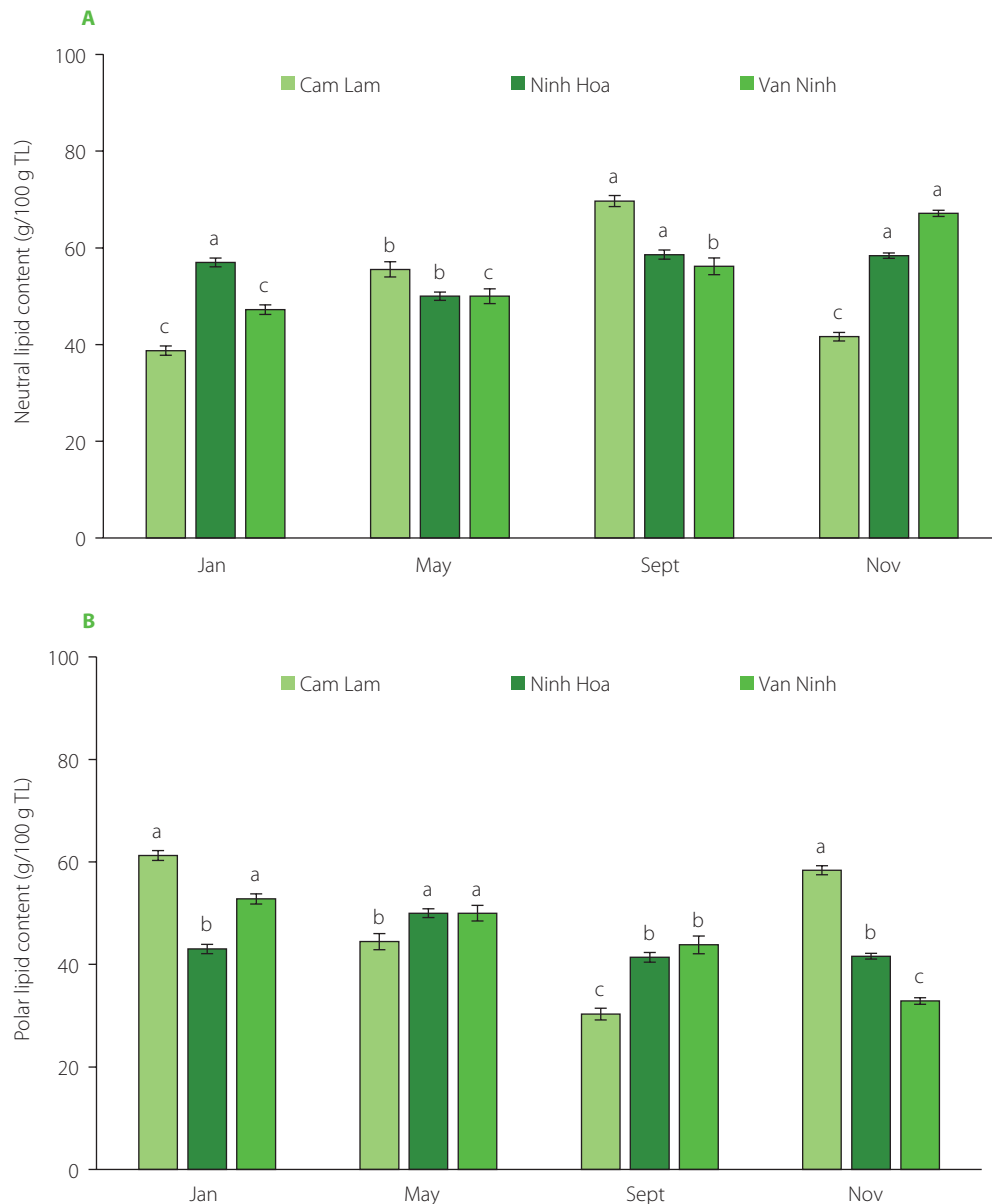


Figure 4. Neutral lipid (A) and polar lipid (B) contents of *Crassostrea gigas* oysters cultured in Khanh Hoa coast at three locations and harvested in different months. Different letters above bars separately for each farming location indicate significant differences ($p < 0.05$). TL, total lipids.

Cam Lam oysters increased from January (38.75 g/100 g TL) to September (69.68 g/100 g TL) and then decreased in November (41.62 g/100 g TL). Polar lipid levels on the other hand decreased from January (61.25 g/100 g TL) to September (30.32 g/100 g TL) and then started to increase again in November (58.38 g/100 g TL). In Ninh Hoa oysters, the percentage of neutral and polar lipids was relatively stable across the four months. Polar lipids are structural components of the membranes, and their content varies little irrespective of the external parameters and nutritional changes [Soudant *et al.*, 1999]. In turn, the neutral lipid content and composition reflect the diet of the oysters and are used as a biomarker in bivalves [Pernet *et al.*, 2006]. The ratio of polar lipids to neutral lipids is an indicator of the nutritional condition of the organism with values ≤ 1 showing good nutritional status [Pogoda *et al.*, 2013]. Triacylglycerols were the main constituent of neutral lipids in *Mytilus* spp. [Fokina *et al.*, 2018], oyster

Crassostrea rhizophorae [Liu *et al.*, 2020], and oyster *Crassostrea gigas* [Saito & Marty, 2010], and it was found that they are part of the principal energy reserves in marine invertebrates. They are accumulated in periods of high food availability and depleted during food scarcity. The relative stability of neutral lipids in oysters harvested in Ninh Hoa, in our study, can be indicative of better food quality and availability at all times. Also, high levels of neutral lipids recovered in November in Van Ninh were probably due to phytoplanktonic blooms during the rainy season. Low levels of neutral lipids in January may suggest low food availability. Increased levels of neutral lipids recorded in May in oysters from the farming areas of Cam Lam and Van Ninh during the spawning season are probably due to the accumulation of lipids and conversion of glycogen into lipids during gametogenesis. In a study on *C. gigas* by Dagorn *et al.* [2016], neutral lipids accounted for 40% in winter (January) and 64.5% in spring

(April). Similar to this study, low levels of neutral lipids were recorded in January. High levels of neutral lipids in this study were consistent with findings from previous studies [Dagorn *et al.*, 2016; Pazos *et al.*, 1996; Pogoda *et al.*, 2013; Saito & Marty, 2010].

■ Fatty acid composition

The contents of fatty acids, total saturated fatty acids (SFAs), monounsaturated fatty acids (MUFAs), and polyunsaturated fatty acids (PUFAs) of muscle lipids of *C. gigas* cultured in the three farming locations are shown in Table 1. Lipids recovered from *C. gigas* were abundant in SFAs (30.89–39.16 g/100 g TL), followed by PUFAs (28.13–35.88 g/100 g TL), and MUFAs (19.32–23.75 g/100 g TL). The main PUFAs were the *n*-3 PUFA with eicosapentaenoic acid (EPA, 20:5*n*3, 9.09–13.77 g/100 g TL) and docosahexaenoic acid (DHA, 22:6*n*3, 6.71–16.47 g/100 g TL) being the dominant fatty acids from the three locations across the harvest season. The major MUFA in oyster muscle was oleic acid (18:1*n*9, 6.96–10.00 g/100 g TL) while the most abundant SFA was palmitic acid (16:0, 21.14–27.27 g/100 g TL). Palmitic acid, EPA, and DHA are major components of phospholipids and are typical of marine animal lipids [Pogoda *et al.*, 2013]. Since EPA and DHA are membrane components, their contents vary slightly throughout the year. Previous studies have also indicated that oyster was abundant in EPA and DHA [Liu *et al.*, 2020; Martino & Cruz, 2004; Saito & Marty, 2010]. EPA levels were slightly higher in this study than these of DHA in general, similar to a study by Pazos *et al.* [1996] in which the contents of EPA in triacylglycerols and phospholipids of *C. gigas* were higher than these of DHA. High EPA levels are a reflection of EPA-rich phytoplankton. EPA has also been shown to have an energetic role [Qin *et al.*, 2021]. The arachidonic acid (C20:4*n*6) is a precursor of prostaglandins which influences reproduction in molluscs [Soudant *et al.*, 1999]. The proportion of *n*-6 fatty acids, especially C20:4*n*6, indirectly shows depletion and accumulation of lipid reserves through an increase or decrease, respectively [Pogoda *et al.*, 2013]. In this study, there was a locational variation in the content of C20:4*n*6 in the profile of oyster fatty acids (Table 1). Lipids recovered from the oysters cultivated in Ninh Hoa had a lower content of this fatty acid compared to the oysters from the other two locations. Low lipid levels in Ninh Hoa oysters can indicate better food availability and quality compared to the other two locations as lipids are accumulated as reserves. The mean PUFAs, SFAs, and MUFAs content of *C. gigas* was not significantly different ($p \geq 0.05$) across the harvest seasons and locations. The order of PUFAs content from the three locations within the year decreased in the following order: January (32.87–35.88 g/100 g TL), November (31.37–33.53 g/100 g TL), September (29.88–32.39 g/100 g TL), and May (28.13–32.91 g/100 g TL). Studies have shown an inverse correlation between temperature and the amount of PUFA in oysters during the different months [Pazos *et al.*, 1996]. The insignificant ($p \geq 0.05$) seasonal variation in the PUFA content of *C. gigas* in our study can be explained by the fact that the water temperature does not vary much throughout the season at three farming locations. Marine bivalves have been indicated to have a special requirement for *n*-3 PUFAs accumulating these rather than *n*-6

[Abad *et al.*, 1995]. This explains the higher levels of *n*-3 PUFAs compared to *n*-6 PUFAs in this study.

In a study by Futagawa *et al.* [2011] on *C. gigas* from two farming areas in Japan, SFAs accounted for 41.0–44.2% of the total lipids while MUFAs and PUFAs accounted for 14.8–22.4% and 35.2–42.2%, respectively. Asha *et al.* [2014] reported that PUFAs constituted the majority of the fatty acid pool in *C. madrasensis* followed by SFAs and lastly MUFAs. Similarly, EPA and DHA were found to be the predominant PUFAs. In a study by Liu *et al.* [2020], PUFAs (39.04–48.77% of total lipids) were the dominant FAs followed by SFAs (26.96–37.09% of total lipids) and MUFAs (19.43–28.85% of total lipids) in *C. talienwhanensis* from the Yellow Sea area. PUFA content in the cited study was higher than that in our study; however, similar to our study, palmitic acid was the most abundant SFA and oleic acid was the dominant MUFA. EPA and DHA were also the most prevalent PUFAs. Pogoda *et al.* [2013] also reported that the FAs of *Ostrea edulis* and *C. gigas* were dominated by palmitic acid (C16:0), EPA, and DHA similar to our study. The fatty acid composition of oysters is influenced by intrinsic (*e.g.*, sex, age, size) and extrinsic factors (*e.g.*, temperature, salinity, and diet) [Martino & Cruz, 2004]. A decrease in temperature leads to increased unsaturation of fatty acids to ensure membrane fluidity. At higher temperatures, an increase in phospholipid content is necessary to counteract excess fluidity, which explains the increased SFAs content in the oyster [Martino & Cruz, 2004].

The *C. gigas* lipid quality, expressed as a thrombogenicity index (TI) and an *n*-3/*n*-6 ratio, varied within the harvest season and farming location (Table 1). The TI order was as follows: September (0.44–0.46), May (0.40–0.44), November (0.38–0.430), and January (0.30–0.42). TI is related to the risk of thrombosis and its high values (>1.0) are considered dangerous to human health [Chakraborty *et al.*, 2016]. The values of TI in this study were less than 1. The second lipid quality parameter, *n*-3/*n*-6 ratio, ranged from 1.45 to 4.55, and lipids recovered from the oysters harvested in Ninh Hoa exhibited its higher values compared to the oysters from the other two farming locations (Table 1). The *n*-3/*n*-6 ratios in our study were slightly higher than those reported by Liu *et al.* [2020] for *C. talienwhanensis*; however, were similar to those published by Martino & Cruz [2004] for mangrove oyster *Crassostrea rhizophorae*. Generally, oysters from tropical areas have been reported to have lower *n*-3/*n*-6 ratios compared to those from temperate areas [Lira *et al.*, 2013]. Linehan *et al.* [1999] found the *n*-3/*n*-6 ratio for *C. gigas* as 5.88 in winter and 4.35 in summer. *n*-3 Fatty acids are important in diets as they play a vital role in body function regulation [Swanson *et al.*, 2012]. However, a high intake of *n*-6 is implicated in the increased incidence of inflammatory diseases as *n*-6 and *n*-3 fatty acids compete for metabolic enzymes [Bhardwaj *et al.*, 2016]. Therefore, the consumption of marine organisms, like oysters, is important as they are rich in *n*-3 fatty acids.

High levels of EPA and DHA, the low TI values, and the high *n*-3/*n*-6 ratios recorded throughout the farming season show the excellent nutritional characteristics of the oysters from Khanh Hoa which could be recommended for human consumption.

Table 1. Fatty acid composition (g/100 g total lipid) and nutritional quality indexes of *Crassostrea gigas* oysters cultured in Khanh Hoa coast at three locations and harvested in different months.

| Fatty acid/ parameter | Cam Lam | | | | | Ninh Hoa | | | | | Van Ninh | | | | | |
|--------------------------|--------------------------|--------------------------|-------------------------|--------------------------|--------------------------|--------------------------|--------------------------|--------------------------|--------------------------|--------------------------|-------------------------|--------------------------|-----|-----|------|-----|
| | Jan | May | Sept | Nov | Jan | May | Sept | Nov | Jan | May | Sept | Nov | Jan | May | Sept | Nov |
| C14:0 | 3.57±0.02 ^b | 3.90±0.03 ^{ab} | 4.27±0.02 ^a | 3.25±0.11 ^{bc} | 2.94±0.06 ^c | 3.13±0.02 ^{bc} | 2.84±0.04 ^c | 2.99±0.06 ^c | 2.80±0.06 ^c | 2.53±0.03 ^d | 3.55±0.06 ^b | 3.92±0.06 ^{ab} | | | | |
| C15:0 | 2.38±0.10 ^b | 0.00±0.00 ^d | 0.00±0.00 ^d | 0.00±0.00 ^d | 1.76±0.00 ^c | 0.00±0.00 ^d | 0.00±0.00 ^d | 1.80±0.00 ^c | 2.80±0.02 ^a | 0.00±0.00 ^d | 0.00±0.00 ^d | 0.00±0.00 ^d | | | | |
| C16:0 | 22.02±0.14 ^c | 22.08±0.21 ^c | 23.17±0.02 ^b | 21.14±0.23 ^c | 22.94±0.15 ^b | 25.63±0.21 ^{ab} | 23.86±0.17 ^b | 24.55±0.26 ^b | 27.27±0.15 ^a | 26.58±0.21 ^{ab} | 23.67±0.23 ^b | 24.02±0.22 ^b | | | | |
| C18:0 | 5.95±0.05 ^{ab} | 5.84±0.11 ^{ab} | 6.10±0.15 ^{ab} | 6.50±0.16 ^{ab} | 5.88±0.09 ^{ab} | 5.63±0.9 ^{bc} | 6.82±0.11 ^a | 5.99±0.06 ^{ab} | 6.29±0.11 ^{ab} | 6.33±0.11 ^{ab} | 6.51±0.11 ^{ab} | 6.86±0.06 ^a | | | | |
| C14:1n9 | 2.98±0.00 ^{ab} | 2.60±0.08 ^b | 2.44±0.07 ^b | 3.25±0.09 ^a | 2.35±0.03 ^b | 2.50±0.01 ^b | 2.27±0.06 ^b | 2.40±0.06 ^b | 3.50±0.06 ^a | 2.53±0.06 ^b | 1.78±0.06 ^c | 2.45±0.04 ^b | | | | |
| C16:1n7 | 2.98±0.01 ^b | 3.25±0.01 ^{ab} | 3.66±0.09 ^{ab} | 2.44±0.10 ^b | 2.35±0.08 ^b | 4.38±0.04 ^a | 2.27±0.06 ^b | 2.99±0.04 ^b | 3.50±0.03 ^{ab} | 3.80±0.05 ^{ab} | 4.14±0.02 ^a | 3.92±0.02 ^{ab} | | | | |
| C17:1n7 | 4.17±0.06 ^{ab} | 4.55±0.06 ^{ab} | 3.66±0.11 ^b | 4.88±0.06 ^a | 3.53±0.01 ^b | 3.75±0.10 ^b | 4.55±0.08 ^{ab} | 4.19±0.01 ^{ab} | 3.50±0.05 ^b | 3.80±0.09 ^b | 4.14±0.04 ^{ab} | 3.43±0.05 ^b | | | | |
| C18:1n9 | 8.33±0.11 ^b | 7.79±0.09 ^{bc} | 7.93±0.12 ^{bc} | 7.32±0.11 ^c | 8.24±0.12 ^b | 10.00±0.14 ^b | 7.39±0.10 ^c | 7.19±0.12 ^c | 9.09±0.06 ^{ab} | 6.96±0.10 ^c | 8.28±0.09 ^b | 8.82±0.09 ^b | | | | |
| C20:1n7 | 3.57±0.07 ^{bc} | 3.25±0.12 ^{bc} | 3.66±0.07 ^{bc} | 5.69±0.08 ^b | 4.12±0.05 ^b | 3.13±0.06 ^{bc} | 2.84±0.07 ^c | 2.99±0.06 ^c | 3.50±0.02 ^{bc} | 2.53±0.06 ^c | 3.55±0.04 ^{bc} | 3.43±0.05 ^{bc} | | | | |
| C18:3n6 | 4.76±0.00 ^b | 5.84±0.17 ^{ab} | 5.49±0.04 ^{ab} | 4.07±0.10 ^c | 4.12±0.06 ^c | 5.63±0.05 ^{ab} | 5.68±0.06 ^{ab} | 5.39±0.07 ^b | 6.29±0.08 ^a | 5.06±0.06 ^b | 5.33±0.01 ^{ab} | 5.88±0.8 ^{ab} | | | | |
| C20:4n6 | 8.33±0.02 ^a | 7.14±0.11 ^b | 6.10±0.14 ^{bc} | 8.13±0.14 ^b | 2.35±0.02 ^e | 2.50±0.06 ^e | 3.98±0.02 ^d | 4.19±0.08 ^d | 4.20±0.01 ^d | 3.80±0.04 ^d | 5.33±0.07 ^c | 5.39±0.07 ^c | | | | |
| C20:5n3 | 11.31±0.12 ^b | 11.04±0.09 ^b | 11.59±0.17 ^b | 9.76±0.12 ^c | 12.94±0.12 ^{ab} | 11.88±0.11 ^b | 9.09±0.09 ^c | 13.77±0.11 ^a | 11.19±0.12 ^b | 10.76±0.10 | 11.83±0.12 ^b | 13.73±0.15 ^a | | | | |
| C22:6n3 | 9.52±0.09 ^c | 7.79±0.15 ^d | 6.71±0.09 ^d | 9.76±0.09 ^c | 16.47±0.16 ^a | 8.13±0.09 ^d | 13.64±0.12 ^b | 10.18±0.12 ^c | 11.19±0.09 ^c | 13.29±0.11 ^b | 7.69±0.09 ^d | 6.86±0.11 ^d | | | | |
| SFA | 33.93±0.14 ^b | 31.82±0.17 ^c | 33.54±0.21 ^b | 30.89±0.22 ^c | 33.53±0.21 ^b | 34.38±0.16 ^b | 33.52±0.19 ^b | 35.33±0.15 ^{ab} | 39.16±0.21 ^a | 35.44±0.20 ^{ab} | 33.73±0.19 ^b | 34.80±0.21 ^b | | | | |
| MUFA | 22.02±0.21 ^{ab} | 21.43±0.24 ^b | 21.34±0.15 ^b | 23.58±0.17 ^a | 20.59±0.19 ^b | 23.75±0.21 ^a | 19.32±0.28 ^{bc} | 19.76±0.17 ^{bc} | 23.08±0.22 ^a | 19.62±0.18 ^{bc} | 21.89±0.21 ^b | 22.06±0.14 ^{ab} | | | | |
| PUFA | 33.93±0.22 ^b | 31.82±0.26 ^{bc} | 29.88±0.31 ^d | 31.71±0.19 ^{bc} | 35.88±0.17 ^a | 28.13±0.16 ^e | 32.39±0.20 ^{bc} | 33.53±0.19 ^b | 32.87±0.19 ^{bc} | 32.91±0.21 ^{bc} | 30.18±0.25 ^d | 31.86±0.24 ^{bc} | | | | |
| Other | 10.12±0.18 ^c | 14.94±0.23 ^a | 15.24±0.11 ^a | 13.82±0.22 ^{ab} | 10.00±0.19 | 13.75±0.16 ^{ab} | 14.77±0.18 ^a | 11.38±0.22 ^b | 4.90±0.16 ^d | 12.03±0.11 ^b | 14.20±0.17 ^a | 11.27±0.21 ^b | | | | |
| n-3/n-6 ratio | 1.59±0.11 ^c | 1.45±0.12 ^c | 1.58±0.08 ^c | 1.60±0.09 ^c | 4.55±0.11 ^a | 2.46±0.10 ^b | 2.35±0.07 ^b | 2.50±0.06 ^b | 2.13±0.12 ^{bc} | 2.71±0.08 ^b | 1.83±0.11 ^c | 1.83±0.11 ^c | | | | |
| TI | 0.39±0.01 ^a | 0.42±0.09 ^a | 0.46±0.11 ^a | 0.40±0.07 ^a | 0.30±0.08 ^b | 0.44±0.10 ^a | 0.39±0.10 ^a | 0.38±0.05 ^a | 0.42±0.08 ^a | 0.40±0.09 ^a | 0.44±0.11 ^a | 0.43±0.10 ^a | | | | |

Results are expressed as mean ± standard deviation (n=3). Means with different lowercase letters in the same row show significant differences (p<0.05). SFA, saturated fatty acids; MUFA, monounsaturated fatty acids; PUFA, polyunsaturated fatty acids; TI, thrombogenicity index.

CONCLUSIONS

The results of this study indicate that both the harvesting season and farming location significantly influenced the lipid profile of muscle of *Crassostrea gigas* cultured in Khanh Hoa province, Vietnam. Oysters harvested from the three farming areas exhibited variations in lipid content, with a higher lipid content determined in the oysters from Ninh Hoa. A decreased lipid content and increased free fatty acid content were found during the two spawning seasons (April and September). Neutral lipids constituted a larger proportion of the total lipids of oysters harvested from the three farming areas. Oysters from Ninh Hoa exhibited lower thrombogenicity index (TI) values and higher $n-3/n-6$ ratios compared to those from Cam Lam and Van Ninh, which indicates their higher nutritional value. Further studies that consider seasonal and locational variations in nutritional components, such as protein, glycogen, mineral content, etc., could be conducted to determine the optimal harvesting time.

ACKNOWLEDGEMENTS

The authors are grateful to the staff and students of the Faculty of Food Technology, Nha Trang University for their kind assistance.

RESEARCH FUNDING

This research is funded by Vietnam National Foundation for Science and Technology Development (NAFOSTED) under Grant Number 106.05-2019.341.

CONFLICT OF INTERESTS

The authors declare that they have no conflict of interest or competing interests.

ORCID IDs

D. Kakooza <https://orcid.org/0000-0002-5953-6286>
 M.V. Nguyen <https://orcid.org/0000-0001-5316-8067>
 A.P.T. Tran <https://orcid.org/0009-0005-7177-6011>
 V.T.T. Tran <https://orcid.org/0009-0006-7094-1756>

REFERENCES

- Abad, M., Ruiz, C., Martinez, D., Mosquera, G., Sánchez, J. (1995). Seasonal variations of lipid classes and fatty acids in flat oyster, *Ostrea edulis*, from San Cibrán (Galicia, Spain). *Comparative Biochemistry and Physiology Part C: Pharmacology, Toxicology and Endocrinology*, 110(2), 109-118. [https://doi.org/10.1016/0742-8413\(95\)00006-A](https://doi.org/10.1016/0742-8413(95)00006-A)
- Anjos, C., Baptista, T., Joaquim, S., Mendes, S., Matias, A.M., Moura, P., Simões, T., Matias, D. (2017). Broodstock conditioning of the Portuguese oyster (*Crassostrea angulata*, Lamarck, 1819): Influence of different diets. *Aquaculture Research*, 48(7), 3859-3878. <https://doi.org/10.1111/are.13213>
- AOCS. (2017). In Official Methods and Recommended Practices of the American Oil Chemists Society, 5th edition. Champaign, IL, USA: AOCS Press.
- Asha, K.K., Anandan, R., Mathew, S., Lakshmanan, P.T. (2014). Biochemical profile of oyster *Crassostrea madrasensis* and its nutritional attributes. *The Egyptian Journal of Aquatic Research*, 40(1), 35-41. <https://doi.org/10.1016/j.ejar.2014.02.001>
- Bernárdez, M., Pastoriza, L., Sampedro, G., Herrera, J.J.R., Cabo, M.L. (2005). Modified method for the analysis of free fatty acids in fish. *Journal of Agricultural and Food Chemistry*, 53(6), 1903-1906. <https://doi.org/10.1021/jf040282c>
- Bhardwaj, K., Verma, N., Trivedi, R.K., Bhardwaj, S., Shukla, N. (2016). Significance of ratio of omega-3 and omega-6 in human health with special reference to flaxseed oil. *International Journal of Biological Chemistry*, 10(1-4), 1-6. <https://doi.org/10.3923/ijbc.2016.1.6>

- Bligh, E.G., Dyer, W.J. (1959). A rapid method of total lipid extraction and purification. *Canadian Journal of Biochemistry and Physiology*, 37(8), 911-917. <https://doi.org/10.1139/o59-099>
- Botta, R., Asche, F., Borsum, J.S., Camp, E.V. (2020). A review of global oyster aquaculture production and consumption. *Marine Policy*, 117, art. no. 103952. <https://doi.org/10.1016/j.marpol.2020.103952>
- Chakraborty, K., Chakkalakal, S.J., Joseph, D., Joy, M. (2016). Nutritional composition of edible oysters (*Crassostrea madrasensis* L.) from the southwest coast of India. *Journal of Aquatic Food Product Technology*, 25(8), 1172-1189. <https://doi.org/10.1080/10498850.2015.1039682>
- Chu, F.L.E., Greaves, J. (1991). Metabolism of palmitic, linoleic, and linolenic acids in adult oysters, *Crassostrea virginica*. *Marine Biology*, 110, 229-236. <https://doi.org/10.1007/BF01313708>
- Dagorn, F., Couzinet-Mossion, A., Kendel, M., Beninger, P.G., Rabesaotra, V., Barnathan, G., Wielgosz-Collin, G. (2016). Exploitable lipids and fatty acids in the invasive oyster *Crassostrea gigas* on the French Atlantic coast. *Marine Drugs*, 14(6), art. no. 104. <https://doi.org/10.3390/md14060104>
- De La Parra, A.M., García, O., San Juan, F.S. (2005). Seasonal variations on the biochemical composition and lipid classes of the gonadal and storage tissues of *Crassostrea gigas* (Thunberg, 1794) in relation to the gametogenic cycle. *Journal of Shellfish Research*, 24(2), 457-467. [https://doi.org/10.2983/0730-8000\(2005\)24\[457:SVOTBC\]2.0.CO;2](https://doi.org/10.2983/0730-8000(2005)24[457:SVOTBC]2.0.CO;2)
- Deranieh, R.M., Joshi, A.S., Greenberg, M.L. (2013). Thin-Layer Chromatography of Phospholipids. In: Rapaport, D., Herrmann, J. (Eds). *Membrane Biogenesis. Methods in Molecular Biology*, Humana Press, Totowa, NJ, 1033, pp. 21-27. https://doi.org/10.1007/978-1-62703-487-6_2
- Dridi, S., Romdhane, M.S., Elcafsi, M. (2007). Seasonal variation in weight and biochemical composition of the Pacific oyster, *Crassostrea gigas* in relation to the gametogenic cycle and environmental conditions of the Bizert Lagoon, Tunisia. *Aquaculture*, 263(1-4), 238-248. <https://doi.org/10.1016/j.aquaculture.2006.10.028>
- FAO. (2022). The State of World Fisheries and Aquaculture 2022. Towards Blue Transformation of the Food and Agriculture Organization of the United Nations. Rome, FAO.
- Fokina, N., Storhaug, E., Bakhmet, I., Maximovich, N., Frantzen, M., Nahrang, J. (2018). Seasonal changes in lipid class content in mussels *Mytilus* spp. from Rakkjorden in the Norwegian Sea and Kandalaksha Bay of the White Sea. *Polar Biology*, 41(10), 2103-2117. <https://doi.org/10.1007/s00300-018-2349-7>
- Futagawa, K., Yoshie-Stark, Y., Ogushi, M. (2011). Monthly variation of biochemical composition of Pacific oysters *Crassostrea gigas* from two main cultivation areas in Japan. *Fisheries Science*, 77(4), 687-696. <https://doi.org/10.1007/s12562-011-0364-5>
- Hurtado, M.A., Racotta, I.S., Arcos, F., Morales-Bojórquez, E., Moal, J., Soudant, P., Palacios, E. (2012). Seasonal variations of biochemical, pigment, fatty acid, and sterol compositions in female *Crassostrea corteziensis* oysters in relation to the reproductive cycle. *Comparative Biochemistry and Physiology Part B: Biochemistry and Molecular Biology*, 163(2), 172-183. <https://doi.org/10.1016/j.cbpb.2012.05.011>
- Kandemir, Ş., Polat, N. (2007). Seasonal variation of total lipid and total fatty acid in muscle and liver of rainbow trout (*Oncorhynchus mykiss* W, 1792) reared in Derbent Dam Lake. *Turkish Journal of Fisheries and Aquatic Sciences*, 7(1), 27-31.
- Lan, N.T., Kovyazin, V.F., Huan, P.T. (2021). Phytoplankton composition of the mangrove ecosystem in Khanh Hoa province, Vietnam. *IOP Conference Series: Earth and Environmental Science*, 876(1), art. no. 012061. <https://doi.org/10.1088/1755-1315/876/1/012061>
- Linehan, L.G., O'Connor, T.P., Burnell, G. (1999). Seasonal variation in the chemical composition and fatty acid profile of Pacific oysters (*Crassostrea gigas*). *Food Chemistry*, 64(2), 211-214. [https://doi.org/10.1016/S0308-8146\(98\)00144-7](https://doi.org/10.1016/S0308-8146(98)00144-7)
- Lira, G.M., Pascoal, J.C.M., Torres, E.A.F.S., Soares, R.A.M., Mendonça, S., Sampaio, G.R., Correia, M.S., Cabral, C.C.V.Q., Cabral Júnior, C.R., López, A.M.Q. (2013). Influence of seasonality on the chemical composition of oysters (*Crassostrea rhizophorae*). *Food Chemistry*, 138(2-3), 786-790. <https://doi.org/10.1016/j.foodchem.2012.11.088>
- Liu, Y.F., Wu, Z.X., Zhang, J., Liu, Y.X., Liu, Z.Y., Xie, H.K., Rakariyatham, K., Zhou, D.Y. (2020). Seasonal variation of lipid profile of oyster *Crassostrea taliwanensis* from the Yellow Sea area. *Journal of Aquatic Food Product Technology*, 29(4), 360-372. <https://doi.org/10.1080/10498850.2020.1737998>
- Martino, R.C., Cruz, G.M.D. (2004). Proximate composition and fatty acid content of the mangrove oyster *Crassostrea rhizophorae* along the year seasons. *Brazilian Archives of Biology and Technology*, 47(6), 955-960. <https://doi.org/10.1590/S1516-89132004000600015>
- Napolitano, G.E., Ackman, R.G. (1992). Anatomical distributions and temporal variations of lipid classes in sea scallops *Placopecten magellanicus* (gmelin) from Georges Bank (Nova Scotia). *Comparative Biochemistry and Physiology Part B: Comparative Biochemistry*, 103(3), 645-650. [https://doi.org/10.1016/0305-0491\(92\)90384-4](https://doi.org/10.1016/0305-0491(92)90384-4)

26. Pazos, A.J., Ruiz, C., García-Martin, O., Abad, M., Sánchez, J. (1996). Seasonal variations of the lipid content and fatty acid composition of *Crassostrea gigas* cultured in E1 Grove, Galicia, NW Spain. *Comparative Biochemistry and Physiology Part B: Biochemistry and Molecular Biology*, 114(2), 171-179. [https://doi.org/10.1016/0305-0491\(96\)00017-X](https://doi.org/10.1016/0305-0491(96)00017-X)
27. Pernet, F., Pelletier, C.J., Milley, J. (2006). Comparison of three solid-phase extraction methods for fatty acid analysis of lipid fractions in tissues of marine bivalves. *Journal of Chromatography A*, 1137(2), 127-137. <https://doi.org/10.1016/j.chroma.2006.10.059>
28. Pogoda, B., Buck, B.H., Saborowski, R., Hagen, W. (2013). Biochemical and elemental composition of the offshore-cultivated oysters *Ostrea edulis* and *Crassostrea gigas*. *Aquaculture*, 400-401, 53-60. <https://doi.org/10.1016/j.aquaculture.2013.02.031>
29. Qin, Y., Li, X., Li, J., Zhou, Y., Xiang, Z., Ma, H., Noor, Z., Mo, R., Zhang, Y., Yu, Z. (2021). Seasonal variations in biochemical composition and nutritional quality of *Crassostrea hongkongensis*, in relation to the gametogenic cycle. *Food Chemistry*, 356, art. no. 129736. <https://doi.org/10.1016/j.foodchem.2021.129736>
30. Rato, A., Pereira, L.F., Joaquim, S., Gomes, R., Afonso, C., Cardoso, C., Machado, J., Gonçalves, J.F.M., Vaz-Pires, P., Magnoni, L.J., Matias, A.M., Matias, D., Bandarra, N.M., Ozório, R.O.A. (2019). Fatty acid profile of pacific oyster, *Crassostrea gigas*, fed different ratios of dietary seaweed and microalgae during broodstock conditioning. *Lipids*, 54(9), 531-542. <https://doi.org/10.1002/lipid.12177>
31. Saito, H., Marty, Y. (2010). High levels of icosapentaenoic acid in the lipids of oyster *Crassostrea gigas* ranging over both Japan and France. *Journal of Oleo Science*, 59(6), 281-292. <https://doi.org/10.5650/jos.59.281>
32. Soudant, P., Van Ryckeghem, K., Marty, Y., Moal, J., Samain, J.F., Sorgeloos, P. (1999). Comparison of the lipid class and fatty acid composition between a reproductive cycle in nature and a standard hatchery conditioning of the Pacific Oyster *Crassostrea gigas*. *Comparative Biochemistry and Physiology Part B: Biochemistry and Molecular Biology*, 123(2), 209-222. [https://doi.org/10.1016/S0305-0491\(99\)00063-2](https://doi.org/10.1016/S0305-0491(99)00063-2)
33. Stewart, J.C.M. (1980). Colorimetric determination of phospholipids with ammonium ferrioxalate. *Analytical Biochemistry*, 104(1), 10-14. [https://doi.org/10.1016/0003-2697\(80\)90269-9](https://doi.org/10.1016/0003-2697(80)90269-9)
34. Su, X.Q., Antonas, K., Li, D., Nichols, P. (2006). Seasonal variations of total lipid and fatty acid contents in the muscle of two Australian farmed abalone species. *Journal of Food Lipids*, 13(4), 411-423. <https://doi.org/10.1111/j.1745-4522.2006.00063.x>
35. Swanson, D., Block, R., Mousa, S.A. (2012). Omega-3 fatty acids EPA and DHA: health benefits throughout life. *Advances in Nutrition*, 3(1), 1-7. <https://doi.org/10.3945/an.111.000893>
36. Truong, T., Nguyen, C., Lam, N.N., Jensen, K. (2014). Seasonal and spatial distribution of mesozooplankton in a tropical estuary, Nha Phu, South Central Viet Nam. *Biologia*, 69(1), 80-91. <https://doi.org/10.2478/s11756-013-0289-9>
37. Tung, N.T., Son, T.P.H. (2019). GIS-based multi-criteria evaluation models for selection of suitable sites for Pacific oyster (*Crassostrea gigas*) aquaculture in the central region of Vietnam. *Journal of Environmental Science and Engineering A*, 8, 141-158. <https://doi.org/10.17265/2162-5298/2019.04.002>
38. Ugalde, S.C., Vu, S.V., Giang, C.T., Ngoc, N.T.H., Tran, T.K.A., Mullen, J.D., Vu, V.I., O'Connor, W. (2023). Status, supply chain, challenges, and opportunities to advance oyster aquaculture in northern Vietnam. *Aquaculture*, 572, art. no. 739548. <https://doi.org/10.1016/j.aquaculture.2023.739548>
39. Ulbricht, T.L.V., Southgate, D.A.T. (1991). Coronary heart disease: seven dietary factors. *The Lancet*, 338(8773), 985-992. [https://doi.org/10.1016/0140-6736\(91\)91846-M](https://doi.org/10.1016/0140-6736(91)91846-M)
40. Viladrich, N., Bramanti, L., Tsounis, G., Chocarro, B., Martínez-Quitana, A., Ambroso, S., Madurell, T., Rossi, S. (2016). Variation in lipid and free fatty acid content during spawning in two temperate octocorals with different reproductive strategies: surface versus internal brooder. *Coral Reefs*, 35, 1033-1045. <https://doi.org/10.1007/s00338-016-1440-1>

Effects of Stewing Modes on Physicochemical Quality and Formation of Flavour Compounds of Chinese Dagu Chicken Soup

Haining Guan^{1,2*} , Xiaojun Xu¹ , Chunmei Feng¹ , Yanli Tian¹ , Dengyong Liu¹ , Xiaoqin Diao¹ 

¹College of Food Science and Technology, Bohai University, Jinzhou, 121013, China
²Cuisine Science Key Laboratory of Sichuan Province, Sichuan Tourism University, Chengdu, 610100, China

This study aimed to evaluate the influences of stewing modes, including high fire short time (HFST, 100°C/1 h), medium-high fire mid-length time (MFMT, 98°C/2 h), medium fire long time (MFLT, 90°C/3 h), and low fire ultra-length time (LFUT, 83°C/4 h) processing, on physicochemical parameters and flavour compound profile of Chinese Dagu chicken soup. The chicken soup prepared under the stewing mode of MFMT had smaller particle size ($d_{3,2}$ of 2.56 μm and $d_{4,3}$ of 1.73 μm), higher zeta potential (8.66 mV), and viscosity than the soups stewed under the other conditions. The umami-taste compounds, such as inosine 5'-monophosphate, and umami free amino acid were the most abundant in the soup stewed by MFMT (53.47 and 59.91 mg/100 mL, respectively). GC-MS results showed that the volatile compounds were mainly hexanal, octanal, heptanal, (*E,E*)-2,4-decadienal, nonanal, and 1-octen-3-ol. Additionally, the results of measurements made with the electronic nose and electronic tongue indicated that the overall flavour of the four chicken soups varied significantly. In general, considering the stability and umami taste of chicken soup, as well as the time-saving need, it is recommended to use the MFMT mode to prepare the chicken soup.

Key words: chicken soup, stewing modes, physicochemical quality, taste components, volatile compounds

INTRODUCTION

Chicken meat is loved food by people all over the world due to its delicate taste and a high nutritional value. It contains essential nutrients, especially proteins with a well-balanced amino acid composition, free amino acids, peptides, and essential trace elements [Ali *et al.*, 2019]. Chicken can be cooked in many ways, but chicken soup is usually an important part of an everyday diet of the Chinese people. While the chicken is cooked, some water-soluble components such as proteins, carbohydrates, vitamins, minerals, oligopeptides, and amino acids will be dissolved into chicken soup and their content in soup will increase with the prolongation of heating time [Meng *et al.*, 2022; Zhang

et al., 2021]. These compounds are dietary nutrients, but some of them also have biological activity. Small molecules of chicken soup, such as carnosine, anserine and taurine, can cause central nervous system excitement, improve antioxidant and immune capacity, increase appetite, and promote digestion [Xiao *et al.*, 2021]. After cooking chicken soup for a long time, native structures of nutrients, such as proteins and carbohydrates, are destroyed and become more easily digestible and absorbable by the human body.

The flavour and texture are important factors affecting consumers' acceptance and preference for soups. The flavour in chicken soup is developed by the thermal reaction of carbohydrates,

*Corresponding Author:

e-mail: hai.ning2001@163.com (H. Guan)

Submitted: 1 September 2023

Accepted: 10 January 2024

Published on-line: 8 February 2024



© Copyright by Institute of Animal Reproduction and Food Research of the Polish Academy of Sciences
© 2024 Author(s). This is an open access article licensed under the Creative Commons Attribution-NonCommercial-NoDerivs License (<http://creativecommons.org/licenses/by-nc-nd/4.0/>).

proteins and lipids in the cooking process, mainly including the Maillard reaction, lipid oxidation, and the interaction between the reaction products [Qi *et al.*, 2023; Zhang *et al.*, 2018]. During this process, flavour precursors, such as water-soluble components and lipids, are dissolved, released, and interact to form volatile and non-volatile compounds [Dashdorj *et al.*, 2015]. Research has shown that stewing conditions, such as time, heating temperature, and heating rate, affect a soup's flavour profile during cooking. Therefore, in recent years, several researches published have focused on the influences of cooking conditions on the flavour components and nutrients in soups [Pérez-Palacios *et al.*, 2017; Zou *et al.*, 2021]. Qi *et al.* [2018] studied the effect of stewing time on taste activity and volatile compound levels in chicken soup. The results have shown that increasing cooking time reduces the content of taste components but increases the aroma level. Our previous study also found that after cooking for 4 h, the changes of flavour components in chicken soups tended to stabilise [Guan *et al.*, 2023]. Zhang *et al.* [2013] investigated the influence of stewing temperature on protein hydrolysates and sensory properties of crucian carp soup and found that the soup made at 85°C had excellent sensory qualities in colour, flavour, and nutritional value. Rotola-Pukkila *et al.* [2015] reported that the heating temperature had a more significant influence on the extraction and release of umami compounds in pork soup than the cooking time. In addition to flavour, texture of the soup is also an essential factor of its quality assessment.

However, the literature available has limited information on the rheological properties and flavour compound formation in soups obtained by different "Huohou" modes. "Huohou" is the most critical technical term in traditional Chinese cooking, originally meaning temperature and duration of heating required for dishes from raw to cooked, and is a key factor affecting cooking results. Chotechuang *et al.* [2018] reported that different combinations of boiling temperature and time can affect chicken bone stock quality. This work aimed to evaluate the influences of different "Huohou" modes on the rheological properties and formation of flavour compounds of Dagu chicken soup. Analyses of the zeta potential, particle size, viscosity, 5'-nucleotide content, and the profiles of amino acids, fatty acids, and volatile compounds in four samples, enabled determining the effect of stewing modes on the physicochemical quality and flavour compound formation of the chicken soup. In this study, based on the traditional experience of making soup in China and our pre-experimental findings, we used four different "Huohou" modes commonly used to stew Chinese Dagu chicken soup, namely, the high fire short time (HFST, 100°C, 1 h), the medium-high fire mid-length time (MFMT, 98°C, 2 h), the medium fire long time (MFLT, 90°C, 3 h), and the low fire ultra-length time (LFUT, 83°C, 4 h).

MATERIALS AND METHODS

Materials and chemicals

The freshly slaughtered Chinese Dagu chickens were provided by Dagu Chicken Breeding Farm Co., Ltd. (Zhuanghe, China). The chicken carcasses were placed in polyethylene bags

and transported to the laboratory on ice. Reference standards of amino acids, inosine 5'-monophosphate (5'-IMP), adenosine 5'-monophosphate (5'-AMP), guanosine 5'-monophosphate (5'-GMP), *n*-alkanes (C7 to C30), and cyclohexanone were obtained from Sigma-Aldrich Co., Ltd. (Shanghai, China). Additionally, sulphuric acid, 4-dimethylaminobenzaldehyde, chloramine T, chloroform, methanol, and sodium chloride were purchased from China National Medicines Co., Ltd. (Beijing, China). All other chemicals used were of analytical grade.

Sample preparation

Each half of the chicken carcass (approximately 800 g) was cut into evenly sized pieces that were put into a high-temperature cooking bag (nylon/polypropylene, moisture-proof, resistant to high temperature, and shock-resistant). Next, clearwater twice the weight of the chicken was added, and the bags were sealed under vacuum [Qi *et al.*, 2017]. The sealed samples were divided into four groups based on different "Huohou" modes, each was placed in an electrical stewpot with different powers, and the same volume of water was added to the pot. The first group was prepared using the stewing model of high fire short time (HFST): heated from room temperature (approximately 23°C) to boiling temperature (100±0.15°C) by an electrical stewpot with a constant power of 1,300 W, then kept at the constant temperature for 1 h. The second group was prepared using the stewing model of medium-high fire mid-length time (MFMT): heated from room temperature to 98±0.15°C by an electrical stewpot with a constant power of 800 W, then kept at the constant temperature for 2 h. The third group was prepared using the stewing model of medium fire long time (MFLT): heated from room temperature to 90±0.16°C by an electrical stewpot with a constant power of 500 W, then kept at the constant temperature for 3 h. The fourth group was prepared using the model of low fire ultra-length time (LFUT): heated from room temperature to microboiling temperature (83±0.16°C) by an electrical stewpot with a constant power of 300 W, then kept at the constant temperature for 4 h. After stewing, the liquid was filtered to remove chicken solids, and the chicken soup was ready.

Total solid and collagen content determination

The content of total solids was determined according to Guan *et al.* [2023]. The solid content was expressed as g/100 mL of soup. The collagen content of the samples was measured as reported by Barido & Lee [2021]. The sample (4 g) was hydrolysed with 30 mL of 3 M sulphuric acid and diluted to a final volume of 250 mL with distilled water. The 4 mL of hydrolysate solution was mixed with 2 mL of 4-dimethylaminobenzaldehyde solution (10%, w/v,) and 2 mL of chloramine T solution (7%, w/v,) in a test tube. The mixtures were heated at 60°C for 20 min, and then cooled at room temperature for 20 min. The absorbance was measured at 558 nm using a spectrophotometer (UV-2550, Shimadzu Co., Kyoto, Japan). The collagen content was calculated by multiplying the hydroxyproline content and 11.1 (the coefficient of hydrolysis of collagen to hydroxyproline), and the result was

expressed as mg/mL soup. The content of hydroxyproline was determined according to the standard curve.

■ Zeta potential and particle size estimation

The zeta potential and particle size of the four samples were evaluated using a Zetasizer Nano ZS-90 analyzer (Malvern Instruments Ltd., Malvern, UK). The volume-weighted mean diameters ($d_{4,3}$) and surface-weighted mean diameters ($d_{3,2}$) were recorded.

■ Rheological behaviour measurements

Rheological measurements were carried out according to the method previously used by Zhu *et al.* [2020]. A rotary rheometer (Discovery HR-1, TA Instruments, New Castle, DE, USA) was used to measure the static and dynamic rheological properties. To this end, 1 mL of the chicken soup was placed on the parallel plate under the rheometer, and the upper parallel plate with a diameter of 40 mm was lowered slowly. The distance between the two parallel plates was 1 mm, and the excess liquid flowing out of the plate was erased. The sample was balanced for 2 min before measurements. Static rheology was used to record the variation of viscosity of the soup with a shear rate (0.1–1000 1/s) at 25°C and test interval of 1,000 μ m. The dynamic rheology was measured in the linear viscoelastic region, and the oscillating stress was fixed. The relationship between shear rate, viscosity, and shear stress was analysed. The correlation between the shear rate and shear stress was determined using Equation (1):

$$\tau = K\dot{\gamma}^n \quad (1)$$

where: τ (Pa) is shear stress, $\dot{\gamma}$ (1/s) is shear rate, K (Pa·sⁿ) is consistency coefficient, and n represents flow index.

■ Free amino acid analysis

Free amino acids (FAAs) were determined according to the method described by Qi *et al.* [2017] with some modifications. Chicken soup (2 mL) was mixed with 3% (*w/v*) sulfosalicylic acid (4 mL), and the mixture was centrifuged at 4°C for 15 min (14,000×*g*). Then, 2 mL of *n*-hexane was mixed with the supernatant and left to stand for 15 min and 2 mL of the aqueous phase was filtered using a 0.22 μ m membrane. The FAAs were analysed in filtrate using an automatic amino acid analyzer (L-8900, Hitachi, Tokyo, Japan). The post-column derivatization was carried out with ninhydrin at 135°C. Each FAA was identified by comparing its retention time with a standard amino acid and quantified using an external standard method. The content of FAAs was expressed as mg/100 mL soup. Taste activity values (TAVs) were calculated as the ratio of the content of an individual amino acid in the chicken soup to its taste threshold value obtained from the reported literature [Meng *et al.*, 2022].

■ 5'-Nucleotide analysis

5'-Nucleotides were determined as described by Qi *et al.* [2021] using a high-performance liquid chromatography (HPLC) system (E2695, Waters Ltd., Milford, CT, USA) equipped with an X Bridge

C18 (5 μ m, 4.6×250 mm). Chicken soup (10 mL) was mixed with perchloric acid (30 mL, 5% *w/v*), then the mixture was centrifuged at 4°C for 15 min (10,000×*g*). The supernatant was adjusted to pH 4.5 with 1 M sodium hydroxide solution, diluted to 100 mL, and filtered through a 0.22 μ m membrane prior to the HPLC analysis. The chromatographic separation was carried out using eluent A (0.05 M KH_2PO_4 , pH 5.4) and eluent B (methanol) in a gradient system (98% A for 14 min, 85% A for 7 min, and 98% A for 9 min) with a flow rate of 1.0 mL/min. UV detector wavelength was 254 nm. The 5'-GMP, 5'-IMP, and 5'-AMP were quantified by comparing the peak area of the nucleotide with that of the external standard, and the results were expressed as g/100 mL of the soup. TAVs were calculated as the ratio of the content of an individual nucleotide in the chicken soup to its taste threshold value obtained from the reported literature [Qi *et al.*, 2017].

■ Determination of fatty acid composition

The total lipids were extracted using the method of Folch *et al.* [1957]. Chicken soup (20 mL) was mixed with 400 mL of a chloroform-methanol solution (2:1, *v/v*), and then filtered after vortexing for 10 s. A saturated sodium chloride solution was mixed with the filtrate and placed for 3 h at 4°C. The chloroform from the lower phase was removed through a rotary evaporator at 45°C, whereas the remaining material was the total lipids.

According to the procedure previously described by Diao *et al.* [2017], with some modification, the lipids were converted to fatty acid methyl esters. Briefly, 50 mg of lipids were dissolved with *n*-hexane (2 mL) and a sodium methoxide reagent (2 M, 0.4 mL) was mixed, then saturated sodium chloride (3 mL) was added. After shaking for 15 s, the mixture was left for 10 min, and the supernatant (1 μ L) filtrated through a 0.22 μ m filter membrane was injected into the 7890-5975 gas chromatography-mass spectrometry (GC-MS) system (Agilent Co., Ltd., Santa Clara, CA, USA) equipped with an Agilent INNOWAX capillary column (30 m × 0.32 mm × 0.25 μ m, Thermo Fisher, Waltham, MA, USA). The injection temperature and detector temperature were 250°C and 230°C, respectively. Helium was used as a carrier gas with a flow rate of 1 mL/min. Oven temperature program was as follows: 140°C (2 min) – 200°C (6°C/min, 2 min) – 230°C (2°C/min, 2 min) – 250°C (4°C/min, 2 min). The fatty acids were matched with the National Institute of Standards and Technology (NIST) 147 library spectra, and those with similarity greater than 90% were selected as identification results. Peak area normalisation method was used for quantitative analysis [Petenuci *et al.*, 2019], and the relative content of individual fatty acids was expressed as g per 100 g of total fatty acids.

■ Volatile compound analysis

The volatile compounds in chicken soups were determined as described by Guan *et al.* [2023] by means of the head space-solid phase microextraction-gas chromatography-mass spectrometry (HP-SPME-GC-MS) method. To this end, 5 g of the chicken soup and 2 μ L of cyclohexanone (1.11 μ g/ μ L) were put into a headspace bottle and SPME fibre (75 μ m CAR/PDMS, Supelco, Bellefonte, PA, USA) was used to collect the flavour compounds

from different samples at 50°C for 30 min. Subsequently, the fibre was inserted into the GC injector port and desorbed at 250°C for 5 min. The GC oven temperature program was as follows: initial temperature 40°C (3 min) – 70°C (3°C/min) – 180°C (5°C/min) – 280°C (10°C/min, 5min). The carrier gas – helium – was used with a constant flow rate of 1 mL/min. The retention time of each compound was converted into a linear retention index (LRI) using *n*-alkanes as a reference. The volatile compounds were identified by comparing LRI values with those reported in the literature [Qi *et al.*, 2017] and the data listed in authentic online databases [http://www.flavornet.org, http://www.odour.org.uk]. The quantification of each volatile compound was carried out by comparing its peak area with that of the internal standard (cyclohexanone), and the content was expressed ng/g of the soup.

The odour activity values (OAVs) of volatile compounds were expressed as the ratio between the concentration of a volatile compound and its threshold value reported in the aqueous phase [Qi *et al.*, 2017]. A compound with an OAV greater than or equal to 1 was considered to be an aroma contributor [Bi *et al.*, 2021].

■ Analysis using electronic tongue and electronic nose

The taste of the samples was measured using an electronic tongue (SA402B e-tongue, Insent, Atsugi, Japan), which had six lipid membrane sensors. To enable the analysis, 35 mL of the chicken soup sample from each group were transferred into a special sample cup and then placed on the automatic sampler of the electronic tongue according to the set sequence. The single sampling time was 120 s, once *per* second. Each group of samples was repeatedly tested 4 times. The taste characteristics of the last three times of data collection were analysed. The response values of the e-tongue were recorded and analysed using principal component analysis (PCA).

The volatile compounds in the chicken soup were analysed by the electronic nose (PEN3 e-nose, Airsense Analytics, Schwerin, Germany) equipped with ten different gas sensors

(Table 1) [Zhang J.X. *et al.*, 2022]. The e-nose sensor was pre-heated and calibrated before the test. After a stable sensor response signal, the sample (10 mL) was placed into a precision-threaded vial (20 mL). After 30 min-enrichment at room temperature, the volatile chemicals in the sample bottle reached saturation. The test was repeated five times, and the last three response values were used as valid data. The response values of the e-nose were analysed using PCA.

■ Sensory evaluation

Chicken soups were tested for sensory characteristics by 10 panelists (5 women and 5 men, aged between 22 and 25) from the Bohai University, Jinzhou, China. The panelists with sensory evaluation experience were recruited and trained in recognizing and describing the intensity ratings of standard references, and three sensory attributes (umami, bitterness and aroma) were used for sensory evaluation. Based on the reported literature [Liang *et al.*, 2022; Qi *et al.*, 2021] with some modifications, the reference materials were 0.15% monosodium glutamate (umami), 0.08% quinine (bitterness), and 100 g of Chinese Dagu chicken leg meat stewed in 200 g of water at 98°C for 2 h (aroma). The training sessions were carried out 4 times for 2 h each time before the sensory analysis. The samples were maintained between 55 and 60°C in a water bath during testing and were randomly named. The panelists assessed the umami, bitterness and aroma of each sample, based on 6-point intensity scales (1–2, weaker; 2–3, weak; 3–4, middle; 4–5, strong; and 5–6, stronger). Panelists rinsed their mouths with drinking water (50 mL) between assessments to eliminate the effects of fatigue and carryover. All panelists scored separately without interference with each other, and the average value was taken as the result.

■ Statistical analysis

All data was presented as the means ± standard deviations (SD) of three independent replicates. The results were analysed by one-way analysis of variance using SPSS 19.0 (IBM, Armonk, NY, USA), followed by Duncan's multiple range test with a significance level of $p < 0.05$. The data from the e-nose and e-tongue were analysed through Origin Pro 2021 software (OriginLab Corporation, Northampton, MA, USA).

RESULTS AND DISCUSSION

■ Solid content and collagen content

The solid content in broths is one of the main indexes used to assess their quality, and it also reflects the overall dissolution effect of nutrients (such as protein, fat, amino acid, *etc.*) during the cooking process of raw materials. The effects of different stewing modes on the solid content of chicken soup are shown in Table 2. The solid content of the chicken soup prepared under different stewing modes was significantly different, and the solid content of the chicken soup stewed by MFLT (90°C, 3 h) was the highest. This may be due to the fact that the solid substance released in the soup mainly come from soluble matter, such as collagen, minerals, glycogen, vitamins, *etc.*, which can rapidly dissolve from chicken's tissues with the extension of stewing

Table 1. Performance of the sensor arrays of the e-nose.

| Sensor number | Sensor name | Sensor sensitivity and general description |
|---------------|-------------|-----------------------------------------------------------------------|
| 1 | W1C | Aromatic compounds |
| 2 | W5S | Very sensitive, broad range of sensitivity, reacts to nitrogen oxides |
| 3 | W3C | Ammonia, sensitive to aromatic ingredients |
| 4 | W6S | Mainly hydrogen |
| 5 | W5C | Short-chain alkane aromatic ingredients |
| 6 | W1S | Sensitive to methane |
| 7 | W1W | Reacts to sulphur compounds, H ₂ S |
| 8 | W2S | Detects alcohol, partially aromatic compounds |
| 9 | W2W | Aromatic compounds, sulphur organic compounds |
| 10 | W3S | Alkanes, especially methane |

time at the higher temperature. Subsequently, insoluble large molecules could be released from the deeper tissues, as was shown in a previous study during tuna head soup preparation [Qian *et al.*, 2019]. However, the chicken soup stewing by LFUT took a long time, and the solid content was lower. This is most likely due to the slow dissolution rate of solids in the meat under the lower stewing temperature. Rotola-Pukkila *et al.* [2015] noted that the cooking temperature played a more significant role than the cooking time in analysing the content of umami compounds in pork meat juice.

Collagen in a denatured state is easy to agglutinate into a gel, thus affecting the viscosity of the soup. Collagen in the hot dissolved state will also make the soup more mellow. The content and dissolution of collagen in chicken soup are related to the stewing temperature and time. Different stewing modes had a significant effect on the collagen content of the chicken soup (Table 2). The highest ($p < 0.05$) collagen content, reaching 5.60 mg/mL, was determined in the chicken soup obtained using the MFLT technology. It might be because medium fire stewing for 3 h was more conducive to collagen dissolution.

■ Particle size and zeta potential

The $d_{4,3}$ and $d_{3,2}$ of particles of each chicken soup prepared under different stewing modes are presented in Table 2. The results showed that, compared with HFST, MFLT, and LFUT soups, the $d_{4,3}$ and $d_{3,2}$ of the particles of the soup prepared using the MFMT technology were smaller. It indicated that the MFMT technology could promote the migration of more components from meat to the soup and the formation of a stable emulsion under the effect of continuous high temperature processing, thus decreasing the particle size [Guan *et al.*, 2023]. Therefore, it was inferred that the stewing modes and dissolving ingredients had strong influences on the particle size in the chicken soup. Also, Diao *et al.* [2016] reported that the increase of $d_{4,3}$ and $d_{3,2}$ was due to the formation of larger droplet-coalesced aggregates by those individual droplets, which greatly reduced the emulsification effect.

The zeta potential of four kinds of soups is depicted in Table 2. The absolute value of zeta potential of the soup stewed by MFMT was the highest (8.66 mV). A high zeta potential (absolute value) reflects higher stability of the soup. The zeta potential affects the repulsive force between particles. Qiu *et al.* [2015] demonstrated that the low zeta potential of emulsion droplets

decreased electrostatic repulsion between neighbouring protein-coated droplets, leading to droplet polymerization. Moriyama *et al.* [2003] also showed that the larger the zeta potential, the smaller particles in the emulsion. In this research, the high zeta potential of chicken soup stewed by MFMT contributed to the small particle sizes.

■ Viscosity

Qi *et al.* [2023] noted that the viscosity was an important indicator of emulsion stability. Furthermore, Zhang M. *et al.* [2022] pointed out the increase of viscosity contributes to the physical stability of emulsions, which may be due to the lower mobility reducing the chance of particle collision. As noted in Figure 1A, with the increase in shear rate, the viscosity of chicken soup rapidly decreased and gradually stabilized, indicating that the chicken soup had the property of shear-thinning and pseudoelasticity. With the increase in shear rate, the water environment around the substances in soups was destroyed, and the interaction force was weakened, which changed the viscosity of the chicken soup and caused shear thinning. At the same shear rate, the viscosity of the chicken soup stewed by MFMT was significantly higher than that of the other soups. This may be because the chicken soup obtained by MFMT technology had a small particle size. Similar results have been noted by Costa *et al.* [2019], who demonstrated that the smaller the particle size in yogurt, the better its dispersion and the higher its viscosity value. Coutinho *et al.* [2019] also reported that the particle size greatly influenced the viscosity of chicken soup. Figure 1B shows that the shear stress of four chicken soups prepared under different stewing modes increased with the increase in shear rate. The non-linear relationship between shear stress and shear rate indicated that the four soups were non-Newtonian fluids. Furthermore, the yield stress occurred in the four samples, and the shear stress of the soup stewed by HFST was lower compared to the other soups. One possible explanation was that the interaction of particles in the chicken soup obtained by the HFST technology formed a weak network structure, and small yield stress was required to destroy the structure [Huang *et al.*, 2020].

■ Free amino acid composition

FAAs, as indispensable precursor substances for producing meat flavour, play an important role in the modulation of chicken soup palatability. It has been reported that the enhancement

Table 2. Solid content, collagen content, particle size, and zeta potential of the chicken soups prepared with different stewing modes.

| Sample | Solid content (g/100 mL) | Collagen content (mg/mL) | Particle size | | Zeta potential (mV) |
|--------|--------------------------|--------------------------|-----------------------------|-----------------------------|-------------------------|
| | | | $d_{3,2}$ (μm) | $d_{4,3}$ (μm) | |
| HFST | 1.76±0.02 ^d | 2.80±0.04 ^c | 3.85±0.07 ^a | 2.13±0.03 ^b | -5.84±0.12 ^b |
| MFMT | 2.13±0.02 ^b | 4.96±0.06 ^b | 2.56±0.10 ^d | 1.73±0.05 ^d | -8.66±0.35 ^c |
| MFLT | 2.28±0.03 ^a | 5.60±0.06 ^a | 3.63±0.03 ^b | 1.89±0.03 ^c | -5.26±0.10 ^a |
| LFUT | 1.93±0.04 ^c | 5.06±0.02 ^b | 2.98±0.10 ^c | 2.42±0.02 ^a | -5.79±0.04 ^b |

Data are expressed as mean ± standard deviation ($n=3$). Different lowercase letters (a-d) in the same column indicate significant differences ($p < 0.05$). HFST, high fire short time; MFMT, medium-high fire mid-length time; MFLT, medium fire long time; LFUT, low fire ultra-length time; $d_{3,2}$, surface-weighted mean diameter; $d_{4,3}$, volume-weighted mean diameter.

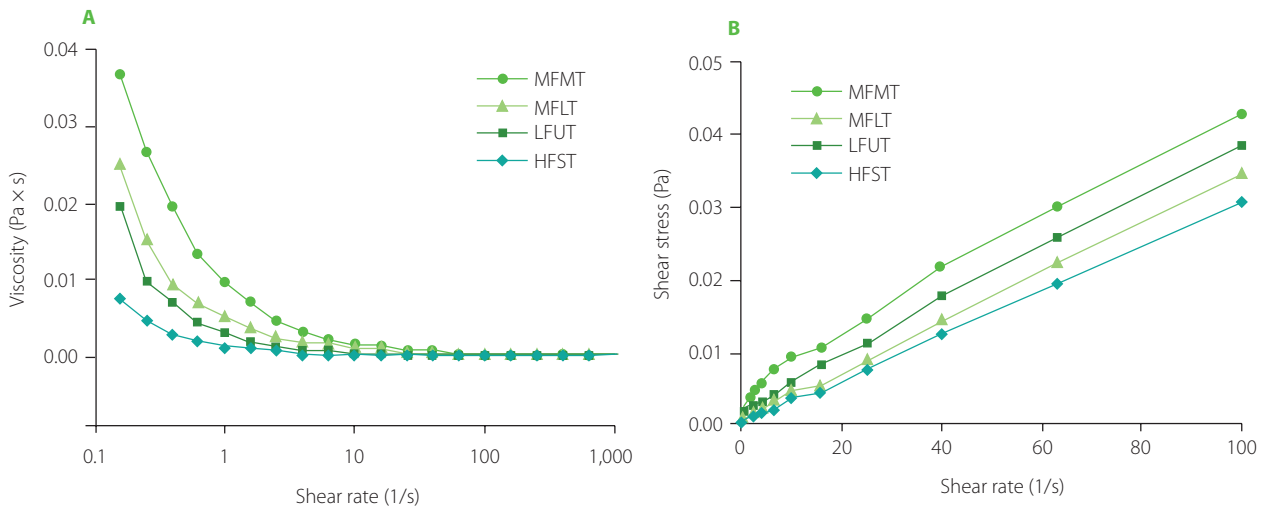


Figure 1. Shear rate viscosity curves (A) and shear stress vs. shear rate curves (B) of the chicken soups prepared with different stewing modes. HFST, high fire short time; MFMT, medium-high fire mid-length time; MFLT, medium fire long time; LFUT, low fire ultra-length time.

in the FAAs of chicken soup may be due to the enhanced migration of FAAs from boiled meat into the soup [Qi *et al.*, 2017]. The delicious taste of soups is not determined by a single kind of amino acids. The balance and interaction between different FAAs, such as sweet amino acids, umami amino acids and bitter amino acids, are the key factors determining the taste of soups. The FAAs composition of the chicken soups prepared with different stewing modes is shown in Table 3. The 17 FAAs identified in the soups were classified into four groups on the basis of their taste (umami, sweet, bitter, or tasteless) [Meng *et al.*, 2022]. Compared with HFST, MFMT, and MFLT, the total FAAs content in the soup stewed by LFUT was the highest, and the content of bitter amino acids was higher than that of umami amino acids, sweet amino acids and tasteless amino acids. The number of bitter amino acids increased significantly due to the increased hydrolysis of proteins and peptides in the crucian carp as the heating temperature increased [Zhang *et al.*, 2013]. Meng *et al.* [2022] also noted that shortening heating time appropriately was necessary to reduce the formation of bitter amino acids and maintain a good taste of bone soup. However, the taste active values (TAV) of the bitter taste FAAs (valine, methionine, isoleucine, leucine, phenylalanine, lysine, and arginine) were low, less than 1 (Table 3); hence, they had little impact on the taste of the chicken soups.

Umami substances can balance food's taste and overall flavour. The high content of umami compounds can make food more palatable. According to the TAV values of FAAs (Table 3), glutamic acid was the main contributor to the umami taste of the chicken soups. Wu & Shiau [2002] also reported that glutamic acid was the predominant free amino acid in chicken soups produced from chicken meat. Zhuang *et al.* [2016] also found that glutamic acid, glycine, and alanine were the major flavour amino acids in cooked crab meat. In our study, the content and TAV value of glutamic acid in the chicken soup from the MFMT group was higher than that of the soups from the other three groups (LFUT, MFLT, and HFST). The lower umami taste FAAs in LFUT

and MFLT groups might be explained by Maillard's reaction because of long-time stewing. While the reason for the low content of umami taste FAAs in the HFST group may be because the short time was not enough to enable the migration of all original FAAs from chicken meat into the soup.

■ 5'-Nucleotide content

5'-Nucleotide has a significant impact on the flavour of meat products and has been widely used as a food flavour enhancer. The nucleotides in chicken soup come from the thermal transfer of nucleotides of chicken meat, which contributes to the chicken soup's flavour [Qi *et al.*, 2022]. The synergies between nucleotides also play a major role in improving overall flavour. The contents of 5'-IMP, 5'-GMP, and 5'-AMP were quantified in the chicken soups prepared with different stewing models (Table 4). 5'-IMP was the most important umami nucleotide in the four kinds of chicken soup because its TAV was greater than 1. Additionally, as reported by Kawai *et al.* [2002], 5'-IMP interacts with a large number of sweet amino acids, such as serine, glycine, and alanine, which have a strong enhancing effect on the umami taste. As shown in Table 4, the 5'-IMP content of the soups of the MFMT group was the highest, while the soups of the HFST group had the lowest 5'-IMP content. This may be due to the fact that rapid heating rate and high temperature of the HFST stewing mode led to the accelerated degradation of 5'-IMP to convert inosine and hypoxanthine during cooking. Zou *et al.* [2018b] also reported that increasing heating temperature promoted the soup's 5'-IMP degradation. Furthermore, Zou *et al.* [2018a] have reported that the synergy of 5'-GMP and 5'-IMP enhanced the umami taste of food. Consistent with 5'-IMP, the content of 5'-GMP in the chicken soups of the MFMT group was higher than in the other groups. The contents of 5'-AMP in the soups of MFMT and LFUT groups were higher than that in the other two groups, but there was no significant difference between these two groups ($p > 0.05$). Although the TAVs of 5'-AMP and 5'-GMP

Table 3. Free amino acid (FAA) composition and their taste activity values (TAVs) of the chicken soups prepared with different stewing modes.

| Free amino acid | Taste threshold (mg/100 mL) | Content in soup (mg/100 mL) | | | | | TAV in soup | | | | | |
|-----------------------|-----------------------------|--------------------------------|--------------------------------|--------------------------------|--------------------------------|-------------------------|-------------------------|-------------------------|-------------------------|-------------------------|-------------------------|-------------------------|
| | | HFST | MFMT | MFLT | LFUT | HFST | MFMT | MFLT | LFUT | LFUT | | |
| Aspartic acid (Asp) | 100 | 14.46±0.34 ^b | 18.14±0.21 ^a | 7.82±0.04 ^d | 9.58±0.13 ^c | 0.14±0.003 ^b | 0.18±0.002 ^a | 0.08±<0.01 ^d | 0.10±0.001 ^c | 0.18±0.002 ^a | 0.08±<0.01 ^d | 0.10±0.001 ^c |
| Glutamic acid (Glu) | 30 | 33.93±0.52 ^b | 41.77±0.39 ^a | 16.56±0.26 ^d | 20.40±0.22 ^c | 1.13±0.017 ^b | 1.39±0.013 ^a | 0.55±0.009 ^d | 0.68±0.007 ^c | 1.39±0.013 ^a | 0.55±0.009 ^d | 0.68±0.007 ^c |
| ΣUmami FAA | | 48.39±0.78^b | 59.91±0.67^a | 24.38±0.35^d | 29.98±0.42^c | – | – | – | – | – | – | – |
| Threonine (Thr) | 260 | 9.87±0.43 ^b | 11.77±0.84 ^a | 9.91±0.37 ^b | 8.19±0.21 ^c | 0.04±0.002 ^a | 0.05±0.003 ^a | 0.04±0.001 ^a | 0.03±<0.01 ^a | 0.05±0.003 ^a | 0.04±0.001 ^a | 0.03±<0.01 ^a |
| Serine (Ser) | 150 | 12.59±0.26 ^b | 15.42±0.36 ^a | 8.59±0.28 ^c | 8.95±0.07 ^c | 0.08±0.002 ^b | 0.10±0.002 ^a | 0.06±0.002 ^c | 0.06±<0.01 ^c | 0.10±0.002 ^a | 0.06±0.002 ^c | 0.06±<0.01 ^c |
| Proline (Pro) | 300 | 5.06±0.03 ^c | 5.81±0.13 ^b | 1.72±0.09 ^d | 13.72±0.14 ^a | 0.02±<0.01 ^a | 0.02±<0.01 ^a | 0.01±<0.01 ^a | 0.05±<0.01 ^a | 0.02±<0.01 ^a | 0.01±<0.01 ^a | 0.05±<0.01 ^a |
| Glycine (Gly) | 130 | 8.73±0.38 ^b | 10.60±0.26 ^a | 4.50±0.23 ^d | 5.50±0.02 ^c | 0.07±0.003 ^b | 0.08±0.002 ^a | 0.03±0.002 ^c | 0.04±<0.01 ^c | 0.08±0.002 ^a | 0.03±0.002 ^c | 0.04±<0.01 ^c |
| Alanine (Ala) | 60 | 13.92±0.41 ^b | 16.75±0.45 ^a | 9.85±0.35 ^d | 11.58±0.46 ^c | 0.23±0.007 ^b | 0.28±0.008 ^a | 0.16±0.006 ^d | 0.19±0.008 ^c | 0.28±0.008 ^a | 0.16±0.006 ^d | 0.19±0.008 ^c |
| ΣSweet FAA | | 50.17±0.96^b | 60.35±0.83^a | 34.57±0.69^d | 47.94±0.84^c | – | – | – | – | – | – | – |
| Valine (Val) | 40 | 9.00±0.48 ^{bc} | 10.44±0.27 ^a | 8.39±0.47 ^c | 9.20±0.64 ^b | 0.23±0.012 ^b | 0.26±0.007 ^a | 0.21±0.01 ^c | 0.23±0.016 ^b | 0.26±0.007 ^a | 0.21±0.01 ^c | 0.23±0.016 ^b |
| Methionine (Met) | 30 | 2.42±0.08 ^c | 2.65±0.06 ^c | 8.23±0.21 ^b | 8.41±0.78 ^a | 0.08±0.003 ^b | 0.09±0.002 ^b | 0.27±0.007 ^a | 0.28±0.26 ^a | 0.09±0.002 ^b | 0.27±0.007 ^a | 0.28±0.26 ^a |
| Isoleucine (Ile) | 90 | 3.36±0.11 ^b | 3.40±0.12 ^b | 3.67±0.06 ^b | 4.24±0.32 ^a | 0.04±0.001 ^a | 0.04±0.001 ^a | 0.04±<0.01 ^a | 0.05±0.004 ^a | 0.04±0.001 ^a | 0.04±<0.01 ^a | 0.05±0.004 ^a |
| Leucine (Leu) | 190 | 4.97±0.05 ^c | 4.95±0.04 ^c | 31.29±0.87 ^a | 28.55±0.69 ^b | 0.03±<0.01 ^c | 0.03±<0.01 ^c | 0.16±0.005 ^a | 0.15±0.003 ^b | 0.03±<0.01 ^c | 0.16±0.005 ^a | 0.15±0.003 ^b |
| Tyrosine (Tyr) | – | 3.09±0.02 ^c | 3.17±0.13 ^c | 29.91±0.63 ^b | 30.88±0.84 ^a | – | – | – | – | – | – | – |
| Phenylalanine (Phe) | 90 | 1.26±0.01 ^c | 1.14±0.05 ^c | 34.94±0.28 ^a | 32.43±0.95 ^b | 0.01±<0.01 ^c | 0.01±<0.01 ^c | 0.39±0.003 ^a | 0.36±0.01 ^b | 0.01±<0.01 ^c | 0.39±0.003 ^a | 0.36±0.01 ^b |
| Lysine (Lys) | 50 | 15.44±0.62 ^b | 20.19±0.68 ^a | 13.80±0.23 ^c | 15.70±0.73 ^b | 0.31±0.01 ^b | 0.40±0.013 ^a | 0.28±0.005 ^c | 0.31±0.015 ^b | 0.40±0.013 ^a | 0.28±0.005 ^c | 0.31±0.015 ^b |
| Histidine (His) | 20 | 4.79±0.23 ^c | 5.53±0.26 ^b | 5.57±0.06 ^b | 6.23±0.09 ^a | 0.24±0.012 ^c | 0.28±0.013 ^b | 0.28±0.003 ^b | 0.31±0.005 ^a | 0.28±0.013 ^b | 0.28±0.003 ^b | 0.31±0.005 ^a |
| Arginine (Arg) | 50 | 7.15±0.35 ^c | 8.34±0.54 ^b | 8.87±0.23 ^b | 9.84±0.35 ^a | 0.14±0.007 ^c | 0.17±0.011 ^b | 0.18±0.005 ^b | 0.20±0.007 ^a | 0.17±0.011 ^b | 0.18±0.005 ^b | 0.20±0.007 ^a |
| ΣBitter FAA | | 51.48±0.85^c | 59.81±0.92^b | 144.67±1.34^a | 145.48±1.65^a | – | – | – | – | – | – | – |
| Cysteine (Cys) | – | 0.40±0.21 ^b | 0.39±0.35 ^b | 0.02±0.01 ^c | 0.59±0.14 ^a | – | – | – | – | – | – | – |
| ΣTasteless FAA | | 0.40±0.21^b | 0.39±0.35^b | 0.02±0.01^c | 0.59±0.14^a | – | – | – | – | – | – | – |
| ΣFAA | | 150.43±1.38^d | 180.43±1.79^c | 203.62±2.14^b | 223.96±1.63^a | – | – | – | – | – | – | – |

Data are expressed as mean ± standard deviation (n=3). Different lowercase letters (a-d) in the same row (separately for content and TAV) indicate significant differences (p<0.05). "–" no reference threshold. HFST, high fire short time; MFMT, medium-high fire mid-length time; MFLT, medium fire long time; LFUT, low fire ultra-length time.

Table 4. 5'-Nucleotide contents and their taste activity values (TAVs) of the chicken soups prepared with different stewing modes.

| 5'-Nucleotide | Taste threshold (mg/100 mL) | Content in soup (mg/100 mL) | | | | TAV in soup | | | |
|---------------|-----------------------------|-----------------------------|-------------------------|-------------------------|-------------------------|-------------------------|-------------------------|-------------------------|-------------------------|
| | | HFST | MFMT | MFLT | LFUT | HFST | MFMT | MFLT | LFUT |
| 5'-GMP | 12.5 | 0.76±0.01 ^d | 1.91±0.03 ^a | 1.23±0.02 ^c | 1.80±0.05 ^b | 0.06±<0.01 ^d | 0.15±<0.01 ^a | 0.10±<0.01 ^c | 0.14±<0.01 ^b |
| 5'-IMP | 25 | 36.55±0.24 ^d | 53.47±0.04 ^a | 49.10±0.35 ^c | 50.83±0.09 ^b | 1.46±0.01 ^d | 2.14±<0.01 ^a | 1.96±0.01 ^c | 2.03±<0.10 ^b |
| 5'-AMP | 50 | 3.82±0.04 ^c | 6.12±0.05 ^a | 5.72±0.18 ^b | 6.00±0.04 ^a | 0.08±<0.01 ^c | 0.12±<0.01 ^a | 0.11±<0.01 ^b | 0.12±<0.01 ^a |

Data are expressed as mean ± standard deviation (n=3). Different lowercase letters (a-d) in the same row (separately for content and TAV) indicate significant differences ($p < 0.05$). HFST, high fire short time; MFMT, medium-high fire mid-length time; MFLT, medium fire long time; LFUT, low fire ultra-length time; 5'-GMP, guanosine 5'-monophosphate; 5'-IMP, inosine 5'-monophosphate; 5'-AMP, adenosine 5'-monophosphate. Taste thresholds were obtained from literature [Qi *et al.*, 2017].

in the four soups were less than 1, the synergistic effect of 5'-AMP and 5'-GMP on umami induction should be considered.

■ Fatty acid composition

Fatty acids are significant precursors of flavour components that affect soup's flavour. Various individual fatty acids have been reported to have important flavour characteristics [He *et al.*, 2023]. Table 5 shows data indicating the influence of different stewing modes on the content of fatty acids in chicken soup. A total of 23 fatty acids were detected in the chicken soups, including 10 saturated fatty acids (SFA), 6 monounsaturated fatty acids (MUFA), and 7 polyunsaturated fatty acids (PUFA). Among them, the main SFA were palmitoleic acid (C16:0) and stearic acid (C18:0), and the main unsaturated fatty acids (USFA) were oleic acid (C18:1) and linoleic acid (C18:2). Han & Zhang [2019] showed that SFA could mask bitterness, whereas Cameron *et al.* [2000] showed that pork flavour correlated positively with the MUFA content. As shown in Table 5, compared to the other stewing modes (HFST, MFLT, and LFUT), the sum of SFA in the chicken soup prepared in the MFMT stewing mode was higher. The relative contents of PUFA in the four samples from high to low were LFUT, MFLT, MFMT, and HFST. This result may be due to the fact that the high-temperature stewing (HFST) accelerated the lipid oxidation rate, which changed the unsaturated fatty acid carbon chain and converted them into aldehydes and alcohols, such as 2-heptanal, 2-nonanal, and 2-octanal [Kim *et al.*, 2020].

■ Volatile compound composition

The results of GC-MS analysis of volatile compounds in chicken soups with different stewing models are shown in Table 6. In total, 34, 36, 51 and 47 volatile compounds were identified in the four chicken soups prepared with stewing models of HFST, MFMT, MFLT, and LFUT, respectively, which indicated that new volatile compounds were formed along with stewing time extension. The volatile compounds from different samples mainly included aldehydes, hydrocarbons, esters, and alcohols. Ba *et al.* [2013] reported that aldehydes were produced upon the thermal oxidation and decomposition of unsaturated fatty acids. For example, hexanal and heptanal are produced by the oxidation of *n*-6 PUFA, and octanal and nonanal are produced by the oxidation of *n*-9 PUFA [Tanimoto *et al.*, 2015]. As displayed in Table 6, aldehydes played an important role in the overall aroma of the cooked chicken soups because of their lower odour thresholds and higher contents. Among all aldehydes identified in the four soups obtained under the different stewing models, the hexanal content was the highest. Qi *et al.* [2017] also found similar results for Chinese yellow-feather chicken soup. Additionally, Yang *et al.* [2011] also noted that the hexanal content represented the flavour formation in cooked meat. Compared to other stewing modes, the chicken soup obtained under the mode of LFUT had the highest hexanal content. This may be because prolonged stewing (4 h) caused more lipids to dissolve from the chicken carcass into the soup and be oxidized to aldehydes.

Table 5. Compositions of fatty acids in the chicken soups prepared with different stewing modes (g/100 g total fatty acids).

| Fatty acid | HFST | MFMT | MFLT | LFUT |
|--------------|-------------------------------|-------------------------------|-------------------------------|-------------------------------|
| C10:0 | 0.00±0.00 ^b | 0.01±0.00 ^a | 0.01±0.00 ^a | 0.01±0.00 ^a |
| C12:0 | 0.03±0.00 ^{ab} | 0.03±0.01 ^b | 0.04±0.01 ^a | 0.04±0.00 ^a |
| C14:0 | 0.62±0.00 ^a | 0.63±0.00 ^a | 0.59±0.00 ^b | 0.52±0.00 ^c |
| C15:0 | 0.10±0.01 ^a | 0.08±0.00 ^b | 0.07±0.00 ^c | 0.10±0.00 ^a |
| C16:0 | 24.61±0.02 ^a | 25.02±0.01 ^a | 21.13±0.06 ^c | 22.54±0.02 ^b |
| C17:0 | 0.13±0.00 ^d | 0.14±0.00 ^c | 0.16±0.00 ^b | 0.21±0.00 ^a |
| C18:0 | 5.95±0.04 ^c | 6.22±0.08 ^b | 6.17±0.03 ^b | 7.14±0.01 ^a |
| C19:0 | 0.00±0.00 ^c | 0.03±0.01 ^b | 0.03±0.00 ^b | 0.04±0.00 ^a |
| C20:0 | 0.08±0.01 ^c | 0.08±0.01 ^c | 0.10±0.01 ^b | 0.15±0.00 ^a |
| C22:0 | 0.00±0.00 ^c | 0.00±0.00 ^c | 0.02±0.00 ^b | 0.03±0.00 ^a |
| ΣSFA | 31.70±0.02^b | 32.21±0.08^a | 28.21±0.09^d | 29.35±0.05^c |
| C14:1 | 0.19±0.01 ^a | 0.19±0.00 ^a | 0.03±0.00 ^b | 0.03±0.00 ^b |
| C16:1 | 6.89±0.01 ^a | 6.44±0.02 ^b | 4.88±0.03 ^c | 4.71±0.01 ^d |
| C17:1 | 0.00±0.00 ^c | 0.13±0.01 ^b | 0.13±0.00 ^b | 0.16±0.00 ^a |
| C18:1 | 45.78±0.05 ^a | 45.19±0.05 ^a | 41.98±0.15 ^b | 31.42±0.16 ^c |
| C19:1 | 0.00±0.00 ^c | 0.00±0.00 ^c | 0.05±0.00 ^b | 0.08±0.00 ^a |
| C20:1 | 0.44±0.01 ^b | 0.45±0.02 ^b | 0.43±0.04 ^b | 0.54±0.00 ^a |
| ΣMUFA | 53.33±0.06^a | 52.51±0.06^b | 47.49±0.11^c | 36.98±0.14^d |
| C18:2 | 14.53±0.05 ^c | 14.75±0.01 ^c | 23.50±0.05 ^b | 33.07±0.15 ^a |
| C18:3 | 0.11±0.00 ^c | 0.00±0.00 ^d | 0.13±0.00 ^b | 0.19±0.01 ^a |
| C16:2 | 0.11±0.00 ^c | 0.11±0.00 ^c | 0.18±0.00 ^b | 0.22±0.00 ^a |
| C20:2 | 0.13±0.00 ^c | 0.13±0.01 ^c | 0.15±0.01 ^b | 0.20±0.03 ^a |
| C20:3 | 0.11±0.00 ^a | 0.11±0.01 ^a | 0.08±0.01 ^b | 0.11±0.00 ^a |
| C20:4 | 0.20±0.00 ^a | 0.18±0.01 ^b | 0.11±0.00 ^d | 0.14±0.00 ^c |
| C22:4 | 0.00±0.00 ^c | 0.05±0.01 ^a | 0.03±0.01 ^b | 0.05±0.00 ^a |
| ΣPUFA | 15.10±0.05^c | 15.30±0.01^c | 24.14±0.04^b | 34.05±0.17^a |

Different lowercase letters (a-d) in the same row indicate significant differences ($p < 0.05$). All data are presented as the mean \pm standard deviation. SFA, saturated fatty acids; MUFA, monounsaturated fatty acids; PUFA, polyunsaturated fatty acids; HFST, high fire short time; MFMT, medium-high fire mid-length time; MFLT, medium fire long time; LFUT, low fire ultra-length time.

Saturated alkanes can be produced by the decarboxylation and cleavage of carbon-carbon bonds in higher fatty acids [Watanabe & Sato, 1971]. Although there were many kinds of alkanes in each chicken soup (Table 6), they did not contribute directly to the flavour due to their long carbon chain. Still, they played a specific role in improving the overall flavour.

Alcohols mainly come from the reduction reaction of carbonyl compounds and oxidation reaction of lipids, and exhibit grass, mushroom and earthy odours [Wan *et al.* 2021]. However, some alcohols and carboxylic acids in meat products react to form esters through esterification. As shown in Table 6, the alcohol content of the chicken soups was affected by stewing temperature and duration. Wettasinghe *et al.* [2000] reported that

1-octen-3-ol was one of the key odour compounds in roasted chicken skin due to its low odour threshold, and that changes in its content can affect the overall flavour. 1-Octen-3-ol, which contributed to mushroom and roasted aroma in chicken soup [Zhang *et al.*, 2018], was detected in all the samples, and its odour intensity was the highest in the MFLT group soups compared to the other samples (HFST, MFMT, and LFUT). One possible explanation was that more lipids were decomposed to form 1-octen-3-ol in the MFLT stewing mode.

Additionally, only three esters were detected at low contents in the four samples by GC-MS, and they may have little impact on odour perception because of their high odour thresholds. Therefore, these volatile compounds were neglected.

Table 6. Volatile compound profile and odour activity values (OAVs) of chicken soups prepared with different stewing modes.

| Compounds | LRI | Odor threshold (ng/g) | Content in soup (ng/g) | | | | OAV in soup | | | |
|-------------------------------|------|-----------------------|----------------------------|----------------------------|----------------------------|-----------------------------|------------------------|------------------------|-------------------------|-------------------------|
| | | | HFST | MFMT | MFLT | LFUT | HFST | MFMT | MFLT | LFUT |
| Hexanal | 806 | 5 | 748±31 ^d | 870±21 ^c | 1981±57 ^b | 2351±34 ^a | 149.6±6.2 ^d | 174.1±4.2 ^c | 396±11 ^b | 470.3±6.8 ^a |
| Heptanal | 905 | 3 | 81.8±6.8 ^c | 282±17 ^b | 511.8±4.8 ^a | 529±15 ^a | 27.3±2.3 ^c | 94.0±5.5 ^b | 170.6±1.6 ^a | 176.4±4.9 ^a |
| Octanal | 1005 | 0.7 | 210.0±2.4 ^d | 257.9±7.4 ^c | 378.7±5.1 ^b | 421.5±7.7 ^a | 300.0±3.4 ^d | 368.5±11 ^c | 541.0±7.2 ^b | 645±11 ^a |
| (E)-2-Octenal | 1013 | 3 | 67.4±3.1 ^d | 140.8±4.0 ^c | 532±30 ^a | 444±11 ^b | 22.5±1.0 ^d | 46.9±1.3 ^c | 177±10 ^a | 148.1±3.5 ^b |
| Nonanal | 1104 | 1 | 244.6±24 ^d | 381±31 ^b | 627.2±1.8 ^b | 764±35 ^a | 245±24 ^d | 381±31 ^c | 627.2±1.8 ^b | 764±35 ^a |
| (E)-2-Nonenal | 1112 | 0.08 | 29.9±2.2 ^c | ND | 105.5±2.8 ^b | 121.3±9.1 ^a | 374±25 ^c | Trace | 1319±35 ^b | 1516±114 ^a |
| Decanal | 1204 | 2 | 6.07±0.71 ^c | 24.3±4.1 ^b | 33.5±1.9 ^b | 41.33±0.83 ^a | 3.03±0.35 ^d | 12.2±2.0 ^c | 16.76±0.96 ^b | 20.67±0.42 ^a |
| (E)-2-Decenal | 1212 | 0.3 | ND | ND | 171.0±2.1 ^b | 288±32 ^a | Trace | Trace | 570.0±7.1 ^b | 961±108 ^a |
| (E,E)-2,4-Decadienal | 1220 | 0.07 | 24.0±2.4 ^d | 105.5±3.9 ^c | 145.2±5.6 ^a | 121.6±9.7 ^b | 342±35 ^d | 1507±56 ^c | 2074±80 ^a | 1738±139 ^b |
| 2-Undecenal | 1311 | NA | ND | ND | 111.9±5.5 ^b | 204±31 ^a | Trace | Trace | Trace | Trace |
| Tridecyclic aldehyde | 1601 | NA | ND | ND | ND | 69.6±1.9 ^a | Trace | Trace | Trace | Trace |
| Myristic aldehyde | 1502 | NA | ND | ND | ND | 9.43±0.51 ^a | Trace | Trace | Trace | Trace |
| Hexadecanal | 1800 | NA | ND | ND | 3.95±0.25 ^a | ND | Trace | Trace | Trace | Trace |
| ΣAldehydes | | | 1438±31^d | 2062±35^c | 4678±75^b | 5439±131^a | | | | |
| 2-Methyl-3-ethyl-1,3-hexadien | 868 | NA | 12.51±0.10 ^b | ND | 53.0±1.3 ^a | ND | Trace | Trace | Trace | Trace |
| 2,5-Dimethyl nonane | 986 | NA | ND | ND | 35.5±2.6 ^a | 18.8±1.2 ^b | Trace | Trace | Trace | Trace |
| 3,3,5-Trimethylheptane | 867 | NA | 49.9±1.9 ^c | ND | 197.2±1.5 ^a | 123.9±2.8 ^b | Trace | Trace | Trace | Trace |
| Undecane | 1115 | NA | ND | ND | 124.9±3.1 ^a | 80.8±1.7 ^b | Trace | Trace | Trace | Trace |
| 1-Iodononane | 1430 | NA | 4.54±0.36 ^d | 19.16±0.64 ^c | 230±15 ^b | 313.8±9.6 ^a | Trace | Trace | Trace | Trace |
| 4-Methylundecane | 1150 | NA | 152.2±7.2 ^c | 400±26 ^a | 70.6±6.1 ^d | 200±13 ^b | Trace | Trace | Trace | Trace |

Table 6 cont. Volatile compound profile and odour activity values (OAVs) of chicken soups prepared with different stewing modes.

| Compounds | LRI | Odor threshold (ng/g) | Content in soup (ng/g) | | | | OAV in soup | | | |
|----------------------------|------|-----------------------|-------------------------|-------------------------|-------------------------|-------|-------------|-------|-------|------|
| | | | HFST | MFMT | MFLT | LFUT | HFST | MFMT | MFLT | LFUT |
| 2,3-Dimethyldecane | 1086 | NA | 72.1±9.5 ^a | 47.7±1.3 ^b | ND | Trace | Trace | Trace | Trace | |
| 2-Methyl-6-ethyl-octane | 986 | NA | 48.8±5.5 ^c | 10.4±2.3 ^d | 296±23 ^a | Trace | Trace | Trace | Trace | |
| 5-(2-methylpropyl)nonane | 1185 | NA | 18.5±1.1 ^d | 123±12 ^a | 92.3±3.3 ^b | Trace | Trace | Trace | Trace | |
| Tridecane | 1313 | 2140 | 16.5±2.6 ^d | 59.8±6.4 ^c | 142.5±8.9 ^a | Trace | Trace | Trace | Trace | |
| Nonadecane | 1910 | NA | 8.1±1.3 ^c | 48.5±7.1 ^b | 64.7±1.6 ^a | Trace | Trace | Trace | Trace | |
| 1-Tetradecene | 1403 | NA | ND | 52.1±6.3 ^b | 77.1±1.4 ^a | Trace | Trace | Trace | Trace | |
| n-Tetradecane | 1413 | NA | 30.8±1.1 ^d | 147±11 ^c | 249.1±5.5 ^a | Trace | Trace | Trace | Trace | |
| 2,4-Dimethyl-undecane | 1185 | NA | 15.08±0.10 ^d | 202±11 ^a | 177±10 ^b | Trace | Trace | Trace | Trace | |
| 3,5-Dimethyloctane | 887 | NA | 22.77±0.20 ^f | ND | 292±10 ^b | Trace | Trace | Trace | Trace | |
| 4-Methyldodecane | 1249 | NA | 20.00±0.98 ^e | 136.0±3.8 ^b | 186.8±8.1 ^a | Trace | Trace | Trace | Trace | |
| 4,6-Dimethyldodecane | 1285 | NA | ND | 853±41 ^c | 1140±114 ^a | Trace | Trace | Trace | Trace | |
| 2,4-Dimethyl-dodecane | 1285 | NA | 63.0±1.2 ^d | 247±13 ^b | 369±18 ^b | Trace | Trace | Trace | Trace | |
| 2,7-Dimethyl-undecane | 1185 | NA | ND | 27.95±0.22 ^b | 34.7±2.1 ^a | Trace | Trace | Trace | Trace | |
| 5-Methyl-5-propylnonane | 1229 | NA | ND | 33.5±3.2 ^b | 37.89±0.26 ^b | Trace | Trace | Trace | Trace | |
| 4-Methyltridecane | 1349 | NA | 3.33±0.26 ^b | 13.27±0.20 ^a | 11.2±1.4 ^a | Trace | Trace | Trace | Trace | |
| Eicosane | 2009 | NA | 23.8±1.5 ^d | 354±26 ^c | 434±23 ^b | Trace | Trace | Trace | Trace | |
| n-Heptadecane | 1711 | NA | 63.8±4.1 ^d | 423±17 ^c | 454.8±4.8 ^b | Trace | Trace | Trace | Trace | |
| Heneicosane | 2109 | NA | 6.91±0.07 ^c | 55.3±2.7 ^b | 57.4±9.3 ^{ab} | Trace | Trace | Trace | Trace | |
| 4-Methyltetradecane | 1448 | NA | 11.5±1.8 ^c | 75.0±3.2 ^a | 63.7±1.9 ^b | Trace | Trace | Trace | Trace | |
| 2,6,10-trimethyl-tridecane | 1419 | NA | ND | 47.1±5.0 ^f | 70±34 ^b | Trace | Trace | Trace | Trace | |
| 4-Methylpentadecane | 1548 | NA | ND | ND | 12.4±1.4 ^a | Trace | Trace | Trace | Trace | |

Table 6 cont. Volatile compound profile and odour activity values (OAVs) of chicken soups prepared with different stewing modes.

| Compounds | LRI | Odor threshold (ng/g) | Content in soup (ng/g) | | | | OAV in soup | | | |
|-----------------------------------------------|------|-----------------------|------------------------------|-----------------------------|-------------------------------|------------------------------|-------------------------|-------------------------|-----------------------|-----------------------|
| | | | HFST | MFMt | MFLT | LFUT | HFST | MFMt | MFLT | LFUT |
| Hexadecane | 1612 | NA | 6.64±0.16 ^d | 172.33±0.07 ^b | 220±10 ^a | 121±16 ^c | Trace | Trace | Trace | Trace |
| 4-Methylhexadecane | 1647 | NA | ND | ND | 7.45±0.36 ^b | 13.13±0.46 ^a | Trace | Trace | Trace | Trace |
| ΣHydrocarbons | | | 614.0±6.5^d | 3579±92^c | 5385±126^a | 4696±83^b | | | | |
| n-Octyl acrylate | 1272 | NA | ND | ND | 23.4±1.3 ^a | 16.39±0.63 ^b | Trace | Trace | Trace | Trace |
| 2,2,4-Trimethyl-1,3-pentanediol diisobutyrate | 1605 | NA | 1.77±0.28 ^c | ND | 13.1±1.3 ^b | 120.8±7.4 ^a | Trace | Trace | Trace | Trace |
| Phthalate isobutyl/nyl ester | 2107 | NA | 1.86±0.07 ^d | 14.1±1.0 ^b | 11.6±1.7 ^b | 8.97±0.84 ^c | Trace | Trace | Trace | Trace |
| ΣEsters | | | 3.63±0.32^c | 14.1±1.0^b | 48.05±0.92^a | 48.8±1.5^a | | | | |
| 1-Octen-3-ol | 969 | 1 | 44.40±0.25 ^d | 52.23±0.87 ^c | 77.8±2.4 ^a | 67.3±1.4 ^b | 44.40±0.25 ^d | 52.23±0.87 ^c | 77.8±2.4 ^a | 67.3±1.4 ^b |
| 11-Methyldodecanol | 1492 | NA | 38.85±0.71 ^d | 228±16 ^c | 170.5±1.0 ^b | 84.0±5.3 ^c | Trace | Trace | Trace | Trace |
| 2-Propyl-1-heptanol | 1194 | NA | 32.04±5.6 ^b | ND | 638±91 ^a | ND | Trace | Trace | Trace | Trace |
| 2-Isopropyl-5-methyl-1-heptanol | 1165 | NA | 17.5±1.1 ^b | 113±18 ^a | 126.0±7.8 ^a | 120.843±7.4 ^a | Trace | Trace | Trace | Trace |
| 1-Tetradecanol | 1535 | NA | ND | 24.7±2.8 ^b | 34.1±1.5 ^a | ND | Trace | Trace | Trace | Trace |
| 2-Hexyl-1-decanol | 1790 | NA | ND | ND | 12.11±0.15 ^b | 15.92±0.12 ^a | Trace | Trace | Trace | Trace |
| ΣAlcohols | | | 137.5±1.3^d | 422±25^b | 1053±46^a | 287.2±9.8^c | | | | |
| 2,4-Di-tert-butylphenol | 1555 | NA | 3.5±0.01 ^c | 38.6±5.1 ^b | 46.0±2.6 ^b | 83.1±6.1 ^a | Trace | Trace | Trace | Trace |
| 11-Methyltriterpenoids | 2343 | NA | ND | 2.57±0.12 ^c | 7.91±0.30 ^b | 31.4±4.0 ^a | Trace | Trace | Trace | Trace |
| ΣOther | | | 3.5±0.01^d | 41.4±5.0^c | 53.9±2.8^b | 95.3±6.7^a | | | | |

Data are expressed as mean ± standard deviation (n=3). Different lowercase letters (a-d) in the same row (separately for content and OAV) indicate significant differences (p<0.05). HFST, high fire short time; MFMt, medium-high fire mid-length time; MFLT, medium fire long time; LFUT, low fire ultra-length time; LRI: linear retention index; NA, not acquired; ND, not detected. Odor thresholds were obtained from literature [Meng et al., 2022] and <http://www.odour.org.uk>

■ Flavour analysed by e-nose and e-tongue

The e-nose system is sensitive to volatile compounds of the sample within the measurable range, and small changes in their content will lead to differences in sensor response. PCA is a technique that reduces the dimensionality of large datasets by creating new uncorrelated variables [Chen *et al.*, 2022]. The volatile compounds of the four soups obtained under different stewing modes were presented in the PCA spatial distribution map (Figure 2A). The first two principal components (PCs) explained a total of 89.9% variation (PC1=83.9%, PC2=6.0%), which indicated that the two principal components contributed to the main feature information of different samples. As shown in Figure 2A, the soups of MFMT and MFLT groups were close to each other, indicating that they had similar odour characteristics. Additionally, MFMT and MFLT were far away from the samples of LFUT and HFST, which indicated that the odour characteristics of MFMT and MFLT samples were significantly different from those of the LFUT and HFST samples.

Principal component analysis was used to determine further differences in odour characteristics between the samples by performing a load analysis on the e-nose response (Figure 2B). Based on the response intensity of ten sensors to a specific characteristic gas, the main characteristic gas in each soup was tentatively speculated. The length of the arrow represents the contribution of compounds to the overall odour profile of the sample [Li *et al.* 2022]. The highest contribution rate in PC1 was found for the HFST sample, followed by the LFUT and MFMT samples, and the highest contribution rate in PC2 was found for the MFLT sample. Additionally, MFMT and MFLT had similar distances from the origin, indicating that they had similar characteristics, which was consistent with the results presented in Figure 2A. As shown in Figure 2B, the sensor's response to hydrogen (W6S), alkanes (W3S), and ammonia (W3C) was higher for the HFST sample; methane (W1S), nitrogen oxides (W5S), and aromatic compounds and sulphur organic compounds (W2W) were the main contributors in the MFLT sample; the W5C sensor responded more strongly to the LFUT and MFMT samples, indicating that they contained higher levels of short-chain alkane aromatic ingredients [Zhang J.X. *et al.*, 2022].

As shown in Figure 2C, the taste of the four chicken soup samples was discriminable, and there was no overlap in the 2D space. The total contribution variance of PC1 and PC2 was 85.1%, which meant that the first two PCs already contained sufficient information to reflect the total variance of the whole dataset. These data demonstrated that the e-nose and the e-tongue could discriminate the different samples. Different stewing modes significantly influenced the odour and taste of the chicken soups.

■ Sensory evaluation

The umami taste, bitterness and aroma of chicken soup have a significant impact on its flavour [Wu *et al.*, 2023]. Therefore, the sensory evaluation was carried out to better understand the effects of different stewing models on the changes in taste and aroma of the soups (Table 7). It could be seen that the chicken soup stewed by MFMT received the highest score for umami taste, while the chicken soup

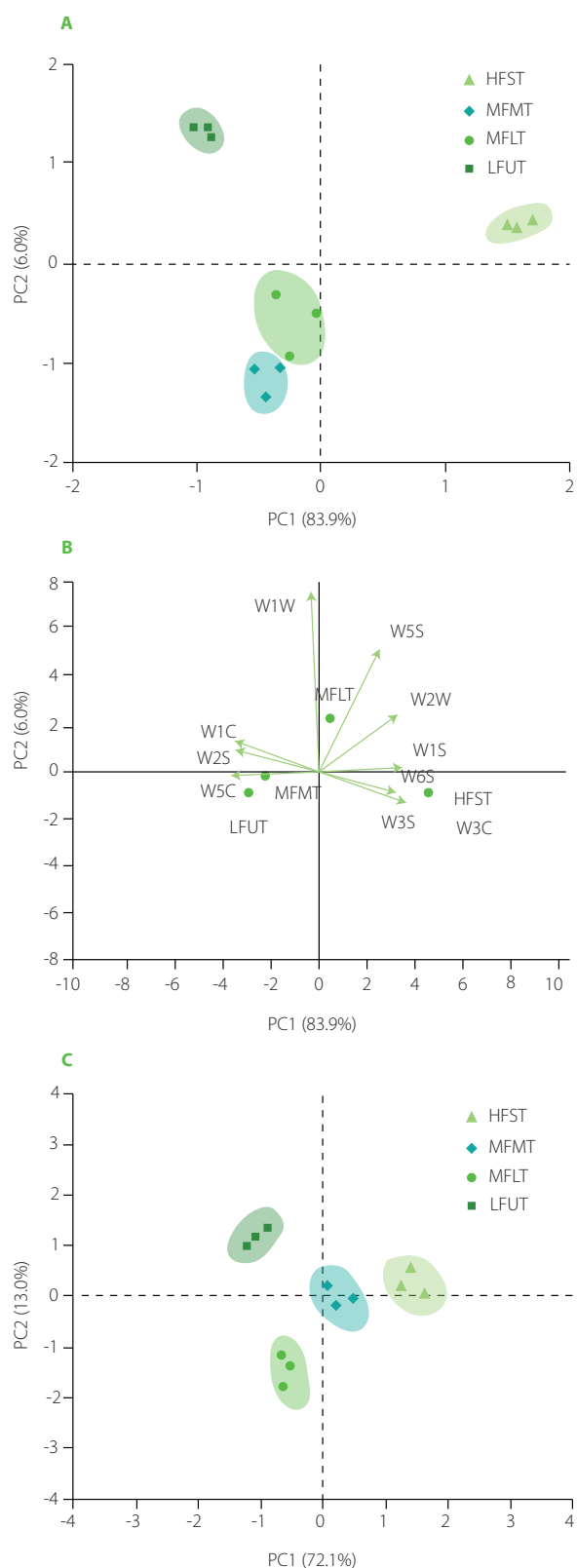


Figure 2. Principal component analysis (PCA) plot (A) and loading plot (B) of the e-nose data and PCA plot (C) of the e-tongue data. HFST, high fire short time; MFMT, medium-high fire mid-length time; MFLT, medium fire long time; LFUT, low fire ultra-length time; W1C, W5S, W3C, W6S, W5C, W1S, W1W, W2S, W2W, and W3S, sensor names (see Table 1 for details).

obtained by MFLT and LFUT received the highest score for its aroma. Bitterness score of the soup stewed by MFLT compared to MFMT was

Table 7. Sensory evaluation of chicken soup prepared with different stewing modes.

| Samples | Umami | Bitterness | Aroma |
|---------|------------------------|------------------------|------------------------|
| HFST | 3.51±0.04 ^d | 1.22±0.01 ^d | 3.14±0.03 ^c |
| MFMT | 5.25±0.03 ^a | 1.59±0.06 ^c | 4.71±0.03 ^d |
| MFLT | 4.61±0.06 ^b | 2.40±0.02 ^b | 5.73±0.04 ^a |
| LFUT | 4.19±0.04 ^c | 2.65±0.04 ^a | 5.36±0.03 ^a |

Different lowercase letters (a-d) in the same column indicate significant differences ($p < 0.05$). HFST, high fire short time; MFMT, medium-high fire mid-length time; MFLT, medium fire long time; LFUT, low fire ultra-length time.

also higher. Prolonging the stewing time appropriately helped to develop aroma, but at the same time, bitterness also increased. However, it was weak and did not affect the overall flavour of the chicken soup. The sensory evaluation results were consistent with the results of e-nose, the e-tongue, and GC-MS.

CONCLUSIONS

Different stewing modes (HFST, MFMT, MFLT, and LFUT) significantly affected chicken soup's stability and flavour compound formation. The chicken soup obtained under the MFMT stewing mode had a high viscosity, small particle size, and higher zeta potential. The contents of the umami components (umami taste FAAs and nucleotides) in the MFMT samples were higher than in the other samples. However, the profile and contents of volatile compounds of the chicken soup prepared under the MFMT stewing mode were different and lower than in the LFUT and MFLT groups, indicating that low temperature and long-time stewing were beneficial to the formation of volatile compounds. Hence, when considering the stability and umami taste of chicken soup, and time-saving, it is appropriate to use the MFMT mode to prepare it.

RESEARCH FUNDING

This work was supported by the Open Foundation Program of Cuisine Science Key Laboratory of Sichuan Province (PRKX2022Z10), the Science and Technology Project of "Unveiling and Commanding" from Liaoning Province (2022JH1/10900011; 2021JH1/10400033), and the Doctoral Research Foundation of Bohai University (05013/0520bs006).

CONFLICT OF INTERESTS

The authors declare no conflicts of interest.

ORCID IDs

X. Diao <https://orcid.org/0000-0002-9863-3943>
 C. Feng <https://orcid.org/0009-0008-2389-6811>
 H. Guan <https://orcid.org/0000-0002-2232-1564>
 D. Liu <https://orcid.org/0000-0003-4588-9985>
 Y. Tian <https://orcid.org/0009-0009-7007-8456>
 X. Xu <https://orcid.org/0000-0002-8710-9783>

REFERENCES

- Ali, M., Lee, S.Y., Park, J.Y., Jung, S., Jo, C., Nam, K.C. (2019). Comparison of functional compounds and micronutrients of chicken breast meat by breeds. *Food Science of Animal Resources*, 39(4), 632–642. <https://doi.org/10.5851/kosfa.2019.e54>
- Ba, H.V., Amna, T., Hwang, I. (2013). Significant influence of particular unsaturated fatty acids and pH on the volatile compounds in meat-like model systems. *Meat Science*, 94(4), 480–488. <https://doi.org/10.1016/j.meatsci.2013.04.029>
- Barido, F.H., Lee, S.K. (2021). Different effect of sodium chloride replacement with calcium chloride on proteolytic enzyme activities and quality characteristics of spent hen samgyetang. *Food Science of Animal Resources*, 41(5), 869–882. <https://doi.org/10.5851/kosfa.2021.e43>
- Bi, J.C., Lin, Z.Y., Li, Y., Chen, F.S., Liu, S.X., Li, C.F. (2021). Effects of different cooking methods on volatile flavor compounds of chicken breast. *Journal of Food Biochemistry*, 45(8), art. no. 13770. <https://doi.org/10.1111/jfbc.13770>
- Cameron, N.D., Enser, M., Nute, G.R., Whittington, F.M., Penman, J.C., Fiske, A.C., Perry, A.M., Wood, J.D. (2000). Genotype with nutrition interaction on fatty acid composition of intramuscular fat and the relationship with flavour of pig meat. *Meat Science*, 55(2), 187–195. [https://doi.org/10.1016/S0309-1740\(99\)00142-4](https://doi.org/10.1016/S0309-1740(99)00142-4)
- Chen, Y.P., Cai, D., Li, W., Blank, I., Liu, Y. (2022). Application of gas chromatography-ion mobility spectrometry (GC-IMS) and ultrafast gas chromatography electronic-nose (uf-GC E-nose) to distinguish four Chinese freshwater fishes at both raw and cooked status. *Journal of Food Biochemistry*, 46(6), SI, art. no. 13840. <https://doi.org/10.1111/jfbc.13840>
- Chotechuan, N., Lokkhumlue, M., Deetae, P. (2018). Effect of temperature and time on free amino acid profile in Thai chicken bone soup stock preparation. *Thai Journal of Pharmaceutical Sciences*, 42(3), 110–117. <https://digital.car.chula.ac.th/tjps/vol42/iss3/1>
- Costa, M.F., Pimentel, T.C., Guimaraes, J.T., Balthazar, C.F., Rocha, R.S., Cavalcanti, R.N., Esmerino, E.A., Freitas, M.Q., Raices, R.S.L., Silva, M.C., Cruz, A.G. (2019). Impact of prebiotics on the rheological characteristics and volatile compounds of Greek yogurt. *LWT – Food Science and Technology*, 105, 371–376. <https://doi.org/10.1016/j.lwt.2019.02.007>
- Coutinho, N.M., Silveira, M.R., Pimentel, T.C., Freitas, M.Q., Moraes, J., Fernandes, L.M., Silva, M.C., Raices, R.S.L., Ranadheera, C.S., Borges, F.O., Neto, R.P.C., Tavares, M.L.B., Fernandes, F.A.N., Nazzaro, F., Rodrigues, S., Cruz, A.G. (2019). Chocolate milk drink processed by cold plasma technology: Physical characteristics, thermal behavior and microstructure. *LWT – Food Science and Technology*, 102, 324–329. <https://doi.org/10.1016/j.lwt.2018.12.055>
- Dashdorj, D., Amna, T., Hwang, I. (2015). Influence of specific tasteactive components on meat flavor as affected by intrinsic and extrinsic factors: an overview. *European Food Research and Technology*, 241, 157–171. <https://doi.org/10.1007/s00217-015-2449-3>
- Diao, X.Q., Guan, H.N., Kong, B.H., Zhao, X.X. (2017). Preparation of diacylglycerol from lard by enzymatic glycerolysis and its compositional characteristics. *Korean Journal Food Science of Animal Resources*, 37(6), 813–822. <https://doi.org/10.5851/kosfa.2017.37.6.813>
- Diao, X.Q., Guan, H.N., Zhao, X.X., Chen, Q., Kong, B.H. (2016). Properties and oxidative stability of emulsions prepared with myofibrillar protein and lard diacylglycerols. *Meat Science*, 115, 16–23. <https://doi.org/10.1016/j.meatsci.2016.01.001>
- Folch, J., Lees, M., Sloane-Stanley, G.H. (1957). A simple method for the isolation and purification of total lipids from animal tissues. *Journal of Biological Chemistry*, 226(1), 497–509. [https://doi.org/10.1016/S0021-9258\(18\)64849-5](https://doi.org/10.1016/S0021-9258(18)64849-5)
- Guan, H.N., Yang, C., Tian, Y.L., Feng, C.M., Gai, S.M., Liu, D.Y., Diao, X.Q. (2023). Changes in stability and volatile flavor compounds of self-emulsifying chicken soup formed during the stewing process. *LWT – Food Science and Technology*, 175, art. no. 114520. <https://doi.org/10.1016/j.lwt.2023.114520>
- Han, Y., Zhang, Z. (2019). Fatty acid-rich trout bone soup demonstrates potential to mask bitterness of food and Chinese medicine. *Journal of Food and Nutrition Research*, 7(3), 224–230. <https://doi.org/10.12691/JFNR-7-3-7>
- He, W., Han, M.L., Bu, Y., Zhu, W.H., Li, J.R. (2023). Flavor mechanism of micro-nanoparticles and correlation analysis between flavor substances in thermoultrasonic treated fishbone soup. *Ultrasonics Sonochemistry*, 93, art. no. 106299. <https://doi.org/10.1016/j.ultsonch.2023.106299>
- Huang, T., Tu, Z., Zou, Z., Shangguan, X., Wang, H., Bansal, N. (2020). Glycosylated fish gelatin emulsion: Rheological, tribological properties and its application as model coffee creamers. *Food Hydrocolloids*, 102, art. no. 105552. <https://doi.org/10.1016/j.foodhyd.2019.105552>
- Kawai, M., Okiyama, A., Ueda, Y. (2002). Taste enhancements between various amino acids and IMP. *Chemical Senses*, 27(8), 739–745. <https://doi.org/10.1093/chemse/27.8.739>
- Kim, J., Utama, D.T., Jeong, H.S., Barido, F.H., Lee, S.K. (2020). Quality characteristics of retort samgyetang marinated with different levels of soy sauce

- and processed at different F_0 values. *Journal of Animal Science and Technology*, 62(5), 713–729.
<https://doi.org/10.5187/jast.2020.62.5.713>
20. Li, W.L., Zheng, L.T., Xiao, Y., Li, L.C., Wang, N., Che, Z.M., Wu, T. (2022). Insight into the aroma dynamics of Dongpo pork dish throughout the production process using electronic nose and GC×GC-MS. *LWT – Food Science and Technology*, 169, art. no. 113970.
<https://doi.org/10.1016/j.lwt.2022.113970>
 21. Liang, L., Duan, W., Zhang, J.C., Huang, Y., Zhang, Y.Y., Sun, B.G. (2022). Characterization and molecular docking study of taste peptides from chicken soup by sensory analysis combined with nano-LC-Q-ToF-MS/MS. *Food Chemistry*, 383, art. no. 132455.
<https://doi.org/10.1016/j.foodchem.2022.132455>
 22. Meng, Q., Zhou, J.W., Gao, D., Xu, E., Guo, M.M., Liu, D.H. (2022). Desorption of nutrients and flavor compounds formation during the cooking of bone soup. *Food Control*, 132, art. no. 108408.
<https://doi.org/10.1016/j.foodcont.2021.108408>
 23. Moriyama, Y., Kawasaki, Y., Takeda, K. (2003). Protective effect of small amounts of sodium dodecyl sulfate on the helical structure of bovine serum albumin in thermal denaturation. *Journal of Colloid and Interface Science*, 257(1), 41–46.
[https://doi.org/10.1016/S0021-9797\(02\)00017-6](https://doi.org/10.1016/S0021-9797(02)00017-6)
 24. Pérez-Palacios, T., Eusebio, J., Ferro Palma, S., Carvalh, M.J., Mir-Bel, J., Antequera, T. (2017). Taste compounds and consumer acceptance of chicken soups as affected by cooking conditions. *International Journal of Food Properties*, 20, sup. 1, art. no.1291678.
<https://doi.org/10.1080/10942912.2017.1291678>
 25. Petenuci, M.E., Santos, V.J.D., Gualda, I.P., Lopes, A.P., Schneider, V.V.A., Jr, O.O.D.S., Visentainer, J.V. (2019). Fatty acid composition and nutritional profiles of *Brycon* spp. from central Amazonia by different methods of quantification. *Journal of Food Science and Technology*, 56(3), 1551–1558.
<https://doi.org/10.1007/s13197-019-03654-4>
 26. Qi, J., Du, C., Yao, X., Yang, C., Zhang, Q., Liu, D. (2022). Enrichment of taste and aroma compounds in braised soup during repeated stewing of chicken meat. *LWT – Food Science and Technology*, 168, art. no. 113926.
<https://doi.org/10.1016/j.lwt.2022.113926>
 27. Qi, J., Jia, C.K., Zhang, W.W., Yan, H.M., Cai, Q.Y., Yao, X.N., Xu, K., Xu, Y., Xu, W.P., Xiong, G.Y., Li, M.Q. (2023). Ultrasonic-assisted stewing enhances the aroma intensity of chicken broth: A perspective of the aroma-binding behavior of fat. *Food Chemistry*, 398, art. no. 133913.
<https://doi.org/10.1016/j.foodchem.2022.133913>
 28. Qi, J., Liu, D.Y., Zhou, G.H., Xu, X.L. (2017). Characteristic flavor of traditional soup made by stewing Chinese yellow-feather chickens. *Journal of Food Science*, 82(9), 2031–2040.
<https://doi.org/10.1111/1750-3841.13801>
 29. Qi, J., Wang, H.H., Zhou, G.H., Xu, X.L., Li, X., Bai, Y., Yu, X.B. (2018). Evaluation of the taste-active and volatile compounds in stewed meat from the Chinese yellow-feather chicken breed. *International Journal of Food Properties*, 20, Sup. 3, S2579–S2595.
<https://doi.org/10.1080/10942912.2017.1375514>
 30. Qi, J., Zhang, W.W., Xu, Y., Xie, X.F., Xiong, G.Y., Xu, X.L., Zhou, G.H., Ye, M. (2021). Enhanced flavor strength of broth prepared from chicken following short-term frozen storage. *Food Chemistry*, 356, art. no. 129678.
<https://doi.org/10.1016/j.foodchem.2021.129678>
 31. Qian, X.L., Fan, X.Y., Su, H., Zhang, J., Tao, N.P., Zhong, J., Wang, X.C., Han, B.S. (2019). Migration of lipid and other components and formation of micro/nano-sized colloidal structure in Tuna (*Thunnus obesus*) head soup. *LWT – Food Science and Technology*, 119, 69–76.
<https://doi.org/10.1016/j.lwt.2019.04.088>
 32. Qiu, C., Zhao, M., Decker, E.A., McClements, D.J. (2015). Influence of anionic dietary fibers (xanthan gum and pectin) on oxidative stability and lipid digestibility of wheat protein-stabilized fish oil-in-water emulsion. *Food Research International*, 74, 131–139.
<https://doi.org/10.1016/j.foodres.2015.04.022>
 33. Rotola-Pukkila, M.K., Pihlajaviita, S.T., Kaimainen, M.T., Hopia, A.I. (2015). Concentration of umami compounds in pork meat and cooking juice with different cooking times and temperatures. *Journal of Food Science*, 80(12), C2711–C2716.
<https://doi.org/10.1111/1750-3841.13127>
 34. Tanimoto, S., Kitabayashi, K., Fukusima, C., Sugiyama, S., Hashimoto, T. (2015). Effect of storage period before reheating on the volatile compound composition and lipid oxidation of steamed meat of yellowtail *Seriola quinqueradiata*. *Fisheries Science*, 81, 1145–1155.
<https://doi.org/10.1007/s12562-015-0921-4>
 35. Wan, P., Liu, J., Chen, D.W. (2021). Analysis of aroma-active compounds in bighead carp head soup and their influence on umami of a model soup. *Microchemical Journal*, 168, art. no. 106436.
<https://doi.org/10.1016/j.microc.2021.106436>
 36. Watanabe, K., Sato, Y. (1971). Gas chromatographic and mass spectral analyses of heated flavor compounds of beef fats. *Agricultural and Biological Chemistry*, 35(5), 756–763.
<https://doi.org/10.1080/00021369.1971.10859984>
 37. Wettasinghe, M., Vasanthan, T., Temelli, F., Swallow, K. (2000). Volatiles from roasted byproducts of the poultry-processing industry. *Journal of Agricultural and Food Chemistry*, 48(8), 3485–3492.
<https://doi.org/10.1021/jf000122a>
 38. Wu, H.C., Shiau, C.Y. (2002). Proximate composition, free amino acids and peptides contents in commercial chicken and other meat essences. *Journal of Food and Drug Analysis*, 10(3), 170–177.
<https://doi.org/10.38212/2224-6614.2753>
 39. Wu, Q.R., Zang, M.W., Wang, S.W., Zhao, B., Zhang, S.L., Li, S., Pan, X.Q., Liu, M., Fu, X.H. (2023). Changes in flavors profiles of stewed bone-in lamb loin during cooking by DHS/GC-MS combined with electronic bionic systems. *Food Bioscience*, 53, art. no. 102767.
<https://doi.org/10.1016/j.fbio.2023.102767>
 40. Xiao, Z.C., Zhang, W.G., Yang, H.T., Yan, Z.Y., Ge, C.R., Liao, G.Z., Su, H.W. (2021). ¹H NMR-based water-soluble lower molecule characterization and fatty acid composition of Chinese native chickens and commercial broiler. *Food Research International*, 140, art. no. 110008.
<https://doi.org/10.1016/j.foodres.2020.110008>
 41. Yang, H.S., Lee, E.J., Moon, S.H., Paik, H.D., Ahn, D.U. (2011). Addition of garlic or onion before irradiation on lipid oxidation, volatiles and sensory characteristics of cooked ground beef. *Meat Science*, 88(2), 286–291.
<https://doi.org/10.1016/j.meatsci.2011.01.002>
 42. Zhang, J.J., Yao, Y.J., Ye, X.Q., Fang, Z.X., Chen, J.C., Wu, D., Liu, D.H., Hu, Y.Q. (2013). Effect of cooking temperatures on protein hydrolysates and sensory quality in crucian carp (*Carassius auratus*) soup. *Journal of Food Science and Technology*, 50, 542–548.
<https://doi.org/10.1007/s13197-011-0376-2>
 43. Zhang, J.X., Zhang, B., Dong, J.Y., Tian, Y.Y., Lin, Y.X., Fang, G.Z., Wang, S. (2022). Identification of mouldy rice using an electronic nose combined with SPME-GC/MS. *Journal of Stored Products Research*, 95, art. no. 101921.
<https://doi.org/10.1016/j.jspr.2021.101921>
 44. Zhang, L.L., Hao, Z.L., Zhao, C., Zhang, Y.Y., Li, J., Sun, B.G., Tang, Y.Z., Yao, M.X. (2021). Taste compounds, affecting factors, and methods used to evaluate chicken soup: A review. *Food Science & Nutrition*, 9(10), 5833–5853.
<https://doi.org/10.1002/fsn3.2501>
 45. Zhang, M., Chen, X.D., Hayat, K., Duhoranimana, E., Zhang, X.M., Xia, S.Q., Xing, F.L. (2018). Characterization of odor-active compounds of chicken broth and improved flavor by thermal modulation in electrical stewpots. *Food Research International*, 109, 72–81.
<https://doi.org/10.1016/j.foodres.2018.04.036>
 46. Zhang, M., Fan, L.P., Liu, Y.F., Li, J.W. (2022). A mechanistic investigation of the effect of dispersion phase protein type on the physicochemical stability of water-in-oil emulsions. *Food Research International*, 157, art. no. 111293.
<https://doi.org/10.1016/j.foodres.2022.111293>
 47. Zhu, Y., Bhandari, B., Prakash, S. (2020). Relating the tribo-rheological properties of chocolate flavoured milk to temporal aspects of texture. *International Dairy Journal*, 110, art. no. 104794.
<https://doi.org/10.1016/j.idairyj.2020.104794>
 48. Zhuang, K.J., Wu, N., Wang, X.C., Wu, X.G., Wang, S., Long, X.W., Wei, X. (2016). Effects of 3 feeding modes on the volatile and nonvolatile compounds in the edible tissues of female Chinese mitten crab (*Eriocheir sinensis*). *Journal of Food Science*, 81(4), S968–981.
<https://doi.org/10.1111/1750-3841.13229>
 49. Zou, J., Xu, M.J., Zou, Y.F., Yang, B. (2021). Chemical compositions and sensory characteristics of pork rib and Silkie chicken soups prepared by various cooking techniques. *Food Chemistry*, 345, art. no. 128755.
<https://doi.org/10.1016/j.foodchem.2020.128755>
 50. Zou, Y., Kang, D., Liu, R., Qi, J., Zhou, G., Zhang, W. (2018a). Effects of ultrasonic assisted cooking on the chemical profiles of taste and flavor of spiced beef. *Ultrasonics Sonochemistry*, 46, 36–45.
<https://doi.org/10.1016/j.ultsonch.2018.04.005>
 51. Zou, Y.H., Zhang, W.G., Kang, D.C., Zhou, G.H. (2018b). Improvement of tenderness and water holding capacity of spiced beef by the application of ultrasound during cooking. *International Journal of Food Science and Technology*, 53(3), 828–836.
<https://doi.org/10.1111/ijfs.13659>

Effects of Freeze-Thaw Cycles on the Flavor of Nanguo Pear

Ge Bai[#], Ya Wang[#], Jianrong Zheng, Xiaomin Zhang, Zhaoyue Zhuang, Danshi Zhu, Xuehui Cao^{*#}

College of Food Science and Technology, Bohai University; National & Local Joint Engineering Research Center of Storage, Processing and Safety Control Technology for Fresh Agricultural and Aquatic Products; Jinzhou, Liaoning, 121013, China

Frozen pears, obtained by repeated freezing and thawing under cold outdoor conditions in winter, are very popular in northeast China. The effects of three freeze-thaw cycles (FT1–FT3) on Nanguo pear flavor were studied under fast (−80°C) and slow (−20°C) freezing conditions. Significant differences were found in the flavor of Nanguo pear after subsequent freeze-thaw cycles. The total soluble solid (TSS) content of fresh pear was 14.17 g/100 g and increased significantly after the first freeze-thaw cycle to 17.57–18.17 g/100 g. Lower TSS content was found in pears after the repeated freeze-thawing process. Citric acid was determined as the main organic acid of Nanguo pear. Its content and the overall content of organic acids decreased successively after each freezing and thawing cycle. The electronic tongue analysis results showed that the sourness of fresh pears generally decreased after their repeated freezing and thawing, that the odor of Nanguo pear changed significantly after freeze-thaw cycles, and that nitrogen oxides and hydrocarbons were the most differentiating odor compounds. The content of ethyl caproate was the highest in the volatile compound profile of the Nanguo pear and ranged from 377.26 to 526.77 µg/kg. In short, after repeated freezing and thawing, the changes in the chemical composition impart the frozen pear a unique flavor.

Key words: *Pyrus ussuriensis*, organic acids, soluble solid content, volatile compounds, e-nose analysis, e-tongue analysis

INTRODUCTION

Nanguo pear (*Pyrus ussuriensis* Maxim.) belongs to Qiuzi pear series and is one of the characteristic fruits in Liaoning province, China [Tao *et al.*, 2019]. Fruits of this plant are sweet and sour with a rich and unique aroma [Wei *et al.*, 2017], which is deeply loved by consumers. In China, these pears are not only eaten as delicious food, but also considered as a cough medicine and diuretic [Cui *et al.*, 2005]. They contain ascorbic acid and phenolic compounds, including arbutin, catechin, chlorogenic acid, quercetin, and rutin, that determine their biological activities, such as antioxidant and anti-inflammatory effects [Chen *et al.*, 2007; Li *et al.*, 2012; Yan *et al.*, 2023].

Nanguo pear is a respiratory climacteric fruit with a relatively short shelf life [Wang *et al.*, 2017]. The ripening and senescence

of the fruit can be appropriately delayed when stored at low temperature, but the browning of the peel occurs easily when the Nanguo pear is brought to room temperature [Zhang *et al.*, 2018]. Freezing is one of the most important long-term storage methods for food, which allows consumers to buy seasonal fruit throughout the year. However, in the process of storage, transportation and consumer processing, frozen food is prone to temperature fluctuations, resulting in freeze-thaw cycles, and food may suffer mechanical damage, nutrient denaturation and loss of water retention ability [Ndraha *et al.*, 2018].

The flavor of fruit is an important characteristic to evaluate its quality, and is closely related to the content of carbohydrates, organic acids and volatile organic compounds [Aprea *et al.*, 2017; Cui *et al.*, 2022]. Luo *et al.* [2021] reported that the contents

*Corresponding Author:

tel.: +86-416-3400870; e-mail: caoxuehuisnow@126.com (X. Cao)
#These authors contributed equally to this article.

Submitted: 21 August 2023

Accepted: 17 January 2024

Published on-line: 16 February 2024



© Copyright by Institute of Animal Reproduction and Food Research of the Polish Academy of Sciences
© 2024 Author(s). This is an open access article licensed under the Creative Commons Attribution-NonCommercial-NoDeriv License (<http://creativecommons.org/licenses/by-nc-nd/4.0/>).

of volatile esters in Nanguo pears peaked during the optimum taste period (OTP) and that especially ethyl butyrate, ethyl caproate and hexyl acetate dominated in the profile of these compounds. Other research also shows that these aroma compounds of Nanguo pear have the advantages of high content and low odor threshold [Zhang & Yin, 2023].

The main purpose of this study was to determine the effects of multiple freeze-thaw cycles on Nanguo pear flavor compounds. Gas chromatography-mass spectrometry (GC-MS) method was used to measure the changes in main volatile esters in Nanguo pear, and electronic nose (e-nose) and electronic tongue (e-tongue) were deployed to comprehensively analyze the differences in the flavor of Nanguo pear. The content of acids and sugars in pears was determined as well, so as to explore the change of Nanguo pear flavor compounds in the freeze-thaw cycles.

MATERIALS AND METHODS

■ Materials and chemicals

Mature pear fruits (variety Nanguo) were hand-harvested from the local commercial orchard in Jinzhou, Liaoning Province, China. The collected material (about 65 kg) was transported to the laboratory of the Bohai University in Jinzhou, Liaoning Province, China, and refrigerated at 4°C in a low-temperature constant incubator (Sanyo MIR 254, Sanyo Electric Co., Ltd, Osaka, Japan) for 24 h before experiments.

■ Freeze-thaw cycles

The refrigerated Nanguo pears were randomly equally divided into 6 groups, 10 kg in each group. In addition, 5 kg was used as a fresh sample. Fruits of experimental groups denoted by the symbols SF – slow freezing (3 groups) and FF – fast freezing (3 groups) were frozen at –20°C and –80°C, respectively, in a refrigerating machine for 24 h. After freezing, the pears were transferred to a low-temperature constant incubator for thawing, and then continued to freeze. This freezing and thawing process was repeated 1, 2 and 3 times at each freezing temperature to obtain the samples with different freeze-thaw cycles (FT1, FT2, FT3, respectively).

■ Determination of the content of total soluble solids

Randomly selected 10 Nanguo pears were peeled and cut into pieces, then beaten into a pulp and filtered with 300-mesh filter cloth, and the filtrate was dropped into a digital refractometer (PAL-3 hand-held sugar meter, ATAGO Co., Ltd, Tokyo, Japan) for determination of the content of total soluble solids (TSS), which was expressed as a g/100 g.

■ Determination of organic acid content

Referring to the method of Zhang *et al.* [2021], high performance liquid chromatography (HPLC), using Shimadzu LC2030 system equipped with a UV detector (Shimadzu Corp., Kyoto, Japan), was applied to determine the content of organic acids. The thawed Nanguo pear flesh tissue (5.0 g), was placed into a spiral-cap centrifuge tube (50 mL). An aliquot of 25 mL of pure water was

added into the test tube, and ultrasonic extraction was performed for 30 min in an ultrasonic bath (KQ-500DE ultrasonic cleaner, Kunshan Ultrasonic Instrument Co., Ltd, Kunshan, Jiangsu Province, China) at 80°C. Then, the mixture was cooled at room temperature and centrifuged at 12,000×g at 4°C for 20 min in the Biofuge Stratos centrifuge (Thermo Scientific, Waltham, MA, USA). After the supernatant was poured out, the purified water was added again to repeat the previous operations. Finally, both supernatants were mixed, and the volume was filled to 50 mL. The extract prepared in this way was filtered through a 0.45 µm syringe, put into a vial, and stored at low temperature until analyzed.

An Eclipse Plus C 18 column (particle size 5 µm, 250×4.6 mm, Agilent, Santa Clara, CA, USA) was used to separate organic acids by HPLC. The mobile phase consisted of methanol (5.0% of the mobile phase volume, v/v) and 0.01 mM dipotassium hydrogen phosphate aqueous solution (95% of the mobile phase volume, v/v). The isocratic elution was carried out with the mobile phase flow rate of 0.5 mL/min. The injection volume was 10 µL, the detection wavelength was set to 210 nm, and the column temperature was maintained at 30°C. Under the same conditions, the standard curve was made from the standards (HPLC grade), including oxalic acid, L-tartaric acid, L-malic acid, shikimic acid and citric acid, which were purchased from Beijing Solaibao Technology Co., Ltd, China. The content of organic acids in pear flesh was expressed as µg/g.

■ Odor analysis using electronic nose

The odor of the pears was analyzed using a portable electronic nose (PEN3 e-nose, Airesense Analytics GmbH, Schwerin, Germany). The e-nose consisted of a sampling system, a unit with metal oxide sensors, and pattern recognition software (Win-Muster 1.6.2.15/May 17, Airesense Analytics GmbH). The response characteristics of each sensor were shown as follows: R1 – aromatic compounds, R2 – nitrogen oxide, R3 – ammonia and aromatic compounds, R4 – hydrogen, R5 – olefin and aromatic compounds, R6 – hydrocarbons, R7 – hydrogen sulfide, R8 – alcohols and partially aromatic compounds, R9 – aromatic compounds and organic sulfides, and R10 – alkanes [Zhu *et al.*, 2020]. The thawed pears were cut into chunks and pulped, then filtered through 300-mesh filter cloth. An aliquot of 15 mL of the filtrate was placed in a 50 mL plastic pipe, which was sealed with three layers of plastic wrap. The sample was left standing for 30 min until the odorous substances accumulated above the liquid. The cleaning time of the e-nose was 100 s, the measurement phase lasted 120 s, and the detection environment was kept at 25°C. To minimize error, the surrounding environment was kept closed during measurement.

■ Taste analysis using electronic tongue

Taste analysis of the samples was performed with an SA402B electronic tongue (Insent/Intelligent Sensor Technology, Inc., Kanagawa, Japan), which could test up to 10 samples at a time. The measuring cup containing samples, positive and negative electrode liquid and reference liquid were placed in the sample

tanks, respectively [Zhu *et al.*, 2020]. The positive electrode liquid contained 30% (v/v) ethanol, 100 mM KCl and 10 mM KOH; the negative electrode liquid contained 30% (v/v) ethanol and 100 mM HCl; and the reference liquid consisted of 30 mM KCl and 0.3 mM tartaric acid. Before testing, the thawed pears were homogenized and filtered, and then centrifuged. The supernatant was 10-fold diluted, then 70 mL of the solution was poured into two 50 mL sample cups. Before starting the measurement, the sensor was inserted for 30 s, then the measurement was performed for another 30 s. The sensor was cleaned automatically after the measurement, and the measurement was repeated four times for each sample. The first measurement cycle was discarded due to instability, and only the later three stable sensor responses were used as the raw data for the sample.

■ Determination of volatile ester profile

Analysis of pear volatile esters was performed using 7890N/5975 GC-MS instrument (Agilent). A portion of 3.0 g of thawed pear flesh was weighed into a 20 mL sample bottle, 5 mL saturated NaCl solution was added, and then 20 μ L cyclohexanone solution with a concentration of 0.475 mg/mL was added as the internal standard [Zhou, 2015]. Two magnetic rosters were put into each sample bottle, and the headspace bottle was sealed. After the closed headspace bottle was shaken well, it was balanced in the magnetic agitator at 45°C for 10 min. Then, the needle handle was pushed to stretch out the extraction head and adsorbed for 30 min. After the adsorption, the extraction head was quickly recovered. The HP-5MS capillary column (30 m \times 0.25 mm \times 0.25 μ m; Agilent) was used to separate volatile compounds. The sample inlet temperature and the ion source temperature were set at 250°C and 230°C, respectively. The column temperature was 40°C and the quadrupole was maintained at 150°C. Helium gas was used as a carrier gas, and its flow rate was 1.2 mL/min. The programmed heating process was as follows: the initial column temperature was set at 40°C for 5 min, and then it was increased to 120°C at the rate of 4°C/min, and kept for 2 min to complete the first heating stage. Then, the temperature was increased to 230°C at a rate of 10°C/min and kept for 6 min to complete the second heating stage. The results were matched with the mass spectrum library data to identify the volatile esters. The peak area of cyclohexanone was used to calculate the content of identified compounds in pear flesh, which was expressed as μ g/kg.

■ Statistical analysis

The experiment was performed three times with three replicates each. The data were statistically processed using the SPSS17.0 (SPSS Inc., Chicago, IL, USA). One-way analysis of variance (ANOVA) with least significant difference (LSD) and Duncan tests were used to compare the samples. The differences at $p < 0.05$ were considered statistically significant. Principal component analysis (PCA) and Linear discriminant analysis (LDA) were performed on the e-nose data using Win-Muster software. Origin 9.5 (OriginLab Corporation, Northampton, MA, USA) was used to plot the changes of each analyzed index.

RESULT AND DISCUSSION

■ Effects of freeze-thaw cycles on the content of total soluble solids of Nanguo pear

Total soluble solid (TSS) is a very important characteristic for the sensory and nutritional quality of food [Keutgen & Pawelzik, 2007a,b; Vu *et al.*, 2023]. TSS of fruits usually refer to soluble sugars, such as glucose and fructose, which reflects the sweetness of fruits [Kanski *et al.*, 2020]. The content of TSS of Nanguo pear fruit after each freeze-thaw cycle is shown in Figure 1. The fresh pears had TSS content of 14.17 g/100 g. This value was similar to that previously reported by Yan *et al.* [2023] for fresh Nanguo pear (14.70 g/100 g), but higher than the contents of 13.4 g/100 g and 8.9 g/100 g reported by Wang *et al.* [2021] and Chen *et al.* [2007], respectively, which may be due to the different origin of the fruit (different growing conditions, different variety). The content of TSS in the freeze-thaw samples was significantly ($p < 0.05$) higher than that in fresh fruits. After the first freeze-thaw cycle, the content of TSS in pears frozen at -20°C was 17.57 g/100 g, and that in fruits of FF-FT1 group was 18.17 g/100 g. Ice crystals formed during the freezing lead to destruction of cell structures and damage to cell walls. The rise in TSS content of pears after freezing may be caused by the destruction of vacuoles by ice crystals and the massive outflow of cell fluid. Repeated freezing and thawing will cause more water loss, which will reduce the TSS content. However, there was a study speculating that the degradation of starch and other substances caused by long-term storage increases the content of soluble sugars [Liu *et al.*, 2019], which explains why the TSS content has increased after three freeze-thaw cycles. Some studies had also pointed out that fructose and glucose contents of slow frozen (-20°C) *Prunus mume* fruits were higher after thawing than of the fast frozen fruits (-50°C) [Chung *et al.*, 2013]. With subsequent freeze-thaw cycles under the two freezing conditions, the content of TSS first decreased and then increased (Figure 1). However, under the same number of freeze-thaw cycles, there was a significant ($p < 0.05$) difference in the content of TSS under the two freezing conditions, indicating that the content of TSS was related to the freezing method.

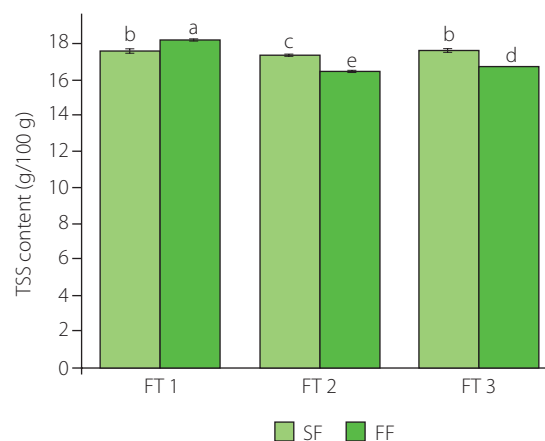


Figure 1. The content of total soluble solids (TSS) in fresh Nanguo pears and after three freeze-thaw cycles (FT1, FT2 and FT3, respectively). SF means freezing at -20°C and FF means freezing at -80°C . Different letters above bars indicate significant differences ($p < 0.05$).

Table 1. The content of organic acids ($\mu\text{g/g}$ flesh) in fresh Nanguo pears and after three freeze-thaw cycles (FT1, FT2 and FT3, respectively) with freezing at -20°C (SF) and -80°C (FF).

| Organic acid | Fresh | SF-FT1 | SF-FT2 | SF-FT3 | FF-FT1 | FF-FT2 | FF-FT3 |
|-----------------|-------------------------------|-------------------------------|-------------------------------|-------------------------------|-------------------------------|-------------------------------|-------------------------------|
| Oxalic acid | 7.34 \pm 0.01 ^a | 5.67 \pm 0.01 ^d | 5.35 \pm 0.00 ^f | 6.15 \pm 0.01 ^b | 5.76 \pm 0.03 ^c | 5.56 \pm 0.03 ^e | 5.56 \pm 0.03 ^e |
| L-Tartaric acid | 6.15 \pm 0.26 ^a | 0.59 \pm 0.05 ^{de} | 0.54 \pm 0.00 ^{de} | 0.29 \pm 0.06 ^e | 2.44 \pm 0.15 ^b | 0.71 \pm 0.06 ^d | 1.77 \pm 0.07 ^c |
| L-Malic acid | 24.30 \pm 0.05 ^a | 13.53 \pm 0.07 ^d | 13.49 \pm 0.09 ^d | 13.27 \pm 0.10 ^d | 15.88 \pm 0.34 ^b | 15.18 \pm 0.07 ^c | 13.01 \pm 0.10 ^d |
| Shikimic acid | 7.13 \pm 0.04 ^a | 2.77 \pm 0.00 ^f | 3.58 \pm 0.04 ^d | 3.37 \pm 0.01 ^e | 6.20 \pm 0.10 ^b | 5.83 \pm 0.04 ^c | 6.18 \pm 0.06 ^b |
| Citric acid | 63.50 \pm 0.04 ^a | 38.26 \pm 0.01 ^b | 37.05 \pm 0.14 ^c | 34.20 \pm 0.18 ^d | 32.17 \pm 0.05 ^e | 26.16 \pm 0.48 ^f | 28.35 \pm 0.26 ^g |
| Sum | 108.41 | 60.81 | 60.01 | 57.27 | 62.45 | 53.45 | 54.88 |

Mean values \pm standard deviation of three replicate measurements were shown. Values with different lowercase letters in the same row were significantly different ($p < 0.05$).

■ Effects of freeze-thaw cycles on organic acid content of Nanguo pear

The composition of organic acids is an important factor influencing the flavor quality and nutritional value of fruits. In addition, organic acids can provide energy for the body, prevent cardiovascular disease by regulating metabolism, while showing excellent bacterial-inhibiting function [Shi *et al.*, 2022].

In organic acid composition of fresh Nanguo pears, the content of citric acid reached 63.50 $\mu\text{g/g}$ and was significantly ($p < 0.05$) higher than those of other acids (Table 1). In other studies, Wang *et al.* [2021] determined the content of citric acid in fresh Nanguo pear at 1.4 mg/g and Chen *et al.* [2007] at 309 mg/kg. These values are different from the results determined in this study, which may be due to differences in the maturity of the purchased pears. The content of citric acid decreased after one freeze-thaw cycle to 38.26 and 32.17 $\mu\text{g/g}$ in both slow (-20°C) and fast (-80°C) freezing conditions, respectively. The opposite phenomenon was observed by Liu *et al.* [2019], who found that the citric acid content in fresh 'Ruane' pears and these pears frozen at -20°C and directly thawed was similar ($p < 0.05$), and even increased when the frozen fruits were stored for 1–12 days. The content of citric acid in pears of FF-FT2 and FF-FT3 groups was lower than that in SF-FT2 and SF-FT3 groups, respectively (Table 1). Contents of oxalic acid, shikimic acid, L-tartaric acid and L-malic acid in pears were also significantly ($p < 0.05$) lower after freeze-thaw cycles compared to fresh fruits. The total amount of five organic acids decreased subsequently after each freeze-thaw cycle, and pears of the FF-FT1 group had slightly higher total organic acid content than the fruits from the other treatment groups. The sum of organic acids in the SF-FT3 group and the FF-FT3 group was very similar, indicating that freezing conditions had no significant effect on the total organic acid content of Nanguo pears when the number of freeze-thaw cycles was high.

■ Effects of freeze-thaw cycles on the odor of Nanguo pear

An electronic nose system is a kind of odor-testing equipment, replacing the human olfactory system, with higher sensitivity and faster detection speed [Zhang *et al.*, 2008]. In Figure 2A, the radar chart is shown established by the e-nose sensor data collection according to the response value of each sample,

and each curve represents the odor intensity of the fresh pears and pears after each freeze-thaw cycle. There were no differences ($p \geq 0.05$) between the samples in the response values of sensors R4, R7 and R9, *e.g.*, to hydrogen, inorganic sulfides such as hydrogen sulfide, and organic sulfides. However, there were significant differences ($p < 0.05$) in sensor R2 and R6 response, indicating that multiple freeze-thaw treatments had the greatest effect on nitrogen oxide and methyl-containing hydrocarbons in pears. The response values of other sensors were also slightly different between samples. These differences might be due to the release of volatile compounds due to the rupture of cell membranes caused by ice crystals during repeated freeze-thaw cycles [Pedrosa-López *et al.*, 2022]. The radar map showed no significant differences between the fruit samples subjected to rapid freezing and slow freezing.

Figure 2B shows the principal component analysis (PCA) diagram of Nanguo pears after 1, 2 and 3 freeze-thaw cycles under different freezing conditions, using the response values of e-nose sensors as variables. The first principal component (PC1) represented 80.21% of total variability, and the second principal component (PC2) – 19.56%. The explanatory rate of total variability was 99.77%, greater than 70–85%, indicating that these two factors held most of the sample information [Chen *et al.*, 2021]. There was significant discrimination along PC1 between the fresh Nanguo pear and the freeze-thaw Nanguo pears, indicating that there were differences in their odor substances. Variables for the SF-FT2 and FF-FT3 samples had partial overlap along the PC1, and the PC2 could not be distinguished effectively. The results showed that the SF-FT2 and FF-FT3 samples had some similar odor substances. Linear discriminant analysis (LDA) was also performed on odor compounds of different pear samples detected by e-nose, and results are shown in Figure 2C. Overall, the data collected for the different freeze-thaw cycles did not overlap significantly (except FF-FT-1 and FF-FT-2 samples), which indicated that the freeze-thaw cycle had a significant effect on the odorant compounds. However, the formation of these volatiles changing during freezing and thawing needs to be further studied.

■ Effect of freeze-thaw cycle on the taste of Nanguo pear

An electronic tongue is a multi-sensor system designed to simulate the unique taste perception ability of human beings. It

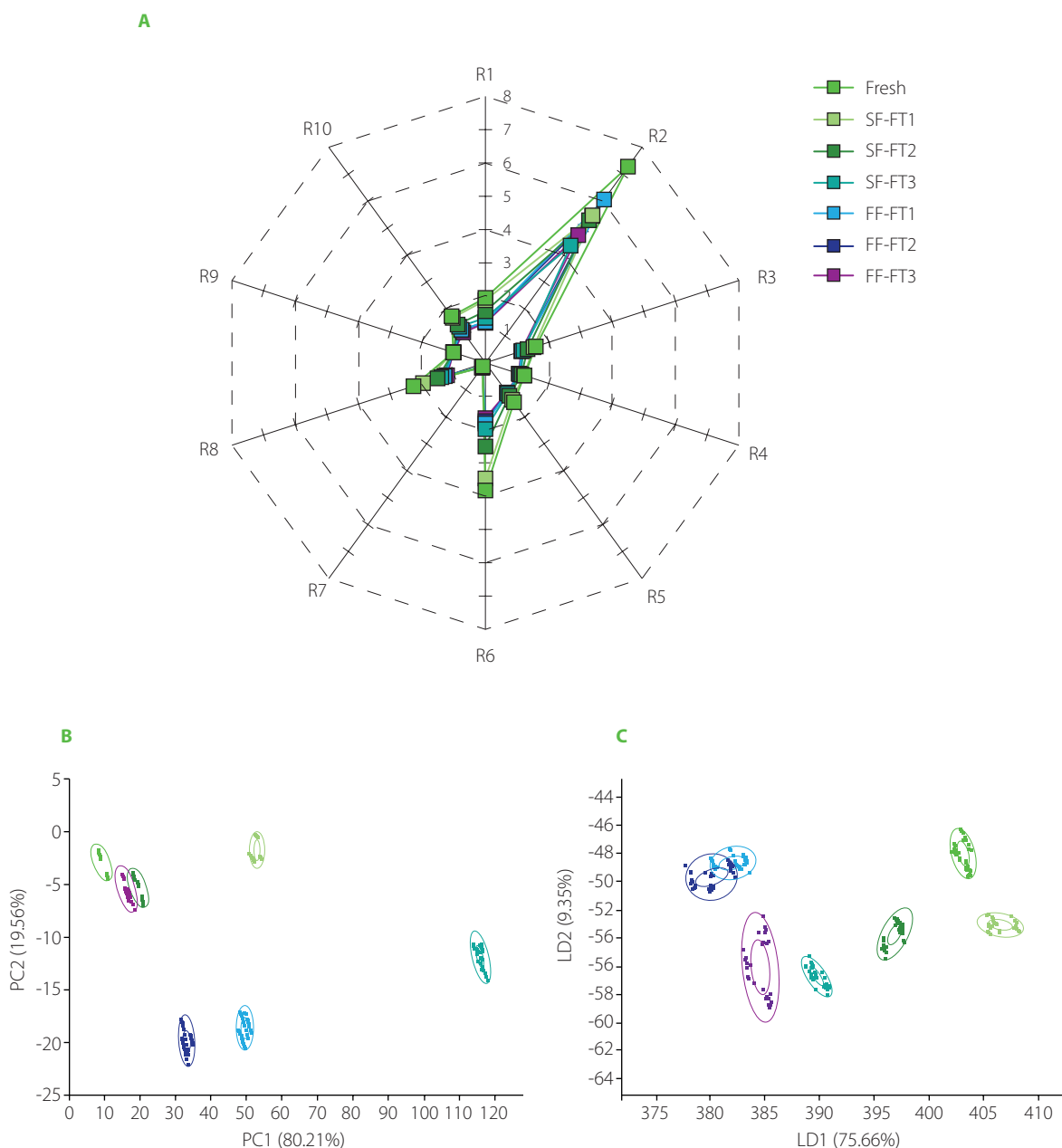


Figure 2. Results of odor analysis by e-nose of Nanguo pear after three freeze-thaw cycles (FT1, FT2 and FT3, respectively). **(A)** Radar diagram of response value of R1–R10 e-nose sensors (R1 – aromatic compounds, R2 – nitrogen oxide, R3 – ammonia and aromatic compounds, R4 – hydrogen, R5 – olefin and aromatic compounds, R6 – hydrocarbons, R7 – hydrogen sulfide, R8 – alcohols and partially aromatic compounds, R9 – aromatic compounds and organic sulfides, R10 – alkanes); **(B)** Principal component analysis (PCA) plot; **(C)** Linear discriminant analysis (LDA) plot. SF means freezing at -20°C and FF means freezing at -80°C .

is used to study the five basic tastes (sweet, salty, sour, bitter, and umami) as well as taste sensations including astringency and pungency [Rosa *et al.*, 2017].

Figure 3A shows the radar diagram of sensor response values in Nanguo pears taste analysis using e-tongue. There were no significant differences ($p \geq 0.05$) in abundance of aftertaste-A (aftertaste-astringent) and aftertaste-B (aftertaste-bitter) among the 7 samples. There were significant differences ($p < 0.05$) between pears of freeze-thaw groups and fresh pears in sour, bitter, astringent, salty and umami taste. Rapid freezing could produce smaller ice crystals than slow freezing due to the rapid temperature drop [Alabi *et al.*, 2020]; hence, it caused less damage to the structure of fruit cells and tissues, and less

cell contents were dissolved, while slow freezing caused greater cell content dissolution, resulting in a large difference in the taste of fast-frozen and slow-frozen Nanguo pears. The results of sour taste analysis showed that, except for the FF-FT1 and SF-FT2 groups, the sourness of pears of the other groups was lower compared to the fresh fruits (Figure 3A). PCA analysis of the signal values of the e-tongue found that PC1 and PC2 represented 47.69% and 32.23% of total variability, respectively (Figure 3B), and the sum of both was 79.92%, indicating that the two principal components were representative. In addition, the distribution of points corresponding to experimental groups in the PCA plot is relatively scattered, which indicates that different freezing methods and the number of freezing and thawing cycles caused

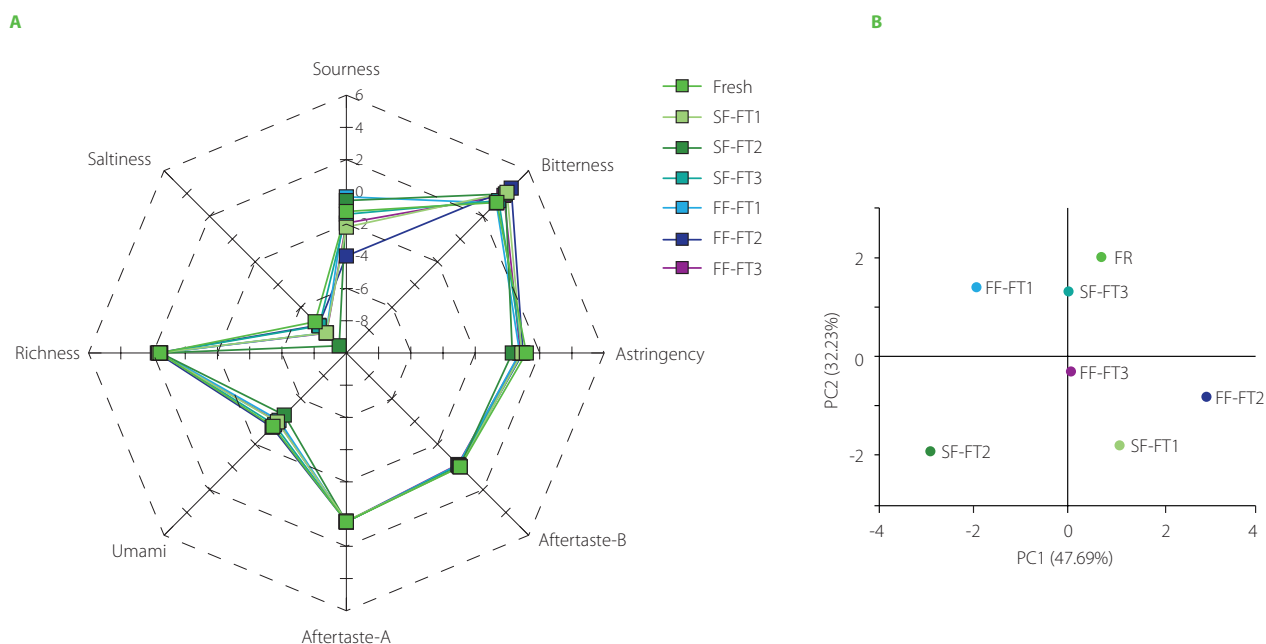


Figure 3. Results of taste analysis by e-tongue of Nanguo pear after three freeze-thaw cycles (FT1, FT2 and FT3, respectively). (A) Radar diagram of response value of e-tongue sensor; (B) Principal component analysis (PCA) plot. SF means freezing at -20°C and FF means freezing at -80°C .

differences in the taste of pears. As mentioned above, these differences could be closely related to the ice crystal formation under different freezing modes. At the same time, the freeze-thaw cycle of pears was a complex process, and the pear flavor change was not only due to the ice crystal interaction; therefore, also the deeper reasons need to be further explored.

■ Effects of freeze-thaw cycles on volatile ester profile of Nanguo pear

Aroma is an important quality feature of fruit. The aroma of fruits was formed by the mixture of many volatile esters, alcohols, aldehydes, ketones and other compounds. The esters are the main volatile compounds that determine the aroma of Nanguo pear [Zhang & Yin, 2023].

Table 2 shows the contents of 24 major volatile esters of Nanguo pear flesh. The total content of esters in fresh pears was $743.86\ \mu\text{g}/\text{kg}$. The sum of esters decreased to $677.74\ \mu\text{g}/\text{kg}$ after one freeze-thaw cycle under slow freezing condition. Then, it increased gradually with the subsequent freeze-thaw cycles. After one freeze-thaw cycle under fast freezing condition, the sum of esters of Nanguo pears was $863.36\ \mu\text{g}/\text{kg}$, which was significantly higher than that of fresh fruits and pears of the SF-FT1 group. With the increase of freeze-thaw cycles, the sum of esters continued to increase and then decreased. In flesh, hexyl acetate, ethyl butyrate, ethyl caproate (ethyl hexanoate) and ethyl (*E,Z*)-2,4-decadienoate were the main esters. The content of ethyl caproate in pear flesh was the highest among esters and ranged from 377.26 to $526.77\ \mu\text{g}/\text{kg}$. This finding is consistent with literature data which reported that ethyl hexanoate was the major volatile compound of Nanguo pears regardless of their ripeness or plant growing locations [Li *et al.*, 2013; Shi *et al.*, 2018]. The odor detection threshold (ODT) value of ethyl caproate is

only $1.2\ \mu\text{g}/\text{kg}$ [Munafo *et al.*, 2016], indicating that ethyl caproate could be the main compound determining the aroma of Nanguo pears. In the previous studies, it was found that the content of ethyl caproate affected the aroma of pineapple and banana [Dou *et al.*, 2020; Steingass *et al.*, 2014]. As the main detected esters, ethyl hexanoate had the greatest effect on the overall ester content of Nanguo pears, so that the content change trend of total esters after freeze-thaw cycles was consistent with that of ethyl caproate.

CONCLUSIONS

There were significant differences in the flavor quality of Nanguo pear after three freeze-thaw cycles. The results of analysis performed with the e-nose showed that the freeze-thaw cycle had the greatest effect on nitrogen oxide and hydrocarbons in Nanguo pears. In terms of sour, bitter, astringent, salty and umami taste, there were significant differences between fresh pears and those treated by the freeze-thaw cycles. Due to the repeated melting and recombination of ice crystals, the structure of the fruits was further damaged, resulting in little correlation between fruit flavor and the number of freeze-thaw cycles.

RESEARCH FUNDING

This work was financed by Basic Research Project of Education Department of Liaoning Province (project NO.LJ2020007).

CONFLICT OF INTERESTS

The authors declare that they have no conflict of interests.

ORCID IDs

G. Bai
X. Cao
Y. Wang

<https://orcid.org/0000-0002-9958-8910>
<https://orcid.org/0000-0002-5434-0938>
<https://orcid.org/0009-0000-5640-4360>

Table 2. The content of volatile esters ($\mu\text{g}/\text{kg}$ flesh) in fresh Nanguo pears and after three freeze-thaw cycles (FT1, FT2 and FT3, respectively) with freezing at -20°C (SF) and -80°C (FF).

| Ester | Fresh | SF-FT1 | SF-FT2 | SF-FT3 | FF-FT1 | FF-FT2 | FF-FT3 |
|----------------------------------------|---------------------------------|---------------------------------|----------------------------------|----------------------------------|-----------------------------------|---------------------------------|----------------------------------|
| Ethyl acetate | 11.48 \pm 0.87 ^{ab} | 11.83 \pm 0.64 ^a | 7.81 \pm 0.50 ^c | 8.46 \pm 0.08 ^c | 7.91 \pm 2.09 ^c | 9.62 \pm 0.88 ^{bc} | 5.19 \pm 0.55 ^d |
| Butyl acetate | 8.65 \pm 0.23 ^d | 10.30 \pm 0.76 ^c | 10.62 \pm 0.22 ^c | 11.92 \pm 0.69 ^b | 14.17 \pm 1.15 ^a | 14.68 \pm 0.56 ^a | 14.26 \pm 0.19 ^a |
| Hexyl acetate | 127.04 \pm 6.98 ^b | 129.78 \pm 1.02 ^b | 138.88 \pm 11.53 ^{ab} | 147.19 \pm 10.74 ^{ab} | 163.36 \pm 39.50 ^{ab} | 151.90 \pm 3.27 ^{ab} | 178.40 \pm 11.77 ^a |
| Heptyl acetate | 4.47 \pm 0.28 ^c | 5.43 \pm 0.39 ^{bc} | 6.21 \pm 1.19 ^{abc} | 6.78 \pm 0.20 ^{abc} | 7.96 \pm 2.40 ^a | 7.55 \pm 0.53 ^{ab} | 8.71 \pm 0.43 ^a |
| Decyl acetate | 0.59 \pm 0.06 ^{bcd} | 0.36 \pm 0.08 ^d | 0.51 \pm 0.06 ^{bcd} | 0.780 \pm 0.04 ^{abcd} | 0.48 \pm 0.17 ^c | 0.72 \pm 0.02 ^{abc} | 0.96 \pm 0.23 ^a |
| Propionic acid ethyl ester | 1.23 \pm 0.13 ^a | 0.48 \pm 0.01 ^c | 0.69 \pm 0.17 ^c | 0.94 \pm 0.13 ^{ab} | ND | 1.13 \pm 0.10 ^a | ND |
| Butyric acid methyl ester | 5.74 \pm 0.80 ^a | 3.02 \pm 0.86 ^c | 3.38 \pm 0.65 ^{bc} | 4.46 \pm 0.53 ^b | 6.35 \pm 0.24 ^a | 4.32 \pm 0.40 ^b | 3.39 \pm 0.24 ^{bc} |
| Ethyl butyrate | 65.02 \pm 3.55 ^a | 52.57 \pm 0.47 ^{ab} | 49.62 \pm 7.06 ^b | 50.88 \pm 0.05 ^{ab} | 57.65 \pm 13.61 ^{ab} | 58.21 \pm 3.82 ^{ab} | 57.38 \pm 0.63 ^{ab} |
| Hexyl butyrate | 2.22 \pm 0.31 ^e | 4.05 \pm 0.12 ^{bc} | 3.93 \pm 0.88 ^{bc} | 4.60 \pm 0.91 ^{ab} | 3.25 \pm 0.53 ^{cd} | 2.85 \pm 0.30 ^{de} | 5.32 \pm 0.01 ^a |
| Ethyl valerate | 4.47 \pm 0.30 ^{ab} | 3.48 \pm 0.29 ^c | 3.90 \pm 0.62 ^{abc} | 3.76 \pm 0.40 ^{bc} | 3.79 \pm 0.68 ^{abc} | 4.75 \pm 0.39 ^a | 4.00 \pm 0.38 ^{abc} |
| Methyl caproate | 29.10 \pm 1.57 ^{ab} | 23.70 \pm 0.55 ^{ab} | 21.15 \pm 0.15 ^b | 28.07 \pm 0.78 ^{ab} | 32.29 \pm 10.54 ^a | 27.69 \pm 0.34 ^{ab} | 19.60 \pm 1.33 ^b |
| Ethyl caproate | 430.41 \pm 6.73 ^{ab} | 377.26 \pm 33.15 ^b | 437.51 \pm 10.72 ^{ab} | 446.10 \pm 9.58 ^{ab} | 495.59 \pm 141.86 ^{ab} | 526.77 \pm 5.31 ^a | 426.92 \pm 25.51 ^{ab} |
| Propyl hexanoate | 1.37 \pm 0.14 ^{cd} | 0.86 \pm 0.27 ^a | 1.14 \pm 0.00 ^{cd} | 0.99 \pm 0.01 ^{ad} | 1.72 \pm 0.36 ^{bc} | 1.85 \pm 0.04 ^b | 2.38 \pm 0.16 ^a |
| Hexyl hexanoate | 2.36 \pm 0.48 ^c | 3.03 \pm 0.67 ^{abc} | 2.95 \pm 0.55 ^{bc} | 5.48 \pm 0.35 ^a | 4.25 \pm 2.79 ^{abc} | 2.68 \pm 0.36 ^{bc} | 5.24 \pm 0.11 ^{ab} |
| Ethyl oenanthate | 5.03 \pm 0.27 ^b | 3.56 \pm 0.24 ^c | 3.49 \pm 0.38 ^c | 2.42 \pm 0.35 ^d | 7.71 \pm 0.35 ^a | 7.47 \pm 0.56 ^a | 4.78 \pm 0.28 ^b |
| Methyl caprylate | 0.53 \pm 0.04 ^{bc} | 0.24 \pm 0.01 ^d | 0.19 \pm 0.03 ^d | 0.13 \pm 0.03 ^d | 1.24 \pm 0.31 ^a | 0.73 \pm 0.00 ^b | 0.37 \pm 0.08 ^{cd} |
| Ethyl <i>trans</i> -2-octenoate | 9.45 \pm 1.73 ^c | 13.23 \pm 0.70 ^{bc} | 16.83 \pm 4.97 ^{ab} | 20.31 \pm 0.51 ^a | 14.79 \pm 5.42 ^{abc} | 16.60 \pm 1.56 ^{ab} | 12.50 \pm 1.22 ^{bc} |
| Ethyl 2-methyl butyrate | 4.49 \pm 0.72 ^d | 13.38 \pm 0.81 ^a | 10.03 \pm 1.64 ^b | 10.69 \pm 1.20 ^b | 7.02 \pm 0.38 ^c | 12.14 \pm 1.31 ^{ab} | 4.71 \pm 0.60 ^d |
| Ethyl 2-hexenoate | 4.64 \pm 0.55 ^a | 4.33 \pm 0.43 ^a | 3.99 \pm 0.50 ^{abc} | 4.65 \pm 0.47 ^a | 3.15 \pm 0.83 ^c | 4.25 \pm 0.23 ^{ab} | 3.36 \pm 0.19 ^{bc} |
| Ethyl 3-hydroxy caproate | 3.50 \pm 1.59 ^a | 0.57 \pm 0.02 ^b | 1.70 \pm 0.55 ^{ab} | 2.09 \pm 0.35 ^b | 0.52 \pm 0.18 ^b | 1.02 \pm 0.27 ^b | 1.93 \pm 0.17 ^{ab} |
| Methyl (<i>E,Z</i>)-2,4-decadienoate | ND | 3.20 \pm 0.29 ^{ab} | 1.78 \pm 1.56 ^b | 7.03 \pm 2.55 ^a | 6.37 \pm 4.31 ^a | 5.55 \pm 0.90 ^{ab} | 4.64 \pm 0.42 ^{ab} |
| 2,4-Ethyl decadienylate | 21.69 \pm 4.11 ^{bc} | 12.36 \pm 3.14 ^c | 20.68 \pm 0.94 ^{bc} | 38.38 \pm 2.08 ^a | 22.83 \pm 18.39 ^{bc} | 27.55 \pm 9.25 ^{ab} | 22.92 \pm 2.73 ^{bc} |
| Ethyl phenylacetate | 0.39 \pm 0.05 ^d | 0.67 \pm 0.06 ^{bc} | 0.55 \pm 0.09 ^{cd} | 0.74 \pm 0.08 ^b | 0.94 \pm 0.07 ^a | 0.82 \pm 0.02 ^{ab} | 0.72 \pm 0.16 ^{bc} |
| Di- <i>iso</i> -butyl phthalate | ND | 0.07 \pm 0.04 | ND | ND | 0.04 \pm 0.00 | ND | ND |
| Sum | 743.86 | 677.74 | 747.53 | 806.83 | 863.36 | 890.85 | 787.66 |

Mean values \pm standard deviation of three replicate measurements were shown. Values with different lowercase letters in the same row were significantly different ($p < 0.05$). ND, not detected.

REFERENCES

- Alabi, K.P., Zhu, Z., Sun, D.W. (2020). Transport phenomena and their effect on microstructure of frozen fruits and vegetables. *Trends in Food Science & Technology*, 101, 63–72. <https://doi.org/10.1016/j.tifs.2020.04.016>
- Apra, E., Charles, M., Endrizzi, I., Corollaro, M.L., Betta, E., Biasioli, F., Gasperi, F. (2017). Sweet taste in apple: The role of sorbitol, individual sugars, organic acids and volatile compounds. *Scientific Reports*, 7(1), art. no. 44950. <https://doi.org/10.1038/srep44950>
- Chen, J., Wang, Z., Wu, J., Wang, Q., Hu, X. (2007). Chemical compositional characterization of eight pear cultivars grown in China. *Food Chemistry*, 104(1), 268–275. <https://doi.org/10.1016/j.foodchem.2006.11.038>
- Chen, Y., Pan, H., Hao, S., Pan, D., Wang, G., Yu, W. (2021). Evaluation of phenolic composition and antioxidant properties of different varieties of Chinese citrus. *Food Chemistry*, 364, art. no. 130413. <https://doi.org/10.1016/j.foodchem.2021.130413>
- Chung, H.S., Kim, D.S., Kim, H.S., Lee, Y.G., Seong, J.H. (2013). Effect of freezing pretreatment on the quality of juice extracted from *Prunus mume* fruit by osmosis with sucrose. *LWT – Food Science and Technology*, 54(1), 30–34. <https://doi.org/10.1016/j.lwt.2013.05.016>
- Cui, B., Liu, S.M., Zheng, T. (2022). Chemotaxonomic identification of key taste and nutritional components in ‘Shushanggan Apricot’ fruits by widely targeted metabolomics. *Molecules*, 27(12), art. no. 3870. <https://doi.org/10.3390/molecules27123870>
- Cui, T., Nakamura, K., Ma, L., Li, J.-Z., Kayahara, H. (2005). Analyses of arbutin and chlorogenic acid, the major phenolic constituents in oriental pear. *Journal of Agricultural and Food Chemistry*, 53(10), 3882–3887. <https://doi.org/10.1021/jf047878k>
- Dou, T.X., Shi, J.F., Li, Y., Bi, F.C., Gao, H.J., Hu, C.H., Li, C.Y., Yang, Q.S., Deng, G.M., Sheng, O., He, W.-D., Yi, G.-J., Dong, T. (2020). Influence of harvest season on volatile aroma constituents of two banana cultivars by electronic nose and HS-SPME coupled with GC-MS. *Scientia Horticulturae*, 265, art. no. 109214. <https://doi.org/10.1016/j.scienta.2020.109214>
- Kanski, L., Naumann, M., Pawelzik, E. (2020). Flavor-related quality attributes of ripe tomatoes are not significantly affected under two common household conditions. *Frontiers in Plant Science*, 11, art. no. 472. <https://doi.org/10.3389/fpls.2020.00472>
- Keutgen, A., Pawelzik, E. (2007a). Modifications of taste-relevant compounds in strawberry fruit under NaCl salinity. *Food Chemistry*, 105(4), 1487–1494. <https://doi.org/10.1016/j.foodchem.2007.05.033>
- Keutgen, A.J., Pawelzik, E. (2007b). Quality and nutritional value of strawberry fruit under long term salt stress. *Food Chemistry*, 107(4), 1413–1420. <https://doi.org/10.1016/j.foodchem.2007.09.071>
- Li, G., Jia, H., Wu, R., Teng, Y. (2013). Changes in volatile organic compound composition during the ripening of ‘Nanguoli’ pears (*Pyrus ussuriensis* Maxim) harvested at different growing locations. *The Journal of Horticultural Science and Biotechnology*, 88(5), 563–570. <https://doi.org/10.1080/14620316.2013.11513007>
- Li, X., Zhang, J.Y., Gao, W.Y., Wang, Y., Wang, H.Y., Cao, J.G., Huang, L.Q. (2012). Chemical composition and anti-inflammatory and antioxidant activities of eight pear cultivars. *Journal of Agricultural and Food Chemistry*, 60(35), 8738–8744. <https://doi.org/10.1021/jf303235h>
- Liu, Y., Wu, Y., Che, F., Zhang, Z., Chen, B. (2019). Physical–chemical composition and quality related changes in ‘Ruener’ pear (*Pyrus ussuriensis*) during freezing–thawing period. *Molecules*, 24(14), art. no. 2611. <https://doi.org/10.3390/molecules24142611>
- Luo, M., Zhou, X., Sun, H., Zhou, Q., Ge, W., Sun, Y., Yao, M., Ji, S. (2021). Insights into profiling of volatile ester and LOX-pathway related gene families accompanying post-harvest ripening of ‘Nanguo’ pears. *Food Chemistry*, 335, art. no. 127665. <https://doi.org/10.1016/j.foodchem.2020.127665>
- Munafo, J.P., Didzbalis, J., Schnell, R.J., Steinhaus, M. (2016). Insights into the key aroma compounds in mango (*Mangifera indica* L. ‘Haden’) fruits by stable isotope dilution quantitation and aroma simulation experiments. *Journal of Agricultural and Food Chemistry*, 64(21), 4312–4318. <https://doi.org/10.1021/acs.jafc.6b00822>
- Ndraha, N., Hsiao, H.I., Vljajic, J., Minfeng, Y., Lin, H.V. (2018). Time-temperature abuse in the food cold chain: Review of issues, challenges, and recommendations. *Food Control*, 89, 12–21. <https://doi.org/10.1016/j.foodcont.2018.01.027>
- Pedrosa-López, M.D.C., Aragón-García, F., Ruiz-Rodríguez, A., Piñeiro, Z., Durán-Guerrero, E., Palma, M. (2022). Effects from the freezing of either whole or crushed grapes on the volatile compounds contents in muscat wines. *Foods*, 11(12), art. no. 1782. <https://doi.org/10.3390/foods11121782>
- Rosa, A., Leone, F., Cheli, F., Chiofalo, V. (2017). Fusion of electronic nose, electronic tongue and computer vision for animal source food authentication and quality assessment – A review. *Journal of Food Engineering*, 210, 62–75. <https://doi.org/10.1016/j.jfoodeng.2017.04.024>
- Shi, F., Zhou, X., Zhou, Q., Tan, Z., Yao, M.M., Wei, B.D., Ji, S.J. (2018). Membrane lipid metabolism changes and aroma ester loss in low-temperature stored Nanguo pears. *Food Chemistry*, 245, 446–453. <https://doi.org/10.1016/j.foodchem.2017.10.091>
- Shi, Y., Pu, D., Zhou, X., Zhang, Y. (2022). Recent progress in the study of taste characteristics and the nutrition and health properties of organic acids in foods. *Foods*, 11(21), art. no. 3408. <https://doi.org/10.3390/foods11213408>
- Steingass, C.B., Grauwet, T., Carle, R. (2014). Influence of harvest maturity and fruit logistics on pineapple (*Ananas comosus* [L.] Merr.) volatiles assessed by headspace solid phase microextraction and gas chromatography–mass spectrometry (HS-SPME-GC/MS). *Food Chemistry*, 150, 382–391. <https://doi.org/10.1016/j.foodchem.2013.10.092>
- Tao, D., Wang, J., Zhang, L., Jiang, Y., Lv, M. (2019). 1-Methylcyclopropene alleviates peel browning of ‘Nanguo’ pears by regulating energy, antioxidant and lipid metabolisms after long term refrigeration. *Scientia Horticulturae*, 247, 254–263. <https://doi.org/10.1016/j.scienta.2018.12.025>
- Vu, N.D., Nguyen, V.M., Tran, T.T. (2023). Effects of pH, total soluble solids, and pectin concentration on color, texture, vitamin C, and sensory quality of mango fruit bar. *International Journal of Food Science*, 2023, 6618300–6618300. <https://doi.org/10.1155/2023/6618300>
- Wang, J., Xin, Z., Qian, Z., Cheng, S., Wei, B., Ji, S. (2017). Low temperature conditioning alleviates peel browning by modulating energy and lipid metabolisms of ‘Nanguo’ pears during shelf life after cold storage. *Postharvest Biology & Technology*, 131, 10–15. <https://doi.org/10.1016/j.postharvbio.2017.05.001>
- Wang, X., Liu, C., Wang, Q., Liu, C., Sun, H., Zhang, M., Lyu, D., Du, G. (2021). A comparative study on antioxidant, anti-inflammatory, antimicrobial activities and chemical composition of *Pyrus ussuriensis* cultivars from northeastern China. *Horticulture, Environment, and Biotechnology*, 62, 477–491. <https://doi.org/10.1007/s13580-020-00322-x>
- Wei, S., Qin, G., Zhang, H., Tao, S., Wu, J., Wang, S., Zhang, S. (2017). Calcium treatments promote the aroma volatiles emission of pear (*Pyrus ussuriensis* ‘Nanguoli’) fruit during post-harvest ripening process. *Scientia Horticulturae*, 215, 102–111. <https://doi.org/10.1016/j.scienta.2016.12.008>
- Yan, X., Dong, T., Yun, X., Tanaka, F., Tanaka, F., Wardana, A.A., Meng, F. (2023). Improving ‘Nanguo’ pear fungal disease and storability by chitosan coating combined with diepoxy-poly (ethylene glycol). *Food Bioscience*, 53, art. no. 102842. <https://doi.org/10.1016/j.fbio.2023.102842>
- Zhang, H., Wang, J., Ye, S. (2008). Prediction of soluble solids content, firmness and pH of pear by signals of electronic nose sensors. *Analytica Chimica Acta*, 606(1), 112–118. <https://doi.org/10.1016/j.jaca.2007.11.003>
- Zhang, L., Wang, J.W., Zhou, X., Shi, F., Ji, S.J. (2018). Effect of ATP treatment on enzymes involved in energy and lipid metabolisms accompany peel browning of ‘Nanguo’ pears during shelf life after low temperature storage. *Scientia Horticulturae*, 240, 446–452. <https://doi.org/10.1016/j.scienta.2018.06.036>
- Zhang, X., Wei, X., Ali, M.M., Rizwan, H.M., Li, B., Li, H., Jia, K., Yang, X., Ma, S., Li, S., Chen, F. (2021). Changes in the content of organic acids and expression analysis of citric acid accumulation-related genes during fruit development of yellow (*Passiflora edulis* f. *flavicarpa*) and purple (*Passiflora edulis* f. *edulis*) passion fruits. *International Journal of Molecular Sciences*, 22(11), art. no. 5765. <https://doi.org/10.3390/ijms22115765>
- Zhang, Z., Yin, Z. (2023). The aroma volatile in ‘Nanguo’ pear: A review. *Horticulturae*, 9(3), art. no. 339. <https://doi.org/10.3390/horticulturae9030339>
- Zhou, X., Dong, L., Li, R., Zhou, Q., Wang, J.W., Ji, S.J. (2015). Low temperature conditioning prevents loss of aroma-related esters from ‘Nanguo’ pears during ripening at room temperature. *Postharvest Biology and Technology*, 100, 23–32. <https://doi.org/10.1016/j.postharvbio.2014.09.012>
- Zhu, D., Ren, X., Wei, L., Cao, X., Ge, Y., Liu, H., Li, J. (2020). Collaborative analysis on difference of apple fruits flavour using electronic nose and electronic tongue. *Scientia Horticulturae*, 260, art. no. 108879. <https://doi.org/10.1016/j.scienta.2019.108879>

Recovery of Proteins from Sweet Potato Cell Liquid by Acidification *via* Inoculation-Enhanced Fermentation and Determination of Functional Properties of Protein Products

Qingshuai Li^{1,2}, Liping Liu^{1,2}, Yanlei Han^{1,2}, Xiangying Zhao^{1,2}, Mingjing Yao^{1,2}, Jing Ma^{1,2}, Mo Han^{1,2}, Jiaxiang Zhang^{1,2*}

¹Shandong Food Ferment Industry Research & Design Institute, Qilu University of Technology (Shandong Academy of Sciences), Jinan 250013, China
²School of Food Science and Engineering, Qilu University of Technology (Shandong Academy of Sciences), Jinan 250353, China

Starch production from fresh sweet potatoes generates process wastewater called sweet potato cell liquid (SPCL), which is rich in sweet potato protein (SPP). Currently, the commonly used protein recovery methods, such as isoelectric point precipitation and ultrafiltration, were not suitable for SPP recovery due to the low protein content of SPCL and the high cost of recovery. The feasibility of recovering SPP by SPCL acidification *via* inoculation-assisted fermentation was investigated in this study. The results indicated that the pH of SPCL could be reduced to approximately 4.0 within 6 h of fermentation with inoculation, resulting in an SPP extraction yield of 55.45% and purity of 66.23 g protein/100 g. With the addition of heating treatment, the extraction yield of SPP increased to 76.97–95.34%, while it maintained the purity of 66.36–70.12 g protein/100 g. The composition analysis revealed that SPP products contained sugars (below 11.5 g/100 g) in addition to protein and trace amounts of lignin and phenolics. Functional properties analysis showed that the SPP recovered by inoculation-enhanced fermentation exhibited better emulsifying and foaming properties, and higher digestibility compared to the SPP precipitated using hydrochloric acid. The method of extracting SPP from SPCL by inoculation-enhanced fermentation, as developed in this study, was a straightforward and cost-effective process that fosters significant potential for industrial applications.

Key words: sweet potato proteins, *Leuconostoc citreum*, protein precipitation, digestibility, emulsification, foaming

INTRODUCTION

Sweet potato is a dicotyledonous plant with tuberous roots, which belongs to the genus *Ipomoea* in the family Convolvulaceae and is an important crop species. The root tubers are a rich source of nutrients and bioactive compounds, including starches, proteins, dietary fibers, soluble sugars, carotenoids and anthocyanins, and various minerals such as calcium, iron, phosphorus, and selenium [Tang *et al.*, 2001]. Sweet potatoes rank as the fourth-largest food crop in China, boasting a yearly harvest that surpasses 100 million tons and dominates more than 80% of the world's output [Mu *et al.*, 2009]. Due to its extensive cultivation and high starch content, it

is frequently utilized in the food industry as a crucial raw material for the production of sweet potato starch [Abegunde *et al.*, 2013]. Starch extraction process produces a large amount of sweet potato cell liquid (SPCL) as a discarded by-product, which contains soluble sugars, proteins, and other nutrients [Tang *et al.*, 2001]. This results in significant environmental pollution and the wastage of a valuable nutrient resource. Proteins are one of the main nutrients in SPCL, with a content range of 0.49–2.24 g/100 g [Mu *et al.*, 2014]. Among the sweet potato proteins (SPP), storage proteins (sporamins) are predominant, which account for more than 80% of the total protein [Maeshima *et al.*, 1985], in addition

*Corresponding Author:

e-mail: jxzh23@163.com (J. Zhang)

Submitted: 23 July 2023

Accepted: 19 January 2024

Published on-line: 9 February 2024



© Copyright by Institute of Animal Reproduction and Food Research of the Polish Academy of Sciences
© 2024 Author(s). This is an open access article licensed under the Creative Commons Attribution-NonCommercial-NoDeriv License (<http://creativecommons.org/licenses/by-nc-nd/4.0/>).

to polyphenol oxidase, β -amylase, and other enzyme proteins [Cheng *et al.*, 2015]. The SPP exhibits a well-balanced amino acid profile and favorable functional properties, such as emulsifying and foaming potential as well as water and oil retention ability [Mu *et al.*, 2017]. Additionally, it exhibits remarkable biological activities including lipid-lowering effects, anticancer potential, and antioxidant activity.

Owing to the high nutritional and application value of SPP, efficient techniques for separation and recovery of proteins from SPCL are important, which can maximize resource utilization and minimize environmental pollution. At present, several techniques have been proposed for the recovery of SPP from SPCL, including isoelectric precipitation [Li *et al.*, 2018], heating precipitation [Mu *et al.*, 2017], ultrafiltration [Zhao *et al.*, 2018], and so on. The isoelectric point protein precipitation is primarily employed. In this method, the pH of SPCL is adjusted to 4.0 through the addition of hydrochloric acid or sulfuric acid, which results in protein precipitation with a yield that ranges from a mere 16.00%, and a corresponding purity level of around 50 g protein/100 g [Arogundade & Mu, 2012]. The yield of isoelectric precipitation could be increased to more than 80% by heating [Mu *et al.*, 2017]. SPCL can also be concentrated using ultrafiltration membranes with a molecular weight cut-off of 10,000 Da, and then SPP is obtained by freeze-drying or adjusting pH of precipitation [Arogundade *et al.*, 2012]. The ultrafiltration method produces relatively high extraction yields (41.30–51.30%) and protein purities (76.00–92.95 g protein/100 g) for SPP [Arogundade & Mu, 2012; Zhao *et al.*, 2018]. However, all the aforementioned techniques are isolation methods used by laboratories to investigate the nature of SPP. At the same time, they are not suitable for the recovery of SPP from SPCL on a larger industrial scale due to the low protein content requiring a large volume of SPCL that needs to be processed.

SPCL is a product of fresh sweet potato processing, carrying a large number of microorganisms. During its storage, the pH gradually decreases to approximately 4.0 due to the spontaneous fermentation, leading to protein precipitation [Li & Mu, 2012]. Manufacturers of sweet potato starch have utilized natural storage fermentation precipitation SPP because it requires no additions and is simple to operate. However, this approach is associated with several drawbacks, including a prolonged protein precipitation period, an unstable process cycle, and suboptimal quality of the recovered SPP.

The present study investigated the feasibility of recovering SPP through artificial inoculation and fermentation. Since the functional properties of proteins play a crucial role in food processing, significantly affecting the texture and sensory properties of food, this study further compared the functional properties of SPPs recovered by isoelectric point precipitation with hydrochloric acid and by fermentation under different conditions. The study results are expected to indicate the possibility for industrial recovery and application of sweet potato protein.

MATERIALS AND METHODS

Materials and reagents

Sweet potato (Ji shu No.25) was provided by Sishui Lifeng Factory in Shandong, China. De Man, Rogosa and Sharpe (MRS) broth

medium was purchased from AOBBOX Biotechnology Co (Beijing, China). Methanol for high-performance liquid-chromatography (HPLC) was purchased from J&K Sciences, Inc (Beijing, China). Other reagents and solvents were purchased from Sinopharm Chemical Reagent (Shanghai, China). All solutions were prepared with ultrapure water.

The *Leuconostoc citreum* strain SFZ-T0 was isolated from the spontaneously fermented SPCL in Sishui Lifeng Factory in Shandong and preserved in the collection of the Shandong Jinan Food Fermentation Institute (China).

Preparation of sweet potato cell liquid

SPCL was prepared in accordance with the production process of a sweet potato starch factory as in a previous study by Li *et al.* [2018]. Fresh sweet potatoes were washed, cut into pieces, mixed with twice their volume of drinking water and pulp. The mixture was then filtered through a 260-mesh filter cloth to remove any residue, after which the pulp was centrifuged at 4,000 \times g for 5 min. The resulting supernatant served as the experimental SPCL.

Recovery of sweet potato protein by isoelectric point precipitation

The slightly modified acid precipitation method, previously used by Zhao *et al.* [2019], was applied to recover SPP from SPCL. The pH of SPCL was adjusted to 4.0 using 2 M hydrochloric acid, sulfuric acid, acetic acid, lactic acid, and citric acid, and the mixture was left at room temperature for 2 h. After centrifugation at 6,000 \times g for 10 min, the precipitate was collected, washed twice with water adjusted to 4.0 by adding a 2 M acid solution, and centrifuged again to remove the supernatant. The precipitate was suspended in deionized water (1:1, w/v) and freeze-dried.

Recovery of sweet potato protein by fermentation

To recover SPP by natural fermentation, the freshly prepared SPCL was incubated at room temperature (25°C) until the pH of the sweet potato juice dropped to 4.0–4.5 and clear stratification of the SPCL occurred. After collecting the precipitate, it was centrifuged at 6,000 \times g for 10 min to remove the supernatant. The precipitate was suspended in deionized water (1:1, w/v) and freeze-dried.

Inoculation-enhanced fermentation was carried out with the *L. citreum* SFZ-T0 strain, previously maintained in the laboratory. It underwent two transfers and activations in the MRS medium before being inoculated with a 5% inoculum into the SPCL medium at 30°C for 24 h. The SPCL medium was prepared from sweet potato juice adjusted to a pH of 5.5, heated at 100°C for 10 min, and then centrifuged to remove the precipitate. After autoclaving at 118°C for 20 min, 0.2% yeast extract was added to the clear liquid whose pH was adjusted to 6.0. Subsequently, a 5% inoculate was added into freshly prepared SPCL and incubated at room temperature until the pH of SPCL dropped to 4.0–4.5 and clear stratification of SPCL occurred. After centrifugation at 6,000 \times g for 10 min, the resulting precipitate was collected, washed twice with water adjusted to pH 4.0, and then subjected to further centrifugation to remove the supernatant. The precipitate was suspended in deionized water (1:1, w/v) and freeze-dried.

After fermentation, the SPCL was heated at different temperatures (40°C, 60°C, 80°C, and 100°C) and centrifuged at 6,000×g for 10 min. The sweet potato protein was obtained by direct heating after the supernatant was removed by centrifugation. In the method of stepwise heating (SH), the protein was first heated to a lower temperature (20°C, 40°C, 60°C, and 80°C), the protein sediment was removed by centrifugation and then heated to a higher temperature (40°C, 60°C, 80°C, and 100°C, respectively), and the supernatant was removed by centrifugation to obtain the sweet potato protein at different segmental temperatures.

■ Chemical composition analysis

Crude protein content was determined by the Kjeldahl method ($N \times 6.25$) [AOAC 1990]. Total sugar content was determined by the phenol-sulfuric acid method [Yue *et al.*, 2022]. Ash content was determined using the scorching constant weight method; the protein products were charred and placed in a muffle oven, where they were ashed at 550°C for 16 h [AOAC 1990].

The lignin content was determined using the method described by Liu *et al.* [2022]. Respectively weighed 1.0 g of the SPP product was dissolved in 10 mL of a 1% (v/v) acetic acid solution, soaked for 45 min, and filtered. The filtration residue, after washing and drying, was soaked in 4 mL of a mixture of ethanol and ether for a few minutes. After filtration, the precipitate was dried, 3 mL of a 72% (w/v) sulfuric acid solution was added, shaken well and left for about 15 h. Then, the beaker with the mixture was placed in a boiling water bath for a few minutes, and then a 0.5 mL barium chloride solution was added. The obtained precipitate was dissolved in 10 mL of H₂SO₄ and K₂Cr₂O₇ mixture. After boiling for 15 min, the KI solution was added and titration was performed with an Na₂S₂O₃ solution. The lignin content (LC) was calculated according to Equation (1):

$$LC = \frac{K \times (a - b)}{n \times 48} \quad (1)$$

where: K is the concentration of Na₂S₂O₃ (M), a is the volume of Na₂S₂O₃ used during blank titration (mL), b is the volume of Na₂S₂O₃ used during sample solution titration (mL), n is the mass of SPP product (g), and value 48 is equivalent of the titration of 1 mol of lignin (characterized by C₁₁H₁₂O₄).

Total phenolic content of SPP products was determined using the method described by Velioglu *et al.* [1988] with slight modifications. SPP products were subjected to ultrasonic extraction with 80% (v/v) methanol for 30 min. The mixture was centrifuged at 2,000×g for 15 min and 200 μL of the supernatant was mixed with 1.5 mL of the Folin–Ciocalteu reagent and 1.5 mL of a sodium carbonate solution (60 g/L). After 90 min at 22°C, the absorbance was measured at 725 nm and results were expressed as gallic acid equivalents (mg GAE/g).

Total flavonoid content of SPP products was determined using the method previously used by Sudewi *et al.* [2017] with slight modifications. The SPP extract (0.1 g) was first added into 3.0 mL of a 0.1 mM aluminum chloride solution, mixed with vortex oscillation for 3 min, and left for 30 min at room

temperature. The absorbance of the mixed solution was measured at the wavelength of 415 nm, and the result was expressed in rutin equivalent (mg RE/g).

The sugar profile of the supernatant after SPCL fermentation was determined using high-performance liquid chromatography (HPLC). The supernatant samples were appropriately diluted, filtered through a 0.45 μm membrane, and then analyzed on a U3000 HPLC system (ThermoFisher Scientific, Waltham, MA, USA). The sugars were separated on a Waters Sugar-Pak column (6.5×300 mm, particle diameter 10 μm; Waters Company, Milford, MA, USA) using 0.01 M ethylenediaminetetraacetic acid calcium disodium salt hydrate as a mobile phase with a flow rate of 0.6 mL/min. Injection volume was 10 μL, and column temperature was 80°C. A differential refractive index detector (RI) was used for detection. The identification of sugars was performed by comparing their peak retention times with those of sugar standards, and the quantification was based on the peak areas.

■ Sweet potato protein functional properties analysis

■ Solubility

The solubility of SPP was determined according to the method described by Mu *et al.* [2009] with slight modifications. An aliquot of 1.0 g of the SPP product was added to 100 mL of distilled water and stirred for 1 h at room temperature. After centrifugation at 4,500×g for 10 min, the supernatant was collected to determine the protein content by the Kjeldahl method [AOAC, 1990]. The solubility (%) was calculated according to Equation (2):

$$\text{Solubility} = \frac{m_1}{m_0} \times 100 \quad (2)$$

where: m_1 (g) and m_0 (g) represent the protein content of the supernatant and the SPP product, respectively.

■ Emulsifying properties

The emulsifying activity index (EAI) and emulsion stability index (ESI) of SPP products were determined according to the method described by Cui *et al.* [2021] with slight modifications. A 1% (w/v) aqueous solution of the SPP sample was prepared. An aliquot of 30 mL of the aqueous solution was mixed with 10 mL of peanut oil and homogenized for 90 s at 10,000 rpm to form an emulsion. The resulting emulsions were left undisturbed for 0 and 20 min before taking a sample of 20 μL, which was then mixed with 5 mL of a 0.1% sodium dodecyl sulfate solution. The absorbance was measured at 500 nm using a spectrophotometer (SH-6600, Jiangsu Sheng Aohua Environmental Protection Technology Co. Ltd, Shanghai, China). The EAI (m²/g) and ESI (min) were calculated according to Equations (3) and (4), respectively:

$$EAI = \frac{2 \times 2.303 \times D \times A_0}{l \times \varphi \times C \times 10,000} \quad (3)$$

$$ESI = \frac{A_0}{A_0 - A_{20}} \times t \quad (4)$$

where: D is the dilution factor (250), l is the length of the optical path (1cm), φ is the oil volume fraction (0.25), C is the amount

of protein *per* unit volume before emulsification (g/mL), A_0 is the absorbance value at 0 min of standing, A_{20} is the absorbance value at 20 min of standing, and t is the standing time (20 min).

■ Foaming properties

The foaming capacity (FC) and foaming stability (FS) of SPP products were determined according to the method described by Kim *et al.* [2021] with slight modifications. A 1% (w/v) aqueous solution of the SPP product (75 mL) was vigorously stirred using a disperser at 10,000 rpm for 2 min to ensure complete protein foam formation. The initial volume of the solution before and after stirring was recorded, followed by another measurement after storage for 30 min. The FC and FS were calculated according to Equations (5) and (6), respectively:

$$FC = \frac{V_2 - V_1}{V_1} \times 100 \quad (5)$$

$$FS = \frac{V_3 - V_1}{V_2 - V_1} \times 100 \quad (6)$$

where: V_1 and V_2 are the volumes (mL) of the dispersion before and after stirring, respectively, V_3 is the volume (mL) of the protein solution after storage for 30 min at room temperature after stirring.

■ Sweet potato protein digestibility analysis

The SPP product (2 g) was transferred into a 50 mL centrifuge tube; then, 30 mL of a pepsin solution (enzyme activity of 2,000 U/g) was added, and the mixture was incubated at a temperature of 37°C for 6 h. Subsequently, 10 mL of a trichloroacetic acid solution with a concentration of 10% (wv) was added to precipitate any undegraded protein present in the mixture, which was then subjected to centrifugation at 6,000×g for 10 min before collecting the resulting precipitate. The collected precipitate was washed twice using water acidified to pH 4.0 and freeze-dried thereafter. The digestibility was calculated according to Equation (7) [Chen, 2023]:

$$\text{Digestibility} = \frac{m_0 - m_1}{m_0} \times 100 \quad (7)$$

where: m_1 (g) and m_0 (g) are the weights of precipitated protein and the SPP product, respectively.

■ Statistical analysis

All experiments were conducted in triplicate, and the results were expressed as mean and standard deviation. Statistical analysis was performed using one-way analysis of variance (ANOVA) with SPSS software (IBM, Shanghai, China) at a significance level of $p < 0.05$. Graphical representation was generated using Origin 2018 (Origin Lab, Northampton, MA, USA).

RESULTS AND DISCUSSION

■ Separation of sweet potato proteins by precipitation with acids

Currently, the isoelectric point precipitation method stood as the most commonly employed technique for SPP recovery from SPCL in research [Arogundade & Mu, 2012; Li *et al.*, 2018]. The pH value of SPCL is usually adjusted to about 4.0 with hydrochloric acid to precipitate SPP and realize protein recovery. In this study, several inorganic and organic acids commonly utilized in the industry (for example, citric acid and acetic acid are widely used in food production as sour agents) were selected to adjust the pH of SPCL for SPP precipitation. The results showed that organic acids, such as lactic acid and citric acid, could also be used for SPP precipitation, with marginally improved rates of SPP recovery and protein purity compared to the inorganic acids (Table 1). The protein content of SPCL was 0.35 g/100 g. It can be calculated that the production of 1,000 kg SPP product required a significant amount of hydrochloric acid (375 L), and even more of lactic and citric acids (750 L). Therefore, there was a substantial demand for acids for SPP separation by pH adjustment, which not only incurred high raw material costs but also generated new sources of pollution without any commercial application potential.

■ Separation of sweet potato protein by microbial fermentation regulating pH and precipitation

During SPCL storage, microorganisms (primarily lactic acid bacteria) may reproduce and cause the SPCL to become acidic, eventually reaching the pH required for protein precipitation [Li & Mu, 2012; Pagana *et al.*, 2014]. However, the composition of natural fermentation microorganisms fluctuates greatly (there are many species in the natural fermentation system, so the growth of species is uncontrollable), leading to prolonged and unstable

TABLE 1. Extraction yield and purity of sweet potato protein (SPP) products from sweet potato cell liquid (SPCL) obtained by isoelectric point precipitation with different acids.

| Acid | Yield (%) | Purity (g protein/100 g) | SPCL volume (L) to produce 1,000 kg of SPP product |
|-------------------|-------------------------|--------------------------|----------------------------------------------------|
| Hydrochloric acid | 47.58±0.22 ^e | 59.48±0.14 ^d | 375±25 ^c |
| Sulfuric acid | 49.66±0.19 ^d | 59.43±0.23 ^d | 150±15 ^d |
| Lactic acid | 51.73±0.27 ^b | 60.19±0.25 ^c | 750±35 ^b |
| Acetic acid | 50.85±0.31 ^c | 60.52±0.12 ^b | 1,000±40 ^a |
| Citric acid | 52.70±0.28 ^a | 61.43±0.24 ^a | 750±32 ^b |

Results are shown as mean±standard deviation ($n=3$). Different letter superscripts in the same column indicate significant differences ($p < 0.05$).

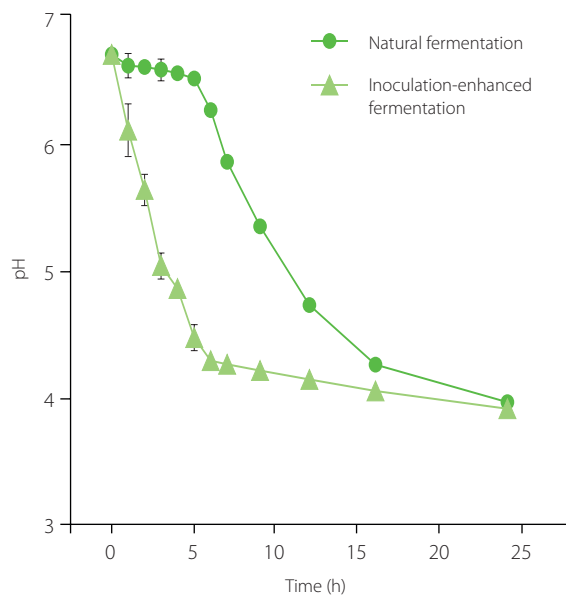


FIGURE 1. Changes in pH during inoculation-enhanced fermentation and natural fermentation of sweet potato cell liquid.

fermentation times, low levels of lactic acid bacteria, and a slower pH decrease [Capozzi *et al.* 2017]. These factors can contribute to SPCL spoilage and protein precipitation failure. In view of this situation, in the early stage, we isolated and screened the SFZ-T0 strain from the natural fermentation sedimentation tank of SPCL, which can rapidly propagate *Leuconostoc citreum* in SPCL (data not shown). Afterwards, we investigated the possibility of precipitating and separating SPP from SPCL through fermentation with the inoculation strain SFZ-T0.

Firstly, a comparison was made between the pH values of SPCL fermented through natural fermentation and those inoculated with strain SFZ-T0. The results shown in Figure 1 indicate that while the pH of naturally fermented SPCL remained unchanged for 4–6 h, it began to decrease after this period and eventually stabilized after 24 h. In contrast, the SPCL inoculated with strain SFZ-T0 exhibited an immediate decline in pH post-inoculation which dropped to about 4.0 within 6–8 h. Meanwhile, the fermentable sugars, such as sucrose, glucose and fructose, in SPCL were rapidly consumed (Table 2),

TABLE 3. Extraction yield and purity of sweet potato protein (SPP) products obtained by inoculation-enhanced fermentation of sweet potato cell liquid (SPCL) at different times.

| Fermentation time (h) | Yield (%) | Purity (g protein/100 g) |
|-----------------------|-------------------------|--------------------------|
| 6 | 55.45±0.21 ^b | 66.23±0.25 ^a |
| 8 | 55.95±0.22 ^a | 66.15±0.15 ^b |
| 10 | 55.19±0.27 ^c | 66.07±0.17 ^b |
| 12 | 55.48±0.25 ^b | 65.43±0.26 ^c |
| 24 | 55.02±0.31 ^d | 63.59±0.19 ^d |
| 48 | 54.43±0.18 ^e | 61.45±0.15 ^e |
| 72 | 53.36±0.17 ^f | 57.77±0.07 ^f |
| 120 | 52.92±0.28 ^g | 56.03±0.14 ^g |
| 168 | 51.15±0.21 ^h | 55.52±0.22 ^h |

Results are shown as mean±standard deviation ($n=3$). Different letter superscripts in the same column indicate significant differences ($p<0.05$).

indicating that strain SFZ-T0 utilized these sugars for acid production, resulting in a rapid decrease of pH in the feed solution to achieve the purpose of protein precipitation. Instead of increasing, the yield and purity of SPP showed a slight decrease with prolonged fermentation time (Table 3), which may be attributed to the bacterial consumption of protein. The optimal extraction yield and purity of SPP were achieved at a fermentation time of 6–8 h.

Inoculation-enhanced fermentation could rapidly precipitate SPP, but it required strain expansion for each batch of inoculation. If each batch of fermentation was inoculated with seed liquid, the cost and difficulty of industrialization would increase. Therefore, this study explored the feasibility of continuous transfer of fermentation broth instead of batch inoculation. As shown in Figure 2, a total of 10 batches with 9 transfer experiments were conducted at a transfer rate of 20%. The results showed that with an increase in the number of transfers, the rate of pH reduction of the SPCL feed increased rather than decreased. The time taken to reach the isoelectric point shortened from approximately 6 h in the first batch to about 5 h in the ninth batch.

TABLE 2. Soluble sugar profile of sweet potato cell liquid unfermented, fermented naturally and fermented with inoculation (g/L).

| Treatment | Fermentation time (h) | Sucrose | Glucose | Fructose |
|-----------------------------------|-----------------------|-------------------------|------------------------|------------------------|
| Without fermentation | 0 | 10.20±0.06 ^a | 2.80±0.03 ^a | 2.73±0.02 ^a |
| Inoculation-enhanced fermentation | 4 | 3.46±0.04 ^b | 0.40±0.01 ^b | 1.07±0.00 ^b |
| | 6 | 0.00±0.00 ^c | 0.00±0.00 ^c | 0.00±0.00 ^c |
| | 8 | 0.00±0.00 ^c | 0.00±0.00 ^c | 0.00±0.00 ^c |
| Natural fermentation | 6 | 8.35±0.03 ^b | 2.35±0.04 ^b | 2.51±0.03 ^b |
| | 12 | 4.74±0.02 ^c | 0.98±0.02 ^c | 1.61±0.02 ^c |
| | 24 | 1.19±0.02 ^d | 0.21±0.01 ^d | 0.36±0.01 ^d |

Results are shown as mean±standard deviation ($n=3$). Different letter superscripts in the same column, separately for inoculation-enhanced fermentation and natural fermentation, indicate significant differences ($p<0.05$).

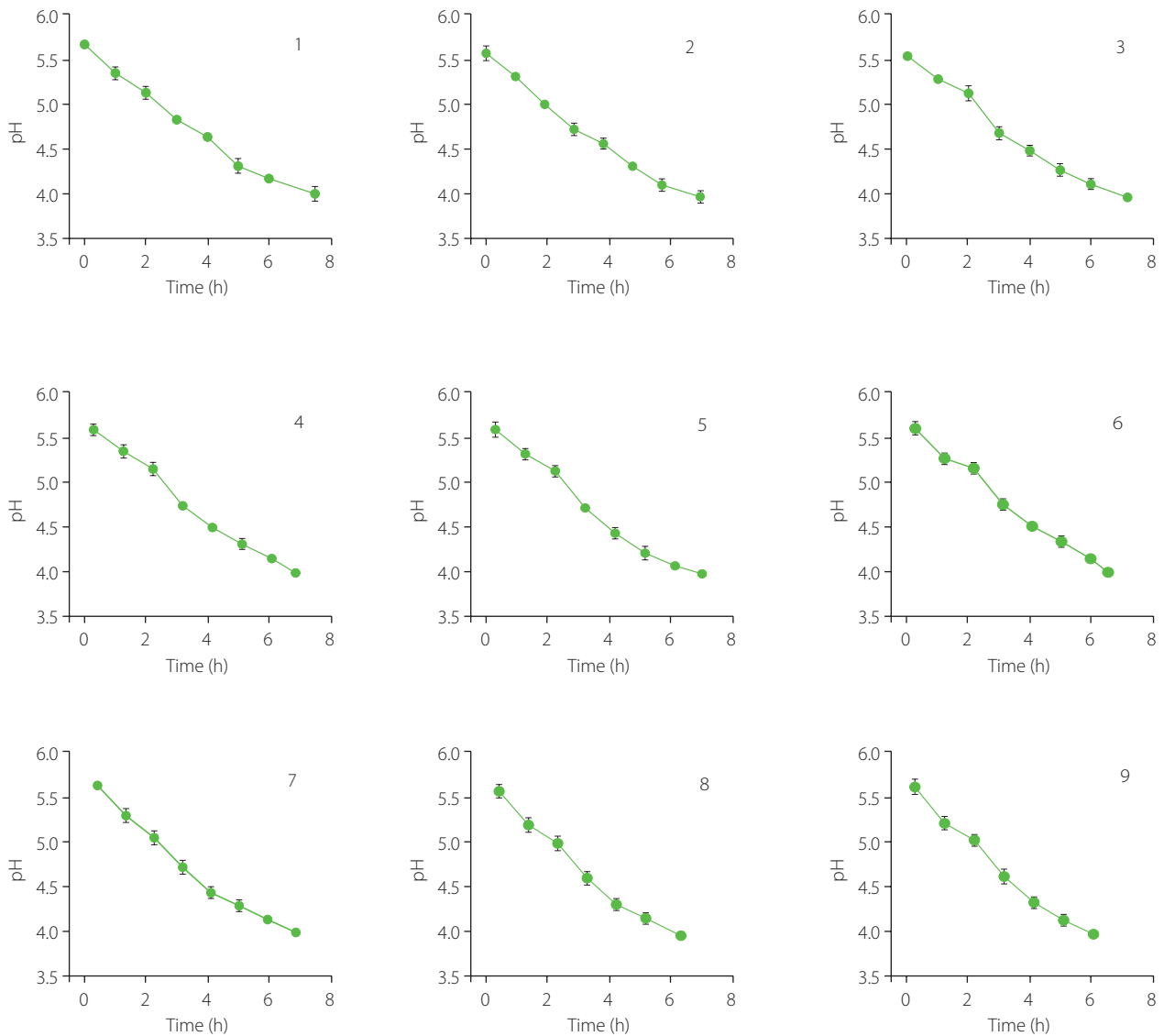


FIGURE 2. Changes in pH in the fermentation broth after batch (1–9) continuous transfer treatment.

Therefore, inoculating strain SFZ-T0 enhanced fermentation, and continuous transfer for SPP recovery from SPCL was a simple, cost-effective method with a commercial application value.

■ Effect of heat treatment on sweet potato protein recovery by microbial fermentation

SPP could be effortlessly and efficiently recovered from SPCL through inoculation-enhanced fermentation, resulting in a higher extraction yield and purity compared to the isoelectric precipitation with hydrochloric acid (extraction yield of 52.70% and 47.58%, respectively, purity of 61.43 and 59.43 g protein/100 g, respectively) (Table 1 and 4). Although the extraction yield of SPP was slightly higher than that reported in the literature for medium isoelectric point precipitated proteins [Arogundade & Mu, 2012], it still remained below 60%, indicating a significant amount of unprecipitated proteins. Heat treatment is a commonly employed technique for improving protein separation and extraction. Mu *et al.* [2017] achieved an extraction yield of over 80% for SPP by utilizing a combination of isoelectric point

TABLE 4. Extraction yield and purity of sweet potato protein (SPP) products obtained by direct heat treatment of sweet potato cell liquid (SPCL) after inoculation-enhanced fermentation.

| SPP product | Yield (%) | Purity (g protein/100 g) |
|-------------|-------------------------|--------------------------|
| F-SPP | 56.78±0.34 ^e | 66.23±0.38 ^d |
| SPP40 | 76.97±0.28 ^d | 66.36±0.32 ^d |
| SPP60 | 85.42±0.37 ^c | 67.15±0.80 ^c |
| SPP80 | 91.45±0.25 ^b | 68.62±0.98 ^b |
| SPP100 | 95.34±0.31 ^a | 70.12±1.63 ^a |

F-SPP, SPP product obtained by inoculation-enhanced fermentation; SPP40, SPP60, SPP80 and SPP100, SPP products obtained by direct heating SPCL to 40°C, 60°C, 80°C and 100°C after inoculation-enhanced fermentation, respectively. Different letter superscripts in the same column indicate significant differences ($p < 0.05$).

precipitation and heat treatment. Therefore, we investigated the effect of heat treatment on the yield of inoculation-enhanced protein fermentation.

TABLE 5. Extraction yield and purity of sweet potato protein (SPP) products obtained by stepwise heat treatment after inoculation-enhanced fermentation.

| SPP | Yield (%) | Purity (g protein/100 g) |
|--------------|-------------------------|--------------------------|
| F-SPP | 56.78±0.34 ^a | 66.23±0.38 ^d |
| SH-SPP20/40 | 20.19±0.31 ^b | 67.41±0.32 ^d |
| SH-SPP40/60 | 8.45±0.32 ^c | 75.43±0.80 ^c |
| SH-SPP60/80 | 6.03±0.31 ^d | 86.49±0.98 ^b |
| SH-SPP80/100 | 3.89±0.28 ^e | 95.19±1.63 ^a |

F-SPP, SPP product obtained by inoculation-enhanced fermentation; SH-SPP20/40, SH-SPP40/60, SH-SPP60/80 and SH-SPP80/100, SPP products obtained by stepwise heating SPCL to 20 and 40°C, 40 and 60°C, 60 and 80°C, and 80 and 100°C after inoculation-enhanced fermentation, respectively. Different letter superscripts in the same column indicate significant differences ($p < 0.05$).

The fermentation broth was heated to different indicated temperatures and then centrifuged to separate the proteins. The results showed that thermal processing significantly enhanced the protein extraction yield (Table 4). When the fermented SPCL was heated from room temperature to 40°C, the yield of SPP extraction increased by around 20% compared to that without heating. Upon reaching a temperature of 100°C, the SPP extraction yield peaked to 95.34%, which was accompanied by an increase in purity. In addition, we conducted a comparison of the yield and purity of SPP extracted through stepwise heating (Table 5) and found out that as the heating temperature increased, the purity of SPP products also increased. The purity of SPP isolated at 80/100°C reached 95.19 g protein/100 g.

■ Chemical composition of sweet potato proteins

As indicated in Table 6, SPP products contained carbohydrates, which had been further analyzed as starch, in addition to protein. Furthermore, SPP products also comprised a small

quantity of ash, lignin, and bioactive compounds such as phenolics. The chemical composition of SPP products was basically the same compared with the report in the related literature, although the proportions between compound contents were slightly different [Arogundade & Mu, 2012]. First of all, the protein content of SPP products after fermentation and heating in our study was significantly higher than that of SPP products extracted by isoelectric point precipitation and ultrafiltration reported in literature [Arogundade *et al.*, 2012]. Due to the low protein content of sweet potato protein recovered by isoelectric point precipitation, the proportion of non-protein compounds in SPP isolated by this method (S-SPP) was relatively high (Table 6). This observation is in accordance with the literature data [Arogundade & Mu, 2012]; the low content of medium electric point precipitated protein correlated with high total phenolic content (3.76 mg GAE/g) and total flavonoid content (3.48 mg CE/g). The purity of SPP isolated through heating increased with temperature elevation while the proportion of non-protein components decreased significantly. Although the purity of the directly heated SPP product was higher, it was still inferior to the stepwise heating, which was caused by the centrifugal removal of the low-purity protein when heated at low temperature, but the content of non-protein compounds of the directly heated protein was higher.

■ Functional properties of sweet potato proteins

■ Solubility

Solubility is a crucial indicator for evaluating the functional properties of plant proteins, and favorable solubility is essential for the functional and nutritional value of the product [Yang *et al.*, 2018]. Table 7 shows the solubility values of SPP extracted using different methods. The solubility of SPP isolated by isoelectric point precipitation and inoculation-enhanced fermentation (S-SPP and F-SPP, respectively) was found to be 72.35%

TABLE 6. Chemical composition of sweet potato protein (SPP) products.

| SPP product | Protein (g/100 g) | Ash (g/100 g) | Total sugar (g/100 g) | Lignin (g/100 g) | Total phenolics (mg GAE/g) | Total flavonoids (mg RE/g) |
|--------------|-------------------------|-------------------------|--------------------------|------------------------|----------------------------|----------------------------|
| S-SPP | 61.43±0.43 ^a | 2.76±0.15 ^a | 11.15±0.21 ^a | 2.13±0.13 ^a | 3.10±0.03 ^a | 3.03±0.03 ^b |
| F-SPP | 66.23±0.38 ^d | 2.15±0.11 ^b | 10.64±0.19 ^b | 1.69±0.10 ^b | 3.16±0.05 ^a | 3.18±0.05 ^a |
| SPP40 | 66.36±0.32 ^d | 2.07±0.08 ^{bc} | 10.51±0.20 ^{bc} | 1.52±0.08 ^b | 3.09±0.04 ^a | 3.16±0.06 ^a |
| SPP60 | 67.15±0.80 ^c | 1.99±0.10 ^{bc} | 10.22±0.17 ^c | 1.43±0.06 ^c | 2.98±0.05 ^b | 3.08±0.02 ^b |
| SPP80 | 68.62±0.98 ^b | 1.93±0.06 ^c | 9.72±0.13 ^d | 1.27±0.07 ^d | 2.77±0.02 ^c | 2.93±0.03 ^c |
| SPP100 | 70.12±1.63 ^a | 1.89±0.02 ^c | 9.33±0.14 ^e | 1.10±0.02 ^e | 2.71±0.00 ^c | 2.82±0.01 ^d |
| SH-SPP20/40 | 67.41±0.32 ^d | 1.45±0.07 ^c | 9.47±0.17 ^c | 1.14±0.06 ^c | 2.85±0.02 ^c | 2.96±0.04 ^c |
| SH-SPP40/60 | 75.43±0.80 ^c | 0.64±0.03 ^d | 6.45±0.13 ^d | 0.87±0.05 ^d | 1.93±0.02 ^d | 2.13±0.03 ^d |
| SH-SPP60/80 | 86.49±0.98 ^b | 0.21±0.01 ^e | 2.69±0.06 ^e | 0.34±0.04 ^e | 0.43±0.01 ^e | 1.01±0.02 ^e |
| SH-SPP80/100 | 95.19±1.63 ^a | 0.00±0.00 ^f | 0.45±0.02 ^f | 0.00±0.00 ^f | 0.06±0.01 ^f | 0.35±0.01 ^f |

S-SPP, SPP product obtained by acid precipitation; F-SPP, SPP product obtained by inoculation-enhanced fermentation; SPP40, SPP60, SPP80 and SPP100, SPP products obtained by direct heating sweet potato cell liquid (SPCL) to 40°C, 60°C, 80°C and 100°C after inoculation-enhanced fermentation, respectively; SH-SPP20/40, SH-SPP40/60, SH-SPP60/80 and SH-SPP80/100, SPP products obtained by stepwise heating SPCL to 20 and 40°C, 40 and 60°C, 60 and 80°C, and 80 and 100°C respectively; GAE, gallic acid equivalent; RE, rutin equivalent. Different letter superscripts in the same column, separately for SPP and SH-SPP samples, indicate significant differences ($p < 0.05$). S-SPP and F-SPP were statistically analyzed with direct heating and stepwise heating, respectively.

TABLE 7. Solubility of sweet potato protein (SPP) products.

| SPP product | Solubility (%) |
|--------------|-------------------------|
| S-SPP | 72.35±1.29 ^b |
| F-SPP | 85.46±1.34 ^a |
| SPP40 | 64.20±1.26 ^c |
| SPP60 | 51.78±0.74 ^d |
| SPP80 | 15.42±0.31 ^e |
| SPP100 | 8.31±0.07 ^f |
| SH-SPP20/40 | 61.30±1.02 ^c |
| SH-SPP40/60 | 49.13±0.64 ^d |
| SH-SPP60/80 | 13.46±0.29 ^e |
| SH-SPP80/100 | 3.80±0.10 ^f |

S-SPP, SPP product obtained by acid precipitation; F-SPP, SPP product obtained by inoculation-enhanced fermentation; SPP40, SPP60, SPP80 and SPP100, SPP products obtained by direct heating sweet potato cell liquid (SPCL) to 40°C, 60°C, 80°C and 100°C after inoculation-enhanced fermentation, respectively; SH-SPP20/40, SH-SPP40/60, SH-SPP60/80 and SH-SPP80/100, SPP products obtained by stepwise heating SPCL to 20 and 40°C, 40 and 60°C, 60 and 80°C, and 80 and 100°C respectively. Different letter superscripts in the same column, separately for SPP and SH-SPP samples, indicate significant differences ($p < 0.05$). S-SPP and F-SPP were statistically analyzed with direct heating and stepwise heating, respectively.

and 85.46%, respectively. The main reason for this difference was that the protein content of F-SPP was higher, and more protein was dissolved under the same conditions. The heat treatment significantly ($p < 0.05$) decreased the solubility of SPP. It was due to the fact that heat treatment could destroy the structure of the protein, which makes it difficult to maintain the original solubility. However, protein extracted by heating below 60°C still exhibited a solubility above 50%, which provided the possibility of SPP functional application.

■ Emulsifying properties

The formation of emulsions required emulsifiers to mix two immiscible liquids, and proteins had long been used as effective emulsifying agents [McClements, 2004]. The emulsifying activity index (EAI) and the emulsion stability index (ESI) were typically used to assess the protein's ability to form stable emulsions [Kumar

et al., 2014]. The results of EAI and ESI analyzed for SPP extracted by different extraction methods are shown in **Table 8**. The EAI of F-SPP (28.30 m²/g) was significantly ($p < 0.05$) higher than that of SPP extracted after stepwise heat treatment (2.10–21.34 m²/g), which was significantly related to the solubility of SPP. It was also better than that of hemp seed protein (8.7 m²/g) [Yao *et al.*, 2023], potato protein (22.80 m²/g) [Hussain *et al.*, 2021] and soybean protein (26.43 m²/g) [Ding, 2021]; most of these different plant proteins were isolated by acid precipitation. The ESI trends of different SPP products differed significantly from their EAI. SPP separated below 60°C showed good emulsion stability. The ESI of SH-SPP40/60 was better than that of F-SPP, and the ESI of SPP separated above 80°C decreased rapidly. Appropriate heat treatment could gradually expose the hydrophobic groups in protein molecules, thereby enhancing the hydrophobic interaction between interfacial proteins and promoting emulsion stability. However, high temperature (80–100°C) may lead to complete denaturation of the sweet potato protein, resulting in protein precipitation and reducing the degree of protein adsorption at the water-oil interface, thereby reducing the stability of the emulsion.

■ Foaming properties

Foam could alter both the texture and flavor of food, with proteins exhibiting favorable foaming properties. The foaming capacity (FC) and foam stability (FS) are two important parameters of protein foaming properties. The foaming properties of sweet potato proteins obtained by different extraction methods are shown in **Table 8**. The F-SPP had the FC of 38.49%, which was higher than that of the SPP isolated *via* isoelectric point precipitation by Mu *et al.* [2017] (FC 30–35%), and other proteins, such as potato protein (FC 20%) [Hussain *et al.*, 2021], peanut protein (FC 26.47%) [He *et al.*, 2023] and mung bean protein (FC 26.10%) [Du *et al.*, 2018]; most of these different plant proteins were isolated by acid precipitation. The results of various stability tests performed for SPP foam were consistent with its foaming ability, which was affected by the reduced solubility caused by heating and subsequently influenced its foam stability [Mir *et al.*, 2021]. F-SPP exhibited good foaming properties in the light of literature data for plant-derived protein isolates [Soria-Hernández *et al.*, 2015].

TABLE 8. Emulsifying and foaming properties, and digestibility of sweet potato protein (SPP) products.

| SPP | Emulsifying activity (m ² /g) | Emulsifying activity (min) | Foaming capacity (%) | Foaming stability (%) | Digestibility (%) |
|--------------|------------------------------------------|----------------------------|-------------------------|-------------------------|-------------------------|
| S-SPP | 22.50±1.15 ^b | 53.44±0.97 ^d | 31.45±1.05 ^b | 50.16±2.04 ^b | 76.19±0.07 ^f |
| F-SPP | 28.30±0.96 ^a | 55.45±1.00 ^c | 38.49±0.95 ^a | 61.15±1.49 ^a | 83.14±0.11 ^e |
| SH-SPP20/40 | 21.34±1.44 ^b | 57.48±0.95 ^b | 25.74±0.74 ^c | 42.45±1.73 ^d | 85.71±0.13 ^d |
| SH-SPP40/60 | 16.09±0.58 ^c | 60.13±0.89 ^a | 21.19±0.94 ^d | 45.13±1.25 ^c | 87.56±0.20 ^c |
| SH-SPP60/80 | 6.42±1.10 ^d | 26.14±0.78 ^e | 11.38±1.06 ^e | 30.35±0.45 ^e | 89.35±0.21 ^b |
| SH-SPP80/100 | 2.10±0.60 ^e | 6.12±0.67 ^f | 4.16±0.44 ^f | 21.78±0.33 ^f | 90.46±0.31 ^a |

SPP, SPP product obtained by acid precipitation; F-SPP, SPP product obtained by inoculation-enhanced fermentation; SH-SPP20/40, SH-SPP40/60, SH-SPP60/80 and SH-SPP80/100, SPP products obtained by stepwise heating SPCL to 20 and 40°C, 40 and 60°C, 60 and 80°C, and 80 and 100°C respectively. Different letter superscripts in the same column indicate significant differences ($p < 0.05$).

■ Digestibility of sweet potato proteins

Digestibility is a crucial nutritional characteristic of the food protein. The higher the digestibility, the better the protein utilization rate and the easier its digestion and absorption. The digestibility of SPP products obtained by different extraction methods are shown in Table 8, indicating that the heat treatment significantly enhanced SPP digestibility. Specifically, when heated to 60°C, the digestibility of SPP exceeded 87%, which was 7.32% higher than that of the F-SPP samples. Moreover, heating at 100°C further increased the digestibility of SH-SPP80/100 to reach up to 90%. This is due to the fact that the high temperature treatment destroys the structure of the protein itself and significantly improves SPP digestibility [Sun *et al.*, 2012], although on the other hand, the functional properties of SPP extracted by heat denaturation may be lost. SPP had been heat-treated after being purified (to a purity of 95 g protein/100 g) by Sun *et al.* [2014]. As the temperature increased, its digestibility increased from 52.8% to 99.6% (at 110°C), while that of the sample heated at 100°C was approximately 80%. Although SPP isolated by heating at higher temperatures (80–100°C) could have worse functional properties, it boasted high protein content and excellent digestibility, rendering it an ideal source of high-quality protein.

CONCLUSIONS

In this study, SPP was recovered from SPCL by artificial inoculation-enhanced fermentation acidification and heating, and the functional properties of the prepared SPP were compared. The results showed that within 6 h of inoculation-enhanced fermentation, the pH level of SPCL could be reduced to less than 4.0, leading to the successful settling of SPP. The extraction yield and purity could be achieved at approximately 55% and 65 g protein/100 g, respectively. Heat treatment at low temperatures (40–60°C) increased the protein extraction yield to 75–85%, while SPP maintained high emulsifying and foaming properties. High-quality SPP products with a protein content ranging from 86 to 95 g/100 g and a digestibility exceeding 90% could be obtained by stepwise heat treatment at high temperatures (60/80–80/100°C).

The present study described a cost-effective and straightforward approach for promoting the industrial recovery of SPP from SPCL through inoculation-enhanced fermentation and continuous transfer. Additionally, the application of assisted heat treatment could produce high-quality SPP products with diverse functional properties, which held a promising application prospect in the food industry.

RESEARCH FUNDING

This work was supported by Key R&D Program of Shandong Province, China (2023TZXD024), the development of plant protein preparation technology and new equipment (2020CXGC010604) and Major Innovation Pilot Project of Integration of Science, Education and Industry of Qilu University of Technology (Shandong Academy of Science) (No. 2022JBZ01-08).

CONFLICT OF INTERESTS

We confirm that there are no conflicts of interest for this article that could influence the outcome.

ORCID IDs

Q. Li

<https://orcid.org/0009-0002-3501-021X>

REFERENCES

- Abegunde, O.K., Mu, T.H., Chen, J.W., Deng, F.M. (2013). Physicochemical characterization of sweet potato starches popularly used in Chinese starch industry. *Food Hydrocolloids*, 33(2), 169-177. <https://doi.org/10.1016/j.foodhyd.2013.03.005>
- AOAC (1990). *Methods of Analysis* (15th ed.). Washington: Association of Official Agriculture Chemistry.
- Arogundade, L.A., Mu, T.H. (2012). Influence of oxidative browning inhibitors and isolation techniques on sweet potato protein recovery and composition. *Food Chemistry*, 134(3), 1374-1384. <https://doi.org/10.1016/j.foodchem.2012.03.035>
- Arogundade, L.A., Mu, T.H., Añón, M.C. (2012). Heat-induced gelation properties of isoelectric and ultrafiltered sweet potato protein isolate and their gel microstructure. *Food Research International*, 49(1), 216-225. <https://doi.org/10.1016/j.foodres.2012.07.061>
- Capozzi, V., Fragasso, M., Romaniello, R., Berbegal, C., Russo, P., Spano, G. (2017). Spontaneous food fermentations and potential risks for human health. *Fermentation*, 3(4), art. no. 49. <https://doi.org/10.3390/fermentation3040049>
- Chen, J. (2023). *In vitro* simulation of protein digestion of formula food for special medical purposes. *Food Industry*, (08), 331-334 (in Chinese).
- Cheng, S., Zhang, Y.F., Zeng, Z. Q., Lin, J., Zhang, Y.W., Ni, H., Li, H.H. (2015). Screening, separating, and completely recovering polyphenol oxidases and other biochemicals from sweet potato wastewater in starch production. *Applied Microbiology & Biotechnology*, 99(4), 1745-1753. <https://doi.org/10.1007/s00253-014-6034-7>
- Cui, Q., Wang, L., Wang, G., Zhang, A., Wang, X., Jiang, L. (2021). Ultrasonication effects on physicochemical and emulsifying properties of *Cyperus esculentus* seed (tiger nut) proteins. *LWT – Food Science and Technology*, 142, art. no. 110979. <https://doi.org/10.1016/j.lwt.2021.110979>
- Ding, D. (2021). Effects of emulsifier on emulsification, physical and chemical properties of soybean protein. *IOP Conference Series: Earth and Environmental Science*, 792(1), art. no. 012017. <https://doi.org/10.1088/1755-1315/792/1/012017>
- Du, M., Xie, J., Gong, B., Xu, X., Tang, W., Li, X., Li, Ch., Xie, M. (2018). Extraction, physicochemical characteristics and functional properties of mung bean protein. *Food Hydrocolloids*, 76, 131-140. <https://doi.org/10.1016/j.foodhyd.2017.01.003>
- He, W.Y., He, K., Liu, X.Y., Ye, L.Y., Lin, X., Ma, L., Yang, P., Wu, X.L. (2023). Modulating the allergenicity and functional properties of peanut protein by covalent conjugation with polyphenols. *Food Chemistry*, 415, art. no. 135733. <https://doi.org/10.1016/j.foodchem.2023.135733>
- Hussain, M., Qayum, A., Zhang, X.X., Hao, X., Liu, L., Wang, Y., Hussein, K., Li, X. (2021). Improvement in bioactive, functional, structural and digestibility of potato protein and its fraction patatin via ultra-sonication. *LWT – Food Science and Technology*, 148, art. no. 111747. <https://doi.org/10.1016/j.lwt.2021.111747>
- Kim, T.K., Yong, H.I., Kim, Y.B., Jung, S., Kim, H.W., Choi, Y.S. (2021). Effects of organic solvent on functional properties of defatted proteins extracted from *Protoetia brevitaris* larvae. *Food Chemistry*, 336, art. no. 127679. <https://doi.org/10.1016/j.foodchem.2020.127679>
- Kumar, K.S., Ganesan, K., Selvaraj, K., Rao, P.V.S. (2014). Studies on the functional properties of protein concentrate of *Kappaphycus alvarezii* (Doty) Doty – an edible seaweed. *Food Chemistry*, 153, 353-360. <https://doi.org/10.1016/j.foodchem.2013.12.058>
- Li, P., Mu, T. (2012). Recovery of sporamin from naturally fermented sweet potato starch slurry by foam fractionation. *International Journal of Food Science Technology*, 47(9), 1889-1895. <https://doi.org/10.1111/j.1365-2621.2012.03046.x>
- Li, Q.R., Luo, J.L., Zhou, Z.H., Wang, G.Y., Chen, R., Cheng, S., Wu, M., Li, H., Ni, H., Li, H.H. (2018). Simplified recovery of enzymes and nutrients in sweet potato wastewater and preparing health black tea and theaflavins with scrap tea. *Food Chemistry*, 245, 854-862. <https://doi.org/10.1016/j.foodchem.2017.11.095>
- Liu, X., Wen, J.F., Jiao, Y.R., Wang Y.L. (2022). Core shell abandoned the determination of cellulose, hemicellulose, and lignin content in the. *Journal of College of Yulin*, 32(02), 6-9 (in Chinese). <https://doi.org/10.16752/j.cnki.jylu.2022.02.002>
- Maeshima, M., Sasaki, T., Asahi, T. (1985). Characterization of major proteins in sweet potato tuberous root. *Phytochemistry*, 24(9), 1899-1902. [https://doi.org/10.1016/S0031-9422\(00\)83088-5](https://doi.org/10.1016/S0031-9422(00)83088-5)
- McClements, D.J. (2004). Protein-stabilized emulsions. *Current Opinion in Colloid and Interface Science*, 9(5), 305-313. <https://doi.org/10.1016/j.cocis.2004.09.003>

20. Mir, N.A., Riar, C.S., Singh, S. (2021). Improvement in the functional properties of quinoa (*Chenopodium quinoa*) protein isolates after the application of controlled heat-treatment: effect on structural properties. *Food Structure*, 28, art. no. 100189.
<https://doi.org/10.1016/j.foostr.2021.100189>
21. Mu, T., Sun, H., Zhang, M., Wang, Ch. (2017). Chapter 2. Sweet potato proteins. In: T. Mu, H. Sun, M. Zhang, Ch. Wang (Eds.). *Sweet Potato Processing Technology*, Academic Press, pp. 49-119.
<https://doi.org/10.1016/B978-0-12-812871-8.00002-7>
22. Mu, T.H., Liu, Y., Zhang, M., Sun, H.N. (2014). Protein recovery from sweet potato starch wastewater by foam separation. *Separation Science and Technology*, 49, 2255-2260.
<https://doi.org/10.1080/01496395.2014.911324>
23. Mu, T.H., Tan, S.S., Xue, Y.L. (2009). The amino acid composition, solubility and emulsifying properties of sweet potato protein. *Food Chemistry*, 112(4), 1002-1005.
<https://doi.org/10.1016/j.foodchem.2008.07.012>
24. Pagana, I., Morawicki, R., Hager, J.T. (2014). Lactic acid production using waste generated from sweet potato processing. *International Journal of Food Science Technology*, 49(2), 641-649.
<https://doi.org/10.1111/ijfs.12347>
25. Soria-Hernández, C., Serna-Saldívar, S., Chuck-Hernández, C. (2015). Physicochemical and functional properties of vegetable and cereal proteins as potential sources of novel food ingredients. *Food Technology & Biotechnology*, 53(3), 269-277.
<https://doi.org/10.17113/ftb.53.03.15.3920>
26. Sudewi, S., Lolo, W.A., Warongan, M., Rifai, Y., Rante, H. (2017). The ability of *Abelmoschus manihot* L. leaf extract in scavenging of free radical DPPH and total flavonoid determination. *IOP Conference Series: Materials Science and Engineering*, 259, art. no. 012020.
<https://doi.org/10.1088/1757-899X/259/1/012020>
27. Sun, M., Mu, T., Sun, H., Zhang, M. (2014). Digestibility and structural properties of thermal and high hydrostatic pressure treated sweet potato (*Ipomoea batatas* L.) protein. *Plant Foods for Human Nutrition*, 69(3), 270-275.
<https://doi.org/10.1007/s11130-014-0426-9>
28. Sun, M., Mu, T., Zhang, M., Arogundade, L.A. (2012). Nutritional assessment and effects of heat processing on digestibility of Chinese sweet potato protein. *Journal of Food Composition and Analysis*, 26(1-2), 104-110.
<https://doi.org/10.1016/j.jfca.2012.03.008>
29. Tang, S.Y. Dai, Y. F. Liu Z.Y. (2001). Treatment of food-processing wastewater. *Beijing: Chemical Industry Press*.
30. Velioglu, Y.S., Mazza, G., Gao, L., Oomah, B.D. (1998). Antioxidant activity and total phenolics in selected fruits, vegetables and grain products. *Journal of Agricultural and Food Chemistry*, 46(10), 4113-4117.
<https://doi.org/10.1021/jf9801973>
31. Yang, J., Liu, G., Zeng, H., Chen, L. (2018). Effects of high pressure homogenization on faba bean protein aggregation in relation to solubility and interfacial properties. *Food Hydrocolloids*, 83, 275-286.
<https://doi.org/10.1016/j.foodhyd.2018.05.020>
32. Yao, S.Y., Li, W., Wu, Y., Martin, G.J.O., Ashokkumar, M. (2023). The impact of high-intensity ultrasound-assisted extraction on the structural and functional properties of hempseed protein isolate (HPI). *Foods*, 12(2), art no. 348.
<https://doi.org/10.3390/FOODS12020348>
33. Yue, F.F., Zhang, J.R., Xu, J.X., Niu, T.F., Lü, X., Liu, M.S. (2022). Effects of mono-saccharide composition on quantitative analysis of total sugar content by phenol-sulfuric acid method. *Frontiers in Nutrition*, 9, art. no. 963318.
<https://doi.org/10.3389/FNUT.2022.963318>
34. Zhao, Z.K., Mu, T.H., Zhang, M., Richel, A. (2019). Effects of high hydrostatic pressure and microbial transglutaminase treatment on structure and gelation properties of sweet potato protein. *LWT – Food Science and Technology*, 115, art. no. 108436.
<https://doi.org/10.1016/j.lwt.2019.108436>
35. Zhao, Z.K., Mu, T.H., Zhang, M., Richel, A. (2018). Chemical forces, structure, and gelation properties of sweet potato protein as affected by pH and high hydrostatic pressure. *Food and Bioprocess Technology*, 11(9), 1719-1732.
<https://doi.org/10.1007/s11947-018-2137-y>

Curcumin Prevents Free Fatty Acid-Induced Lipid Accumulation *via* Targeting the miR-22-3p/*CRLS1* Pathway in HepG2 Cells

Yuanyuan Mei^{1,2#} , Xiaoting Sun^{1,2,3#} , Shi-Ying Huang^{1#} , Xiaowen Wu^{1,2,3}, Kuo-Ting Ho^{3,4} , Liming Lu⁵ ,
Chaoxiang Chen^{1,2} , Jian Li^{1,2} , Jingwen Liu¹ , Guiling Li^{1,2*} 

¹College of Ocean Food and Biological Engineering, Jimei University, Xiamen, Fujian 361021, P. R. China

²Fujian Marine Functional Food Engineering Technology Research Center, Xiamen, Fujian 361021, P. R. China

³Hi. Q Biomedical Laboratory, Taiwan Investment Zone, Quanzhou, Fujian, 362123, P. R. China

⁴Center for Precision Medicine, Yi He Hospital, Taiwan Investment Zone, Quanzhou, Fujian, 362123, P. R. China

⁵Shanghai Institute of Immunology, Shanghai Jiaotong University School of Medicine, Shanghai, 200025, P. R. China

Dysregulated lipid metabolism in liver is an important hallmark of non-alcoholic fatty liver disease (NAFLD), which may be modulated by dietary polyphenols or microRNAs (miRNAs). However, the underlying epigenetic regulatory mechanism of polyphenols remain unclear. The current study aimed to address how miRNA mediates hepatic lipid metabolic control of curcumin, a polyphenolic food supplement. The results showed that 24 h treatment with 5–20 μ M curcumin prevented free fatty acid-induced lipid accumulation by around 10–50% in HepG2 cells, which was attenuated by pre-transfection with 40 nM miR-22-3p mimic for 48 h. In consequence, transfection with 40 nM miR-22-3p inhibitor for 48 h significantly reduced lipid accumulation by around 10%. And, 48 h overexpression of miR-22-3p targeting cardioplipin synthase 1 (*CRLS1*) gene, which encodes a mitochondrial phospholipid synthase, showed a similar regulatory effect. Thus, miR-22-3p and *CRLS1* showed opposite effects in modulating lipid metabolism, which probably involved mitochondrial control. In summary, this study demonstrated that curcumin improved hepatic lipid metabolism *via* targeting the miR-22-3p/*CRLS1* pathway. Identification of the epigenetic regulatory mechanism underlying lipid metabolism may thereby facilitate alleviation of metabolic disorders by natural polyphenols.

Key words: polyphenol, epigenetics, liver, steatosis, mitochondria

INTRODUCTION

Lipids are key components of biofilms and essential nutrients of human body. Lipid metabolism includes the processes of lipid uptake, transportation, *de novo* synthesis and decomposition, which produce a variety of intermediates to facilitate maintaining cellular homeostasis and regulating organism functions [Kloska *et al.*, 2020]. Aberrant lipid metabolism is involved in the pathogenesis of a variety of human diseases [Yoon *et al.*, 2021]. Liver is the major organ responsible for the homeostatic regulation between lipid accumulation and removal. Besides lipid uptakes

from food, free fatty acids transferred from blood and *de novo* synthesized lipids are the main sources of intrahepatic lipids. As far as the dynamic balance of liver lipids is disrupted, lipids may abnormally accumulate in liver, which eventually results in liver metabolic disorders. For instance, aberrant accumulation of triglycerides in liver may lead to liver steatosis, a hallmark feature of non-alcoholic fatty liver disease (NAFLD) [Arab *et al.*, 2018]. NAFLD represents a kind of metabolic stress-related liver disease, which is closely associated with obesity, diabetes, cardiovascular diseases and other metabolic disorders [Lionardo

*Corresponding Author:

tel.: 86-5926181487; fax: 86-5926180470; e-mail: glli2016@jmu.edu.cn (G. Li)

#These authors contributed equally.

Submitted: 8 November 2023

Accepted: 22 January 2024

Published on-line: 13 February 2024



© Copyright by Institute of Animal Reproduction and Food Research of the Polish Academy of Sciences

© 2024 Author(s). This is an open access article licensed under the Creative Commons Attribution-NonCommercial-NoDerivs License (<http://creativecommons.org/licenses/by-nc-nd/4.0/>).

et al., 2018]. Without timely intervention, NAFLD may develop into non-alcoholic steatohepatitis (NASH), liver cirrhosis, or even liver cancers, which severely impairs human health and lifespan.

The pathogenesis of NAFLD has not been completely elucidated, which may have hampered its effective drug treatment. Great efforts have been focused on exploring for novel medicines and interventions in lifestyle or diets to reduce NAFLD incidence and progression [Hernandez-Rodas *et al.*, 2015]. Fortunately, a series of studies indicated that NAFLD can be effectively treated by herbal extracts with anti-hyperlipidemic and hepatoprotective activities [Abenavoli *et al.*, 2021]. As a natural polyphenolic compound, curcumin has served as a food additive and pigment. It is also widely used as an effective herbal medicine to relieve various health problems, probably due to its multi-functional activities. In recent years, a series of clinical and animal studies demonstrated that curcumin can mitigate hepatic lipid accumulation and exhibit anti-hepatitis effect in mice and human [Zhao *et al.*, 2022], thereby showing good therapeutic potential for NAFLD and other metabolic disorders. Li *et al.* [2021] reported that 10-week food supplementation with 0.2% curcumin significantly reduced the body fat, hepatic steatosis, insulin resistance and serum lipopolysaccharide levels of obese mice. A clinical study also revealed that 102 NAFLD patients who received 8-week curcumin treatment showed significantly reduced hepatic steatosis without safety concerns [Rahmani *et al.*, 2016]. However, due to the complex pathogenesis of NAFLD and the complicated molecular targets of curcumin, the physiological roles and action mechanism of curcumin in cellular lipid metabolism are not completely understood.

MicroRNAs (miRNAs) are ~22 nt small non-coding RNAs, the aberrant expression of which is closely associated with human metabolic diseases [Agbu & Carthew, 2021]. They have become potential therapeutic targets for different health problems. miRNAs may be involved in the occurrence and development of NAFLD *via* at least three different pathways. 1) Regulating lipid uptake through the modulation of membrane transporters. For instance, miR-26a was shown to target *CD36* to inhibit lipid uptake in HepG2 cells [Ding *et al.*, 2019]. 2) Regulating *de novo* lipid synthesis by targeting different enzymes. For instance, both miR-27a and miR-103 targeted and inhibited the expression of fatty acid synthase (*FAS*) and stearoyl-S-CoA desaturase 1 (*SCD1*), two key enzymes involved in fatty acid synthesis, to regulate hepatic lipid metabolism and thereby alleviate NAFLD [Zhang *et al.*, 2017; 2020]. 3) Regulating fatty acid β -oxidation in mitochondria. Veitch *et al.* [2022] reported that miR-30e overexpression significantly promoted exogenous fatty acid β -oxidation (FAO) in mitochondria without affecting endogenous FAO.

As one of the most abundant liver miRNAs, miR-22-3p was shown to have a physiological role in regulating lipid and metabolic homeostasis [Castaño *et al.*, 2022; Panella *et al.*, 2023]. Although it has been demonstrated that miR-22-3p repression improved lipid metabolism in mouse and human liver [Hu *et al.*, 2020; Thibonnier *et al.*, 2020], some studies showed opposite results [Gjorgjieva *et al.*, 2020; 2022]. The exact regulatory effect and action mechanism of miR-22-3p in lipid metabolism

may differ due to diverse cell types and pathological statuses investigated. Interestingly, miR-22-3p is a common polyphenol-controlled miRNA [Hayakawa *et al.*, 2022]. Previously, we also reported that miR-22-3p was one of the molecular targets of curcumin [Sun *et al.*, 2023]. Therefore, it is interesting to address whether curcumin regulates lipid metabolism in hepatocytes by controlling miR-22-3p and its downstream effectors.

Inducing a high-fat *in vitro* HepG2 cellular model by free fatty acid (FFA), this study aimed to address whether and how miR-22-3p modulated the effect of curcumin on lipid metabolism. The data revealed that curcumin effectively prevented FFA-induced lipid accumulation in HepG2 cells, which was mitigated by miR-22-3p overexpression. Furthermore, both inhibition of miR-22-3p and overexpression of *CRLS1*, a target gene of miR-22-3p and key mitochondrial regulating gene, significantly reduced lipid accumulation in HepG2 cells. Hepatic steatosis can be attributed to aberrant lipogenesis. The effects of miR-22-3p and *CRLS1* on lipogenesis were also investigated. Taken together, this study is of significance to elucidate the epigenetic regulatory mechanism underlying hepatic lipid metabolism. It may also provide insights into the development and utilization of natural food supplements to relieve lipid metabolic disorders, such as NAFLD and obesity.

MATERIALS AND METHODS

■ Cell culture and treatment

The human hepatoma cell line HepG2 was obtained from the Cell Bank of the Chinese Academy of Sciences in Shanghai. HepG2 cells used in this study have a passage number not higher than 20. HepG2 cells were cultured in Gibco's DMEM (Grand Island, NY, USA) that contained 10% fetal bovine serum (FBS; Gemini, Calabasas, CA, USA) and a 1% penicillin/streptomycin antibiotic mixture (Gibco, Grand Island, NY, USA) at 37°C with 5% CO₂ in a humidified incubator (ThermoFisher, Waltham, MA, USA). Except for specified, around 5×10⁵ HepG2 cells *per* well were seeded in a 12-well plate and cultured to nearly 75% confluency. Then, a 1 mM FFA mixture (oleic acid to palmitic acid ratio of 2:1) was added for 24 h to induce lipid accumulation according to a previously described method [Gómez-Lechón *et al.*, 2007]. To test curcumin's activity, HepG2 cells were co-incubated with curcumin (Sigma-Aldrich, Saint Louis, MO, USA) and the FFA mixture for 24 h. The amount of curcumin was chosen as previously described [Shan *et al.*, 2022]. Curcumin was dissolved in DMSO (Amresco, Solon, OH) and added to cells at 1% (*v/v*), and DMSO served as a vehicle control.

■ Cell transfection and free fatty acid induction

HepG2 cells were grown to around 75% confluency in the 12-well culture plate, followed by transfection with 40 nM miRNA (Ribobio, Guangzhou, China) or the pCMV-CRLS1 plasmid at 1.5 μ g/well for 48 h using Lipofectamine 2000 Transfection Reagent (Invitrogen, Carlsbad, CA, USA) in accordance with the manufacturer's protocols. The cells were then exposed to 1 mM FFA for 24 h before further investigation. The pCMV-CRLS1 plasmid was previously prepared [Sun *et al.*, 2023].

Oil Red O staining and lipid semi-quantification assay

The cells were *in situ* stained with an Oil Red O staining solution to visualize accumulation of intracellular lipid droplets, as referred to the instructions of an Oil Red O stain kit (Solarbio, Beijing, China) with modifications. Briefly, the cells were fixed with 10% formalin for 20 min at room temperature and washed twice with distilled water. Following further washing with 60% (*v/v*) isopropanol for 20–30 s, the cells were stained with a freshly water-diluted Oil Red O dye (0.5% stock solution and H₂O in 3:2, *v/v*, ratio) for 20 min and then rinsed with distilled water to remove excessive dye. The stained cells were photographed under a light microscope, followed by lipid semi-quantification assay. To quantify the accumulated intracellular lipid levels, the Oil Red O-stained cells were immersed in isopropanol with 40 min vibration at room temperature to dissolve lipid droplets and the optical absorbance was measured at 510 nm [Chen *et al.*, 2020]. The relative lipid amount was calculated as compared to that of control optical absorbance.

Determination of intracellular triglyceride and total cholesterol contents

The intracellular triglyceride (TG) and total cholesterol (TC) contents were determined using the corresponding assay kits from Jiancheng Biotechnology (Nanjing, China) following the manufacturer's instructions. The lipid contents were normalized to the total protein amount, and the control TG or TC level was set as 1.0.

Measurement of mRNA expression levels

The mRNA expression level was quantified using the quantitative real-time PCR (qRT-PCR) assay. Total cellular RNA was first isolated with Invitrogen's TRIzol reagent, and 1 µg of total RNA was reversely transcribed into cDNA molecules using the Toyobo's ReverTra Ace qPCR RT Master Mix kit (Osaka, Japan). qRT-PCR was then performed with 2 µL of properly diluted cDNA as a template *per* 20 µL of a reaction mix and primers at 100 nM, using the Accurate Biology's 2x SYBR Green Premix Pro Taq HS mix (Changsha, China), under the ABI7300 real-time PCR detection system (Applied Biosystems, Waltham, MA, USA). The PCR reactions were carried out as follows: denaturing at 95°C for 5 min, followed by 40 amplification cycles at 95°C for 5 s and 60°C for 31 s. *β-actin* was used as a reference gene. The relative gene expression levels were calculated by the 2^{-ΔΔCT} method, as ΔCT = CT (tested gene) – CT (reference gene) and ΔΔCT = ΔCT (sample) – ΔCT (control). The primer sequences used in this study were as listed in Table 1 and Table S1.

Statistical analysis

All experiments were performed with duplicate biological repeats for at least three times and data were presented as the mean ± standard deviation (SD) (*n*≥3). The difference between two groups was evaluated using an unpaired Student's *t*-test, and the differences among multiple groups were determined by one-way analysis of variance (ANOVA), and then subjected to Duncan's analysis for multiple comparisons. Differences were considered statistically significant at *p*<0.05 or *p*<0.01.

Table 1. The primer sequences used in this study.

| Gene name | Forward (5' → 3') | Reverse (5' → 3') |
|----------------|--------------------------|---------------------------|
| <i>β-actin</i> | ACCTTCTACAATGAGCT-GCG | CCTGGATAGCAACGTA-CATGG |
| <i>CRLS1</i> | TTGTCAATGACGAGA-ATTGGCT | GCCAGTTTCGAG-CAATAAATCC |
| <i>SREBP-1</i> | GTGGCGGCTGCATTGA-GAGTGAG | AGGTACCCGAGGGCATC-CGAGAAT |
| <i>PPARγ</i> | GAGCCCAAGTTT-GAGTTTGC | GCAGGTTGTCTTGAAT-GTCTTC |
| <i>FAS</i> | CAAGAACTGCACGGAG-GTGT | AGCTGCCAGAGTCG-GAGAAC |
| <i>LXRα</i> | CGCACTACATCTGC-CACAGT | TCAGGCGGATCT-GTCTTCT |

CRLS1, cardiolipin synthase 1; *SREBP-1*, sterol-regulatory element binding protein-1; *PPARγ*, peroxisome proliferators-activated receptor γ; *FAS*, fatty acid synthase; *LXRα*, liver X receptor α.

RESULTS AND DISCUSSION

NAFLD represents a spectrum of liver diseases that are characterized by dysregulated hepatic lipid metabolism and is closely related to hepatocellular carcinoma [Degaspero & Colombo, 2016]. Although the prevalence of NAFLD is increasing worldwide annually, currently there is no pharmaceutical therapy available for NAFLD. However, it is generally recognized that the most effective treatment for NAFLD is patient's lifestyle intervention, particularly physical activity and diet. In recent years, a series of studies have also indicated that plant polyphenols (such as resveratrol and curcumin) and plant extracts with polyphenols (such as tea extract), can effectively alleviate or prevent NAFLD *via* various pathways [Abenavoli *et al.*, 2021]. However, the pathogenesis of NAFLD and the function mechanism of polyphenols remain largely unknown.

In general, the primary hepatocyte is the best model for *in vitro* NAFLD research to reveal its pathogenesis and treatment. However, due to the limited culture passages, poor reproducibility and ethical issues of primary culture, the immortalized hepatocyte-derived HepG2 cell has become a commonly used substitutive model and shows similar response to free fatty acid induction [Abenavoli *et al.*, 2021; Gómez-Lechón *et al.*, 2007]. Oleic acid (OA) and palmitic acid (PA) are the most abundant fatty acid components of hepatic triglycerides [Rafiei *et al.*, 2019]. Both OA and PA were able to induce lipid accumulation in hepatocytes. OA was more adipogenic but less apoptotic than PA, however, the FFA mixture (2OA/1PA) combines the advantages of both acids [Gómez-Lechón *et al.*, 2007]. Hence, a 1 mM FFA mixture was used in this study to induce an *in vitro* high-fat hepatic cellular model of HepG2 cells.

Curcumin prevented lipid accumulation in free fatty acid-induced HepG2 cells

To evaluate the effect of curcumin on lipid accumulation in HepG2 cells, the cell viability was first determined by the 3-(4,5-dimethylthiazol-2-yl)-2,5-diphenyltetrazolium bromide (MTT) assay in FFA and curcumin treated cells. It was shown that curcumin (up to 20 µM) did not exhibit obvious cytotoxic effect in HepG2 cells,

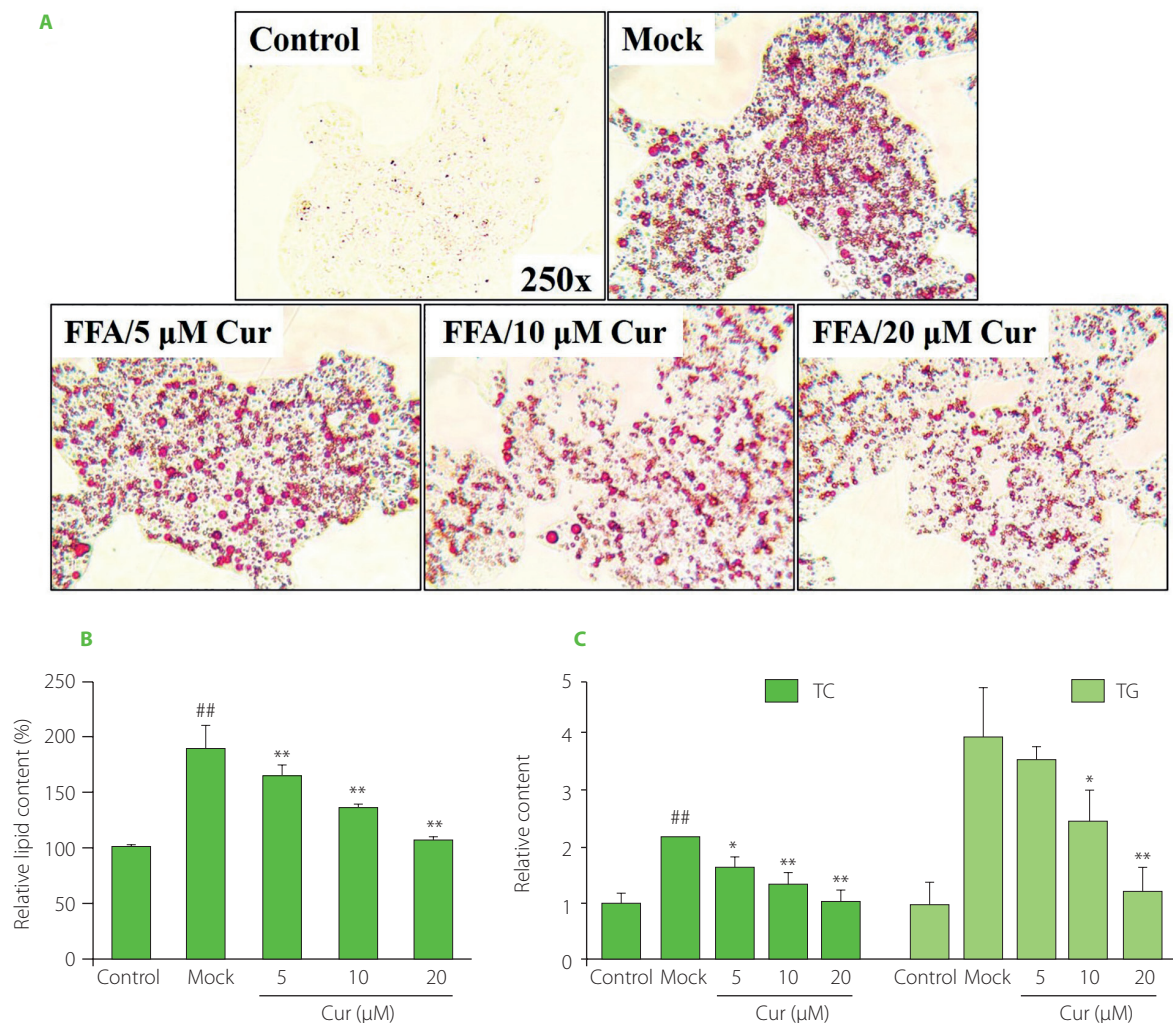


Figure 1. Curcumin prevented free fatty acid (FFA)-induced lipid accumulation in HepG2 cells. Cells were co-treated with 1 mM FFA mixture and various amounts of curcumin as indicated for 24 h before the assessment of cellular lipid levels. **(A)** Representative Oil Red O staining images. **(B)** Lipid semi-quantification of Oil Red O-stained cells. The control lipid content was set as 100%. **(C)** The total cholesterol (TC) and triglyceride (TG) contents. The TC and TG levels in control cells were set as 1.0. ^{##} $p < 0.01$, compared with untreated control cells; ^{*} $p < 0.05$ or ^{**} $p < 0.01$, compared with mock cells. Cur, curcumin; Mock, FFA-induced control cells.

however, a dramatic decrease in cell viability was observed upon 40 μM curcumin treatment (Figure S1A). Therefore, HepG2 cells were treated with no higher than 20 μM curcumin in the following assays. High-fat HepG2 cells were then induced by a 1 mM FFA mixture for 24 h without affecting cellular viability. And additional curcumin treatment did not significantly affect the cell viability, which remained constant after 24 h (Figure S1B). Therefore, in the subsequent assays, HepG2 cells were co-treated with 1 mM FFA and 5–20 μM curcumin for 24 h to evaluate curcumin's effect on lipid accumulation without cytotoxic impact.

Oil Red O staining was then carried out in FFA and curcumin co-treated cells. The results showed that FFA exposure significantly induced lipid accumulation. However, curcumin co-treatment markedly decreased the amount of lipid droplets with a dose-dependent effect (Figure 1A). Further lipid semi-quantification assay results showed that FFA-induced lipid deposition was dramatically reduced by 5–20 μM curcumin by around 10–50%, which was consistent with the results of Oil Red O staining (Figure 1B). One of the characteristics of NAFLD is the dysregulation of liver lipid

metabolism related to TG [Arab *et al.*, 2018; Degasperi & Colombo, 2016]. TG and cholesterol represent the main groups of lipids in cells. TG serves as a storage form of cellular lipids, and cholesterol is the precursor of various lipid signaling molecules [Friedman *et al.*, 2018]. Their total contents were also measured. As shown in Figure 1C, the intracellular TC and TG levels were increased by about 2.2-fold and 4-fold, respectively, upon 24 h FFA treatment in HepG2 cells. However, this stimulatory effect was attenuated by curcumin with a dose-dependent effect. Upon 20 μM curcumin treatment, the TC and TG levels were reduced to less than 50% of that of mock cells and similar to that of control cells. All these data indicated that curcumin promoted lipid metabolism, which was consistent with previous *in vivo* and *in vitro* studies [Li *et al.*, 2021; Rahmani *et al.*, 2016; Tian *et al.*, 2018].

■ Curcumin inhibited lipid accumulation by down-regulating miR-22-3p expression

miRNAs have been reported to be involved in the pathogenesis of fatty liver diseases with therapy potentials [Agbu & Carthew,

2021]. They may regulate lipid metabolism through downstream pathways and function as potential drug targets for NAFLD. For example, miR-122 inhibition upregulated its target gene *SIRT1*, a lipogenesis inhibitor that can activate the AMPK pathway to eventually prevent FFA-induced lipogenesis [Long *et al.*, 2019]. And miR-32-5p may activate SREBP-mediated adipogenesis, eventually promoting liver lipid accumulation and metabolic disorders [Wang *et al.*, 2023]. In addition, miR-122, miR-33, miR-34a and miR-21 are potential biomarkers for NAFLD and closely related to its progression [Gjorgjieva *et al.*, 2019]. Interestingly, curcumin can exert its physiological activity *via* miRNA regulation [Hayakawa *et al.*, 2022]. Our recent study also showed that miR-22-3p was downregulated by curcumin and modulated its antioxidant activity [Sun *et al.*, 2023]. miR-22-3p is known to be

involved in cytokine production, tumor and metabolic diseases, and is also involved in regulation of lipid metabolism [Panella *et al.*, 2023], however, with controversial effects [Castaño *et al.*, 2022; Gjorgjieva *et al.*, 2020; Hu *et al.*, 2020].

To address whether and how miR-22-3p also modulates curcumin's activity in controlling lipid metabolism, the expression level of miR-22-3p and its function in HepG2 cells were further examined. Compared with the control, FFA induction significantly increased miR-22-3p expression level. And additional curcumin treatment significantly declined the miR-22-3p level to around 60% (Figure S2A). Thus, the miR-22-3p expression level varied along with altered lipid amount in HepG2 cells. It was elevated by FFA but downregulated by curcumin. Moreover, miR-22-3p attenuated curcumin's effect in preventing lipid

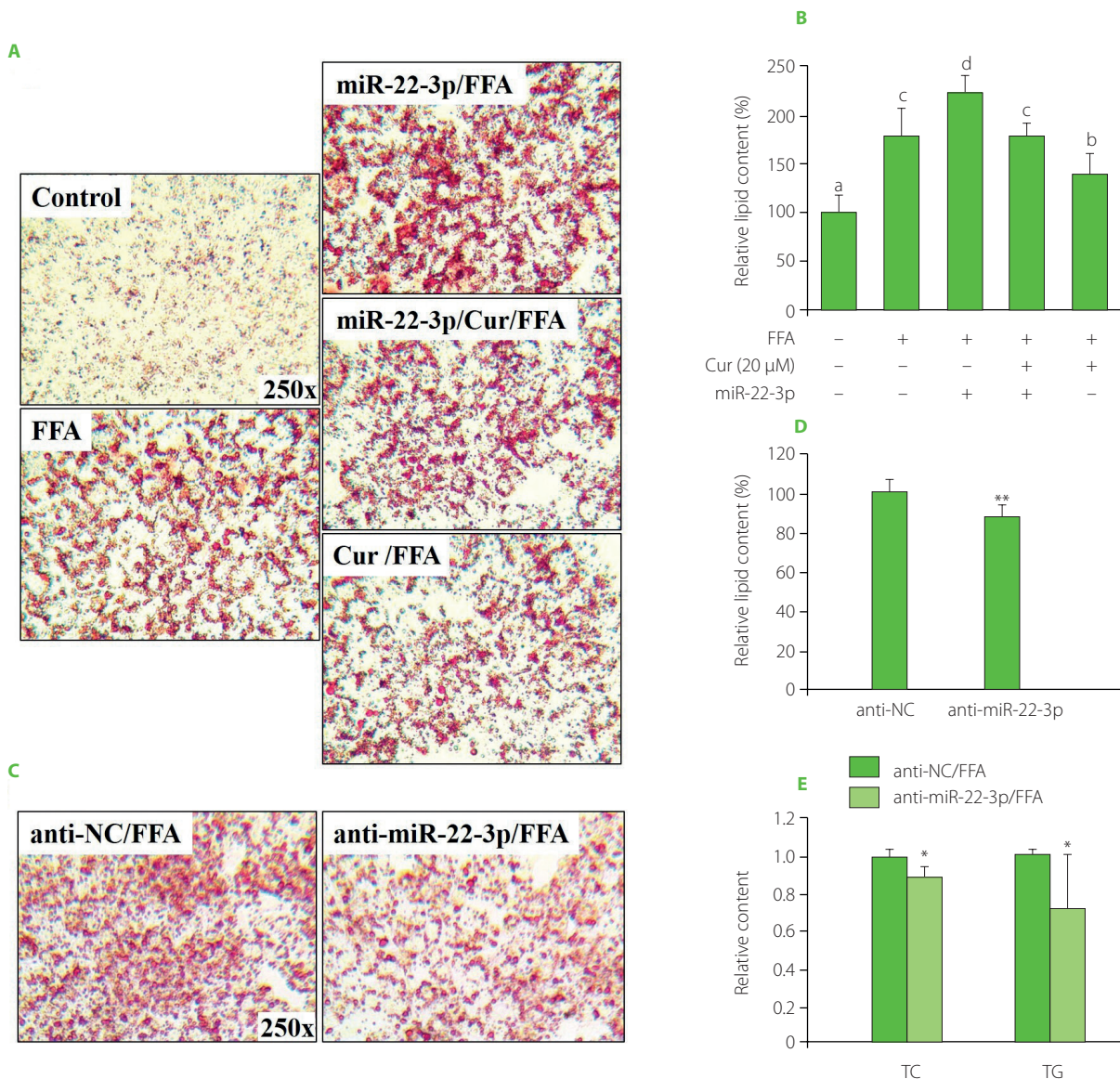


Figure 2. miR-22-3p modulated curcumin's effect on preventing free fatty acid (FFA)-induced lipid accumulation in HepG2 cells. (A–B) miR-22-3p overexpression reversed curcumin's effect on preventing lipid accumulation. Cells that were transfected with 40 nM miR-22-3p mimic for 48 h, and then co-treated with 1 mM FFA and 20 μ M curcumin (Cur) for 24 h. (A) Representative Oil Red O staining images. (B) Lipid semi-quantification of Oil Red O-stained cells. Different low case numbers on top of the columns indicate statistically significant differences among samples. (C–E) miR-22-3p repression significantly prevented lipid accumulation in HepG2 cells. The cells were transfected with 40 nM miR-22-3p inhibitor (anti-miR-22-3p) for 48 h and then stimulated with 1 mM FFA for 24 h. (C) Representative Oil Red O staining images. (D) Lipid semi-quantification of Oil Red O-stained cells. (E) The total cholesterol (TC) and triglyceride (TG) contents. The TC and TG contents in control cells were set as 1.0. * p <0.05 or ** p <0.01, compared with control cells that were transfected with miRNA inhibitor control (anti-NC).

accumulation. The results showed that curcumin-caused lipid reduction in HepG2 cells was reversed by miR-22-3p, as red lipid droplets and the total lipid contents were significantly increased by 48 h pre-transfection of miR-22-3p in the curcumin-treated cells (Figure 2A–B). All these data indicated that miR-22-3p is involved in modulating curcumin's activity in lipid control.

To further verify the effect of miR-22-3p on FFA-induced lipid accumulation, HepG2 cells were transfected with miR-22-3p inhibitor for 48 h and then stimulated by FFA for 24 h before lipid assessment. Compared with the control, deposition of red lipid droplets and the total lipid contents were significantly reduced upon miR-22-3p inhibition (Figure 2C–D). In addition, miR-22-3p repression significantly reduced the TC and TG contents to around 80% and 60%, respectively, as compared to the control cells (Figure 2E). Thus, miR-22-3p may function to promote hepatic lipid accumulation. Taken together, these results indicated that curcumin reduced FFA-induced lipid accumulation by downregulating miR-22-3p. miR-22-3p is a molecular target of curcumin to control lipid metabolism. Interestingly, miR-22-3p is a downstream effector of nuclear receptor farnesoid X receptor (*FXR*), which is regulated by curcumin in liver [Yan *et al.*, 2018; Zhao *et al.*, 2021]. Therefore, downregulation of miR-22-3p by curcumin may be mediated by *FXR*.

■ The *CRLS1* gene overexpression decreased lipid accumulation in HepG2 cells

miRNAs are involved in the regulation of cellular physiology and lipid metabolism *via* modulation of their target genes. For instance, miR-34a regulated macrophage cholesterol efflux and transport *via* targeting the *ABCA1* and *ABCG1* genes [Xu *et al.*, 2020]. And miR-17-5p upregulated adipogenic differentiation in 3T3-L1 cells *via* repressing *Tcf7l2*, a Wnt signaling pathway effector [Tian *et al.*, 2018]. Our previous study showed that the *CRLS1* gene is a target gene of miR-22-3p [Sun *et al.*, 2023]. *CRLS1* encodes cardiolipin synthase 1, which catalyzed the final step of mitochondrial cardiolipin synthesis. Cardiolipin is highly expressed in liver and plays an important role in hepatocyte lipid metabolism [Tu *et al.*, 2020]. The current study showed that the *CRLS1* gene expression was significantly decreased in FFA-induced HepG2 cells, but significantly increased by around 40% upon additional 20 μ M curcumin treatment (Figure S2A). In consistent, transfection with miR-22-3p inhibitor significantly promoted *CRLS1* gene expression in the FFA-induced mock cells (Figure S2B).

Considering the regulatory effect of miR-22-3p on lipid accumulation, *CRLS1* may be also involved in lipid metabolic control. Therefore, a pCMV-*CRLS1* overexpression plasmid [Sun

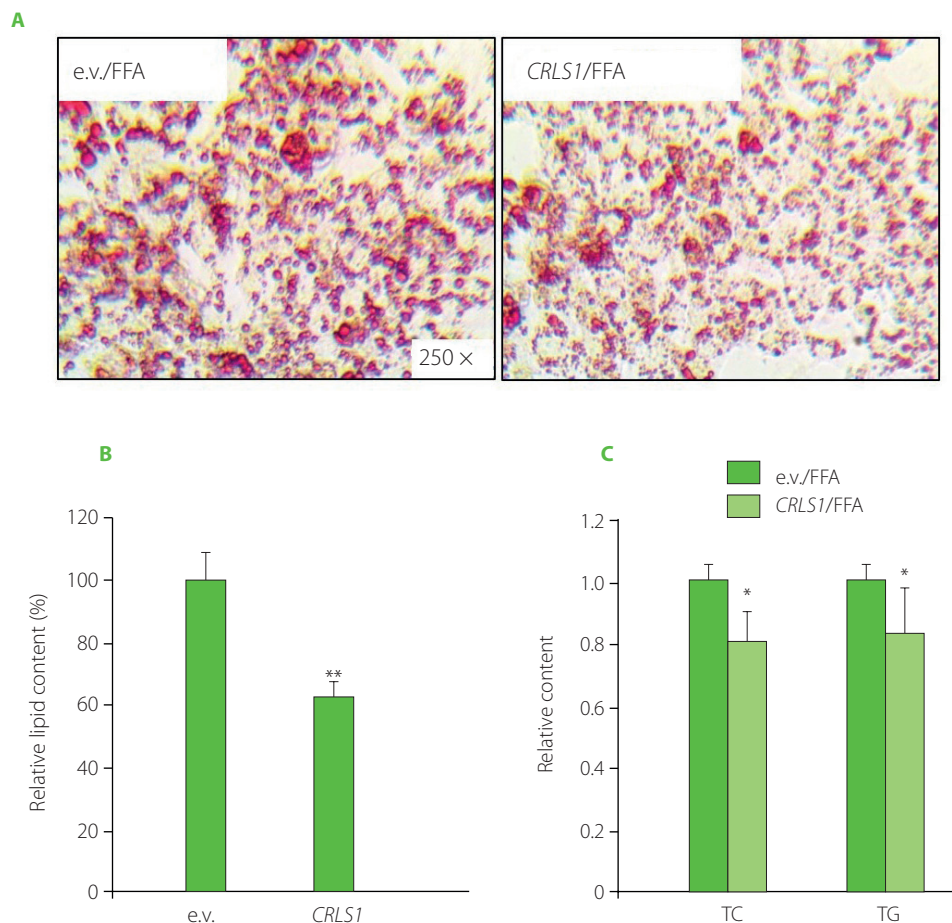


Figure 3. *CRLS1* overexpression prevented free fatty acid (FFA)-induced lipid accumulation in HepG2 cells. The cells were transfected with the pCMV-*CRLS1* vector (*CRLS1*) for 48 h and then treated with 1 mM FFA for 24 h. (A) Representative Oil Red O staining cell images. (B) Lipid semi-quantification of Oil Red O-stained cells. (C) Quantification of the total cholesterol (TC) and triglyceride (TG) contents. The TC and TG contents of control cells were set as 1.0. * $p < 0.05$ or ** $p < 0.01$, compared with control cells that were transfected with an empty vector (e.v.).

et al., 2023] was transfected into HepG2 cells for 48 h, followed by FFA-stimulation. There was a significant decrease in lipid droplets and cellular lipid content upon pCMV-CRLS1 transfection (Figure 3A–B), which was consistent with miR-22-3p inhibition or curcumin treatment. Meanwhile, *CRLS1* overexpression decreased the intracellular TC and TG levels by around 20% and 15%, respectively (Figure 3C). These data indicated that *CRLS1* overexpression prevented lipid accumulation in FFA-induced HepG2 cells, which resembled the effect of miR-22-3p repression or curcumin treatment. Our study result was consistent with the findings reported by Kawata *et al.* [2017] who demonstrated that an MCH1 receptor antagonist showed anti-obesity and anti-hepatosteatosis effect along with elevated cardioliplip level in liver. And miR-22-3p may promote lipid accumulation via inhibiting *CRLS1* expression and activity, which further affects mitochondrial lipid metabolism and mitochondrial functions.

■ Both miR-22-3p and *CRLS1* modulated the expression of lipogenic genes

The imbalance between synthesis and decomposition of fatty acids may lead to the accumulation of lipids. Lipid synthesis is regulated by a variety of enzymes and transcription factors via different metabolic pathways. *FAS* encodes fatty acid synthase, the key enzyme for *de novo* fatty acid synthesis [Yoon *et al.*, 2021]. The nuclear receptor peroxisome proliferators-activated receptor γ (*PPAR* γ) promotes steatosis [Lee *et al.*, 2012]. The sterol-regulatory element binding protein-1 (*SREBP-1*) is involved in cholesterol metabolism and regulates TC synthesis, and liver X receptor (*LXR*) was shown to activate *SREBP-1c* and upregulate the expression of *FAS* [Calkin & Tontonoz, 2012; Zhao *et al.*, 2022]. To elucidate the possible molecular mechanism underlying modulation of lipid accumulation in HepG2 cells, the expression of genes associated with lipogenesis was further examined. As shown in Figure 4A, the lipogenic genes, including *SREBP-1*, *PPAR* γ , *FAS* and *LXR* α , were all dramatically upregulated by FFA, indicating lipid generation. However, additional curcumin treatment for 24 h significantly suppressed expression of these genes. Therefore, curcumin downregulated lipogenic gene expression, which was in line with its activity in preventing lipid accumulation or steatosis [Rahmani *et al.*, 2016].

Furthermore, the mRNA levels of *SREBP-1*, *PPAR* γ , *FAS* and *LXR* α genes were dramatically reduced in cells transfected with miR-22-3p inhibitor for 48 h, which was similar to curcumin regulation (Figure 4A–B). Similarly, expression of these genes was significantly reduced upon *CRLS1* overexpression in FFA-stimulated HepG2 cells for 48 h (Figure 4C). Therefore, both miR-22-3p repression and *CRLS1* overexpression reduced lipogenesis, which resembled the regulation by curcumin. Besides *CRLS1*, miR-22-3p may target multiple mRNAs and regulate different enzymes or signal molecules in lipid metabolism. For instance, miR-22-3p was shown to target *PPAR* α and *SIRT1* [Azar *et al.*, 2020]. The current study showed that lipogenic *PPAR* γ , *SREBP-1*, *FAS* and *LXR* α genes were also regulated by miR-22-3p and *CRLS1*. *PPAR* γ is a ligand-activated transcription factor that controls fatty acid metabolism and glycerophospholipid metabolism. Activated

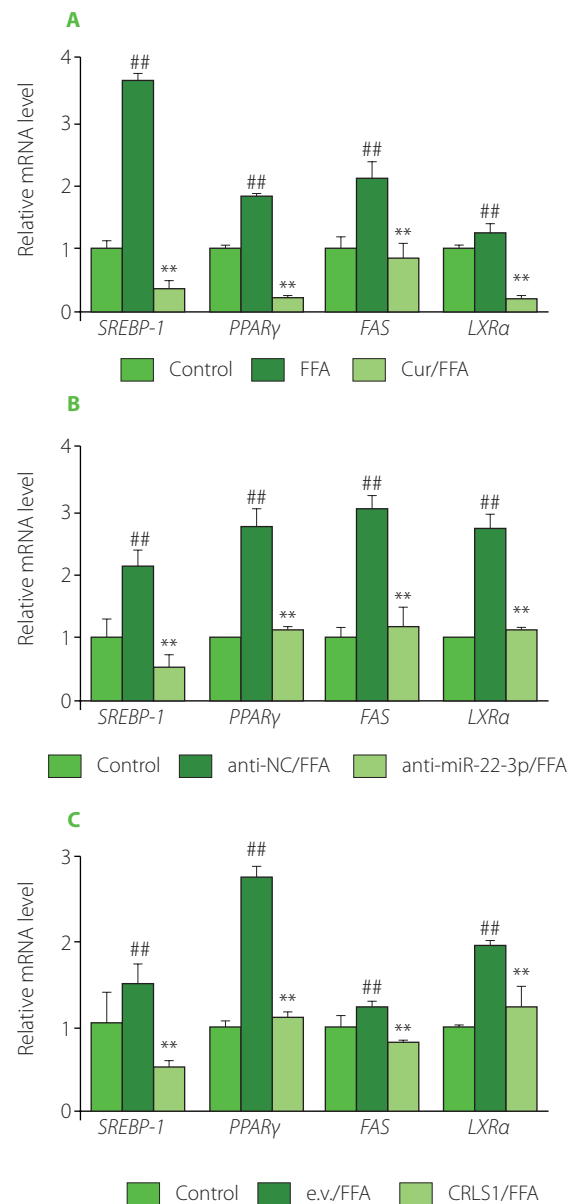


Figure 4. Both miR-22-3p repression and *CRLS1* overexpression resembled curcumin's effect on preventing the expression of lipogenic genes. (A) Effect of curcumin on the expression of genes involved in lipogenesis. The cells were co-treated with 20 μ M of curcumin and 1 mM free fatty acid (FFA) for 24 h before subsequent quantitative real-time PCR (qRT-PCR) assay. (B–C) The expression of lipogenic genes was significantly decreased by miR-22-3p repression or *CRLS1* overexpression. The cells were transfected with miR-22-3p inhibitor (anti-miR-22-3p) or the *CRLS1* overexpression vector (*CRLS1*) for 48 h and then stimulated with 1 mM FFA for 24 h, followed by qRT-PCR assay. (B) Transfection with miR-22-3p inhibitor. (C) Transfection with the pCMV-*CRLS1* vector. The mRNA expression level was set as 1.0 in control cells. ## p <0.01, compared with control cells; ** p <0.01, compared with FFA-induced mock cells. Cur, curcumin; anti-NC, miRNA inhibitor control; e.v., empty vector.

PPAR γ promotes the expression of proteins involved in lipid uptake, TG storage and lipid droplet formation [Lee *et al.*, 2012]. In addition, the *PPAR* γ -*LXR* α -*ABCA1/ABCG1* pathway is associated with cholesterol efflux [Zhang *et al.*, 2023]. *SREBPs* regulate cholesterol and fatty acid synthesis, and *SREBP-1* mainly activates genes required for fatty acid and TG synthesis. And *FAS* is a downstream gene of *SREBP-1* in lipid metabolism [Zhao *et al.*, 2022]. Therefore, curcumin may reduce lipogenesis by downregulating the miR-22-3p/*CRLS1* pathway, and eventually preventing

steatosis. Curcumin may also regulate other lipid metabolic branches, as indicated by controlling the expression of genes involved in fatty acid β -oxidation and cholesterol metabolism (Figure S3). However, the exact transcriptional mechanism remains to be elucidated, and the control of gene expression/activity by miR-22-3p/*CRLS1* is still in progress.

It has been suggested that simple steatosis can lead to the progression of NAFLD along with oxidative stress or mitochondrial dysfunction [Buzzetti *et al.*, 2016]. To address whether and how miR-22-3p/*CRLS1* controls oxidative stress in high-fat hepG2 cells, the cellular ROS levels were measured. The results showed that FFA-induced oxidative stress in HepG2 cells was significantly decreased upon inhibiting miR-22-3p or promoting *CRLS1* expression, resembling the antioxidant effect of curcumin (Figure S4). *CRLS1* was previously shown to control oxidative stress in hepatic LO2 cells [Sun *et al.*, 2023]. Tu *et al.* [2020] also reported downregulated *CRLS1* expression in a mouse NASH model, which further promoted NASH through downstream activating transcription factor3 (*ATF3*). The mitochondria play important roles in controlling hepatic cellular redox balance and lipid metabolism. However, long-term stress, such as oxidative stress and lipid accumulation, may lead to mitochondrial dysfunction [Wang *et al.*, 2022]. *CRLS1* catalyzes the biosynthesis of cardiolipin, a key mitochondrial regulator and also precursor of lipid signal molecules. Peng *et al.* [2018] demonstrated that the progression of NAFLD may be attributed to mitochondrial dysfunction and that cardiolipin level increased in early NAFLD but decreased in NASH, which suggested cardiolipin-mediated mitochondrial control in early NAFLD. Therefore, the current study also provides a mechanistic link between NAFLD and mitochondria regulation.

CONCLUSIONS

The regulation of lipid metabolism by miRNAs is very complicated. There are a variety of miRNA species involved, which is also linked to the target mRNA network. Besides binding to the 3'-untranslated region (UTR) of target mRNAs in most cases, miRNA may bind to 5'-UTR or coding sequence (CDS) of target mRNAs to control their expression. In addition, a single miRNA may have multiple targets to function in different pathways, or even exhibiting opposite effects in different hepatic steatosis models. The target gene may also be controlled by different miRNAs and show different regulatory functions. Moreover, *in vivo* and *in vitro* research data may differ, and data may even differ in different tissues of the same body. Finally, the expression and activity of miRNAs and target mRNAs do not always link with each other. Therefore, addressing the epigenetic regulation by miRNAs in lipid metabolism is of significance to reveal the pathogenesis of related liver diseases. It may also provide novel insights into the pre-diagnosis and treatment of hepatic lipid disorders.

SUPPLEMENTARY MATERIALS

The following are available online at <http://journal.pan.olsztyn.pl/Curcumin-Prevents-Free-Fatty-Acid-Induced-Lipid-Accu->

[mulation-via-Targeting-the-miR,182927,0,2.html](http://journal.pan.olsztyn.pl/Curcumin-Prevents-Free-Fatty-Acid-Induced-Lipid-Accumulation-via-Targeting-the-miR,182927,0,2.html); Materials and Methods: Cell viability assay; Determination of miRNA expression level; Measurement of cellular reactive oxygen species level **Table S1**. Additional primer sequences used in this study. **Figure S1**. Effect of curcumin on the viability of non-induced or free fatty acid (FFA)-induced HepG2 cells. **Figure S2**. The expression of miR-22-3p and *CRLS1* varied along with altered intracellular lipid level. **Figure S3**. Curcumin regulated the expression of genes involved in fatty acid β -oxidation and cholesterol metabolism. **Figure S4**. miR-22-3p repression and *CRLS1* overexpression resembled curcumin's effect on decreasing free fatty acid (FFA)-induced oxidative stress in HepG2 cells.

RESEARCH FUNDING

This work was supported by the National Natural Science Foundation of China (31771972), the Natural Science Foundation of Fujian Province (2017J01447), Fujian Province Young and Middle-aged Teachers Education Research Project (JAT200247), the opening project of National & Local Joint Engineering Research Center of Deep Processing Technology for Aquatic Products (Z823288), the Science and Technology Project of Quanzhou (2017Z003) and the High-level Talent Innovation Project of Quanzhou (2019CT007).

CONFLICT OF INTERESTS

The authors declare that they have no conflicts of interest.

ORCID IDs

Ch. Chen
S.-Y. Huang
K.-T. Ho
G. Li
J. Li
J. Liu
L. Lu
Y. Mei
X. Sun

<https://orcid.org/0000-0003-2147-5219>
<https://orcid.org/0000-0002-0370-1553>
<https://orcid.org/0000-0001-7224-1338>
<https://orcid.org/0000-0002-0940-6010>
<https://orcid.org/0000-0002-3444-3788>
<https://orcid.org/0000-0001-7231-6483>
<https://orcid.org/0000-0002-2544-966X>
<https://orcid.org/0009-0007-7216-3983>
<https://orcid.org/0000-0001-7616-8991>

REFERENCES

1. Abenavoli, L., Larussa, T., Corea, A., Procopio, A.C., Boccuto, L., Dallio, M., Federico, A., Luzzza, F. (2021). Dietary polyphenols and non-alcoholic fatty liver disease. *Nutrients*, 13(2), art. no. 494. <https://doi.org/10.3390/nu13020494>
2. Agbu, P., Carthew, R.W. (2021). MicroRNA-mediated regulation of glucose and lipid metabolism. *Nature Reviews Molecular Cell Biology*, 22(6), 425-438. <https://doi.org/10.1038/s41580-021-00354-w>
3. Arab, J.P., Arrese, M., Trauner, M. (2018). Recent insights into the pathogenesis of nonalcoholic fatty liver disease. *Annual Review of Pathology: Mechanisms of Disease*, 13(1), 321-350. <https://doi.org/10.1146/annurev-pathol-020117-043617>
4. Azar, S., Udi, S., Drori, A., Hadar, R., Nemirovski, A., Vemuri, K.V., Miller, M., Sherill-Rofe, D., Arad, Y., Gur-Wahnon, D., Li, X., Makriyannis, A., Ben-Zvi, D., Tabach, Y., Ben-Dov, I.Z., Tam, J. (2020). Reversal of diet-induced hepatic steatosis by peripheral CB1 receptor blockade in mice is p53/miRNA-22/SIRT1/PPAR α dependent. *Molecular Metabolism*, 42, art. no. 101087. <https://doi.org/10.1016/j.molmet.2020.101087>
5. Buzzetti, E., Pinzani, M., Tsochatzis, E.A. (2016). The multiple-hit pathogenesis of non-alcoholic fatty liver disease (NAFLD). *Metabolism*, 65(8), 1038-1048. <https://doi.org/10.1016/j.metabol.2015.12.012>
6. Calkin, A.C., Tontonoz, P. (2012). Transcriptional integration of metabolism by the nuclear sterol-activated receptors LXR and FXR. *Nature Reviews Molecular Cell Biology*, 13(4), 213-224. <https://doi.org/10.1038/nrm3312>
7. Castaño, C., Novials, A., Párrizas, M. (2022). Exosomes from short-term high-fat or high-sucrose fed mice induce hepatic steatosis through different pathways. *Cells*, 12(1), art. no. 169. <https://doi.org/10.3390/cells12010169>

8. Chen, Y., Wang, Y., Lin, W., Sheng, R., Wu, Y., Xu, R., Zhou, C., Yuan, Q. (2020). AFF1 inhibits adipogenic differentiation via targeting TGM2 transcription. *Cell Proliferation*, 53(6), art. no. e12831. <https://doi.org/10.1111/cpr.12831>
9. Degasperi, E., Colombo, M. (2016). Distinctive features of hepatocellular carcinoma in non-alcoholic fatty liver disease. *The Lancet Gastroenterology & Hepatology*, 1(2), 156-164. [https://doi.org/10.1016/S2468-1253\(16\)30018-8](https://doi.org/10.1016/S2468-1253(16)30018-8)
10. Ding, D., Ye, G., Lin, Y., Lu, Y., Zhang, H., Zhang, X., Hong, Z., Huang, Q., Chi, Y., Chen, J., Dong, S. (2019). MicroRNA-26a-CD36 signaling pathway: Pivotal role in lipid accumulation in hepatocytes induced by PM2.5 liposoluble extracts. *Environmental Pollution*, 248, 269-278. <https://doi.org/10.1016/j.envpol.2019.01.112>
11. Friedman, S.L., Neuschwander-Tetri, B.A., Rinella, M., Sanyal, A.J. (2018). Mechanisms of NAFLD development and therapeutic strategies. *Nature Medicine*, 24(7), 908-922. <https://doi.org/10.1038/s41591-018-0104-9>
12. Gjorgjieva, M., Ay, A.-S., Correia de Sousa, M., Delangre, E., Dolicka, D., Sobolewski, C., Maeder, C., Fournier, M., Sempoux, C., Foti, M. (2022). MiR-22 deficiency fosters hepatocellular carcinoma development in fatty liver. *Cells*, 11(18), art. no. 2680. <https://doi.org/10.3390/cells11182860>
13. Gjorgjieva, M., Sobolewski, C., Ay, A.-S., Abegg, D., Correia de Sousa, M., Portius, D., Berthou, F., Fournier, M., Maeder, C., Rantakari, P., Zhang, F.-P., Poutanen, M., Picard, D., Montet, X., Nef, S., Adibekian, A., Foti, M. (2020). Genetic ablation of MiR-22 fosters diet-induced obesity and NAFLD development. *Journal of Personalized Medicine*, 10(4), art. no. 170. <https://doi.org/10.3390/jpm10040170>
14. Gjorgjieva, M., Sobolewski, C., Dolicka, D., Correia de Sousa, M., Foti, M. (2019). miRNAs and NAFLD: from pathophysiology to therapy. *Gut*, 68(11), 2065-2079. <https://doi.org/10.1136/gutjnl-2018-318146>
15. Gómez-Lechón, M.J., Donato, M.T., Martínez-Romero, A., Jiménez, N., Castell, J.V., O'Connor, J.-E. (2007). A human hepatocellular *in vitro* model to investigate steatosis. *Chemico-Biological Interactions*, 165(2), 106-116. <https://doi.org/10.1016/j.cbi.2006.11.004>
16. Hayakawa, S., Ohishi, T., Oishi, Y., Isemura, M., Miyoshi, N. (2022). Contribution of non-coding RNAs to anticancer effects of dietary polyphenols: chlorogenic acid, curcumin, epigallocatechin-3-gallate, genistein, quercetin and resveratrol. *Antioxidants*, 11(12), art. no. 2352. <https://doi.org/10.3390/antiox11122352>
17. Hernandez-Rodas, M.C., Valenzuela, R., Videla, L.A. (2015). Relevant aspects of nutritional and dietary interventions in non-alcoholic fatty liver disease. *International Journal of Molecular Sciences*, 16(10), 25168-25198. <https://doi.org/10.3390/ijms161025168>
18. Hu, Y., Liu, H.X., Jena, P.K., Sheng, L., Ali, M.R., Wan, Y.Y. (2020). miR-22 inhibition reduces hepatic steatosis via FGF21 and FGFR1 induction. *JHEP Reports*, 2(2), art. no. 100093. <https://doi.org/10.1016/j.jhepr.2020.100093>
19. Kawata, Y., Okuda, S., Hotta, N., Igawa, H., Takahashi, M., Ikoma, M., Kasai, S., Ando, A., Satomi, Y., Nishida, M., Nakayama, M., Yamamoto, S., Nagisa, Y., Takekawa, S. (2017). A novel and selective melanin-concentrating hormone receptor 1 antagonist ameliorates obesity and hepatic steatosis in diet-induced obese rodent models. *European Journal of Pharmacology*, 796, 45-53. <https://doi.org/10.1016/j.ejphar.2016.12.018>
20. Kloska, A., Weśnierska, M., Malinowska, M., Gabig-Cimińska, M., Jakóbkiewicz-Banecka, J. (2020). Lipophagy and lipolysis status in lipid storage and lipid metabolism diseases. *International Journal of Molecular Sciences*, 21(17), art. no. 6113. <https://doi.org/10.3390/ijms21176113>
21. Lee, Y.J., Ko, E.H., Kim, J.E., Kim, E., Lee, H., Choi, H., Yu, J.H., Kim, H.J., Seong, J.-K., Kim, K.-S., Kim, J.-w. (2012). Nuclear receptor PPAR γ -regulated monoacyl-glycerol O-acyltransferase 1 (MGAT1) expression is responsible for the lipid accumulation in diet-induced hepatic steatosis. *Proceedings of the National Academy of Sciences of the United States of America*, 109(34), 13656-13661. <https://doi.org/10.1073/pnas.1203218109>
22. Li, S., You, J., Wang, Z., Liu, Y., Wang, B., Du, M., Zou, T. (2021). Curcumin alleviates high-fat diet-induced hepatic steatosis and obesity in association with modulation of gut microbiota in mice. *Food Research International*, 143, art. no. 110270. <https://doi.org/10.1016/j.foodres.2021.110270>
23. Lonardo, A., Nascimben, F., Mantovani, A., Targher, G. (2018). Hypertension, diabetes, atherosclerosis and NAFLD: Cause or consequence? *Journal of Hepatology*, 68(2), 335-352. <https://doi.org/10.1016/j.jhep.2017.09.021>
24. Long, J.K., Dai, W., Zheng, Y.W., Zhao, S.P. (2019). miR-122 promotes hepatic lipogenesis via inhibiting the LKB1/AMPK pathway by targeting Sirt1 in non-alcoholic fatty liver disease. *Molecular Medicine*, 25(1), art. no. 26. <https://doi.org/10.1186/s10020-019-0085-2>
25. Panella, R., Petri, A., Desai, B.N., Fagoonee, S., Cotton, C.A., Nguyen, P.K., Lundin, E.M., Wagshal, A., Wang, D.-Z., Näär, A.M., Vlachos, I.S., Maratos-Flier, E., Altruda, F., Kauppinen, S., Pandolfi, P.P. (2023). MicroRNA-22 is a key regulator of lipid and metabolic homeostasis. *International Journal of Molecular Sciences*, 24(16), art. no. 12870. <https://doi.org/10.3390/ijms241612870>
26. Peng, K.-Y., Watt, M.J., Rensen, S., Greve, J.W., Huynh, K., Jayawardana, K.S., Meikle, P.J., Meex, R.C.R. (2018). Mitochondrial dysfunction-related lipid changes occur in nonalcoholic fatty liver disease progression. *Journal of Lipid Research*, 59(10), 1977-1986. <https://doi.org/10.1194/jlr.M085613>
27. Rafei, H., Omidian, K., Bandy, B. (2019). Dietary polyphenols protect against oleic acid-induced steatosis in an *in vitro* model of NAFLD by modulating lipid metabolism and improving mitochondrial function. *Nutrients*, 11(3), art. no. 541. <https://doi.org/10.3390/nu11030541>
28. Rahmani, S., Asgari, S., Askari, G., Keshvari, M., Hatampour, M., Feizi, A., Sahebkar, A. (2016). Treatment of non-alcoholic fatty liver disease with curcumin: A randomized placebo-controlled trial. *Phytotherapy Research*, 30(9), 1540-1548. <https://doi.org/10.1002/ptr.5659>
29. Shan, D., Wang, J., Di, Q., Jiang, Q., Xu, Q. (2022). Steatosis induced by non-phenol in HepG2 cells and the intervention effect of curcumin. *Food & Function*, 13(1), 327-343. <https://doi.org/10.1039/D1FO02481G>
30. Sun, X., Li, Y., Lin, Y., Mei, Y., Lin, L., Ho, K.-T., Huang, K., Zhan, J., Chen, C., Zeng, J., Wu, D., Li, J., Liu, J., Li, G. (2023). MiR-22-3p modulated the antioxidant activity of curcumin via targeting the cardioplin synthase gene CRLS1 in LO2 cells. *Journal of Functional Foods*, 104, art. no. 105541. <https://doi.org/10.1016/j.jff.2023.105541>
31. Thibonnier, M., Esau, C., Ghosh, S., Wargent, E., Stocker, C. (2020). Metabolic and energetic benefits of microRNA-22 inhibition. *BMJ Open Diabetes Research & Care*, 8(1), art. no. e001478. <https://doi.org/10.1136/bmjdr-2020-001478>
32. Tian, L., Song, Z., Shao, W., Du, W.W., Zhao, L.R., Zeng, K., Yang, B.B., Jin, T. (2018). Curcumin represses mouse 3T3-L1 cell adipogenic differentiation via inhibiting miR-17-5p and stimulating the Wnt signalling pathway effector Tcf712. *Cell Death & Disease*, 8(1), art. no. e2559. <https://doi.org/10.1038/cddis.2016.455>
33. Tu, C., Xiong, H., Hu, Y., Wang, W., Mei, G., Wang, H., Li, Y., Zhou, Z., Meng, F., Zhang, P., Mei, Z. (2020). Cardioplin synthase 1 ameliorates NASH through activating transcription factor 3 transcriptional inactivation. *Hepatology*, 72(6), 1949-1967. <https://doi.org/10.1002/hep.31202>
34. Veitch, S., Njock, M.S., Chandry, M., Siraj, M.A., Chi, L., Mak, H., Yu, K., Rathnakumar, K., Perez-Romero, C.A., Chen, Z., Alibhai, F.J., Gustafson, D., Raju, S., Wu, R., Zarrin Khat, D., Wang, Y., Caballero, A., Meagher, P., Lau, E., Pepic, L., Cheng, H.S., Galant, N.J., Howe, K.L., Li, R.K., Connelly, K.A., Husain, M., Delgado-Olguin, P., Fish, J.E. (2022). MiR-30 promotes fatty acid beta-oxidation and endothelial cell dysfunction and is a circulating biomarker of coronary microvascular dysfunction in pre-clinical models of diabetes. *Cardiovascular Diabetology*, 21(1), art. no. 31. <https://doi.org/10.1186/s12933-022-01458-z>
35. Wang, Y.-D., Wu, L.-L., Mai, Y.-N., Wang, K., Tang, Y., Wang, Q.-Y., Li, J.-Y., Jiang, L.-Y., Liao, Z.-Z., Hu, C., Wang, Y.-Y., Liu, J.-J., Liu, J.-H., Xiao, X.-H. (2023). miR-32-5p induces hepatic steatosis and hyperlipidemia by triggering *de novo* lipogenesis. *Metabolism*, 146, art. no. 155660. <https://doi.org/10.1016/j.metabol.2023.155660>
36. Wang, Y., Chen, C., Chen, J., Sang, T., Peng, H., Lin, X., Zhao, Q., Chen, S., Eling, T., Wang, X. (2022). Overexpression of NAG-1/GDF15 prevents hepatic steatosis through inhibiting oxidative stress-mediated dsDNA release and AIM2 inflammasome activation. *Redox Biology*, 52, art. no. 102322. <https://doi.org/10.1016/j.redox.2022.102322>
37. Xu, Y., Xu, Y., Zhu, Y., Sun, H., Juguilon, C., Li, F., Fan, D., Yin, L., Zhang, Y. (2020). Macrophage miR-34a is a key regulator of cholesterol efflux and atherosclerosis. *Molecular Therapy*, 28(1), 202-216. <https://doi.org/10.1016/j.jymthe.2019.09.008>
38. Yan, C., Zhang, Y., Zhang, X., Aa, J., Wang, G., Xie, Y. (2018). Curcumin regulates endogenous and exogenous metabolism via Nrf2-FXR-LXR pathway in NAFLD mice. *Biomedicine & Pharmacotherapy*, 105, 274-281. <https://doi.org/10.1016/j.biopha.2018.05.135>
39. Yoon, H., Shaw, J.L., Haigis, M.C., Greka, A. (2021). Lipid metabolism in sickness and in health: Emerging regulators of lipotoxicity. *Molecular Cell*, 81(18), 3708-3730. <https://doi.org/10.1016/j.molcel.2021.08.027>
40. Zhang, F., Li, Y., Xin, W., Wang, L., Zhang, Y., Xu, H., Wang, H., Zhao, H., Yang, H., Si, N., Bian, B. (2023). Gypenosides and capsaicinoids in combination ameliorates high-fat-diet-induced rat hyperlipidemia via the PPAR γ -LXR-ABCA1/ABCG1 pathway. *Journal of Functional Foods*, 108, art. no. 105714. <https://doi.org/10.1016/j.jff.2023.105714>

41. Zhang, M., Sun, W., Zhou, M., Tang, Y. (2017). MicroRNA-27a regulates hepatic lipid metabolism and alleviates NAFLD via repressing FAS and SCD1. *Scientific Reports*, 7(1), art. no. 14493. <https://doi.org/10.1038/s41598-017-15141-x>
42. Zhang, M., Tang, Y., Tang, E., Lu, W. (2020). MicroRNA-103 represses hepatic *de novo* lipogenesis and alleviates NAFLD via targeting FASN and SCD1. *Biochemical and Biophysical Research Communications*, 524(3), 716-722. <https://doi.org/10.1016/j.bbrc.2020.01.143>
43. Zhao, Q., Lin, X., Wang, G. (2022). Targeting SREBP-1-mediated lipogenesis as potential strategies for cancer. *Frontiers in Oncology*, 12, art. no. 952371. <https://doi.org/10.3389/fonc.2022.952371>
44. Zhao, T., Wang, J., He, A., Wang, S., Chen, Y., Lu, J., Lv, J., Li, S., Wang, J., Qian, M., Li, H., Shen, X. (2021). Mebhydrolin ameliorates glucose homeostasis in type 2 diabetic mice by functioning as a selective FXR antagonist. *Metabolism*, 119, art. no. 154771. <https://doi.org/10.1016/j.metabol.2021.154771>

Effect of Infrared Drying on the Drying Kinetics and the Quality of Mango (*Mangifera indica*) Powder

Phuoc-Bao-Duy Nguyen^{1,2} , Thi-Van-Linh Nguyen^{3,*} , Thi-Thuy-Dung Nguyen³ 

¹Faculty of Electrical and Electronics Engineering, Ho Chi Minh University of Technology (HCMUT), 268 Ly Thuong Kiet Street, District 10, Ho Chi Minh City, Vietnam

²Vietnam National University Ho Chi Minh City, Linh Trung Ward, Thu Duc District, Ho Chi Minh City, Vietnam

³Department of Food Technology, Institute of Applied Technology and Sustainable Development, Nguyen Tat Thanh University, 300A Nguyen Tat Thanh Street, District 4, Ho Chi Minh City, Vietnam

Mango powder is a nutrient-dense substance that can be used directly or as a supplement in food items. However, due to the high sugar content, the removal of moisture from mango was difficult. This study investigated an infrared drying technique for removing moisture from mango pulp to produce powder products. The experiment was designed in a three-factor full factorial design with the following variables: drying temperature (70, 75, and 80°C), maltodextrin content (0, 6, and 9 g/100 g pulp), and total soluble solid content (11 and 16°Brix). The findings indicated that the Weibull model was the most appropriate for describing the moisture removal of mango pulp during infrared drying. Higher temperature and maltodextrin content, along with reduced total soluble solid content, resulted in improved quality of the mango powder. Furthermore, the optimal drying conditions for mango powder were found as 11°Brix, 80°C, and 9% maltodextrin content, which could ensure the highest retention of total phenolics (59.874%), retention of reducing sugars (71.044%), total acidity (10.141%), and retention of DPPH radical scavenging activity (65.051%). To fully benefit from the rewards of infrared drying, it is essential to establish suitable pretreatment conditions or use additives to preserve component quality.

Key words: antioxidant activity, fruit powder, phenolics, pulp drying, Weibull model

INTRODUCTION

Mango (*Mangifera indica* L.) is one of the most widely consumed tropical fruits due to its high nutritional and economic values [Occena-Po, 2006]. It has been found to contain numerous bioactive phytochemicals, including phenolics, terpenoids, carotenoids, and phytosterols with antioxidant, anti-inflammatory, immunomodulatory, antibacterial, anti-diabetic, anti-cancer, and anti-microbial benefits [Mirza *et al.*, 2021]. However, mango fruits are extremely perishable and delicate; thus special care must be taken during their transport and storage. Mangoes are a very marketable commodity, and the processing sector can increase its value by transforming them into frozen goods, pulp,

and powders among which mango powder holds a lot of promise as a nutritional supplement because of its high nutritional value [Owino & Ambuko, 2021]. Nevertheless, the production of mango powder faces many difficulties because the high sugar content of the fruits hinders moisture removal to reach the final desired moisture content, whereas the stickiness and clumping lessen the recovery rate of product and make the drying process more challenging to operate [Djantou *et al.*, 2007]. Therefore, the main technical problem is to achieve the final moisture content as well as to prevent the adverse phenomenon of stickiness and clumping that occurs during the drying of mango [Truong *et al.*, 2005]. The stickiness of high-sugar products has been

*Corresponding Author:

e-mail: ntvlinh@ntt.edu.vn (T.V.L. Nguyen)

Submitted: 15 October 2023

Accepted: 23 January 2024

Published on-line: 1 March 2024



© Copyright by Institute of Animal Reproduction and Food Research of the Polish Academy of Sciences
© 2024 Author(s). This is an open access article licensed under the Creative Commons Attribution-NonCommercial-NoDerivs License (<http://creativecommons.org/licenses/by-nc-nd/4.0/>).

determined to be directly associated with the glass transition temperature (the value at which amorphous polymer chains below the phase transition point shift from the crystalline state to the elastic state, symbolized as T_g , is low) [Roos *et al.*, 1996]. At the same time, dried products are prone to clumping when grinding or during storage [Roos *et al.*, 1996; Slade *et al.*, 1991]. Two methods commonly used to overcome these problems are (i) product formulation, and (ii) process optimization [Djantou *et al.*, 2012]. The powder quality and the drying performance can be enhanced through the addition of additives to reduce the moisture content to an appropriate value [Bhandari *et al.*, 1993].

Mangoes are dried using a wide variety of techniques around the globe; for example, Pott *et al.* [2005] improved the quality of unsulfided mango slices by drying at high temperature (80°C) for about 6 h while Wang *et al.* [2018] evaluated the thermal efficiency of the indirect forced convection solar drying and analyzed the drying kinetics of mango. Furthermore, Caparino *et al.* [2012] investigated the physical and microstructural properties of mango powder affected by different drying processes and concluded that Refractance Window® (RW) drying produced mango powder that was on par with that of the freeze-dried powder and even higher in quality than the spray-dried one. The same conclusion in terms of the drying efficiency of the RW method was verified in the study by Zotarelli *et al.* [2017]. Spray-drying technique is considered a suitable technique in the production of fruit powders thanks to its short drying time, which effectively reduces the loss caused by the decomposition of chemical compounds in the product along with the product moisture of 2–5 g/100 g, water activity of 0.2–0.6, and increased storage stability [Marques *et al.*, 2007; Tan *et al.*, 2011]. The application of the RW drying technique to mango pulp resulted in the production of high-quality mango powder, thereby demonstrating the effectiveness of the high heat drying technique in removing water from mango pulp and overcoming the stickiness that is the primary issue with spray drying [Nguyen *et al.*, 2022a,b].

A new drying technology of the fourth generation, such as infrared (IR) drying, can be applied to the drying of mango pulp, particularly thin layers with high contact surfaces [Allanic *et al.*, 2017]. The emitted radiation is of a narrow wavelength and the heat transfer efficiency is between 80% and 90% [Sadin *et al.*, 2014]. Uniform heating, reduced processing time, increased heat transfer and energy absorption rate, and a better end product are some of the benefits of using IR drying [Zhu & Pan, 2009]. For instance, the IR approach accelerated the drying process of apples by 50% as compared to the convection heat method [Nowak & Lewicki, 2004]. Therefore, the combination of IR and hot air provides a synergistic effect, which leads to a more efficient drying process [Afzal *et al.*, 1999; Nawirska *et al.*, 2009]. The application of infrared drying to mango sections has been the subject of research [Doymaz, 2017; Yao *et al.*, 2020]. Doymaz [2017] reported that the final moisture content of dried mango slices was around 0.15 g water/g dry weight (DW), which corresponds to 13 g/100 g on a wet basis. Another investigation conducted by Yao *et al.* [2020] exposed a moisture content of about 0.20 g water/g DW, which corresponds to 16.7 g/100 g on a wet

basis. These moisture contents were considered inappropriate for the grinding process performed in the production of fruit powder. At this time, empirical evidence regarding the drying of mango pulp *via* infrared is lacking. However, the fruit powder manufacturing sector shows great potential for implementing infrared drying technology, owing to its easy scalability and remarkable energy efficiency. Based on the favorable findings observed in the production of mango powder *via* RW drying of mango pulp, it is believable to suggest that infrared drying could exhibit remarkable efficacy when applied to mango powder. Thus, the purpose of this study was to assess the impact of IR drying conditions on drying characteristics and quality of resulting mango powder from mango pulp. These experimental results will contribute to the improvement in production towards the best quality and lowest production cost.

MATERIALS AND METHODS

■ Material and its pretreatment

Mature and evenly ripe mango (*Mangifera indica* L.) fruits were collected in Thanh Phuoc hamlet (Thanh Phong commune, Thanh Phu district, Ben Tre province, Vietnam) with soft texture and characteristic aroma. After being washed, peeled and sliced, mango slices were steamed for 3 min and then cooled immediately in cold water, followed by grinding in a commercial blender and sieving through 16-mesh sieves. Afterward, distilled water was used to adjust the mango pulp to 11 and 16°Brix. Mango pulp was subsequently sealed in polypropylene bags and frozen at –18°C until it could be employed again.

■ Chemicals

Chemicals used in the study were purchased from Sigma-Aldrich (Singapore), including 2,2-diphenyl-1-picrylhydrazyl (DPPH) radical (purity 99%), 6-hydroxy-2,5,7,8-tetramethylchroman-2-carboxylic acid (Trolox, purity 99%), gallic acid (purity 99%), 3,5-dinitrosalicylic acid (DNS, purity 99%), and Folin-Ciocalteu reagent (FCR). Maltodextrin (dextrose equivalent of 16–20), used as a carrier, was purchased from Merck Millipore (Burlington, MA, USA).

■ Experimental design and infrared drying operation

In this study, an infrared drying system was self-fabricated in a laboratory setting which has previously been effectively applied to drying avocado powder [Nguyen *et al.*, 2021]. The drying system consisted of a drying chamber (length × width × height of 64×23×27 cm) equipped with an infrared radiation module (ITT 1000W 235V-01X0, maximum capacity of 1,000 W, Germany) placed 20 cm away from the surface of drying materials. Infrared radiation was controlled through a thermometer with an accuracy of 0.5°C and a delay of 0.5 s. The three-factor full factorial design including total soluble solids (11 and 16°Brix), drying temperature (70, 75, and 80°C), and maltodextrin content (0, 6, and 9 g/100 g pulp) was used. The moisture content of the dried samples was measured at 5-min intervals by an MB23 moisture analyzer (Ohaus, Parsippany, NJ, USA) for which the drying was discontinued at the moisture content of 0.04 g/g DW. The mathematical model and kinetic parameters for the infrared drying

of mango pulp were then determined based on the experimental data of the moisture content change during drying. Besides, retention of total phenolic content (TPC), retention of reducing sugars (RS), total titratable acidity (TA) and retention of DPPH radical scavenging activity of mango powder were used to analyze the influence of factors on the infrared drying of mango pulp.

■ Mathematical models for thin-layer drying curves

During prolonged drying, for the moisture content at equilibrium state is comparatively small compared to that at different time intervals (M_t , g water/g DW) or the initial value (M_0 , g water/g DW), the moisture ratio (MR) should be determined according Equation (1) [Pala *et al.*, 1996]:

$$MR = \frac{M_t}{M_0} \quad (1)$$

Many mathematical models have been proposed to predict how foods will dry [Onwude *et al.*, 2016]. This study fitted drying curves to the semi-theoretical and empirical models.

Newton (Lewis) model (Equation 2): The simplest model to describe the drying characteristics of some agricultural products with assumptions that the drying material is arranged sufficiently thin, the air velocity is high, and temperature and relative humidity are constant during drying.

$$MR = \exp(-kt) \quad (2)$$

Page model (Equation 3): The experimental model evolved from the Newton model to reduce the error by adding a dimensionless constant (n).

$$MR = \exp(-kt^n) \quad (3)$$

Henderson and Pabis model (Equation 4): The model was derived from the initial term in the general solution of the second Fick diffusion law, operating under the assumption that the general solution approaches being equal to the initial term when the drying process continues for an extended period of time.

$$MR = a \times \exp(-kt) \quad (4)$$

Logarithmic model (Equation 5): The model transformed from the Henderson and Pabis model by adding the empirical constant (c).

$$MR = a \times \exp(-kt) + c \quad (5)$$

Midilli model (Equation 6): The model transformed from the Henderson and Pabis model by combining exponential and linear terms.

$$MR = a \times \exp(-kt^n) + bt \quad (6)$$

Weibull model (Equation 7): Experimental model, developed from experimental data.

$$MR = a - b \times \exp \left[- \left(\frac{t}{\beta} \right)^\alpha \right] \quad (7)$$

The coefficient of determination (R^2) and the root mean square error (RMSE) were calculated to determine the power of the tested models according Equation (8) and Equation (9), respectively.

$$R^2 = 1 - \frac{\sum_{i=1}^N (M_{\text{exp},i} - M_{\text{pre},i})^2}{\sum_{i=1}^N (MR_{\text{exp}} - MR_{\text{pre},i})^2} \quad (8)$$

$$RMSE = \sqrt{\frac{1}{N} \sum_{i=1}^N (M_{\text{exp},i} - M_{\text{pre},i})^2} \quad (9)$$

where, $M_{\text{exp},i}$ and $M_{\text{pre},i}$ are the experimental and predicted moisture ratio, MR_{exp} is the mean value of the experimental dimensionless moisture ratio, and N is the number of observations.

■ Determination of the effective moisture diffusivity

Fick's second law of diffusion was applied to the mango pulp, which was regarded as an infinite flat plate, in order to determine the movement of moisture. The equation for diffusion is given below (Equation 10):

$$\frac{\partial M}{\partial t} = D_{\text{eff}} \nabla^2 M \quad (10)$$

where, M is the moisture content (g water/g DW), D_{eff} is the effective moisture diffusivity (m^2/s), and t is time (s).

Crank [1975] provided a general analytical solution for the thin-layer drying under certain conditions, including but not limited to: homogeneous and isotropic product sizes; constant product characteristics; minimal shrinkage; minimal external resistance to heat and mass transfer; sole surface evaporation; uniform initial moisture distribution; constant moisture diffusivity. The answer was as follows (Equation 11):

$$MR = \frac{8}{\pi^2} \sum_{n=0}^{\infty} \frac{1}{(2n+1)^2} \exp \left(- (2n+1)^2 \pi^2 \frac{D_{\text{eff}}}{L^2} t \right) \quad (11)$$

where, MR is the dimensionless moisture ratio, L is the thickness (m), n is the term in series expansion, and t is time (s).

The initial term in the previous series expansion (where $n=0$) was regarded as an approximation for extended drying periods (Equation 12):

$$MR = \frac{8}{\pi^2} \exp \left(- \pi^2 \frac{D_{\text{eff}}}{L^2} t \right) \quad (12)$$

The effective moisture diffusivity was calculated using the non-linear least square method based on the Levenberg-Marquardt method [Marquardt, 1963].

■ Chemical analysis

■ Preparation of analytical solution

To prepare the analytical solutions for total phenolic content and antioxidant activity determinations, 0.5 g of powder was extracted with 10 mL of 60% (v/v) methanol under sonication (40 KHz, 240 W, 5 min) in the Pro 100-40D ultrasonic cleaner (Asonic, Ljubljana, Slovenia), followed by being cooled for 20 min at

10°C and centrifuged (1,220×g, 10 min) in the PLC-05 centrifuge (Gemmy Industrial Corp., Taipei, Taiwan). The extraction was then repeated and the supernatant was finally collected for analysis. The analytical samples for the determination of reducing sugar content and total acidity were prepared following the same procedure using distilled water as a solvent.

■ Total phenolic content determination

Total phenolic content was determined following the International Organization for Standardization (ISO) 14502-1:2005 method [ISO, 2005] which is based on the chromophore formed between phenolics and FCR under alkaline conditions. Briefly, aliquots (0.6 mL) were mixed successively with 1.5 mL of FCR and 1.2 mL of 7.5% Na₂CO₃ before the absorbance measurement at 765 nm using the UV-9000 spectrometer (Metash, Shanghai, China). Total phenolic content, which was calculated as mg of gallic acid equivalent *per g* of dried powder (mg GAE/g DW) using the gallic acid standard curve, was used to further estimate its retention (TPC Ret) during drying according to Equation (13).

$$\text{TPC Ret (\%)} = \frac{C_{\text{TPC, after drying}}}{C_{\text{TPC, before drying}}} \times 100\% \quad (13)$$

where: $C_{\text{TPC, before drying}}$ and $C_{\text{TPC, after drying}}$ were the TPC in the sample before drying and after drying, respectively.

■ Antioxidant activity determination – DPPH assay

DPPH radical scavenging activity was evaluated according to the procedure described by Brand-Williams *et al.* [1995] with minor changes, which is based on the reduction in violet color caused by the reaction of antioxidants and DPPH radical. Briefly, sample aliquots (150 µL) were reacted with 2,850 µL of a working DPPH radical solution (absorbance of 1.10±0.02 at 515 nm) for 30 min in the darkness before being measured for absorbance at the same wavelength. DPPH radical scavenging activity (RSA), which was calculated as mg Trolox equivalent *per g* of dried powder (mg TE/g DW) using the Trolox standard curve, was used to further estimate its retention (RSA Ret) during drying according to Equation (14).

$$\text{RSA Ret (\%)} = \frac{C_{\text{RSA, after drying}}}{C_{\text{RSA, before drying}}} \times 100\% \quad (14)$$

where: $C_{\text{RSA, before drying}}$ and $C_{\text{RSA, after drying}}$ were the DPPH radical scavenging activity of the sample before drying and after drying, respectively.

■ Reducing sugar content determination

The reducing sugar (RS) content was determined according to DNS assay [Miller, 1959] by mixing 1 mL of samples with 1 mL of DNS reagent under boiling conditions for 10 min. After sample cooling to ambient temperature, distilled water (2 mL) was added, and absorbance was measured at 540 nm to estimate the RS content and its retention (RS Ret) during drying from Equation (15).

$$\text{RS Ret (\%)} = \frac{C_{\text{RS, after drying}}}{C_{\text{RS, before drying}}} \times 100\% \quad (15)$$

where: $C_{\text{RS, before drying}}$ and $C_{\text{RS, after drying}}$ were the reducing sugar of the sample before drying and after drying, respectively.

■ Total titratable acidity determination

The extract (10 mL) was titrated with standard NaOH solution in the presence of phenolphthalein as an indicator. The titration stopped when the solution attained a pale pink color that persisted for 30 s. Total titratable acidity (TA) was calculated by Equation (16).

$$\text{TA (\%)} = \frac{V_{\text{NaOH}}}{V_{\text{sample}}} \times 0.0064 \times 1,000 \quad (16)$$

where: V_{NaOH} and V_{sample} were the volume of titrated NaOH solution and extract sample, respectively.

■ Optimization method

The study employed a numerical optimization technique to simultaneously optimize multiple responses using Design Expert version 13.0 (Stat-Ease, Inc., Minneapolis, MN, USA). To address the desire to find a solution that accommodates various responses, the objectives were combined into an overall composite function, denoted as $D(x)$, referred to as the desirability function. This function is defined by Equation (17) [Myers *et al.*, 2016].

$$D(x) = \sqrt[n]{d_1 \times d_2 \times \dots \times d_n} \quad (17)$$

where: d_1, d_2, \dots, d_n are responses and n is the total number of responses in the observations.

The function $D(x)$ represents the optimal intervals for each response (d_i). Desirability is a quantitative measure that varies between zero (indicating the least desirable condition) and one (representing the most desirable condition) at the desired outcome. Numerical optimization identifies the point that maximizes the desirability function [Myers *et al.*, 2016].

■ Statistical analysis

Experiments were conducted in triplicates, and data were fitted by the non-linear least square method based on the Levenberg-Marquardt method. After one-way analysis of variance (ANOVA), Tukey's honestly significant difference test was performed. StatPlus software (AnalystSoft, Brandon, FL, USA) was used to analyze the Pearson correlations between variables.

RESULTS AND DISCUSSION

■ Drying characteristics of mango pulp during infrared drying

The changes in moisture ratio and drying rate under different IR drying conditions of mango pulp are shown in Figures 1 and 2, respectively. As can be seen in Figure 1, drying times can be reduced by increasing drying temperatures. Drying time, however, was proportional to the amount of maltodextrin or total soluble solids in the mango pulp. In the meantime, the lower total soluble solids required a lower amount of maltodextrin, and higher drying temperature led to the higher drying rate. Also, based on the drying rate curve data (Figure 2), infrared drying of mango pulp proceeded primarily in the deceleration stage.

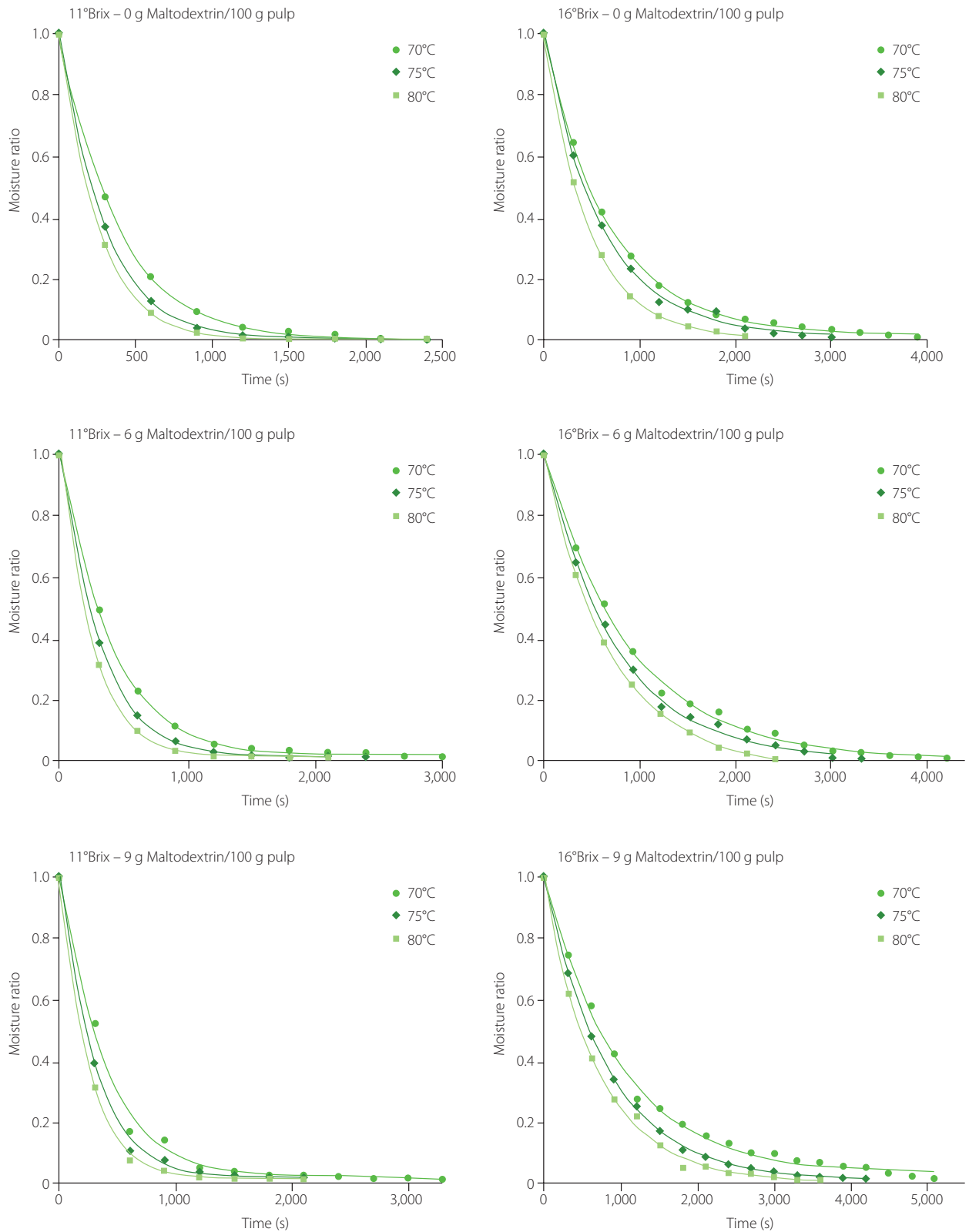


Figure 1. The change of moisture content vs time in infrared drying of mango pulp under different conditions including temperature of 70–80°C, maltodextrin content of 0–9 g/100 g pulp, and total soluble solids of pulp at 11 and 16°Brix. DW, dry weight.

Experimental data on moisture ratio was used to select a model that characterizes the moisture removal in mango pulp during IR drying. The mathematical model was chosen based on its highest coefficient of determination (R^2) and the lowest root

mean square error (RMSE), all of which were presented as mean values (Table 1). The high R^2 values accompanied with the low errors were used to rank the mathematical models in the descending order of Weibull > Midilli > Logarithmic > Page >

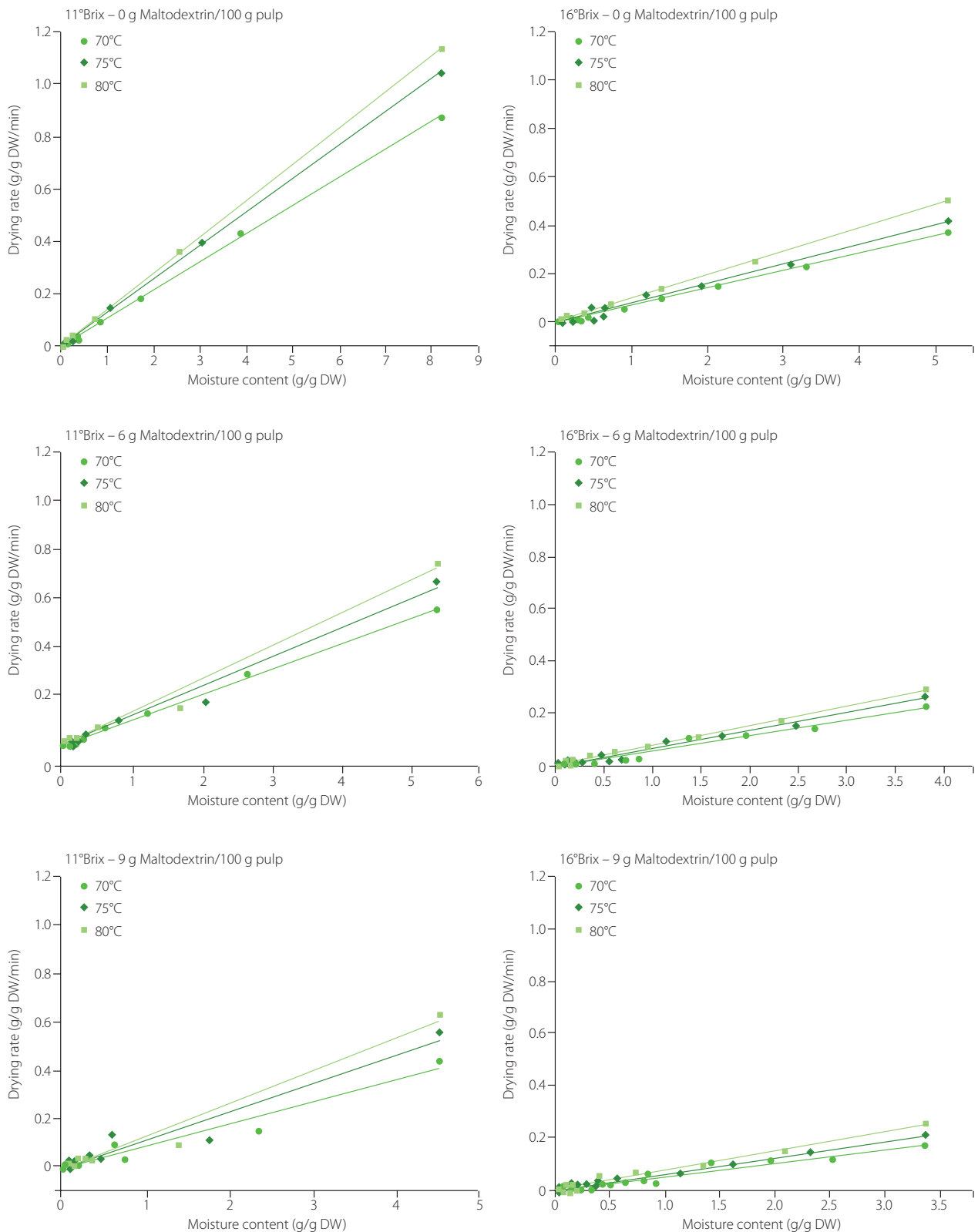


Figure 2. Drying rate curves of infrared drying of mango pulp at different conditions including temperature of 70–80°C, maltodextrin content of 0–9/100 g pulp, and total soluble solids of pulp at 11 and 16°Brix. DW, dry weight.

Henderson and Pabis > Newton models. Apparently, the Weibull model was the best predictive among the models investigated. This conclusion is not in agreement with the report of Onwude *et al.* [2016], who suggested that the Midilli model was the best to characterize the thin layer drying of fruits and vegetables.

However, the experimental data was not assessed on the Weibull model in these investigations. On the other hand, Midilli and Weibull models have been reported as the most compatible with experimental data in several research, including those looking at the drying of persimmon slices [Doymaz, 2012] and sliced

Table 1. Results of non-linear regression analysis of kinetic models of infrared drying of mango pulp and values of effective moisture diffusivity (D_{eff}).

| Temperature (°C) | Total soluble solids (°Brix) | Maltodextrin (g/100 g pulp) | Newton | | Page | | Henderson&Pabis | | Logarithmic | | Midilli | | Weibull | | Deff (m ² /s) |
|----------------------|------------------------------|-----------------------------|----------------|----------------|----------------|----------------|-----------------|----------------|----------------|----------------|----------------|---------------|----------------|---------------|--------------------------|
| | | | R ² | RMSE | R ² | RMSE | R ² | RMSE | R ² | RMSE | R ² | RMSE | R ² | RMSE | |
| 70 | 11 | 0 | 0.9999 | 0.00513 | 0.9999 | 0.00542 | 0.9999 | 0.00593 | 0.9999 | 0.00493 | 0.9999 | 0.00708 | 0.9999 | 0.00652 | 9.274×10^{-10} |
| | | 6 | 0.9992 | 0.01115 | 0.9995 | 0.01019 | 0.9992 | 0.01246 | 0.9998 | 0.00640 | 0.9998 | 0.00911 | 0.9998 | 0.00755 | 8.734×10^{-10} |
| | | 9 | 0.9926 | 0.02586 | 0.9932 | 0.02593 | 0.9927 | 0.02701 | 0.9931 | 0.02759 | 0.9952 | 0.02672 | 0.9948 | 0.02538 | 8.416×10^{-10} |
| 75 | 16 | 0 | 0.9987 | 0.01215 | 0.9995 | 0.00861 | 0.9988 | 0.01305 | 0.9996 | 0.00806 | 0.9996 | 0.00890 | 0.9997 | 0.00832 | 4.865×10^{-10} |
| | | 6 | 0.9967 | 0.01972 | 0.9970 | 0.02011 | 0.9967 | 0.02127 | 0.9970 | 0.02214 | 0.9998 | 0.00911 | 0.9971 | 0.02449 | 3.767×10^{-10} |
| | | 9 | 0.9929 | 0.02657 | 0.9946 | 0.02471 | 0.9930 | 0.02810 | 0.9956 | 0.02378 | 0.9952 | 0.02672 | 0.9956 | 0.02568 | 3.086×10^{-10} |
| 80 | 11 | 0 | 0.9999 | 0.00489 | 0.9999 | 0.00447 | 0.9999 | 0.00565 | 0.9999 | 0.00290 | 0.9999 | 0.00042 | 0.9999 | 0.00383 | 1.236×10^{-10} |
| | | 6 | 0.9998 | 0.00669 | 0.9999 | 0.00556 | 0.9998 | 0.00773 | 0.9999 | 0.00284 | 0.9977 | 0.02825 | 0.9999 | 0.00366 | 11.58×10^{-10} |
| | | 9 | 0.9969 | 0.01768 | 0.9970 | 0.01840 | 0.9969 | 0.01873 | 0.9975 | 0.01774 | 0.9996 | 0.00866 | 0.9984 | 0.01531 | 11.37×10^{-10} |
| Average value | 16 | 0 | 0.9974 | 0.01944 | 0.9977 | 0.02034 | 0.9974 | 0.02173 | 0.9977 | 0.02353 | 0.9977 | 0.02871 | 0.9978 | 0.02859 | 5.608×10^{-10} |
| | | 6 | 0.9974 | 0.01921 | 0.9977 | 0.02017 | 0.9974 | 0.02145 | 0.9976 | 0.02345 | 0.9977 | 0.02852 | 0.9977 | 0.02846 | 4.509×10^{-10} |
| | | 9 | 0.9996 | 0.00720 | 0.9996 | 0.00733 | 0.9996 | 0.00774 | 0.9996 | 0.00783 | 0.9996 | 0.00866 | 0.9996 | 0.00873 | 4.035×10^{-10} |
| Average value | 11 | 0 | 0.9999 | 0.00238 | 0.9999 | 0.00209 | 0.9999 | 0.00291 | 0.9999 | 0.00075 | 0.9999 | 0.00432 | 0.9999 | 0.00423 | 14.78×10^{-10} |
| | | 6 | 0.9998 | 0.00678 | 0.9999 | 0.00515 | 0.9998 | 0.00782 | 0.9999 | 0.00122 | 0.9997 | 0.01322 | 0.9999 | 0.00143 | 14.59×10^{-10} |
| | | 9 | 0.9986 | 0.01290 | 0.9986 | 0.01382 | 0.9986 | 0.01394 | 0.9992 | 0.01155 | 0.9966 | 0.02998 | 0.9997 | 0.00754 | 14.02×10^{-10} |
| Average value | 16 | 0 | 0.9999 | 0.00408 | 0.9990 | 0.00427 | 0.9999 | 0.00471 | 0.9999 | 0.00533 | 0.9999 | 0.00739 | 0.9999 | 0.00738 | 7.614×10^{-10} |
| | | 6 | 0.9993 | 0.01104 | 0.9993 | 0.01220 | 0.9993 | 0.01275 | 0.9996 | 0.01157 | 0.9997 | 0.01322 | 0.9998 | 0.01254 | 5.444×10^{-10} |
| | | 9 | 0.9963 | 0.02186 | 0.9966 | 0.02325 | 0.9964 | 0.02391 | 0.9964 | 0.02660 | 0.9966 | 0.02998 | 0.9966 | 0.02988 | 4.909×10^{-10} |
| Average value | | | 0.9980 | 0.01304 | 0.9983 | 0.01289 | 0.9981 | 0.01427 | 0.9985 | 0.01268 | 0.01605 | 0.9986 | 0.01605 | 0.9987 | 0.01386 |

lemongrass [Nguyen *et al.*, 2019] while the latter model can also be utilized to identify the drying kinetics such as convective drying of sliced mango [Corzo *et al.*, 2010], pepino fruit (*Solanum muricatum* Ait.) [Uribe *et al.*, 2011], quince [Tzempelikos *et al.*, 2015], and longan [Ju *et al.*, 2018]. Therefore, in this study, we confirm that the Weibull model is the most suitable to characterize the moisture removal of mango pulp under IR drying.

The effective moisture diffusivity during the IR drying of mango pulp has been determined and values are presented in **Table 1**. The correlation between the effective moisture diffusivity and process condition parameters ($R^2=0.99$, $p<0.0001$) was described by Equation (18):

$$D_{\text{eff}} \times 10^{10} = 8.356 - 3.372x_1 + 1.935x_2 - 0.724x_3 - 0.893x_1x_2 - 0.297x_1x_3 \quad (18)$$

where, x_1 , x_2 , and x_3 correspond to the coding levels of total soluble solids, drying temperature, and maltodextrin content, respectively.

It is shown that the lowest effective moisture diffusivity ($3.086 \times 10^{-10} \text{ m}^2/\text{s}$) was observed at drying conditions of 70°C, 16°Brix, and 9% maltodextrin, whereas 80°C, 11°Brix, and 0% maltodextrin resulted in the highest D_{eff} value of $14.78 \times 10^{-10} \text{ m}^2/\text{s}$. These results were consistent with those reported for thin layer drying of fruits and vegetables [Onwude *et al.*, 2016]

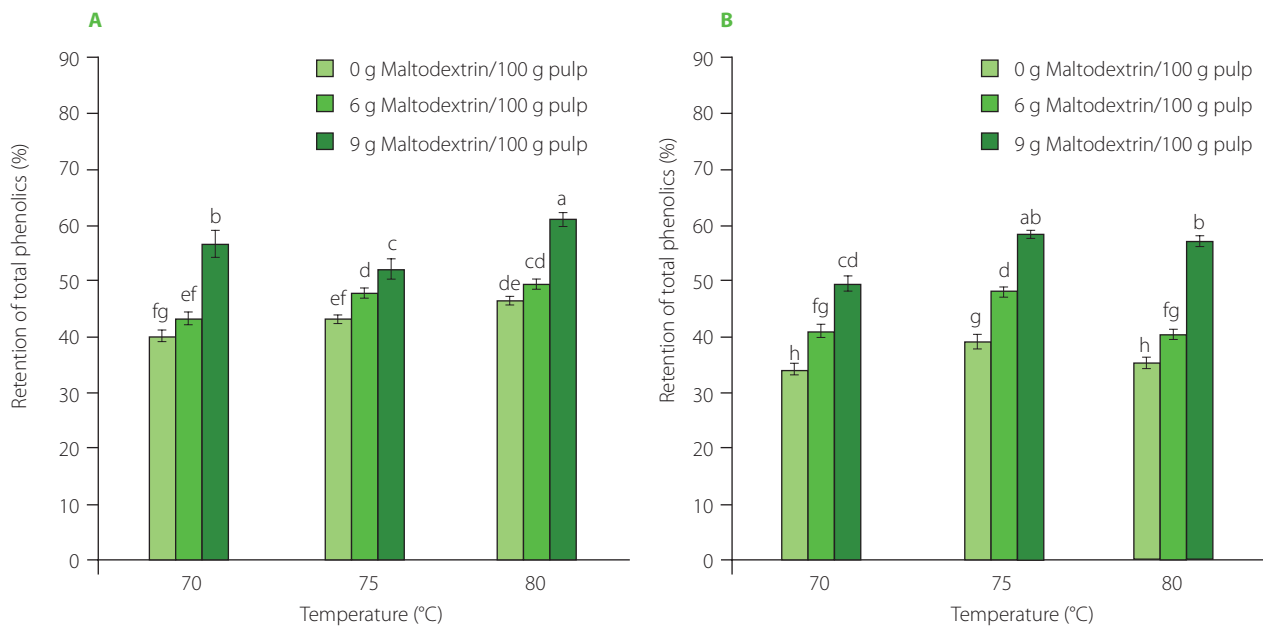


Figure 3. The retention of total phenolic content in mango powder obtained by infrared drying of pulp at different conditions. (A) The results for drying pulp with total soluble solids (TSS) of 11°Brix. (B) The results for drying pulp with TSS of 16°Brix. The same letters above bars of both graphs indicated that the values are not significantly different ($p \geq 0.05$).

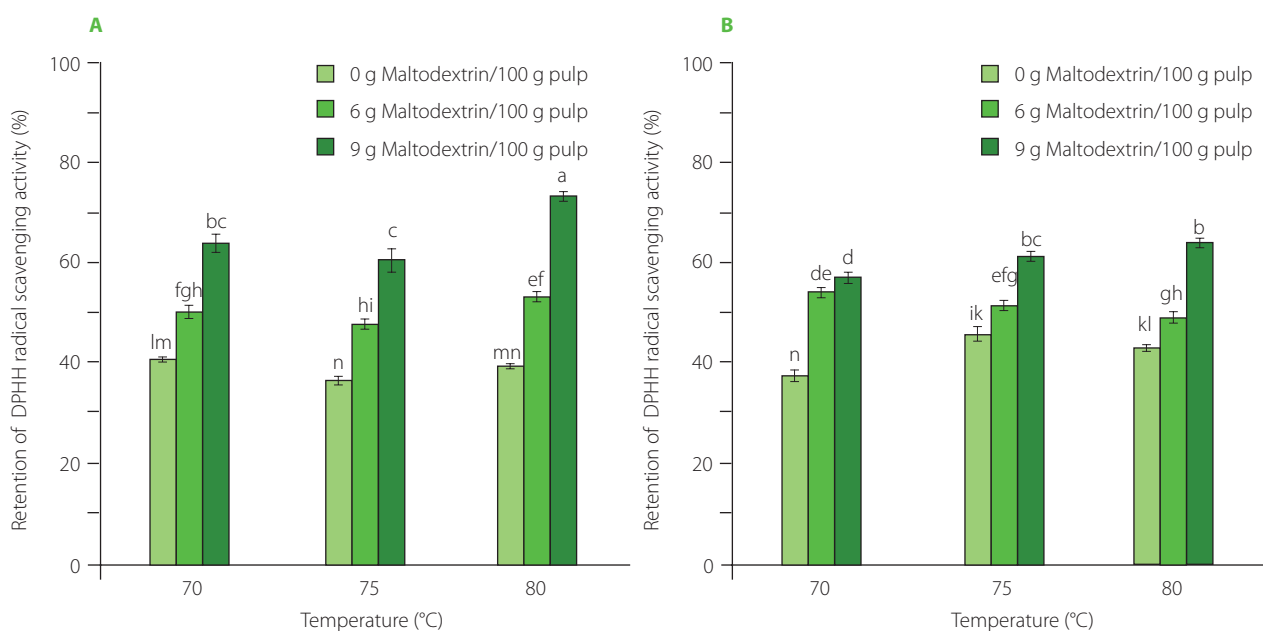


Figure 4. The retention of DPPH radical scavenging activity in mango powder obtained by infrared drying of pulp at different conditions. (A) The results for drying pulp with total soluble solids (TSS) of 11°Brix. (B) The results for drying pulp with TSS of 16°Brix. The same letters above bars of both graphs indicated that the values are not significantly different ($p \geq 0.05$).

and IR drying of tomatoes at 60–80°C (1.094×10^{-9} to 4.468×10^{-9} m²/s) [Sadin *et al.*, 2014], carrots at 60–80°C (2.38×10^{-9} to 10.30×10^{-9} m²/s) [Wu *et al.*, 2014], bell peppers at 50–80°C (1.75×10^{-10} to 8.97×10^{-10} m²/s) [Nasiroglu & Kocabiyyik, 2009], anise at 60–80°C (5.022×10^{-10} to 9.557×10^{-10} m²/s) [Wen *et al.*, 2020], and blueberries at 60–90°C (2.24×10^{-10} to 16.4×10^{-10} m²/s) [Shi *et al.*, 2008]. It is possible to infer that even supposing the same IR drying temperature, the drying of mango pulp showed a greater D_{eff} value than the drying of bell peppers, anise, and blueberries, but a lower value than during drying of tomatoes and carrots.

■ Effects of infrared drying on the quality of mango powder

The effects of IR drying conditions on the quality of mango powder including the retention of total phenolic content, DPPH radical scavenging activity, reducing sugars and the value of total titratable acidity are presented in Figure 3, 4, 5 and 6, respectively. The results demonstrate that higher temperatures and increased maltodextrin content, together with decreased total soluble solid content, enhanced the retention of TPC, RS, RSA (TPC Ret, RS Ret, and RSA Ret, respectively), and TA. The correlation between the quality indicators of mango powder and process condition parameters were described by Equations (19)–(22).

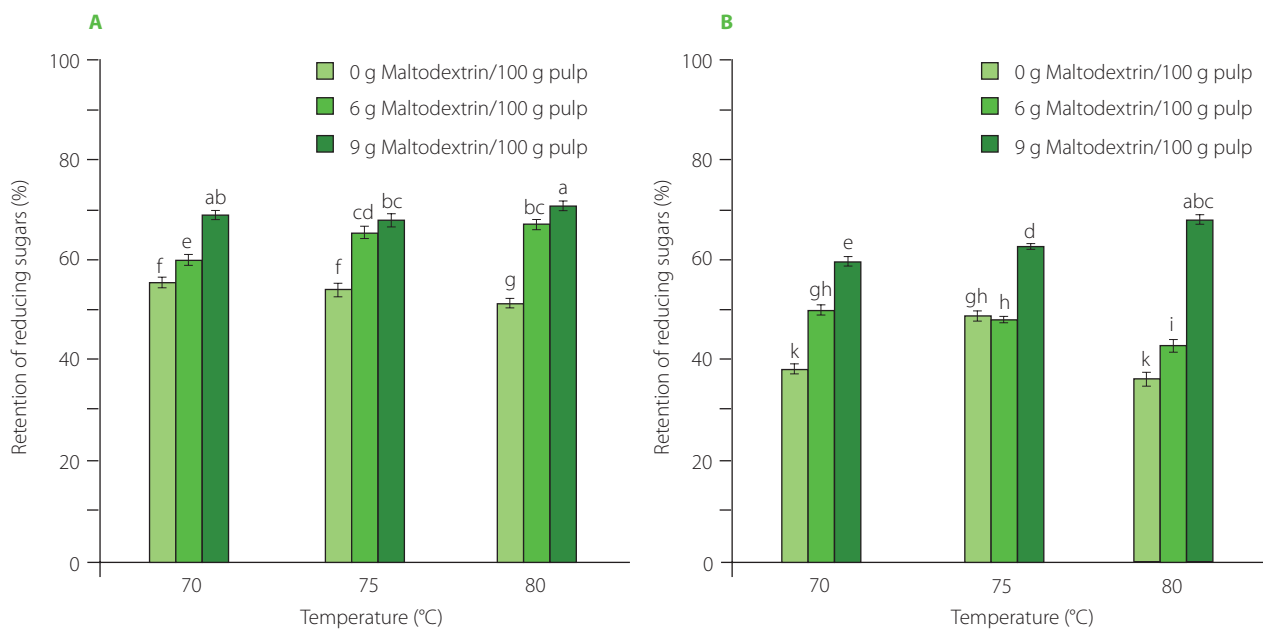


Figure 5. The retention of reducing sugars in mango powder obtained by infrared drying of pulp at different conditions. (A) The results for drying pulp with total soluble solids (TSS) of 11°Brix. (B) The results for drying pulp with TSS of 16°Brix. The same letters above bars of both graphs indicated that the values are not significantly different ($p \geq 0.05$).

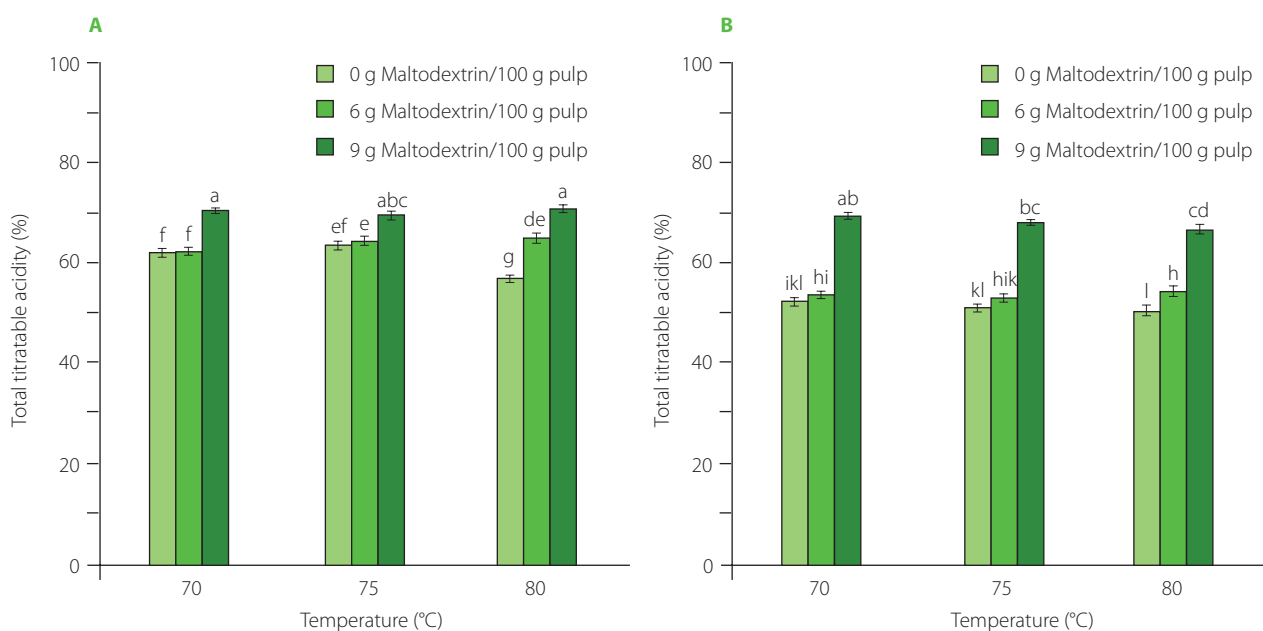


Figure 6. The total titratable acidity in mango powder obtained by infrared drying of pulp at different conditions. (A) The results for drying pulp with total soluble solids (TSS) of 11°Brix. (B) The results for drying pulp with TSS of 16°Brix. The same letters above bars of both graphs indicated that the values are not significantly different ($p \geq 0.05$).

$$\text{TPC Ret (\%)} = 41.68 - 1.97x_1 + 2.07x_2 + 8.03x_3 + 6.12x_3^2 \quad (19)$$

$$(R^2 = 0.86, p < 0.0001)$$

$$\text{RSA Ret (\%)} = 46.58 - 0.11x_1 + 1.57x_2 + 11.43x_3 + 5.36x_3^2 \quad (20)$$

$$(R^2 = 0.88, p < 0.0001)$$

$$\text{RS Ret (\%)} = 55.60 - 5.94x_1 + 0.39x_2 + 9.11x_3 \quad (21)$$

$$(R^2 = 0.81, p < 0.0001)$$

$$\text{TA (\%)} = 7.83 - 0.51x_1 - 0.067x_2 + 0.92x_3 + 0.95x_3^2 \quad (22)$$

$$(R^2 = 0.90, p < 0.0001)$$

where, x_1 , x_2 , and x_3 are corresponding to the coding levels of total soluble solids, drying temperature, and maltodextrin content, respectively.

The above regression equations also clearly indicate that the retention of TPC, RS, RSA, and the value of TA were all positively correlated with either the IR temperature or the maltodextrin content.

During thermal processes, the degradation of phenolics is mainly due to the action of enzymes, such as polyphenol oxidase (PPO) and peroxidase (POD) [Tomás-Barberán & Espín, 2001]. For mangoes, PPO and POD were most effective at 50–60°C [Korbel *et al.*, 2013] and were inactivated at high temperatures, *i.e.* 70–90°C [Queiroz *et al.*, 2008]. According to Sultana *et al.* [2012], intense heat treatment was able to form new phenolic compounds. During the high-temperature drying, the drying time was shortened, indicating a shorter decomposition reaction time [Nguyen *et al.*, 2020]. It is deduced that a rise in temperature will result in the increased retention of phenolic compounds in mango pulp, which was strengthened by the highest retention of phenolics found in some studies on the high-temperature drying, such as RW drying at 90°C [López *et al.*, 2010] and 95°C [Shende & Datta, 2020] of blueberries and mango pulp, respectively. Regarding the carrier, the increase in maltodextrin content in mango pulp retained phenolics possibly because this carrier hindered the exposure of these bioactives in mango pulp with oxygen, leading to limited degradation [Osorio *et al.*, 2011]. Besides, the addition of maltodextrin to the pulp increased the dry matter, showing high binding capacity to water [Radosta & Schierbaum, 1990], which in turn lowered the water activity and limited the phenolic decomposition. These results are in accordance with findings from other studies on sapodilla (*Manilkara zapota*) powder [Chong & Wong, 2017] and avocado (*Persea Americana* Mill.) powder [Nguyen *et al.*, 2023].

Mango is rich in sugars, including reducing sugars such as glucose and fructose [Ribeiro & Schieber, 2010]. During the high-temperature drying, a high-sugar material, like mango, will easily lose reducing sugar content, primarily due to the Maillard reaction [Jaeger *et al.*, 2010]. As a result, the Maillard process accelerated the loss of reducing sugars at higher drying temperatures. However, an increase in the maltodextrin content limits the exposure of the substrates, thereby markedly reducing the extent of sugar losses. Total titratable acidity was shown to be significantly affected by maltodextrin

Table 2. Coefficients of Pearson correlations between the retention of DPPH radical scavenging activity (RSA), retention of total phenolic content (TPC), retention of reducing sugars (RS), and the values of total titratable acidity (TA).

| | Retention of RSA | Retention of TPC | Retention of RS |
|------------------|---------------------------------------|--------------------|--------------------|
| Retention of TPC | 0.853 ($p=0$) | | – |
| Retention of RS | 0.719 ($p=9.48 \times 10^{-10}$) | 0.856 ($p=0$) | |
| TA | 0.663 ($p=4.56 \times 10^{-8}$) | 0.819 ($p=0$) | 0.915 ($p=0$) |

content and drying temperature. Specifically, a greater amount of maltodextrin helped form a barrier to minimize the nutrient loss during heat treatment while the depletion of acidic compounds increased mostly at higher temperatures with increased thermal energy.

The investigation also revealed the positive correlations between the retention of TPC, RS, RSA, and the value of TA as shown in Table 2. The findings indicated that the retention of TPC exhibited significant correlation with the retention of DPPH radical scavenging activity with a correlation coefficient of 0.853 ($p < 0.01$). This implies that the capacity of mango powder to scavenge DPPH radicals displayed a similar pattern to that of the content of phenolic compounds, which are known for their antioxidant properties [Huyut *et al.*, 2017; Sikwese & Duodu, 2007]. Thanks to their specific chemical structure, these molecules can scavenge free radicals and also prevent their further production in the presence of transition metal ions as catalysts [Huyut *et al.*, 2017; Sikwese & Duodu, 2007]. The retention of TPC also exhibited a strong positive connection with the retention of RS, and values of TA (Table 2). The similar trend of changes in TPC, RS, and TA could be inferred in the infrared drying process of mango pulp under the conditions used in the study.

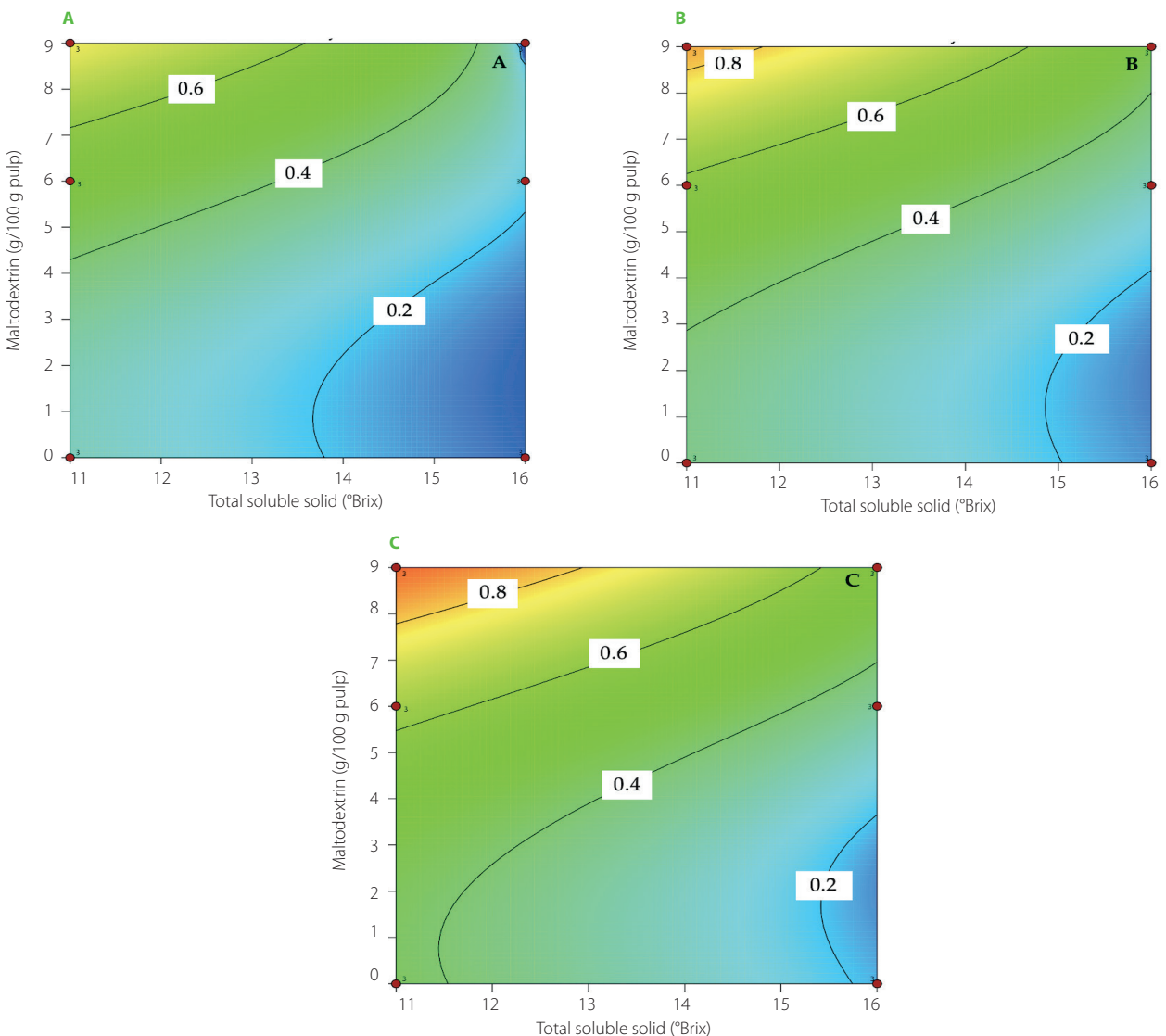
■ Optimization of infrared drying for mango pulp

This study applied a numerical optimization technique to simultaneously optimize multiple responses, such as effective moisture diffusivity, DPPH radical scavenging activity retention, TPC retention, RS retention, and TA value. The specific objectives for each factor and response were selected, and distinct weights were given to each objective to adjust the form of the desirability function (Table 3). The contour plot of the desirability function for mango pulp under various IR drying settings are displayed in Figure 7. The desirability function reached the highest value of 0.916 (Table 3). The predicted values for all independent and dependent parameters resulting from the optimization process using the desirability function are shown in Table 3. The optimal values of control parameters were 11°Brix, 80°C, and 9% maltodextrin content. Under these specific drying conditions, the mango powder was achieved with the highest retention of TPC (59.874%), retention of RS (71.044%), TA (10.141%), retention of RSA (65.051%), and D_{eff} ($14.033 \times 10^{-10} \text{ m}^2/\text{s}$).

Table 3. Criteria for optimization of factors and responses and their values of optimal point within the desirability region for infrared drying of mango pulp.

| Factor/Response | Lower limit | Upper limit | Importance | Prediction | Experiment | Error (%) |
|--------------------------------------------|-------------------------|--------------------------|------------|--------------------------|-------------------------|-----------|
| Total soluble solids ($^{\circ}$ Brix) | 11 | 16 | 3 | 11 | 11 | - |
| Maltodextrin (g/100 g pulp) | 0 | 9 | 3 | 9 | 9 | - |
| Temperature ($^{\circ}$ C) | 70 | 80 | 3 | 80 | 80 | - |
| Effective moisture diffusivity (m^2/s) | 3.086×10^{-10} | 14.780×10^{-10} | 5 | 14.033×10^{-10} | 14.02×10^{-10} | 0.0927 |
| Retention of RSA (%) | 35.70 | 74.10 | 5 | 65.051 | 65.05 | 0.0015 |
| Retention of TPC (%) | 33.34 | 62.10 | 5 | 59.874 | 59.87 | 0.0067 |
| Retention of RS (%) | 34.91 | 71.87 | 5 | 71.044 | 71.04 | 0.0056 |
| Total titratable acidity (%) | 6.96 | 10.00 | 5 | 10.141 | 9.88 | 2.6417 |
| Desirability | - | - | - | 0.916 | - | - |

RSA, DPPH radical scavenging activity; TPC, total phenolic content; RS, reducing sugars.

**Figure 7.** The contour plot of the desire function for mango pulp under various infrared drying conditions. (A) 70 $^{\circ}$ C, (B) 75 $^{\circ}$ C, and (C) 80 $^{\circ}$ C.

CONCLUSIONS

In this study, infrared drying of mango pulp under different conditions was performed. The Weibull model was useful for describing the decline in mango pulp's moisture content

during infrared drying. The effectiveness of infrared drying of mango pulp was greatly influenced by drying temperature, total soluble solid content, and maltodextrin content. Temperature had a positive effect on water removal while total

soluble solid content and maltodextrin showed the opposite effect. Moreover, total phenolics and DPPH radical scavenging activity were better retained with increasing IR temperature (from 70 to 80°C) or maltodextrin content (from 0 to 9 g/100 g pulp). Therefore, it is important to set adequate pretreatment conditions or employ additives to maintain powder's quality in order to take advantage of the infrared drying. Finally, the findings indicated that the implementation of infrared drying of mango pulp with 11°Brix and 9% maltodextrin content at 80°C would ensure the highest quality of mango powder.

ACKNOWLEDGEMENTS

The authors would like to thank Nguyen Tat Thanh University for permission and for providing facilities, as well as Ho Chi Minh City University of Technology (HCMUT) and VNU-HCM for supporting this study. We also wish to thank Ms. Dao Hai Nguyen for supplying mango fruits during the research period, and to Ms. Huynh Thi To Na and Ms Vo Pham Quynh Tram for supporting the collection of data during the beginning stages of the research.

RESEARCH FUNDING

This research is funded by Nguyen Tat Thanh University, Ho Chi Minh city, Vietnam under grant 2021.01.023.

CONFLICT OF INTERESTS

The authors declare no conflict of interest.

ORCID IDs

P.B.D. Nguyen
T.T.D. Nguyen
T.V.L. Nguyen

<https://orcid.org/0000-0001-6827-919X>
<https://orcid.org/0000-0002-1701-0729>
<https://orcid.org/0000-0003-1471-6352>

REFERENCES

- Afzal, T.M., Abe, T., Hikida, Y. (1999). Energy and quality aspects during combined FIR-convection drying of barley. *Journal of Food Engineering*, 42(4), 177–182. [https://doi.org/10.1016/S0260-8774\(99\)00117-X](https://doi.org/10.1016/S0260-8774(99)00117-X)
- Allanic, N., Le Bideau, P., Glouannec, P., Deterre, R. (2017). An experimental study on infrared drying kinetics of an aqueous adhesive supported by polymer composite. *Heat and Mass Transfer*, 53(1), 223–231. <https://doi.org/10.1007/s00231-016-1816-3>
- Bhandari, B., Senoussi, A., Dumoulin, E., Lebert, A. (1993). Spray drying of concentrated fruit juices. *Drying Technology*, 11(5), 1081–1092. <https://doi.org/10.1080/07373939308916884>
- Brand-Williams, W., Cuvelier, M.-E., Berset, C. (1995). Use of a free radical method to evaluate antioxidant activity. *LWT – Food Science and Technology*, 28(1), 25–30. [https://doi.org/10.1016/S0023-6438\(95\)80008-5](https://doi.org/10.1016/S0023-6438(95)80008-5)
- Caparino, O., Tang, J., Nindo, C., Sablani, S., Powers, J., Fellman, J. (2012). Effect of drying methods on the physical properties and microstructures of mango (Philippine 'Carabao' var.) powder. *Journal of Food Engineering*, 111(1), 135–148. <https://doi.org/10.1016/j.jfoodeng.2012.01.010>
- Corzo, O., Bracho, N., Alvarez, C. (2010). Weibull model for thin-layer drying of mango slices at different maturity stages. *Journal of Food Processing and Preservation*, 34(6), 993–1008. <https://doi.org/10.1111/j.1745-4549.2009.00433.x>
- Crank, J. (Ed) (1975). Chapter 4: Diffusion in a plane sheet. In *The Mathematics of Diffusion*. 2nd edition, Oxford University Press, pp. 44–68.
- Djantou, E., Mbofung, C.M., Scher, J., Desobry, S. (2007). A modelling approach to determine the effect of pre-treatment on the grinding ability of dried mangoes for powder production (*Mangifera indica* var Kent). *Journal of Food Engineering*, 80(2), 668–677. <https://doi.org/10.1016/j.jfoodeng.2006.07.003>
- Djantou, E., Mbofung, C., Scher, J., Phambu, N., Mraael, J. (2012). Alternation drying and grinding (ADG) technique: A novel approach for producing ripe mango powder. *LWT – Food Science and Technology*, 44(7), 1585–1590. <https://doi.org/10.1016/j.lwt.2011.01.022>
- Doymaz, İ. (2012). Evaluation of some thin-layer drying models of persimmon slices (*Diospyros kaki* L.). *Energy Conversion and Management*, 56, 199–205. <https://doi.org/10.1016/j.enconman.2011.11.027>
- Doymaz, İ. (2017). Microwave and infrared drying characteristics of mango slices. *Celal Bayar University Journal of Science*, 13(3), 681–688. <https://doi.org/10.18466/cbayarfbe.339337>
- Huyut, Z., Beydemir, Ş., Gülçin, İ. (2017). Antioxidant and antiradical properties of selected flavonoids and phenolic compounds. *Biochemistry Research International*, 2017, art. no. 7616791. <https://doi.org/10.1155/2017/7616791>
- ISO. (2005). ISO 14502-1:2005, Determination of substances characteristic of green and black tea—Part 1: Content of total polyphenols in tea-colorimetric method using Folin-Ciocalteu reagent. In *ISO 14502-1 International Standardization*. International Organization for Standardization Switzerland, p. 10.
- Jaeger, H., Janositz, A., Knorr, D. (2010). The Maillard reaction and its control during food processing. The potential of emerging technologies. *Pathologie Biologie*, 58(3), 207–213. <https://doi.org/10.1016/j.patbio.2009.09.016>
- Ju, H.-Y., Zhao, S.-H., Mujumdar, A., Fang, X.-M., Gao, Z.-J., Zheng, Z.-A., Xiao, H.-W. (2018). Energy efficient improvements in hot air drying by controlling relative humidity based on Weibull and Bi-Di models. *Food and Bioprocess Technology*, 11, 20–29. <https://doi.org/10.1016/j.fbp.2018.06.002>
- Korbel, E., Servent, A., Billaud, C., Brat, P. (2013). Heat inactivation of polyphenol oxidase and peroxidase as a function of water activity: A case study of mango drying. *Drying Technology*, 31(13–14), 1675–1680. <https://doi.org/10.1080/07373937.2013.808659>
- López, J., Uribe, E., Vega-Gálvez, A., Miranda, M., Vergara, J., Gonzalez, E., Di Scala, K. (2010). Effect of air temperature on drying kinetics, vitamin C, antioxidant activity, total phenolic content, non-enzymatic browning and firmness of blueberries variety O'Neil. *Food and Bioprocess Technology*, 3(5), 772–777. <https://doi.org/10.1007/s11947-009-0306-8>
- Marquardt, D.W. (1963). An algorithm for least-squares estimation of nonlinear parameters. *Journal of the Society for Industrial and Applied Mathematics*, 11(2), 431–441. <https://doi.org/10.1137/0111030>
- Marques, L.G., Ferreira, M.C., Freire, J.T. (2007). Freeze-drying of acerola (*Malpighia glabra* L.). *Chemical Engineering and Processing: Process Intensification*, 46(5), 451–457. <https://doi.org/10.1016/j.cep.2006.04.011>
- Miller, G.L. (1959). Use of dinitrosalicylic acid reagent for determination of reducing sugar. *Analytical Chemistry*, 31(3), 426–428. <https://doi.org/10.1021/ac60147a030>
- Mirza, B., Croley, C.R., Ahmad, M., Pumarol, J., Das, N., Sethi, G., Bishayee, A. (2021). Mango (*Mangifera indica* L.): A magnificent plant with cancer preventive and anticancer therapeutic potential. *Critical Reviews in Food Science and Nutrition*, 61(13), 2125–2151. <https://doi.org/10.1080/10408398.2020.1771678>
- Myers, R.H., Montgomery, D.C., Anderson-Cook, C.M. (Eds). (2016). Chapter 7: Multiple Response Optimization. In: *Response Surface Methodology: Process and Product Optimization Using Designed Experiments*. 4th edition, John Wiley & Sons, pp. 325–356.
- Nasıroglu, S., Kocabiyik, H. (2009). Thin-layer infrared radiation drying of red pepper slices. *Journal of Food Process Engineering*, 32(1), 1–16. <https://doi.org/10.1111/j.1745-4530.2007.00195.x>
- Nawirska, A., Figiel, A., Kucharska, A.Z., Sokół-Łętowska, A., Biesiada, A. (2009). Drying kinetics and quality parameters of pumpkin slices dehydrated using different methods. *Journal of Food Engineering*, 94(1), 14–20. <https://doi.org/10.1016/j.jfoodeng.2009.02.025>
- Nguyen, T., Nguyen, Q., Nguyen, P., Tran, B., Huynh, P.T. (2020). Effects of drying conditions in low-temperature microwave-assisted drying on bioactive compounds and antioxidant activity of dehydrated bitter melon (*Momordica charantia* L.). *Food Science & Nutrition*, 8(7), 3826–3834. <https://doi.org/10.1002/fsn3.1676>
- Nguyen, T.V., Nguyen, M.D., Nguyen, D.C., Bach, L.G., Lam, T.D. (2019). Model for thin layer drying of lemongrass (*Cymbopogon citratus*) by hot air. *Processes*, 7(1), art. no. 21. <https://doi.org/10.3390/pr7010021>
- Nguyen, T.-V.-L., Ngo, P.-T., Huynh, T.-T.-N., Vo, P.-N.-T., Hoang, T.-N.-A., Nguyen, P.-B.-D. (2022a). Refractance window drying of mango pulp (*Mangifera indica*): Impact of hydrocolloids on drying characteristics and color parameters. *AIP Conference Proceedings*, 2610(1), art. no. 060022. <https://doi.org/10.1063/5.0100826>
- Nguyen, T.-V.-L., Nguyen, Q.-D., Nguyen, P.-B.-D. (2022b). Drying kinetics and changes of total phenolic content, antioxidant activity and color pa-

- rameters of mango and avocado pulp in refractance window drying. *Polish Journal of Food and Nutrition Sciences*, 72(1), 27–38.
<https://doi.org/10.31883/pjfn/144835>
29. Nguyen, T.-V.-L., Nguyen, Q.-D., Nguyen, T.-T.-D., Nguyen, P.-B.-D. (2021). Effects of infrared drying conditions and maltodextrin addition on some physicochemical characteristics of avocado (*Persea americana*) pulp powder. *Applied Sciences*, 11(24), art no. 11803.
<https://doi.org/10.3390/app112411803>
 30. Nguyen, T.-V.-L., Nguyen, T.-T.-D., Huynh, Q.-T., Nguyen, P.-B.-D. (2023). Effect of maltodextrin on drying rate of avocado (*Persea Americana* Mill.) pulp by refractance window technique, and on color and functional properties of powder. *Polish Journal of Food and Nutrition Sciences*, 73(2), 187–195.
<https://doi.org/10.31883/pjfn/163982>
 31. Nowak, D., Lewicki, P.P. (2004). Infrared drying of apple slices. *Innovative Food Science & Emerging Technologies*, 5(3), 353–360.
<https://doi.org/10.1016/j.ifset.2004.03.003>
 32. Occena-Po, L.G. (2006). Chapter 33: Banana, mango, and passion fruit. In: Y.H. Hui (Ed.), *Handbook of Fruits and Fruit Processing*. 1st edition. Blackwell Publishing Ames, Iowa, USA, pp. 635–650.
<https://doi.org/10.1002/9780470277737.ch33>
 33. Onwude, D.I., Hashim, N., Janius, R.B., Navu, N.M., Abdan, K. (2016). Modeling the thin-layer drying of fruits and vegetables: A review. *Comprehensive Reviews in Food Science and Food Safety*, 15(3), 599–618.
<https://doi.org/10.1111/1541-4337.12196>
 34. Osorio, C., Forero, D.P., Carriazo, J.G. (2011). Characterisation and performance assessment of guava (*Psidium guajava* L.) microencapsulates obtained by spray-drying. *Food Research International*, 44(5), 1174–1181.
<https://doi.org/10.1016/j.foodres.2010.09.007>
 35. Owino, W.O., Ambuko, J.L. (2021). Mango fruit processing: Options for small-scale processors in developing countries. *Agriculture*, 11(11), art. no. 1105.
<https://doi.org/10.3390/agriculture11111105>
 36. Pala, M., Mahmutoğlu, T., Saygi, B. (1996). Effects of pretreatments on the quality of open-air and solar dried apricots. *Food/Nahrung*, 40(3), 137–141.
<https://doi.org/10.1002/food.19960400308>
 37. Pott, I., Neidhart, S., Mühlbauer, W., Carle, R. (2005). Quality improvement of non-sulphited mango slices by drying at high temperatures. *Innovative Food Science & Emerging Technologies*, 6(4), 412–419.
<https://doi.org/10.1016/j.ifset.2005.05.004>
 38. Queiroz, C., Mendes Lopes, M.L., Fialho, E., Valente-Mesquita, V.L. (2008). Polyphenol oxidase: Characteristics and mechanisms of browning control. *Food Reviews International*, 24(4), 361–375.
<https://doi.org/10.1080/87559120802089332>
 39. Radosta, S., Schierbaum, F. (1990). Polymer-water interaction of maltodextrins. Part III: Non-freezable water in maltodextrin solutions and gels. *Starch-Stärke*, 42(4), 142–147.
<https://doi.org/10.1002/star.19900420405>
 40. Ribeiro, S.M.R., Schieber, A. (2010). Chapter 34: Bioactive compounds in mango (*Mangifera indica* L.). In: R.R. Watson, V.R. Preedy (Eds.), *Bioactive Foods in Promoting Health: Fruits and Vegetables*. Elsevier, pp. 507–523.
<https://doi.org/10.1016/B978-0-12-374628-3.00034-7>
 41. Roos, Y., Karel, M., Kokini, J. (1996). Glass transitions in low moisture and foods: Effects on shelf life and quality. *Food Technology (Chicago)*, 50(11), 95–108.
 42. Sadin, R., Chegini, G.-R., Sadin, H. (2014). The effect of temperature and slice thickness on drying kinetics tomato in the infrared dryer. *Heat and Mass Transfer*, 50(4), 501–507.
<https://doi.org/10.1007/s00231-013-1255-3>
 43. Shende, D., Datta, A.K. (2020). Optimization study for refractance window drying process of Langra variety mango. *Journal of Food Science and Technology*, 57(2), 683–692.
<https://doi.org/10.1007/s13197-019-04101-0>
 44. Shi, J., Pan, Z., McHugh, T.H., Wood, D., Hirschberg, E., Olson, D. (2008). Drying and quality characteristics of fresh and sugar-infused blueberries dried with infrared radiation heating. *LWT – Food Science and Technology*, 41(10), 1962–1972.
<https://doi.org/10.1016/j.lwt.2008.01.003>
 45. Sikwese, F., Duodu, K.G. (2007). Antioxidant effect of a crude phenolic extract from sorghum bran in sunflower oil in the presence of ferric ions. *Food Chemistry*, 104(1), 324–331.
<https://doi.org/10.1016/j.foodchem.2006.11.042>
 46. Slade, L., Levine, H., Reid, D.S. (1991). Beyond water activity: Recent advances based on an alternative approach to the assessment of food quality and safety. *Critical Reviews in Food Science & Nutrition*, 30(2–3), 115–360.
<https://doi.org/10.1080/10408399109527543>
 47. Sultana, B., Anwar, F., Ashraf, M., Saari, N. (2012). Effect of drying techniques on the total phenolic. *Journal of Medicinal Plant Research*, 6(1), 161–167.
<https://doi.org/10.5897/JMPR11.916>
 48. Tan, L.W., Ibrahim, M.N., Kamil, R., Taip, F.S. (2011). Empirical modeling for spray drying process of sticky and non-sticky products. *Procedia Food Science*, 1, 690–697.
<https://doi.org/10.1016/j.profoo.2011.09.104>
 49. Tomás-Barberán, F.A., Espín, J.C. (2001). Phenolic compounds and related enzymes as determinants of quality in fruits and vegetables. *Journal of the Science of Food and Agriculture*, 81(9), S1, 853–876.
<https://doi.org/10.1002/jsfa.885>
 50. Truong, V., Bhandari, B.R., Howes, T. (2005). Optimization of cocurrent spray drying process for sugar-rich foods. Part II—Optimization of spray drying process based on glass transition concept. *Journal of Food Engineering*, 71(1), 66–72.
<https://doi.org/10.1016/j.jfoodeng.2004.10.018>
 51. Tzempelikos, D.A., Vouros, A.P., Bardakas, A.V., Filios, A.E., Margaris, D.P. (2015). Experimental study on convective drying of quince slices and evaluation of thin-layer drying models. *Engineering in Agriculture, Environment and Food*, 8(3), 169–177.
<https://doi.org/10.1016/j.eaef.2014.12.002>
 52. Uribe, E., Vega-Gálvez, A., Di Scala, K., Oyanadel, R., Saavedra Torrico, J., Miranda, M. (2011). Characteristics of convective drying of pepino fruit (*Solanum muricatum* Ait.): Application of Weibull distribution. *Food and Bioprocess Technology*, 4(8), 1349–1356.
<https://doi.org/10.1007/s11947-009-0230-y>
 53. Wang, W., Li, M., Hassanien, R.H.E., Wang, Y., Yang, L. (2018). Thermal performance of indirect forced convection solar dryer and kinetics analysis of mango. *Applied Thermal Engineering*, 134, 310–321.
<https://doi.org/10.1016/j.applthermaleng.2018.01.115>
 54. Wen, Y.-X., Chen, L.-Y., Li, B.-S., Ruan, Z., Pan, Q. (2020). Effect of infrared radiation-hot air (IR-HA) drying on kinetics and quality changes of star anise (*Illicium verum*). *Drying Technology*, 39(1), 1–14.
<https://doi.org/10.1080/07373937.2019.1696816>
 55. Wu, B., Ma, H., Qu, W., Wang, B., Zhang, X., Wang, P., Wang, J., Atungulu, G.G., Pan, Z. (2014). Catalytic infrared and hot air dehydration of carrot slices. *Journal of Food Process Engineering*, 37(2), 111–121.
<https://doi.org/10.1111/jfpe.12066>
 56. Yao, L., Fan, L., Duan, Z. (2020). Effect of different pretreatments followed by hot-air and far-infrared drying on the bioactive compounds, physicochemical property and microstructure of mango slices. *Food Chemistry*, 305, art. no. 125477.
<https://doi.org/10.1016/j.foodchem.2019.125477>
 57. Zhu, Y., Pan, Z. (2009). Processing and quality characteristics of apple slices under simultaneous infrared dry-blanching and dehydration with continuous heating. *Journal of Food Engineering*, 90(4), 441–452.
<https://doi.org/10.1016/j.jfoodeng.2008.07.015>
 58. Zotarelli, M.F., da Silva, V.M., Durigon, A., Hubinger, M.D., Laurindo, J.B. (2017). Production of mango powder by spray drying and cast-tape drying. *Powder Technology*, 305, 447–454.
<https://doi.org/10.1016/j.powtec.2016.10.027>

High-Fiber Extruded Purple Sweet Potato (*Ipomoea batatas*) and Kidney Bean (*Phaseolus vulgaris*) Extends the Feeling of Fullness

Eny Palupi^{1*}, Naufal M. Nurdin¹, Ghina Mufida¹, Fadhilah N. Valentine¹, Rictor Pangestika¹, Rimbawan Rimbawan¹, Ahmad Sulaeman¹, Dodik Briawan¹, Fitry Filianty²

¹Department of Community Nutrition, Faculty of Human Ecology, IPB University, Indonesia

²Department of Food Industrial Technology, Faculty of Agroindustrial Technology, Padjadjaran University, Indonesia

Low intake of dietary fiber is closely related to an increased risk of various non-communicable diseases globally. This study aimed to develop a formulation for high-fiber extrudate based on purple sweet potato and kidney bean and evaluate the nutritional value of the products and their satiety index after consumption. Optimization of the formula was carried out using four levels of purple sweet potato flour substitution with kidney bean flour: 0, 20, 30, and 40% (w/w). The extrudates were obtained using a double-screw extruder at 60°C, with the auger, screw, and cutter speeds of 40, 40 and 50 Hz, respectively. The satiety index determination involved 16 subjects with body mass index in optimal range, and data from the visual analogue scale (VAS) questionnaire were used at 0, 30, 60, 90, 120, 150, and 180 min after consumption of the test food. The product with the highest substitution (40%) of kidney bean was selected as the best based on the sensory acceptability and nutritive value – contents of protein and total fiber were 13.20 and 17.00 g in 100 g dry matter, respectively. The estimated shelf-life of this extrudate was 19 months. Satiety index values for commercial cereals, extruded purple sweet potato, and extruded purple sweet potato with kidney bean were 99, 104, and 140, respectively. This research showed that the consumption of high-fiber extruded sweet potato with kidney bean could significantly extend the feeling of fullness with low energy contribution so that it might prevent excess calorie intake contributing to overweight and obesity.

Key words: calorie, extruded food, high-fiber food, satiety, obesity

INTRODUCTION

Obesity is a chronic inflammatory condition that is characterized by an increase in total body fat. As many as 39% of world adults aged over 18 years are overweight, with 13% classified as obese [WOF, 2023]. The consumption of foods high in energy, fat, and simple carbohydrates, combined with a low fiber intake and a lack of balanced energy expenditure, can act as triggers for obesity [Lasimpala *et al.*, 2021]. Alongside the prevalence of obesity, the risk of metabolic syndrome issues also increases, being an initial bridge to various non-communicable diseases.

A high-fiber diet plays a critical role in controlling various health-related biomarkers, including blood glucose, blood pressure, cholesterol levels, and others [Khalid *et al.*, 2022]. However, majority of adults globally consume less than 20 g of fiber *per day* [Stephen *et al.*, 2017], whereas the recommended fiber intake for adult ranges from 25 to 29 g *per day* [Reynolds *et al.*, 2019]. Fiber aids in smooth bowel movements and prevents constipation. It also forms a matrix with carbohydrates in food, slowing down digestion and glucose absorption to maintain stable blood glucose levels. Additionally, the fermentation of fiber in the large

***Corresponding Author:**

e-mail: enypalupi@apps.ipb.ac.id (E. Palupi)

Submitted: 31 August 2023

Accepted: 12 February 2024

Published on-line: 7 March 2024



© Copyright by Institute of Animal Reproduction and Food Research of the Polish Academy of Sciences
© 2024 Author(s). This is an open access article licensed under the Creative Commons Attribution-NonCommercial-NoDeriv License (<http://creativecommons.org/licenses/by-nc-nd/4.0/>).

intestine helps maintain pH balance and gut microbiota, reducing the risk of colorectal cancer [Dhingra *et al.*, 2012].

Purple sweet potato (*Ipomoea batatas* L.) is a common tuber found in Indonesia. It might be served as a staple food containing up to 2.01–3.87 g/100 g of fiber in their fresh matter. Even in the form of flour, purple sweet potatoes have a high fiber content of up to 11.9 g/100 g [Huang *et al.*, 1999; Palupi *et al.*, 2023]. Kidney bean (*Phaseolus vulgaris* L.) is a type of legume known for its nutritional value as 100 g of kidney bean flour contains 13.12 g of fiber [Palupi *et al.*, 2023]. These two foods not only have a high fiber content, but they also contain proteins with noticeable essential amino acids [Audu & Aremu, 2011; Kurnianingsih *et al.*, 2021]. According to Herreman *et al.* [2020], the combination of proteins of tubers and legumes represents one of the suitable plant-based amino acid profiles. Purple sweet potato was detected as poor in methionine [Kurnianingsih *et al.*, 2020], whereas, among common legumes, kidney beans are considered high in methionine, *i.e.*, 0.105 g/100 g [Margier *et al.*, 2018].

A diet rich in fiber and high-quality protein can help people with obesity and pre-diabetes feel fuller for longer periods of time, improve their lipid profiles, and lose weight by lowering insulin resistance [Clark & Slavin 2013; Dhillon *et al.*, 2016; Lesgards, 2023; Rebello *et al.*, 2014; Starr *et al.*, 2019]. As a result, this kind of diet is also linked to a lower risk of developing a number of diseases linked to the metabolic syndrome [Amankwaah *et al.*, 2017; Glynn *et al.*, 2022; Reynolds *et al.*, 2020]. A previous study reported that a high-quality protein diet helped prevent cardiovascular disease and type II diabetes by ameliorating the blood lipid profile and insulin resistance index in obese middle-aged and older adults [Starr *et al.*, 2019].

Considering the above, it seems reasonable to make an effort to formulate a product from purple sweet potatoes and kidney beans, which can serve as a source of fiber and valuable protein, increasing the feeling of satiety and reducing the need for additional meals that could lead to excessive caloric intake. A product that can be formulated using purple sweet potatoes and kidney beans is flakes. These products are typically consumed for breakfast due to their convenience [Priebe & McMonagle, 2016]. The aim of our research was to optimize the formulation of a high-fiber extrudate using purple sweet potatoes and kidney beans and characterize the nutritional, physical and sensory characteristics of the final product, as well as the satiety index after consumption, as part of an initiative to enhance fiber intake in the population.

MATERIALS AND METHODS

■ Materials

There were two main materials that have been used in this research, *i.e.*, purple sweet potato and kidney bean. The variety of purple sweet potato was Ayamurasaki, which was procured from the local farmer in Dramaga, Bogor, Indonesia. In a single run of purple sweet flour, as many as 100 kg of tubers have been used. A common kidney bean (50 kg) was purchased from the local market (Bogor, Indonesia).

■ Production of purple sweet potato and kidney bean flakes

The production of flakes from purple sweet potato and kidney bean was consisting of three main stages, *i.e.*, tuber flour production, legumes flour production, and ingredient mixing followed by extrusion. The production of purple sweet potato flour began with cleaning the sweet potatoes to remove any soil adhering to their skin. Once cleaned, the sweet potatoes were manually cut into medium-sized pieces (3×3 cm), which were then steamed at a temperature of 100°C for 20 min using a PM-3A steamer (Armfield, Bogor, Indonesia) with a capacity of approximately 15 kg of cut sweet potatoes. Subsequently, the steamed sweet potatoes were mashed using a planetary mixer (Gansons, Bombay, India) until smooth. The mass was then dried using a model T of double drum dryer (Simon Dryers, Nottingham, UK) at a temperature of 110°C. The drying process resulted in purple sweet potato sheets and various-sized pieces that were still slightly moist. Therefore, they were further dried in a cabinet dryer (Gelenkwellendienst H. Orth GmbH, Ludwigshafen, Germany) for a minimum of 90 min at 60°C. Once the sheets and pieces were completely dry, they were ground using a ZS A300 pin disc mill (Phoenix, Jakarta, Indonesia) to obtain purple sweet potato flour with a particle size <0.25 mm (screen with 60 mesh). A single batch of purple sweet potato flour yielded as much as 46% of the fresh tuber weight.

As for the production of kidney bean flour, the kidney beans were washed and sorted to remove poor quality beans, such as rotten, sprouted, broken, and dried before soaking at room temperature (approximately 25°C) for 30 min. The soaked kidney bean was boiled using a PM-3A steam jacket kettle (Armfield) for 60 min until softened. This boiling was performed to fully cook the beans and enhance the texture (softened), palatability, and ease the subsequent grinding. Subsequently, the cooked kidney bean was finely mashed using a planetary mixer (Gansons). The drying of mashed kidney bean was performed using a double drum dryer (Simon Dryers) and a cabinet dryer (Gelenkwellendienst H.), followed by further grinding using a ZS A300 pin disc mill (Phoenix), similar to the processing of purple sweet potato flour. The yield of obtaining flour from kidney beans was as much as 80%.

The development and testing of the purple sweet potato and kidney bean extrudate formulations were conducted as a trial-and-error process before producing the final extruded product. This stage aimed to assess the feasibility of the product concept and estimate formulas for the best quality products. The feasibility and the quality of the concept and formula were tested based on the qualitative sensory evaluation by the selected panelists who met International Organization for Standardization (ISO) standard of sensory panelist [ISO 8586:2014]. The results of this evaluation are shown in [Table S1](#) in Supplementary Materials. The development and optimization also included determining the temperature and time of extrusion. The final formulas, F0, F1, F2, and F3 (with different ratios of sweet potato flour to kidney bean flour – 100:0, 80:20, 70:30, 60:40 (*w/w*), respectively), used to obtain extruded purple sweet potato and kidney bean

TABLE 1. Formulas (F0–F3) of extrudates.

| Ingredient (g) | F0 | F1 | F2 | F3 |
|----------------------------------------------------|-------|-------|-------|-------|
| Main ingredients | | | | |
| Purple sweet potato flour | 2,100 | 1,680 | 1,470 | 1,260 |
| Kidney bean flour | 0 | 420 | 630 | 840 |
| Complements | | | | |
| Rice flour | 330 | 330 | 330 | 330 |
| Corn flour | 45 | 45 | 45 | 45 |
| Milk powder | 25 | 25 | 25 | 25 |
| Salt | 10 | 10 | 10 | 10 |
| Liquid ingredients (10% of dry ingredients) | | | | |
| Emulsifier | 1 | 1 | 1 | 1 |
| Water | 200 | 200 | 200 | 200 |
| Oil | 50 | 50 | 50 | 50 |

products are presented in Table 1. The dry ingredients, such as purple sweet potato flour, kidney bean flour, rice flour, cornstarch, milk powder, and salt, were mixed until well blended. Separately, the liquid ingredients, such as water, oil, and emulsifier, were homogeneously combined. Subsequently, all the ingredients were mixed together using a Ueno noodle machine (Siraitodai Fhutuu Tokyo Manufacture, Japan) before being fed into the Twinscrew Bex 2256 extruder (Berto Food & Beverage Processing Machines, Jakarta, Indonesia). This extruder features three different speed settings, *i.e.*, auger, screw, and cutter. The auger, also known as the feeder screw, is located at the beginning of extrusion process and is responsible for feeding the raw material into the extruder. The screw is located inside the extruder barrel and plays an important role in melting, mixing, and shaping the material as it moves along the barrel. The cutter is located at the end of the extrusion process. The faster the cutter operates the smaller the size of the resulting product. The extrusion temperature, auger, screw, and cutter speed were monitored, as well as the selection of the appropriate mold during the development and optimization of the formulation. The optimal extrusion temperature has been achieved at 60°C for the third temperature setting, with the first and second temperature settings were turned off. This setting is suitable for raw materials with a water content of up to 15%. During the trial process, the optimal speed settings were also obtained for the auger, screw, and cutter, with speeds set at 40, 40, and 50 Hz, respectively, where 10 Hz equals to 600 rpm. Based on the formulas F0, F1, F2 and F3 (Table 1), four extrudates of purple sweet potato with kidney bean substitution (E0, E1, E2 and E3, respectively) were produced. The flakes were then cooled at room temperature (25°C) for 30 min before being packaged in aluminum foil using a sealer. These products were subsequently subjected to determination of color and texture characteristics, sensory evaluation, analysis of nutrients, shelf-life and satiety index. As many as three experiments were performed for physical, sensory, and nutritional analysis. While

the assessment of shelf-life has been conducted through eight batches of experiments as eight time series experiment. Furthermore, as many as three batches of production have been carried out for satiety index assessment, with all batches being homogenized prior to the packing and testing.

■ Physical characteristics analysis

The analysis of the physical characteristics included the assessment of the color and texture of the extrudates. The color analysis was conducted using an AMT511 Chroma Meter (Amstast, Lakeland, FL, USA), which measures the color of the samples based on the CIE Lab system. This system provides color measurement results expressed in L^* , a^* , and b^* coordinates, which represent lightness (dark-bright), redness (green-red), and yellowness (blue-yellow), respectively. The texture of the flakes was tested for hardness using a CT3-100 Brookfield texture analyzer (Brookfield, Toronto, Canada).

■ Nutrient content determination

The nutrient content analysis of purple sweet potato and kidney bean extrudates includes determining the moisture content using the gravimetric AOAC International method [AOAC 952.10, 2005], ash content using the gravimetric method [AOAC 923.03, 2005], lipid content using the direct extraction method with a Soxhlet apparatus [AOAC 922.06, 1922], protein content using the Kjeldahl method [AOAC 920.87, 1920], and total fiber content using the enzymatic-gravimetric method [AOAC 985.29, 2003]. Carbohydrate content was estimated on the basis of balance. Results of nutrient content were expressed based on dry matter (DM) of extrudates.

■ Sensory evaluation

The sensory evaluation consisted of two tests, *i.e.*, quantitative descriptive analysis (QDA) and overall acceptance rating test, also known as the hedonic test. QDA has been done by involving

8 trained panelists which met the requirements specified by ISO standard [ISO 8586:2014]. In QDA, the assessors participated in a focus group discussion (FGD) to determine the representative attributes, attribute definitions, and the standard scales to be used. The panelists then quantified each attribute by using 10-point intensity scales (weak-strong intensity) in a separate testing booth and recorded their ratings on evaluation sheets. The gathered data was processed and presented in a radar chart format.

The overall acceptance rating test was conducted to determine how well the products were accepted by the panelists. In this test, the level of acceptance of each attribute was measured using a 9-point hedonic scale, with 1 being “dislike extremely” and 9 being “like extremely”. In this research, the observed attributes were appearance, aroma, finger-feel texture, taste, mouthfeel, aftertaste, and overall perception. The panelists involved at this test were 40 initiated assessors, who have previously conducted sensory evaluations and understand the rules of sensory testing but have not yet been selected as assessors.

■ Shelf-life estimation

The flakes were stored at three different temperatures, *i.e.*, 25, 35, and 45°C, at 1 till 8 weeks to estimate their self-life. Only E3 has been used for shelf-life estimation. Sensory acceptability (S) of extrudate was used as a parameter defining changes during storage. Sensory evaluation of acceptability was performed by 8 selected assessors at 1–7 scale with following interpretation, 7 – equal or better to control, 6 – slight difference to control, 5 – more distinct difference but still acceptable, 4 – beginning to lose acceptability, 3 – more distinct loss of acceptability, 2 – very distinct loss of acceptability, and 1 – unacceptable. The control here was the fresh E3, which was produced on the day of testing. It has been assumed that the test food would start to lose acceptability at S_4 or $\ln S = \ln 4 = 1.386$. The shelf-life was predicted based on the regression equation of each storage temperature. Temperature of 30°C was used to calculate the final estimated shelf-life [Hough, 2010].

■ Satiety index determination

The satiety index assessment has been approved by the Ethics Committee of IPB University in Bogor, Indonesia, with the approval number 857/IT3.KEPMSM-IPB/SK/2023. It was measured after consumption of the flakes with 0% kidney beans flour (E0) and with 40% kidney beans flour (E3) compared with commercial cereals and using white bread as the reference. White bread was made from flour (all-purpose flour/medium protein) (70.4 g/100 g), water (10.0 mL/100 g), sugar (6.3 g/100 g), shortening (4.5 g/100 g), sweet whey powder (4.2 g/100 g), salt (2.1 g/100 g), yeast (0.8 g/100 g), and whole milk powder (0.8 g/100 g). The design used in this study was a partial crossover study, where each subject was given isocaloric food with 240 kcal after 10 h fasting. The test foods were given four times on four different days, but on the same day, all subjects were given the same type of food. There was a 3-day interval or washout period between the test foods to allow the subjects’

physiological conditions to return to their baseline [Becker *et al.*, 2022; Nolan *et al.*, 2016].

A total of 16 subjects was included in the study, following Forde’s [2018] recommendation of requiring 15–18 subjects to compare satiety between products. The subjects participating in this research met the inclusion and exclusion criteria. The inclusion criteria were as follows: individuals with body mass index (BMI) in optimal range (BMI 18.5–22.9 kg/m²), man or woman aged between 20–22 years, willing to be interviewed and complete the questionnaire, not currently on any specific diet, willing to undergo measurements of body weight, height, body composition, and participate in all activities, and not allergic to nuts. On the other hand, the exclusion criteria were suffering from chronic illnesses or complications.

The data was obtained through the completion of questionnaires and direct measurements on the subjects. The primary data included subject characteristics (name, age, and gender), anthropometry (height and weight), satiety levels, as well as the macro-nutrient content of the test foods, (white bread, commercial cereals, extruded purple sweet potato, and extruded purple sweet potato with kidney bean). Data related to the subjects’ nutritional status was collected through direct measurements using a digital floor scale for body weight (HN-289, Omron, Kyoto, Japan) and a microtoise for height (GEA SH2A stature meter, Bogor, Indonesia). Data was collected through a visual analogue scale (VAS) satiety score questionnaire at 0, 30, 60, 90, 120, 150, and 180 min after consumption of the food products, which was then used to calculate the area under the curve for each flake type and compare it with the area under the curve for white bread to determine the satiety index (%) for each subject [Forde, 2018]. Moreover, the curve was calculated using a trapezoid system for satiety parameters including hunger, fullness, desire, and food intake. The curve was scaled in units of time of sampling (counted in hour) and fullness index, which was expressed as a ruler scale at mm. Therefore, the area under the curve was expressed as mm².

■ Statistical analysis

Data processing in this research was conducted using Excel 2010 for Windows software (Microsoft, Redmond, WA, USA) and Statistical Product and Service Solution (SPSS) 16.0 software (IBM, Armonk, NY, USA). The processed and analyzed data included the results of color and texture analysis, sensory evaluations, shelf-life estimation and nutrient content, as well as satiety index. The data was then subjected to one-way analysis of variance (ANOVA) using SPSS software (IBM) and further tested with Duncan post hoc test if significant effects were found among the treatments. Results of the analysis were considered significantly different if $p < 0.05$.

RESULTS AND DISCUSSION

■ Formulation and processing

The key steps in optimizing the formula for extruded products with purple sweet potato and kidney bean were adjusting the composition of additional flours, reducing or eliminating

certain ingredients, and controlling the moisture content of the raw dough. It was also important to optimize the extruder settings, including the extrusion temperature based on thermo-control and the rotations of the screw, auger, and cutter. For this purpose, a series of trial-and-error experiments were carried out. The selection of the extrusion temperature and machine speed settings was performed based on the optimization trials conducted as part of preliminary research. Thirteen trials (Table S1) were conducted to develop the formulation and determine the extruder's auger, screw, and cutter rotations, as well as the dough's moisture content to achieve an optimal product quality. The screw type and also its speed have a significant impact on the rheological properties of the final product [Tomaszewska-Ciosk *et al.*, 2012].

During the development of the extrudate formula, liquid ingredients (water, oil and emulsifier) were added (Table 1). They played a vital role in the drying process during the extrusion and in forming a matrix between starch and protein present in the dough. When heated, the starch experiences high pressure during extrusion, causing the dough to expand as it exits the extruder, resulting in expanded products. Without the addition of water to the product, the extruded dough cannot fully be formed, leading to non-expansion or burnt dough, causing it to adhere inside the extruder and obstructing extrusion [Yacu, 2020]. On the other hand, excessive liquid level leads to a resulting product with a soggy or mushy texture. The addition of oil to the dough could increase the crispiness of the product and prevent hollowness in the final products. This is because oil can reduce the friction between the dough and the extruder

screw, thus preventing a rapid increase in temperature due to mechanical friction in the extruder. In this study, based on the preliminary research, the optimal liquid percentage was determined to be 10% (*w/w*) with oil-to-water ratio of 1:4 (*w/v*).

The extruder employed in this study was a double-screw extruder equipped with three thermo-controls. Temperature for extrusion was reached at 60°C regulated only on the third thermo-control of the machine. Meanwhile, thermo-controls 1 and 2 remained switched off. This configuration is suitable for dough with a water content of less than 15 g/100 g [Budi *et al.*, 2016]. If the dough's water content exceeds 15 g/100 g, all thermo-controls must be activated [Budi *et al.*, 2016]. Trials conducted at higher temperatures (>60°C) resulted in a burnt product. The low heating setting was chosen as the flours used in this study were fully cooked during the flouring stages. Through experimentation, it was determined that the optimal settings for the auger and screw speeds during the extrusion process of this study were 40 Hz, while the cutter speed was set at 50 Hz. A detailed evaluation of the trials is provided in Table S1.

■ Physical, nutritional and sensory characteristics

The selected formulas (Table 1) were used to obtain extrudates based on purple sweet potato without or with kidney bean substitution. The physical, chemical and sensory characteristics of these products are shown in Table 2. As the percentage of kidney bean flour substitution increased in the extruded formulation, there was a corresponding increase in lightness (L^*) and yellowness (b^*), but a decrease in redness (a^*) of products. The significant variances in extrudate color, particularly

TABLE 2. Physical and nutritional characteristics of extrudates.

| Characteristic | E0 | E1 | E2 | E3 |
|------------------------------------------|---------------------------|----------------------------|--------------------------|--------------------------|
| Physical characteristics | | | | |
| L^* | 47.57±1.23 ^d | 51.22±1.29 ^c | 53.11±0.88 ^b | 56.14±0.99 ^a |
| a^* | 27.88±0.83 ^a | 24.64±2.58 ^{ab} | 23.54±1.56 ^b | 21.57±1.41 ^c |
| b^* | -9.17±0.69 ^c | -2.02±2.10 ^b | -2.65±0.37 ^b | 3.12±0.50 ^a |
| Hardness (N) | 124.44±22.36 ^b | 194.25±44.35 ^{ab} | 207.8±10.55 ^a | 232.2±81.27 ^a |
| Nutrient content and energy value | | | | |
| Moisture (g/100 g) | 5.58±0.08 ^a | 5.48±0.18 ^a | 5.41±0.11 ^a | 5.25±0.12 ^a |
| Ash (g/100 g DM) | 2.80±0.06 ^c | 2.99±0.01 ^b | 3.12±0.04 ^{ab} | 3.26±0.05 ^a |
| Protein (g/100 g DM) | 5.51±0.19 ^d | 9.33±0.19 ^c | 11.50±0.09 ^b | 13.20±0.11 ^a |
| Lipid (g/100 g DM) | 0.56±0.08 ^b | 0.67±0.07 ^{ab} | 0.76±0.05 ^{ab} | 0.87±0.04 ^a |
| Carbohydrate (g/100 g DM) | 85.57±0.25 ^a | 81.54±0.29 ^b | 79.23±0.28 ^c | 77.43±0.14 ^d |
| Energy (kcal/100 g) | 369.28±0.47 ^a | 369.47±1.03 ^a | 369.70±0.32 ^a | 370.35±0.49 ^a |
| Total fiber (g/100 g DM) | 16.47±0.09 ^b | 16.58±0.01 ^b | 17.04±0.11 ^a | 17.00±0.04 ^a |
| Soluble fiber (g/100 g DM) | 5.67±0.04 ^a | 4.46±0.15 ^b | 4.11±0.02 ^b | 3.25±0.11 ^c |
| Insoluble fiber (g/100 g DM) | 10.80±0.13 ^d | 12.12±0.09 ^c | 12.93±0.13 ^b | 13.75±0.07 ^a |

E0, E1, E2, and E3, extrudates obtained on the basis of formulas with different ratios of sweet potato flour to kidney bean flour – 100:0, 80:20, 70:30, 60:40 (*w/w*), respectively; L^* , lightness; a^* , redness; b^* , yellowness; DM, dry matter. Values with different superscript letters (a–d) in a row are significantly different at $p < 0.05$.

the reduced redness observed in the flakes with the higher bean portion. The presence of anthocyanin in purple sweet potatoes seemed the plausible reason for this phenomenon. These pigments, found in significant quantities in purple sweet potatoes (ranging from 3.31 to 13.9 mg/g), are known to influence coloration [Rodríguez-Mena *et al.*, 2023]. Our prior investigation revealed that although some of these anthocyanins undergo degradation during flour extrusion, their presence remains notable in the end product [Palupi *et al.*, 2023]. The hardness of the extrudates also varied depending on the proportion of kidney bean flour in the formula – higher kidney bean flour content led to a higher hardness (Table 2). Visually, the produced flakes in our study exhibited a dense consistency with a slightly flat, concave round shape and a slight porosity. The number of pores increased with the quantity of kidney beans used. It is worth noting that the extrusion process has a significant impact on the composition and physical appearance of the products [Lisiecka *et al.*, 2021; Ménabréaz *et al.*, 2021].

A similar pattern was also observed in the content of key nutrients in the extrudates. With increased kidney bean substitution, the levels of ash (crude minerals), protein, lipid, and total fiber increase (Table 2). The extrudate with 40% bean substitution had the highest contents of crude minerals, protein, lipid, and fiber at 3.26, 13.20, and 0.87, 17.00 g in 100 g of dry matter (DM), respectively. It is worth paying attention to the content of soluble and insoluble fiber in the formulated flakes. Higher kidney bean flour substitution led to an increase in insoluble fiber content and a significant decrease in soluble fiber content ($p < 0.05$). This phenomenon may be attributed to kidney beans' higher total fiber content compared to purple sweet potatoes, which predominantly consists of insoluble fiber [Kan *et al.*, 2017]. According to Leite *et al.* [2022], purple sweet potatoes contain fiber ranging from 6.5 to 12.6% of their dry matter, depending on the variety. The fiber content of purple sweet potatoes is primarily composed of cellulose, hemicellulose, and pectin, at 2.7, 3.6, and 0.47%, respectively [Yuansah & Laga, 2023]. In contrast, kidney beans are known to contain 26.3% fiber in their dry matter, primarily composed of cellulose and hemicellulose [Kan *et al.*, 2017].

Flakes are a ready-to-eat food product that meets the nutritional needs of individuals seeking a convenient source of essential nutrients [Priebe & McMonagle, 2016]. This product is well-suited to be part of a breakfast menu. The breakfast menu is capable of satisfying 22.4% of the daily energy requirement and provides 32.7% of the daily protein requirement, 21.8% of the daily fat requirement, 21.5% of the daily carbohydrate requirement, and 33.6% of the daily dietary fiber requirement for adults aged 19–64 years, both males and females [Gibney *et al.*, 2018]. A single breakfast serving of the extrudate with purple sweet potato and kidney bean optimized in our study (50 g), when accompanied by a glass of fresh cow's milk, a boiled egg, and a medium-sized banana, can adequately fulfill the breakfast requirements of adults. This developed product is also suitable for consumption by children, as supported by previous studies

indicating that children generally show a strong preference for extruded food products made from ingredients like potatoes, sweet potatoes, fruit extracts, and various cereals [Gumul *et al.*, 2023; Natabirwa *et al.*, 2020; Potter *et al.*, 2013; Shah *et al.*, 2019]. Children's inclination toward crispy textures, visually appealing appearances, and easy-to-consume food products contributes to their acceptance [Natabirwa *et al.*, 2020]. Past studies have utilized ready-to-eat extrudates as supplemental foods to enhance nutrient intake in children [Gumul *et al.*, 2023; Natabirwa *et al.*, 2020; Potter *et al.*, 2013; Shah *et al.*, 2019]. Furthermore, the extrudate obtained in our study from a formula with 40% replacement of purple sweet potato flour with kidney bean flour has a potential to be labeled as a high-fiber, source of protein, and low-fat food item. The cut off of each claim is 6, 12, 3 g per 100 g flakes, respectively [Indonesian Food and Drug Authority 2022].

The result of QDA showed that the higher portion of the purple sweet potato flour in the extrudate formula provided a greater smoothness and homogeneity, a reduced porosity, a stronger tuber flavor with a milder earthy and beany undertone, and a sweeter taste of the final products (Figure 1). Additionally, it was noted that the purple sweet potato resulted in a harder mouthfeel and a less earthy aftertaste. Purple sweet potato contributed to sweet taste and tuber flavor. Moreover, the significant content of carbohydrate in purple sweet potato [Kurnianingsih *et al.*, 2020] seemed to support the consistency of the mixture, making its texture smoother. While, the kidney bean contributed to the beany and earthy flavor. The substitution of kidney beans at 20%, 30%, and 40% did not significantly influence ($p \geq 0.05$) the overall acceptance level (Figure 1), with acceptance ratings consistently above six on a nine-point hedonic scale, corresponding to a "like moderately" according to the categorization proposed by Wichchukit & O'Mahony [2014]. Consequently, the extrudate with 40% kidney bean (E3) substitution was further evaluated for shelf-life and satiety index. The extrudate without a bean substitute and commercially available breakfast cereals were used for comparison.

■ Shelf-life estimation

Determining the shelf-life of a food product is a critical step before it is introduced to consumers. This process is essential to ensure food safety, protect consumers, and maintain product quality. In this study, the shelf-life estimation was conducted using a sensory approach, which is known for its sensitivity compared to other methods [Hough, 2010]. A first-order kinetic reaction was chosen as the model for shelf-life estimation. Like many common foods, the developed product experiences a faster rate of deterioration as storage time and temperature increase (Figure 2). The correlation between these factors was particularly pronounced at higher storage temperatures. The equation with a lower slope was derived for 45°C ($y = -0.0716x + 1.8891$), in contrast to the equations for 35°C and 25°C, which were $y = -0.0184x + 1.9667$ and $y = -0.0075x + 1.9684$, respectively. By applying these formulations, a shelf-life estimation graph

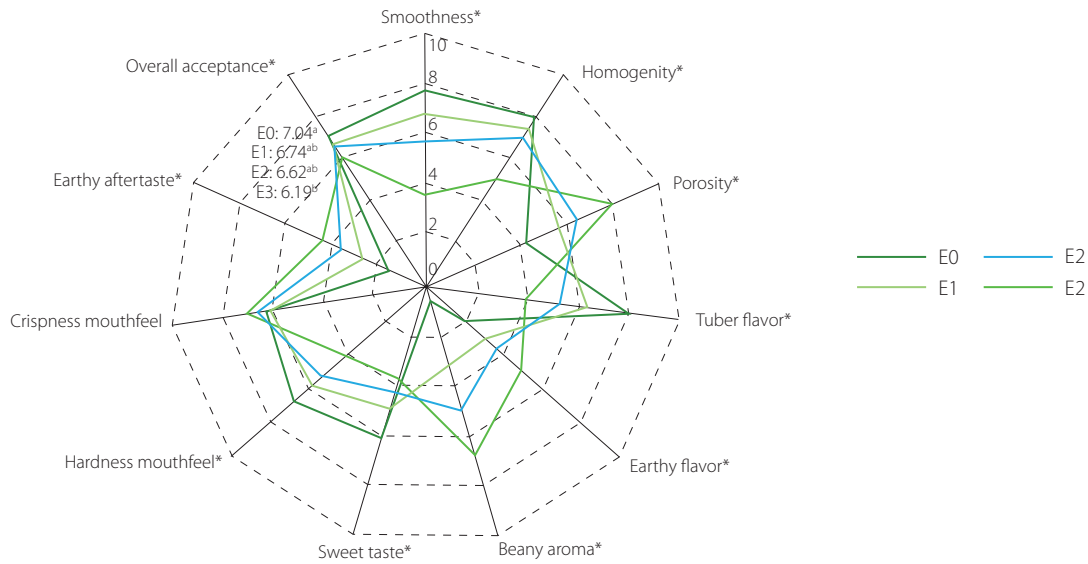


Figure 1. Quantitative descriptive analysis (QDA) results and overall acceptance rating of extrudates (E0, E1, E2, and E3) obtained on the basis of formulas with different ratios of sweet potato flour to kidney bean flour – 100:0, 80:20, 70:30, 60:40 (w/w), respectively. *, Significantly different at $p < 0.05$. Values of overall acceptance with different superscript letters are significantly different at $p < 0.05$.

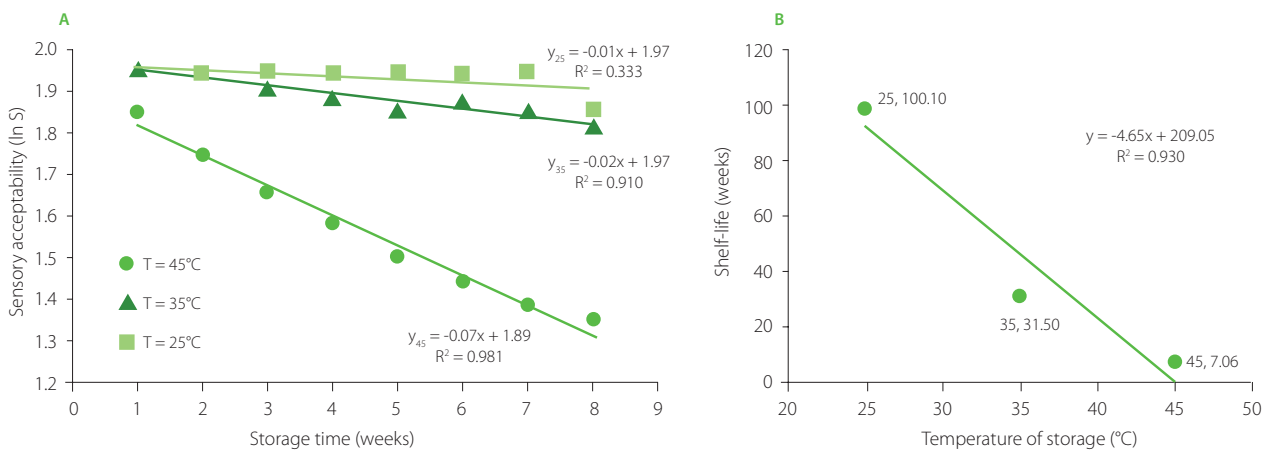


Figure 2. Sensory acceptability on eight storage times (A) and estimated shelf-life (B) of the extrudates made of purple sweet potato flour with kidney bean flour substitution. T, temperature of storage; S, sensory acceptability at 1–7 scale with the following interpretation: 7 – equal or better to control, 6 – slight difference to control, 5 – more distinct difference but still acceptable, 4 – beginning to lose acceptability, 3 – more distinct loss of acceptability, 2 – very distinct loss of acceptability, and 1 – unacceptable; the test food start to lose acceptability at $S=4$ or $\ln S = \ln 4 = 1.386$. Control sample, the fresh E3 which was produced on the day of testing.

was constructed for different temperatures, resulting in the final equation: $y = -4.6472x + 208.84$. Assuming that the anticipated storage temperature will be around 30°C, the estimated safe storage time was 19 months. This is a favorable estimation, indicating that the developed product can be stored at room temperature for over a year without a significant reduction in acceptability.

Satiety index

The satiety index serves as a measure of how filling and satisfying a food is, and it provides valuable information into its potential to control hunger and regulate food intake. This experiment enabled the researchers to compare the satiety effects of the test foods, providing insights into their potential as satisfying food options. Many factors contributed to the satiety index, one of them being nutrient content. Between products examined in our study,

commercial cereals had the highest energy value (370 kcal/100 g) and total carbohydrate content (83.14 g/100 g) (Table 3). In contrast, the extruded purple sweet potato with kidney bean had the highest protein content (12.5/100 g) and higher fiber content (16.1 g/100 g) compared to commercial cereals.

The study revealed significant differences in satiety indexes after consumption of extrudates based on purple sweet potato with and without kidney bean and commercial cereal. The satiety index for the tested foods, in the order of commercial cereal, extruded purple sweet potato, and extruded purple sweet potato with kidney bean, were 99.29, 103.87 and 140.03, respectively (Table 3). The satiety index computed for the extruded purple sweet potato with kidney bean (E3) was significantly higher compared to that calculated for commercial cereals, indicating that the addition of kidney bean to purple sweet potato flakes resulted in a greater

TABLE 3. Nutritional characteristics of food products used to assess the satiety index and results of this assessment.

| Characteristic | White bread | Commercial cereals | Extruded purple sweet potato | Extruded purple sweet potato with kidney bean |
|------------------------------------------|--------------------------|--------------------------|------------------------------|-----------------------------------------------|
| Energy value (kcal/100 g) | 238.70±1.62 ^c | 370.24±4.27 ^a | 286.56±0.47 ^b | 286.48±0.49 ^b |
| Protein content (g/100 g) | 9.90±0.04 ^b | 9.90±0.05 ^b | 5.20±0.19 ^c | 12.50±0.11 ^a |
| Lipid content (g/100 g) | 4.70±0.02 ^a | 1.30±0.37 ^b | 0.54±0.04 ^b | 0.80±0.04 ^b |
| Total carbohydrate content (g/100 g) | 48.38±3.62 ^c | 83.14±1.70 ^a | 80.8±0.34 ^{ab} | 73.4±0.25 ^b |
| Available carbohydrate content (g/100 g) | 39.28±0.32 ^d | 79.80±0.11 ^a | 65.24±0.25 ^b | 57.26±0.14 ^c |
| Total dietary fiber content (g/100 g) | 9.10±3.30 ^{ab} | 3.33±1.59 ^b | 15.55±0.09 ^a | 16.11±0.11 ^a |
| Soluble fiber content (g/100 g) | 2.66±0.96 ^b | 0.64±0.31 ^c | 5.64±0.03 ^a | 3.08±0.02 ^b |
| Insoluble fiber content (g/100 g) | 6.44±2.34 ^{bc} | 2.66±1.28 ^c | 9.86±0.06 ^{ab} | 13.02±0.09 ^a |
| Water content (mL/100 g) | 35.37±0.37 ^a | 2.57±0.28 ^c | 7.03±0.08 ^b | 6.85±0.12 ^b |
| Weight (g) of serving (240 kcal) | 100 | 51.3 | 66.3 | 66.3 |
| Hunger (mm×h) | 17.89±1.32 ^{ab} | 20.54±2.06 ^a | 15.15±1.85 ^{ab} | 13.39±1.94 ^b |
| Fullness (mm×h) | 30.54±1.78 ^{ab} | 28.73±1.64 ^b | 33.32±1.84 ^{ab} | 35.98±1.82 ^a |
| Desire to eat (mm×h) | 19.87±2.22 ^{ab} | 22.51±2.15 ^a | 16.49±2.17 ^{ab} | 12.96±2.04 ^b |
| Food intake (mm×h) | 20.72±1.77 ^{ab} | 22.80±2.05 ^a | 16.78±2.05 ^{ab} | 14.10±2.10 ^b |
| Satiety index (%) | Reference | 99.29±7.43 ^b | 103.87±22.47 ^{ab} | 140.03±29.46 ^a |

Values with different superscript letters (a–d) in a row are significantly different at $p < 0.05$.

sense of fullness. At the determination at 180-min, the visual analogue scale (VAS) score for the sensation of fullness resulting from the consumption of extruded tuber with kidney bean was 49.84 mm (Figure 3). This score was subsequently utilized in conjunction with the regression equation derived from white bread as a reference ($y = -0.30x + 87.96$). Then, the calculation yielded a projected duration of 126 min for white bread to induce the same level of fullness. Consequently, it can be inferred that the consumption of extruded tuber with kidney bean led to an extended feeling of fullness by 54 min compared to the white bread.

The study suggests that fiber was the primary factor responsible for prolonging the feeling of satiety compared to protein, carbohydrates, lipids, and water. The fiber content showed a significant correlation with feelings of hunger ($p=0.02$, $r=-0.30$), fullness ($p=0.00$, $r=0.35$), desire to eat ($p=0.00$, $r=-0.40$), and food intake ($p=0.00$, $r=-0.38$). Thus, consuming foods high in fiber can increase the feeling of fullness (satiety), making the extruded purple sweet potato with kidney bean a potential source of fiber to improve daily fiber intake and prevent overeating. The testing method used in this study can be applied to try other satiating foods based on total energy. However, during fasting periods after satiety testing, subjects should not be allowed to leave the area to minimize variations in physical activity and any disruptions that could affect satiety perception.

CONCLUSIONS

In conclusion, this research optimized the formula of flakes from the extrusion of purple sweet potatoes with kidney beans. The extrudate obtained on the basis of the selected formula,

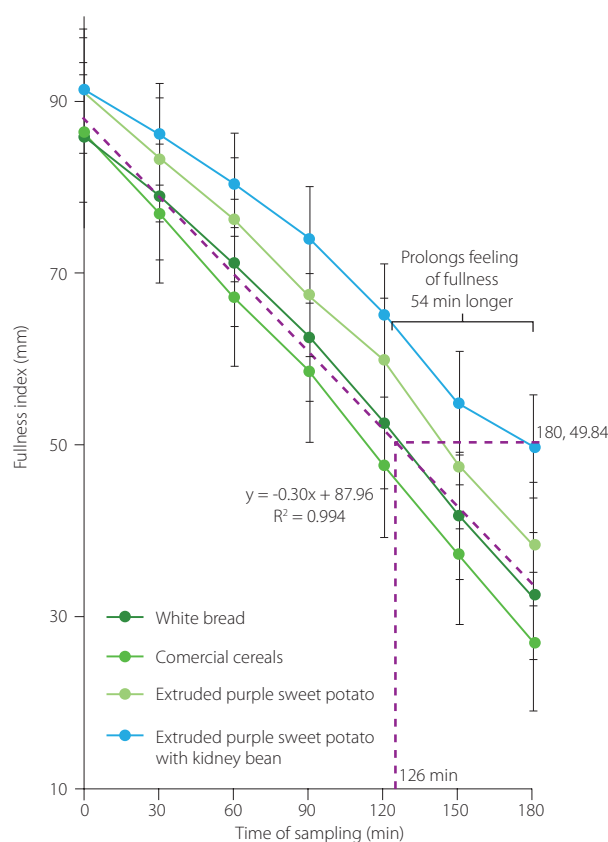


Figure 3. The visual analogue scale (VAS) for fullness index at fasting intervals of 30, 60, 90, 120, 150, and 180 min after the consumption of extrudate made of purple sweet potato flour with and without kidney bean flour compared with commercial cereals and white bread (as reference) which showed that the consumption of extruded purple sweet potato with kidney bean substitution led to an extended feeling of fullness by 54 min compared to white bread.

which replaced 40% of purple sweet potato flour with kidney bean flour, showed good sensory acceptability, nutritional value (high contents of protein and fiber), and caused a high satiety index after consumption. The estimated shelf-life of flakes was as much as 19 months. This product might provide an alternative fiber-rich food that has been proved to prolong the feeling of fullness compared to the reference and commercial food, so it is expected to prevent eating more food, which is an initial trigger for excess calorie intake. However, before mass production of this extrudate, future research is needed on its physical properties such as its wetting capacity, rehydration, milk absorption, and sedimentation. To ensure the safety of extrudates for mass production, it is also necessary to assess the content of heavy metals and microbiological tests. Furthermore, future research could investigate the long-term effects of consuming extruded purple sweet potatoes, especially as a main breakfast food, on other biological markers like blood glucose level and lipid profile.

SUPPLEMENTARY MATERIALS

The following are available online at <http://journal.pan.olsztyn.pl/High-Fiber-Extruded-Purple-Sweet-Potato-Ipomoea-batas-and-Kidney-Bean-Phaseolus,183995,0,2.html>. Table S1. Optimization of the development of extruded purple sweet potato and kidney beans.

INFORMED CONSENT STATEMENT

This research has obtained permission from the Commission on Research Ethics Involving Human Subjects, IPB University Number: 857/IT3.KEPMSM-IPB/SK/2023.

RESEARCH FUNDING

The authors acknowledge to IPB University for financial support of the research as a “Young Lecturer Grant” for this research entitled “High Fiber and Antioxidants Extruded Purple Sweet Potato to Prevent Obesity and Non-Communicable Diseases” No. RKA B1.006.02 and the Article Processing Charge. The authors also would like to thank for the support of research grant from Southeast Asian Regional Center for Graduate Study and Research in Agriculture (SEARCA).

CONFLICT OF INTERESTS

The authors declare no conflict of interest.

ORCID IDs

| | |
|----------------|-------------------------------------------------------------------------------------------|
| D. Briawan | https://orcid.org/0000-0002-3241-4983 |
| F. Filianty | https://orcid.org/0000-0002-2956-3566 |
| G. Mufida | https://orcid.org/0009-0009-0236-4717 |
| N.M. Nurdin | https://orcid.org/0000-0002-0532-9492 |
| E. Palupi | https://orcid.org/0000-0003-2029-3106 |
| R. Pangestika | https://orcid.org/0009-0007-7503-5741 |
| R. Rimbawan | https://orcid.org/0000-0002-2421-5933 |
| A. Sulaeman | https://orcid.org/0000-0002-9618-7214 |
| F.N. Valentine | https://orcid.org/0009-0007-2141-7947 |

REFERENCES

- Aguilar-Avila, D.S., Martinez-Flores, H.E., Morales-Sanchez, E., Reynoso-Camacho, R., Garnica-Romo, Ma.G. (2023). Effect of extrusion on the functional properties and bioactive compounds of tamarind (*Tamarindus indica* L.) shell. *Polish Journal of Food and Nutrition Sciences*, 73(3), 278-288. <https://doi.org/10.31883/pjfn/170815>
- Amankwaah, A.F., Sayer, R.D., Wright, A.J., Chen, N., McCrory, M.A., Campbell, W.W. (2017). Effects of higher dietary protein and fiber intakes at breakfast on postprandial glucose, insulin, and 24-h interstitial glucose in overweight adults. *Nutrients*, 9(4), art. no. 352. <https://doi.org/10.3390/nu9040352>
- AOAC International. 2005. Official Method 923.03. Ash of Flour. 18th edition. AOAC International, Gaithersburg, Maryland, USA.
- AOAC International. 2005. Official Method 925.10. Solid (Total) and Moisture in Flour. 18th edition. AOAC International, Gaithersburg, Maryland, USA.
- AOAC International. 2005. Official Method 985.29. Insoluble, Soluble, and Total Dietary Fiber in Foods. Enzymatic-Gravimetric. 18th edition. AOAC International, Gaithersburg, Maryland, USA.
- AOAC International. 1922. Official Method 922.06. Fat in Flour. 15th edition. AOAC International, Gaithersburg, Maryland, USA.
- AOAC International. 1920. Official Method 920.87. Protein (total) in Flour. 15th edition. AOAC International, Gaithersburg, Maryland, USA.
- Audu, S.S., Aremu, M.O. (2011). Effect of processing on chemical composition of red kidney bean (*Phaseolus vulgaris* L.) flour. *Pakistan Journal of Nutrition*, 10(11), 1069-1075. <https://doi.org/10.3923/pjn.2011.1069.1075>
- Becker, A.M., Holze, F., Grandinetti, T., Klaiher, A., Toedtli, V.E., Kolaczynska, K.E., Duthaler, U., Varghese, N., Eckert, A., Grünblatt, E., Liechti, M.E. (2022). Acute effects of psilocybin after escitalopram or placebo pretreatment in a randomized, double-blind, placebo-controlled, crossover study in healthy subjects. *Clinical Pharmacology & Therapeutics*, 111(4), 886-895. <https://doi.org/10.1002/cpt.2487>
- Budi, F.S., Hariyadi, P., Budijanto, S., Syah, D. (2016). Effect of dough moisture content and extrusion temperature on degree of gelatinization and crystallinity of rice analogues. *Journal of Developments in Sustainable Agriculture*, 10(2), 91-100. <https://doi.org/10.11178/jdsa.10.91>
- Clark, M.J., Slavin, J.L. (2013). The effect of fiber on satiety and food intake: A systematic review. *Journal of the American College of Nutrition*, 32(3), 200-211. <https://doi.org/10.1080/07315724.2013.791194>
- Dhillon, J., Craig, B.A., Leidy, H.J., Amankwaah, A.F., Anguah, K.O.B., Jacobs, A., Jones, B.L., Jones, J.B., Keeler, C.L., Keller, C.E., McCrory, M.A., Rivera, R.L., Slebodnik, M., Mattes, R.D., Tucker, R.M. (2016). The effects of increased protein intake on fullness: a meta-analysis and its limitations. *Journal of the Academy of Nutrition and Dietetics*, 116(6), 968-983. <https://doi.org/10.1016/j.jand.2016.01.003>
- Dhingra, D., Michael, M., Rajput, H., Patil, R.T. (2022). Dietary fibre in foods: A review. *Journal of Food Science and Technology*, 49, 255-266. <https://doi.org/10.1007/s13197-011-0365-5>
- Forde, C.G. (2018). Chapter 7: Measuring satiation and satiety. In: G. Ares, P. Varela (Eds.), *Methods in Consumer Research*, Volume 2, Woodhead Publishing, pp. 151–182. <https://doi.org/10.1016/B978-0-08-101743-2.00007-8>
- Gibney, M.J., Barr, S.I., Bellisle, F., Drewnowski, A., Fagt, S., Livingstone, B., Masset, G., Moreiras, V.G., Moreno, L.A., Smith, J., Vieux, F., Thielecke, F., Hopkins, S. (2018). Breakfast in human nutrition: The international breakfast research initiative. *Nutrients*, 10(5), art. no. 559. <https://doi.org/10.3390/nu10050559>
- Glynn, E.L., Fleming, S.A., Edwards, C.G., Wilson, M.J., Evans, M., Leidy, H.J. (2022). Consuming a protein and fiber-based supplement preload promotes weight loss and alters metabolic markers in overweight adults in a 12-week, randomized, double-blind, placebo-controlled trial. *The Journal of Nutrition*, 152(6), 1415-1425. <https://doi.org/10.1093/jn/nxac038>
- Gumul, D., Berski, W., Zięba, T. (2023). The influence of fruit pomaces on nutritional, pro-health value and quality of extruded gluten-free snacks. *Applied Sciences*, 13(8), art. no. 4818. <https://doi.org/10.3390/app13084818>
- Herreman, L., Nommensen, P., Pennings, B., Laus, M.C. (2020). Comprehensive overview of the quality of plant- and animal-sourced proteins based on the digestible indispensable amino acid score. *Food Science & Nutrition*, 8(10), 5379-5391. <https://doi.org/10.1002/fsn3.1809>
- Hough G. (Ed.) (2010). Chapter 3: Design of sensory shelf-life experiments, In: *Sensory Shelf Life Estimation of Food Products*. 1st Edition, US: CRC Press, Boca Raton, USA, pp. 63-82. <https://doi.org/10.1201/9781420092943>
- Huang, A.S., Tanudjaja, L., Lum, D. (1999). Content of alpha-, beta-carotene, and dietary fiber in 18 sweetpotato varieties grown in Hawaii. *Journal of Food Composition and Analysis*, 12(2), 147-151. <https://doi.org/10.1006/jfca.1999.0819>
- Indonesian Food and Drug Authority. (2022). Regulation of Indonesian Food and Drug Authority Number 1 of 2022 About Monitoring Claims on Processed Food Label and Food Advertisement. Jakarta: Indonesian Food and Drug Authority.

22. ISO 8586. (2014). Sensory analysis – General guidelines for the selection, training and monitoring of selected assessors and expert sensory assessors.
23. Kan, L., Nie, S., Hu, J., Wang, S., Cui, S.W., Yawen, L., Xu, S., Wu, Y., Wang, J., Bai, Z., Xie, M. (2017). Nutrients, phytochemicals and antioxidant activities of 26 kidney bean cultivars. *Food and Chemical Toxicology*, 108(Part B), 467-477. <https://doi.org/10.1016/j.fct.2016.09.007>
24. Khalid, W., Arshad, M.S., Jabeen, A., Muhammad Anjum, F., Qaisrani, T.B., Suleria, H.A.R. (2022). Fiber-enriched botanicals: A therapeutic tool against certain metabolic ailments. *Food Science & Nutrition*, 10(10), 3203-3218. <https://doi.org/10.1002/fsn3.2920>
25. Kurnianingsih, N., Ratnawati, R., Nazwar, T.A., Ali, M., Fatchiyah, F. (2020). A comparative study on nutritional value of purple sweet potatoes from West Java and Central Java, Indonesia. *Journal of Physics: Conference Series*, 1665(1), art. no. 012011. <https://doi.org/10.1088/1742-6596/1665/1/012011>
26. Kurnianingsih, N., Ratnawati, R., Nazwar, T.A., Ali, M., Fatchiyah, F. (2021). Purple sweet potatoes from East Java of Indonesia revealed the macronutrient, anthocyanin compound and antidepressant activity candidate. *Medical Archives*, 75(2), 94-100. <https://doi.org/10.5455/medarh.2021.75.94-100>
27. Lasimpala, L., Nuryani, N., Ramadhani, F., Kau, M. (2021). Dietary patterns and knowledge of metabolic syndrome among adults. *Gorontalo Journal of Nutrition and Dietetic*, 1(2), 64-73 (in Indonesian).
28. Leite, C.E.C., Souza, B.D.K.F., Manfio, C.E., Wamser, G.H., Alves, D.P., de Francisco, A. (2022). Sweet potato new varieties screening based on morphology, pulp color, proximal composition, and total dietary fiber content via factor analysis and principal component analysis. *Frontiers in Plant Science*, 13, art. no. e852709. <https://doi.org/10.3389/fpls.2022.852709>
29. Lesgards, J.F. (2023). Benefits of whey proteins on type 2 diabetes mellitus parameters and prevention of cardiovascular diseases. *Nutrients*, 15(5), art. no. 1294. <https://doi.org/10.3390/nu15051294>
30. Lisiecka, K., Wójtowicz, A., Sujak, A. (2021). Effect of composition and processing conditions on selected properties of potato-based pellets and microwave-expanded snacks supplemented with fresh beetroot pulp. *Polish Journal of Food and Nutrition Sciences*, 71(2), 211–236. <https://doi.org/10.31883/pjfn/138321>
31. Margier, M.M., George, S., Hafnaoui, N., Remond, D., Nowicki, M., Chaffaut, L.D., Amiot, M.-J., Reboul, E. (2018). Nutritional composition and bioactive content of legumes: characterization of pulses frequently consumed in France and effect of the cooking method. *Nutrients*, 10(11), art. no. 1668. <https://doi.org/10.3390/nu10111668>
32. Ménabréaz, T., Dorsaz, M., Bocquel, D., Udrisard, I., Kosinska-Cagnazzo, A., Andlauer, W. (2021). Goji berry and whey protein concentrate enriched rice extrudates – Physical properties and accessibility of bioactives. *Polish Journal of Food and Nutrition Sciences*, 71(1), 29-37. <https://doi.org/10.31883/pjfn/131269>
33. Natabirwa, H., Nakimbugwe, D., Lung'aho, M., Tumwesigye, K.S., Muyonga, J.H. (2020). Bean-based nutrient-enriched puffed snacks: Formulation design, functional evaluation, and optimization. *Food Science Nutrition*, 8(9), 4763-4772. <https://doi.org/10.1002/fsn3.1727>
34. Nolan, S.J., Hambleton, I., Dwan, K. (2016). The use and reporting of the cross-over study design in clinical trials and systematic reviews: a systematic assessment. *PLoS ONE*, 11(7), art. no. e0159014. <https://doi.org/10.1371/journal.pone.0159014>
35. Palupi, E., Delina, N., Nurdin, N.M., Navratilova, H.F., Rimbawan, R., Sulaeman, A. (2023). Kidney bean substitution ameliorates the nutritional quality of extruded purple sweet potatoes: Evaluation of chemical composition, glycemic index, and antioxidant capacity. *Foods*, 12(7), art. no. 1525. <https://doi.org/10.3390/foods12071525>
36. Potter, R., Stojceska, V., Plunkett, A. (2013). The use of fruit powders in extruded snacks suitable for children's diets. *LWT – Food Science and Technology*, 51(2), 537-544. <https://doi.org/10.1016/j.lwt.2012.11.015>
37. Priebe, M.G., McMonagle, J.R. (2016). Effects of ready-to-eat-cereals on key nutritional and health outcomes: A systematic review. *PLoS ONE*, 11(10), art. no. e0164931. <https://doi.org/10.1371/journal.pone.0164931>
38. Rebello, C., Greenway, F.L., Dhurandhar, N.V. (2014). Functional foods to promote weight loss and satiety. *Current Opinion in Clinical Nutrition & Metabolic Care*, 17(6), 596-604. <https://doi.org/10.1097/MCO.0000000000000110>
39. Reynolds, A., Mann, J., Cummings, J., Winter, N., Mete, E., Te Morenga, L. (2019). Carbohydrate quality and human health: a series of systematic reviews and meta-analyses. *The Lancet*, 393(10170), 434-445. [https://doi.org/10.1016/S0140-6736\(18\)31809-9](https://doi.org/10.1016/S0140-6736(18)31809-9)
40. Reynolds, A.N., Akerman, A.P., Mann, J. (2020). Dietary fibre and whole grains in diabetes management: Systematic review and meta-analyses. *PLoS Medicine*, 17(3), art. no. e1003053. <https://doi.org/10.1371/journal.pmed.1003053>
41. Rodríguez-Mena, A., Ochoa-Martínez, L.A., González-Herrera, S.M., Rutiaga-Quiñones, O.M., González-Laredo, R.F., Olmedilla-Alonso, B. (2023). Natural pigments of plant origin: Classification, extraction and application in foods. *Food Chemistry*, 398, art. no. 133908. <https://doi.org/10.1016/j.foodchem.2022.133908>
42. Shah, F.U.H., Sharif, M.K., Bashir, S., Ahsan, F. (2019). Role of healthy extruded snacks to mitigate malnutrition. *Food Reviews International*, 35(4), 299-323. <https://doi.org/10.1080/87559129.2018.1542534>
43. Starr, K.N.P., Connelly, M.A., Orenduff, M.C., McDonald, S.R., Sloane, R., Huffman, K.M., Kraus, W.E., Bales, C.W. (2019). Impact on cardiometabolic risk of a weight loss intervention with higher protein from lean red meat: Combined results of 2 randomized controlled trials in obese middle-aged and older adults. *Journal of Clinical Lipidology*, 13(6), 920-931. <https://doi.org/10.1016/j.jacl.2019.09.012>
44. Stephen, A., Champ, M., Cloran, S., Fleith, M., Van Lieshout, L., Mejbourn, H., Burley, V. (2017). Dietary fibre in Europe: Current state of knowledge on definitions, sources, recommendations, intakes and relationships to health. *Nutrition Research Reviews*, 30(2), 149-190. <https://doi.org/10.1017/S095442241700004X>
45. Tomaszewska-Ciosk, E., Golachowski, A., Drożdż, W., Borczkowski, T., Borczkowska, H., Zdybel, E. (2012). Selected properties of single- and double-extruded potato starch. *Polish Journal of Food and Nutrition Sciences*, 62(3), 171–177. <https://doi.org/10.2478/v102222-011-0034-4>
46. Wichchukit, S., O'Mahony, M. (2014). The 9-point hedonic scale and hedonic ranking in food science: some Reappraisals and alternatives. *Journal of the Science of Food and Agriculture*, 95(11), 2167-2178. <https://doi.org/10.1002/jsfa.6993>
47. WOF, World Obesity Federation. (2023). World Obesity Atlas 2023. UK.
48. Yacu, W. (2020). Chapter 3: Extruder screw, barrel, and die assembly: General design principles and operation. In: G.M. Ganjyal (Ed.). *Extrusion Cooking*, 2nd Edition, Woodhead Publishing & Cereals & Grains Assoc. Bookstore, pp. 73-117. <https://doi.org/10.1016/B978-0-12-815360-4.00003-1>
49. Yuansah, S.C., Laga, A. (2023). Enzymatic saccharification of purple sweet potato flour by α -amylase, xylanase, mannanase and amyloglucosidase for liquid sugar production. *IOP Conference Series: Earth and Environmental Science*, 1182(1), art. no. 012044. <https://doi.org/10.1088/1755-1315/1182/1/012044>

Current Perspective About the Effect of a Ketogenic Diet on Oxidative Stress – a Review

Natalia Drabińska

Food Volatilomics and Sensomics Group, Faculty of Food Science and Nutrition, Poznan University of Life Sciences, Poznań, Poland

Oxidative stress (OS) plays a pivotal role in the development of many diseases. Therefore, many efforts have been undertaken to minimize the consequences of OS or improve antioxidant defense systems. One solution expected to improve redox homeostasis is the ketogenic diet (KD). KD is a low-carbohydrate, high-fat diet leading to a ketosis state. The shift in metabolism occurring in ketosis can affect the reactive oxygen species (ROS)-producing pathways and influence the expression of enzymes involved in redox homeostasis. Therefore, this review summarizes and discusses existing knowledge about KD and ROS homeostasis. The available tools for evaluating OS status are presented, listing their potential and drawbacks. An important aspect is the summary of the current knowledge about the effect of KD on OS conducted *in vitro*, *in vivo*, and in clinical trials. Finally, the review addresses future studies needed to understand the connection between KD and OS.

Key words: ketogenic diet, oxidative stress, antioxidant, oxidation, lipids

ABBREVIATIONS

4-HNE, 4-hydroxynonenal; 8-oxo-dG, 7,8-dihydroxy-8-oxo-2'-deoxyguanosine; AAPH, 2,2'-azobis(2-methylpropionamide) dihydrochloride; ACL, antioxidant capacity in lipids; ACW, antioxidant capacity in water; AGEs, advanced glycation end products; ALEs, advanced lipoxidation end products; AOPPs, advanced oxidation protein products; ATP, adenosine triphosphate; BMI, body mass index; CAT, catalases; CUPRAC, cupric ion reducing antioxidant capacity; DNPH, dinitrophenylhydrazine; ELISA, enzyme-linked immunosorbent assay; ERK, extracellular signal-regulated kinase; F₂-IsoPs, F₂-isoprostanes; Foxo3a, forkhead box O3; GPx, glutathione peroxidase; GR, glutathione reductase; GSH, glutathione; GSK3β, glycogen synthase 3; GSSG, glutathione disulfide; GST, glutathione transferase; HAT, hydrogen atom transfer; HDACs, histone deacetylases; HDL, high-density lipoprotein; HEK293, human embryonic kidney 293; KD, ketogenic diet; LGIT, low glycemic index treatment; MAD, modified Atkins

diet; MCT, medium-chain triglycerides; MCTKD, medium-chain triglycerides-based KD; MDA, malonaldehyde; MPO, myeloperoxidase; Mt2, metallothionein-2; NAD⁺, nicotinamide adenine dinucleotide; NADPH, nicotinamide adenine dinucleotide phosphate; NEAC, nonenzymatic antioxidant capacity; NOX, NADPH oxidases; NQO1, quinone oxidoreductase; Nrf2, NF E2-related factor 2; ORAC, oxygen radical absorbance capacity; OS, oxidative stress; oxLDL, oxidized low-density lipoprotein; PCL, photochemiluminescence; PUFAs, polyunsaturated fatty acids; RNS, reactive nitrogen species; ROS, reactive oxygen species; SCOT, succinyl-CoA: 3-ketoacid CoA-transferase; SET, single electron transfer; SOD, superoxide dismutase; TAC, total antioxidant capacity; TBA, thiobarbituric acid; TBARS, thiobarbituric acid-reactive substances; TRAP, total radical-trapping antioxidant parameter; UCP, uncoupling protein; VLCKD, very low-caloric ketogenic diet; VOCs, volatile organic compounds; XDH, xanthine dehydrogenase; XO, xanthine oxidase.

*Corresponding Author:

e-mail: natalia.drabinska@up.poznan.pl (N. Drabińska)

Submitted: 18 January 2024

Accepted: 22 February 2024

Published on-line: 7 March 2024



© Copyright by Institute of Animal Reproduction and Food Research of the Polish Academy of Sciences
 © 2024 Author(s). This is an open access article licensed under the Creative Commons Attribution-NonCommercial-NoDerivs License (<http://creativecommons.org/licenses/by-nc-nd/4.0/>).

INTRODUCTION

The interest in the impact of diet on human health has surged over the last few years. Consumers are increasingly mindful of their food choices, seeking ways to enhance their health through the selection of appropriate food products. Furthermore, individuals are paying greater attention to the physiological effects and endeavouring to comprehend the intricate biochemical processes. Consequently, the food industry and numerous scientific groups have developed a growing array of functional foods, novel foods, and bioactive compound-enriched foodstuffs [Moolwong *et al.*, 2023; Nguyen *et al.*, 2023; Ta *et al.*, 2023; Wiczorek *et al.*, 2022]. Additionally, there is a rise in the development of new diets and diversification of applied dietary plans. Various diets have been applied and proposed for weight management [Johnston *et al.*, 2014], of these the ketogenic diet (KD) is currently gaining in popularity [Drabińska *et al.*, 2021].

The increase in the prevalence of noncommunicable diseases observed in recent years can be considered a consequence of a rapid rise in obesity prevalence [WHO, 2016, 2023]. One of the factors contributing to the development of obesity-related consequences is oxidative stress (OS). It can be attributed to cellular damage caused by reactive oxygen species (ROS) combined with the underproduction of antioxidant mechanisms. Moreover, disturbances in redox metabolism can lead to the development of immunological diseases and cancer [Nathan & Cunningham-Bussel, 2013]. Consequently, the significance of OS in the pathogenesis of diseases is garnering attention, focusing on understanding ongoing mechanisms and eventually targeting OS in applied therapies in the future [Nathan & Cunningham-Bussel, 2013].

This review summarizes and discusses existing knowledge about KD and ROS homeostasis. Additionally, it presents the available tools for evaluating OS status, listing their potential and drawbacks. Finally, the review addresses future studies needed to understand the connection between KD and OS.

KETOGENIC DIET

KD is a dietetic regime entailing a high consumption of fat with a low intake of carbohydrates, leading to the ketosis state. It is a diet consisting of various fat sources, such as plant-based oils, nuts, avocado, meat, cheeses, high-fat dairy products and simultaneously limiting carbohydrate sources, such as bakery goods, potatoes and grains. Compared to other low-carbohydrate diets, KD is distinguished by the shift of metabolism into ketosis. The ketosis state is a physiological process, where the concentration of ketone bodies (β -hydroxybutyrate, acetoacetic acid and acetone) in the bloodstream exceeds 0.5 mmol/L with a normal level of glucose and insulin [Paoli, 2014]. In the case of glucose scarcity, ketone bodies are used as a source of energy. From a biochemical point of view, KD mimics the starvation or fasting state, during which the body shifts from glucose as a main source of energy to ketone body utilization and enhanced gluconeogenesis and ketogenesis.

Originally, KD was developed to treat medically intractable epilepsy due to its neuroprotective properties [Ułamek-Kozioł *et*

al., 2019]. The mechanisms of the neuroprotective effects of KD remain unclear; however, a potential mechanism is related to the normalization of energy dysregulation. KD has been found not only to reduce the frequency of seizures in patients with epilepsy [Keene, 2006] but also may help with Alzheimer's disease [Ota *et al.*, 2019], improve motor functions and cognitive functions in Parkinson's disease [Phillips *et al.*, 2018], and support other neurodegenerative diseases [Zhao *et al.*, 2006]. Recently, the interest in the applications of KD is wider. Reported health benefits being the consequences of KD include the normalization of glycaemia and insulin sensitivity, mitigating the severity of type 2 diabetes, fast reduction of body weight in the first stage of KD, improved autophagy and many others [Liśkiewicz *et al.*, 2021]. However, to observe the beneficial effects of KD, the adaptation step is required. The adaptation to ketosis usually takes 4–6 weeks and is often characterized by unpleasant symptoms, including headache, lack of energy, irritability, dizziness, constipation, and muscle cramps [Bostock *et al.*, 2020; Harvey *et al.*, 2018]. Since many of these side effects are similar to flu, the common name used by the general public is “keto flu”. These symptoms result from the loss of electrolytes with urine due to lower levels of insulin responsible for the reuptake of mainly sodium and potassium, the dehydration which is typical of all high-fat diets, and the lack of glucose to provide energy when the body still has not shifted into the utilization of ketone bodies [Harvey *et al.*, 2018]. Usually, the symptoms pass after reaching nutritional ketosis and can be reduced by a higher intake of water, medium-chain triglycerides (MCT), and electrolytes. The body needs to prepare for the increased level of ketone bodies, which can enter the non-hepatic cells *via* monocarboxylic transporters, and it is suggested that the expression of monocarboxylate transporters increases after 4–6 weeks of ketosis [Barry *et al.*, 2018].

It is also worth mentioning that KD is not a suitable diet for everyone as it may be harmful to individuals with liver and kidney diseases, type 1 diabetes, and cardiovascular diseases, although these risks are not sufficiently scientifically proven [Watanabe *et al.*, 2020]. Moreover, it is suggested that since it is a diet limiting the consumption of many food products, long-term adherence to KD may lead to nutritional deficiencies and consequences like anaemia and osteoporosis [Crosby *et al.*, 2021]. Therefore, the appropriate optimization of KD, securing the intake of a sufficient amount of fibre, vitamins, and elements is required.

KD extends into various types, which makes it difficult to compare the existing results. Depending on the fat intake or calorie intake, and consequently the ketosis state, a few types of KD can be distinguished, including classical KD, Atkins diet, modified Atkins diet (MAD), MCT-based KD (MCTKD), low glycemic index treatment (LGIT), and very low-caloric KD (VLCKD) [Barzegar *et al.*, 2021; Moreno *et al.*, 2016]. The most restrictive is the classical KD, where the weight ratio of fat to carbohydrates and proteins together is 4:1, which consists of approx. 90% of fat intake. This diet is used only for the treatment of non-responsive epilepsy and is characterized by low palatability. The Atkins diet was the first approach to apply KD for obesity management. It consists of four phases: (1) induction with limit of 20 g

of carbohydrates daily; (2) increase of carbohydrate intake to 25–50 g daily; (3) the consumption of carbohydrates reaches 80 g *per day* and is followed until the desirable bodyweight is obtained, and (4) up to 100 g of carbohydrates is allowed and is followed to maintain the weight reduction. Notably, only the first one is actually ketogenic. In later steps, the carbohydrate intake is increased preventing ketosis from being maintained. The MAD is a more palatable version of KD. In this diet, only the first phase of the Atkins diet is maintained for the whole time, making this diet more palatable and maintaining the neuroprotective properties of the KD. The application of MCT allows for the further reduction of fat intake without compromising the ketosis state. MCT is the most efficient in ketone body formation and a more accessible form of energy for non-hepatic cells among the fat sources. LGIT is characterized by the lowest proportion of fat (approx. 60–65%) and the consumption of products only with low glycemic index. Finally, VLCKD is a dietetic regime providing only 500–700 kcal daily and is usually applied before bariatric surgery in clinical conditions [Pilone *et al.*, 2018].

The wide array of KD types makes it difficult to clearly conclude the physiological effects of its administration. Importantly, not every study referring to KD measured the state of ketosis,

and probably in some studies KD was not actually applied. According to Zilberter & Zilberter [2018], the “ketogenic ratio” they had developed can be calculated to ensure that the diet is actually ketogenic. The authors evaluated 62 clinical trials which reported following the KD, and only 25 had an acceptable ketogenic ratio. Therefore, the lack of the ketosis measurement and insufficient ketogenic ratio may lead to incorrect conclusions from the studies with reported KD.

OXIDATIVE STRESS

Reactive oxygen species (ROS) are highly reactive molecules generated as a by-product of metabolism, which are involved in cell signalling, redox homeostasis and the host defense system. ROS family includes superoxide, hydrogen peroxide, singlet oxygen, organic peroxides, hypohalous acids and ozone (Table 1). Apart from ROS, also other molecules, such as nitrogen species (nitric oxide and nitroxyl anion), hydrogen sulfide and its anion, and carbon monoxide, can be considered as reactive signalling molecules [Nathan & Cunningham-Bussell, 2013]. The sources of ROS can be exogenous (air pollution, γ -irradiation, drugs) or endogenous, such as mitochondrial respiratory chain, nicotinamide adenine dinucleotide phosphate (NADPH) oxidases,

Table 1. Reactive species.

| Reactive oxygen species | | Other reactive species | |
|---------------------------------------------|------------------------------------------------|------------------------------------------------|--------------------------------------------|
| Free radicals | Nonradicals | Free radicals | Nonradicals |
| Superoxide anion radical ($O_2^{\cdot-}$) | Hydrogen peroxide (H_2O_2) | Atomic chlorine (Cl \cdot) | Hypohalous acids |
| Hydroxyl radical (OH \cdot) | Organic hydroperoxide (ROOH) | Atomic bromine (Br \cdot) | Hypochlorite (OCl $^-$) |
| Peroxyl radical (ROO \cdot) | Singlet molecular oxygen [$O_2(^1\Delta_g)$] | Nitric oxide = nitrogen monoxide (NO \cdot) | Chloramines (RNHCl) |
| Alkoxy radical (RO \cdot) | Electronically excited carbonyls (RCO) | Nitrogen dioxide (NO $_2^{\cdot}$) | Hypobromite (OBr $^-$) |
| | Ozone (O_3) | Thiyl radical (RS \cdot) | Nitrite (NO $_2^-$) |
| | | | Nitroxyl anion (NO $^-$) |
| | | | Peroxynitrite (ONOO $^-$) |
| | | | Peroxynitrate (O_2NOO^-) |
| | | | Nitrosoperoxycarbonate (ONOOCO $_2$) |
| | | | Thiol (RSH), thiolate (RS $^-$) |
| | | | Disulfide (RSSR) |
| | | | Sulfenate (RSO $^-$) |
| | | | Sulfinate (RSO $_2^-$) |
| | | | Sulfonate (RSO $_3^-$) |
| | | | Hydrogen sulfide (H_2S) |
| | | | Polysulfide (H_2S_x), $x \geq 2$ |
| | | | Acetaldehyde |
| | | | Acrolein |
| | | | Methylglyoxal |
| | | | 4-Hydroxy-nonenal |
| | | | Electronically excited (triplet) carbonyls |
| | | | Selenite |
| | | | Selenate |
| | | | Selenocysteine |
| | | | Selenomethionine |

lipoygenases, cyclooxygenases, cytochrome P450 enzymes, metal storage proteins and many others.

Oxidative stress (OS) is a state when the production of ROS is higher than their catabolism [Nathan & Cunningham-Bussel, 2013]. When the ROS concentration is too high, the OS is induced, leading to the development of pathological states [Qu *et al.*, 2021]. The catabolism of ROS is conducted mainly *via* enzymatic reactions with superoxide dismutases (SOD), catalases (CAT), enzymes of the glutathione redox cycle, thioredoxin reductases, peroxiredoxins and methionine sulfoxide reductases [Nathan & Cunningham-Bussel, 2013]. Moreover, non-enzymatic reactions with ascorbate, pyruvate, α -ketoglutarate, and oxaloacetate can lead to ROS depletion. The body homeostasis is maintained despite the ROS production, and many injuries caused by ROS can be reversed. On the other hand, some oxidative damages, such as carbonylation on the amino acid side of the protein, cannot be reversed and require cell degradation. It is considered that the biological importance of redox processes is equal to phosphorylation-dephosphorylation reactions [Sies *et al.*, 2017].

OS is an important factor in many diseases; however, it remains unclear whether redox imbalance is a cause or the consequence of disease states [Sies *et al.*, 2017]. In obesity, the malfunction of adipose tissue with exceeded energy intake over the energy expenditure triggers metabolic stress, which leads to increased inflammatory responses, which then results in the interrelated complications including glucose intolerance, hypertension, insulin resistance, dyslipidemia, liver diseases, stroke and cancer. OS is linked to impaired insulin signalling. Increased ROS levels can interfere with insulin receptor signalling, promoting insulin resistance in target tissues, such as muscle and adipose tissue. This can lead to reduced glucose uptake by cells and, consequently, glucose intolerance. Moreover, ROS can cause endothelial dysfunction, reducing the bioavailability of nitric oxide. This leads to impaired blood vessel dilation and increased vascular resistance [Ho *et al.*, 2013]. Finally, chronic inflammation and OS can damage DNA, leading to mutations and promoting carcinogenesis [Alhamzah *et al.*, 2023]. OS contributes to a cascade of events that can lead to serious health consequences. Therefore, managing OS is a potential strategy for preventing or mitigating these complications.

OS has been repeatedly suggested to be involved in the progression of neurodegenerative diseases, such as Alzheimer's disease, Parkinson's disease and amyotrophic lateral sclerosis. A significant oxidation of lipids, proteins, and DNA is typical of these diseases [Bedard & Krause, 2007]. Such damages have the potential to induce cell death through various mechanisms, either by inhibiting crucial processes or by upregulating toxic cascades.

METHODS OF OXIDATIVE STRESS EVALUATION

The importance of OS in the development of various pathological states in the human body has raised the need for methods allowing the evaluation of its level. The methods aim to assess the biological redox status, the health-beneficial effects of dietary antioxidants, and the progression and risk of disease

developments. Since OS is a process involving many metabolic pathways, there is no single marker enabling its level assessment. Therefore, a combination of different markers is analyzed to provide the most comprehensive view of OS. Despite the numerous markers proposed over the last decades, there is a lack of consensus regarding their efficacy, standardization, validation, and reproducibility [Marrocco *et al.*, 2017]. The choice of specific markers should depend on the experimental design, type of samples and the available analytical techniques. Markers with the clinical significance are mainly measured in the blood samples and urine [Jørs *et al.*, 2020], but can also be measured in saliva or exhaled breath [Bartoli *et al.*, 2011; Pelclova *et al.*, 2018]. This section further presents the most commonly used non-invasive markers for clinical trials and discusses their potentials and limitations.

■ Markers of reactive oxygen species-induced modifications

Long-term exposure to high levels of ROS can lead to structural modifications of cellular compartments, including lipids, proteins, and nucleic acids. This can result in the systemic or tissue-specific formation of by-products, alteration of protein functions, and changes in gene expressions. Based on this, specific markers related to ROS-induced modifications can be defined and summarized in [Figure 1](#).

■ Protein modification products

Proteins including enzymes, may be damaged by OS, leading to conformational modifications that result in a loss or impairment of enzymatic activity [Davies, 2016]. Protein modifications include chain fragmentation, site-specific amino acid modifications, proteolysis susceptibility, changes in the electric charge, and alterations in enzymatic activity. Various amino acid residues can undergo oxidative changes, such as sulfur-containing residues undergoing oxidation, aromatic and aliphatic groups undergoing hydroxylation, tyrosine residues undergoing nitration, cysteine residues undergoing nitrosylation and glutathionylation, aromatic groups and primary amino groups undergoing chlorination, and some amino acid residues being converted to carbonyl derivatives [Davies, 2016]. Moreover, oxidation can lead to the disruption of the polypeptide chain, resulting in conformational changes.

The most widely used markers of oxidative protein damage are carbonyl compounds (aldehydes and ketones) [Marrocco *et al.*, 2017]. Their formation involves the covalent modification of the side chains of specific amino acid, such as lysine, arginine, proline, and threonine. The measurement of carbonyl compounds is usually done *via* dinitrophenylhydrazine (DNPH) assay, western blotting and mass spectrometry [Kehm *et al.*, 2021].

Another marker of OS is 3-nitrotyrosine, which is the main product of nitration of tyrosine residues in the protein in the presence of reactive nitrogen species (RNS), such as peroxynitrite [Kehm *et al.*, 2021]. During this process, a nitro ($-\text{NO}_2$) group is substituted to the phenolic ring of tyrosine. The presence of 3-nitrotyrosine can be detected using techniques such as immunoblotting or mass spectrometry.

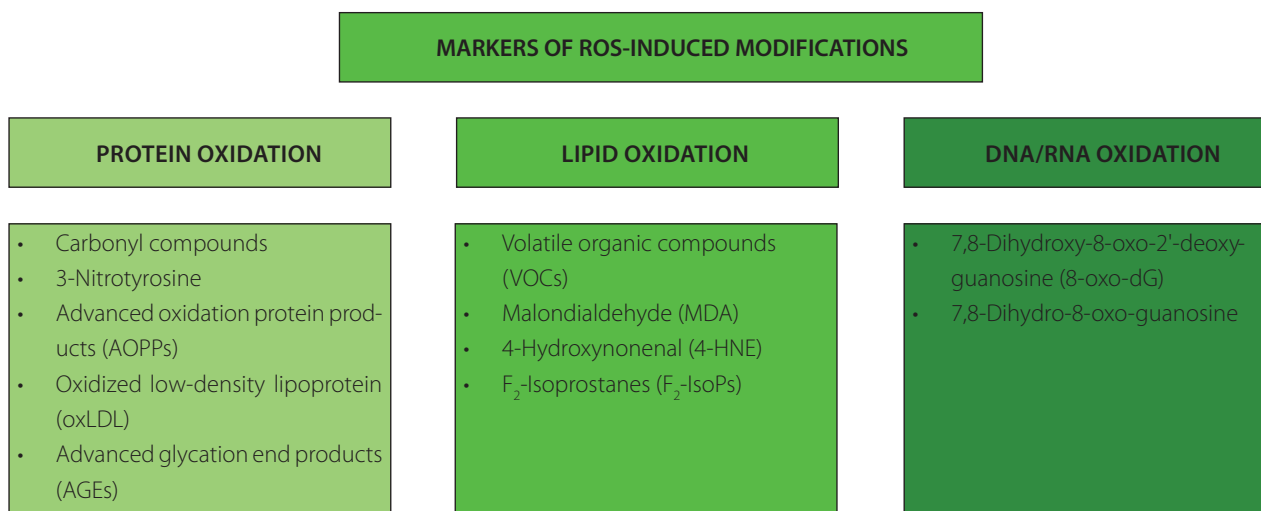


Figure 1. The most commonly used markers of oxidative stress representing reactive oxygen species (ROS)-induced modifications.

The reaction of proteins with chlorinated oxidants can lead to the formation of advanced oxidation protein products (AOPPs), with 3-chloro-tyrosine and 3,5-dichloro-tyrosine as the main examples [Marrocco *et al.*, 2017]. Elevated levels of AOPPs have been detected in the inflammatory diseases, diabetes, and the kidney failure [Cristani *et al.*, 2016; Taylor *et al.*, 2015]. The level of AOPPs is usually measured using the colorimetric techniques.

Oxidized low-density lipoprotein (oxLDL) has also been proposed as a marker of OS and cardiovascular diseases. Nonetheless, employing oxLDL as a biomarker for OS has faced criticism due to the varied nature of oxidation products, the limited specificity of antibodies, and the divergent outcomes observed depending on the deployed assay [Frijhoff *et al.*, 2015; Marrocco *et al.*, 2017]. Moreover, the most commonly used assays to measure oxLDL, detect also the native LDL; therefore, serious doubts have been raised regarding the efficacy of oxLDL as an indicator of OS and its clinical relevance in predicting cardiovascular and related diseases beyond that offered by LDL cholesterol alone.

The formation of advanced glycation end products (AGEs) is often associated with OS and is enhanced by the ROS. Therefore, although it is not a direct marker of OS, it is commonly measured to establish hyperglycemic, hyperlipidemic and OS conditions [Frijhoff *et al.*, 2015]. AGEs are a group of heterogeneous compounds formed upon a non-enzymatic reaction between reducing sugars and amino groups of proteins, lipids, or nucleic acids, called Maillard reaction. This process occurs both endogenously (due to aging) and exogenously (AGEs delivered from diet). Accumulation of AGEs can lead to the cross-linking of proteins, modifying their structure and function. This can affect the normal physiological functions of proteins and contribute to aging-related complications. AGEs can be measured using the immunoassays, fluorescence spectroscopy and western blotting [Kehm *et al.*, 2021]. Since AGEs are a very heterogeneous group of compounds, individual AGEs, like pentosidine and N^ε-(carboxymethyl)lysine can be measured using liquid and gas chromatography coupled to mass spectroscopy [Frijhoff *et al.*, 2015].

■ Lipid oxidation products

Products of lipid oxidation have been widely used for the assessment of OS because polyunsaturated fatty acids (PUFAs) are very prone to oxidation in the presence of ROS due to their double bonds. The biochemical pathways of single PUFA oxidation can result in the formation of over 100 different volatile and semi-volatile compounds, which can be classified into alkanes, alkenes, aldehydes and their derivatives, carboxylic acids, esters, furans and epoxides, as presented in a mechanistic study of Ratcliffe *et al.* [2020]. This study can open the possibility of finding new biomarkers of OS using the analysis of volatile organic compounds (VOCs).

Aldehydes originating from lipids exhibit high reactivity, leading them to readily engage with proteins to create Michael adducts, commonly referred to as advanced lipoxidation end products (ALEs) [Frijhoff *et al.*, 2015]. To date, the most commonly analyzed lipid peroxidation products include malonaldehyde (MDA) and 4-hydroxynonenal (4-HNE). Both these markers can be measured using enzyme-linked immunosorbent assay (ELISA) kits as well as deploying the chromatographic methods [Ligor *et al.*, 2015; Zhang *et al.*, 2019]. MDA, alkenals, and alkadienals collectively form the group known as thiobarbituric acid-reactive substances (TBARS). These substances can undergo a reaction with two equivalents of thiobarbituric acid (TBA), resulting in the formation of a pink adduct complex. This complex can be conveniently measured using colorimetric or fluorometric assays [Marrocco *et al.*, 2017]. However, due to its low specificity, this method received a lot of criticism [Frijhoff *et al.*, 2015].

The interaction of PUFAs in membrane phospholipids with free ROS results in the formation of F₂-isoprostanes (F₂-IsoPs), which are chemically stable prostaglandin-like isomers. Initially generated within lipid membranes as a consequence of OS, F₂-IsoPs are subsequently released in free form through phospholipase action. Notably, their measurement is not influenced by dietary lipid content [Marrocco *et al.*, 2017]. These molecules serve as dependable markers for evaluating *in vivo* OS status [Dreiβigacker *et al.*, 2010; Il'yasova *et al.*, 2004]. Analyzing F₂-IsoPs

in biological fluids and exhaled breath condensate provides an estimation of total body production, while examining F₂-IsoPs esterified in specific tissues offers insights into the localization and quantification of OS in those areas. It is crucial to consider that measurements of both MDA and 15(S)-8-*iso*-prostaglandin F_{2α} by gas chromatography-mass spectrometry in plasma samples may be notably compromised in the presence of hemolysis [Dreißigacker *et al.*, 2010]. As mentioned before, F₂-IsoPs can be measured using chromatographic methods as well as commercially available immunoenzymatic tests.

■ Nucleic acid modification products

ROS and RNS are the main sources of induced DNA damages. This process results in various DNA modifications, including nucleotide oxidation, strand breakage, loss of bases, and the formation of adducts [Dizdaroglu *et al.*, 2002]. The hydroxyl radical (HO•) is capable of reacting with all purine and pyrimidine bases, as well as the deoxyribose backbone, yielding diverse products, the major of which being 7,8-dihydroxy-8-oxo-2'-deoxyguanosine (8-oxo-dG) [Marrocco *et al.*, 2017]. As for RNA damage, the resulting 7,8-dihydro-8-oxo-guanosine is considered a marker of OS, associated with diabetes and neurodegenerative diseases [Broedbaek *et al.*, 2011; Jorgensen *et al.*, 2013]. The markers of nucleic acid oxidation can be measured both in bloodstream and in urine using chromatographic and immunoenzymatic methods [Marrocco *et al.*, 2017].

■ Markers of reactive oxygen species generation

Certain enzymes that produce ROS, usually found intracellularly, can also be detected in the bloodstream, regardless of the mechanism behind their release. Among these enzymes, xanthine oxidase (XO), myeloperoxidase (MPO) and NADPH oxidases (NOX) stand out (Figure 2). Elevated circulating levels of ROS-generating enzymes may potentially lead to an increased production of ROS. However, this outcome depends on various factors, including the availability of the substrate and whether the ROS generated by these enzymes surpass the antioxidant defense mechanisms [Frijhoff *et al.*, 2015]. In some instances, the formation of a metabolite or a reaction product is applied to measure the enzyme activity *in vivo*.

XO plays a role in the oxidation of xanthine to uric acid, producing ROS, specifically H₂O₂ [Nishino *et al.*, 2008], rather than previously thought superoxide anion (O₂^{•-}) [Frijhoff *et al.*, 2015]. The recognition of XO involvement in ischemia-reperfusion

injury has led to clinical trials with XO inhibitors in cardiovascular disease, prompting investigations into measuring circulating XO [Yapca *et al.*, 2013]. It is worth noting that XO inhibition not only impacts ROS production but also has additional effects, such as reducing hyperuricemia by decreasing uric acid levels, which could potentially improve cardiovascular diseases. Uric acid, while acting as an antioxidant, also exhibits proinflammatory properties through NALP3 inflammasome activation [Martinon *et al.*, 2006]. During OS, XO is converted from xanthine dehydrogenase (XDH), which then produces ROS. In physiological conditions, there is a thermodynamic equilibrium between XDH and XO [Nishino *et al.*, 2008]. XDH can transform into XO through the thiol oxidation, and the formation of a disulfide bond or proteolysis can then lock the enzyme in the XO form [Nishino *et al.*, 2008].

Another ROS-inducing enzyme is myeloperoxidase (MPO), which is a peroxide enzyme containing heme pigment, mainly expressed in neutrophils, and is the only human enzyme capable of producing hypochlorous acid (HOCl). The MPO/HOCl system plays a crucial role in the neutrophil defense system against the microorganisms [Aratani, 2018]. HOCl is generated from H₂O₂ and induces the chlorinative stress due to its high oxidative activity, reacting with lipids, proteins and DNA [Chen *et al.*, 2020]. Elevated levels of MPO are implicated in the development of various cardiovascular diseases [Aratani, 2018; Marrocco *et al.*, 2017]. To use MPO as a marker, the level of specific products of MPO/HOCl system should be measured, such as 3-chlorotyrosine [Afshinnia *et al.*, 2017].

NADPH oxidase (NOX) is a group of membrane-bound enzymes. Seven distinct NOX isoforms have been identified in humans (NOX1, NOX2, NOX3, NOX4, NOX5, DUOX1, and DUOX2) [Magnani & Mattevi, 2019]. Alongside the mitochondrial enzymes of the respiratory chain, NOXs are acknowledged as the primary contributors to cellular ROS generation. They generate superoxide (NOX1-3, NOX5) or hydrogen peroxide (NOX4, DUOX1-2) through an NADPH-dependent mechanism [Magnani & Mattevi, 2019]. Deficiency in NOX may result in immunosuppression, absence of otoconogenesis, or hypothyroidism. Conversely, elevated NOX activity is implicated in numerous pathologies, notably cardiovascular diseases and neurodegeneration [Bedard & Krause, 2007]. The measurement of NOX activity has many limitations; however, some attempts have been made to develop more reliable assays using, *i.a.*, electron paramagnetic resonance, as described by Zielonka *et al.* [2017].

■ Markers of antioxidant defense system

■ Antioxidant enzymes

Antioxidant enzymes play an important role in protecting cells from the damaging effects of ROS and OS, thereby maintaining redox homeostasis. These enzymes neutralize ROS and prevent oxidative damage to cellular components, including lipids, proteins, and nucleic acids. The main antioxidant enzymes comprise SOD, CAT, and glutathione-dependent enzymes such as glutathione peroxidase (GPx), glutathione reductase (GR) and glutathione transferase (GST) [Marrocco *et al.*, 2017].

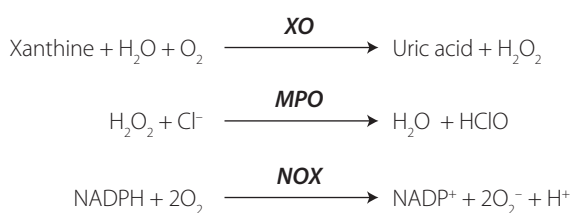


Figure 2. The simplified chemical reactions catalyzed by the reactive oxygen species (ROS)-producing enzymes. XO, xanthine oxidase; MPO, myeloperoxidase; NOX, NADPH oxidases.

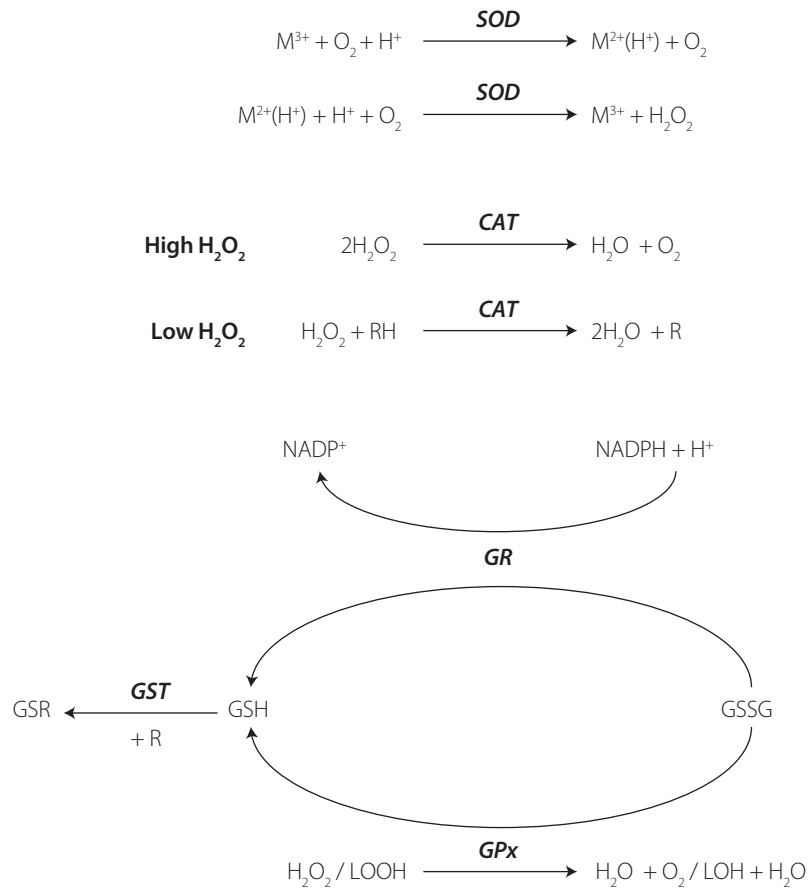


Figure 3. The simplified chemical reactions catalyzed by the antioxidant enzymes. SOD, superoxide dismutase; CAT, catalase; GR, glutathione reductase; GPx, glutathione peroxidase; GST, glutathione transferase; GSH, reduced glutathione; GSSG, oxidized glutathione; GSR, conjugate of GSH with electrophiles; R, electrophile.

SODs constitute a family of enzymes catalyzing the dismutation of O_2 into oxygen and hydrogen peroxide, subsequently processed by other enzymes like catalases. Regarded as the most potent antioxidant enzyme, SOD exhibits a high catalytic rate and high resistance to physico-chemical stress [Bafana *et al.*, 2011]. SODs can be categorized into four distinct groups based on the metal cofactors found in their active sites: copper-zinc-SOD (Cu,Zn-SOD), iron SOD (Fe-SOD), manganese SOD (Mn-SOD), and nickel SOD [Bafana *et al.*, 2011]. These various forms of SODs can be found in different organisms across biological kingdoms and reside in different subcellular compartments. The metallic cofactor plays a crucial role in SOD activity, as depicted in **Figure 3**. SOD activity can be evaluated by analyzing the inhibition of the reduction rate of a tetrazolium salt through the O_2 generated by a xanthine/XO enzymatic system, pyrogallol autoxidation, and the commercially available ELISA assays [Karim *et al.*, 2018; Marrocco *et al.*, 2017].

CAT is an enzyme that converts hydrogen peroxide into water and oxygen, playing a crucial role in reducing hydrogen peroxide generated by SOD and other metabolic processes in peroxisomes, and that exhibits different effects based on hydrogen peroxide concentrations [Sepasi Tehrani & Moosavi-Movahedi, 2018]. At high levels, CAT converts two molecules of hydrogen peroxide in a single reaction due to its catalytic activity. At lower concentrations, it demonstrates peroxidatic

activity, oxidizing hydrogen donors, such as alcohols, heavy metals, and hormones (**Figure 3**). Its activity can be measured using spectrophotometric assays [Bártíková *et al.*, 2017; Karim *et al.*, 2018; Marrocco *et al.*, 2017; Papierska *et al.*, 2022].

Glutathione serves as the primary redox agent in the majority of aerobic organisms, existing in reduced (GSH) and oxidized (glutathione disulfide, GSSG) states. The ratio between GSH and GSSG is commonly used to measure the cellular OS using commercial assays and high-performance liquid chromatography [Chatuphonprasert *et al.*, 2019]. GPx oxidizes GSH to GSSG during reduction of H_2O_2 or organic hydroperoxides to water and alcohols. Subsequently, GSSG is reduced to GSH via reaction of GR, utilizing the reducing power of NADPH [Deponet, 2013]. Functioning as an intracellular antioxidant, glutathione interacts with electrophiles (R) forming GSR compounds through the enzymatic action of GST. A simplified pathway of glutathione metabolism is presented in **Figure 3**. The activity of glutathione-dependent enzymes can be measured using the fixed-time assay measuring H_2O_2 consumption and the continuous monitoring of GSSG formation [Marrocco *et al.*, 2017].

■ Nonenzymatic antioxidant capacity

Apart from enzymes, there are various nonenzymatic compounds possessing antioxidant capacity, including endogenous substances (uric acid, thiols, bilirubin) and exogenous

compounds derived from the diet, such as polyphenols, ascorbic acid, tocopherols and others [Marrocco *et al.*, 2017]. Various methods can be deployed to measure antioxidant capacity, expressed as moles of oxidants neutralized *per* litre of body fluid. Detailed information about assays used to measure nonenzymatic antioxidant capacity (NEAC), also known as total antioxidant capacity (TAC), can be found elsewhere [Ialongo, 2017; Pellegrini *et al.*, 2020]. Therefore, only selected, commonly used methods will be described below. Two types of methods can be distinguished based on the possible reactions: (1) hydrogen atom transfer (HAT), where the quenching capacity of free radicals by hydrogen donation is measured, and (2) single electron transfer (SET), where the reducing capacity toward any molecule by electron donation is measured. The chemical reaction and examples of each method are presented in **Figure 4**.

Oxygen radical absorbance capacity (ORAC) is a method that measures the oxidative degradation of a fluorescent molecule (either β -phycoerythrin or fluorescein) in a mixture containing free radical generators, such as azo-initiator compounds. The ORAC assay can only measure substances capable of trapping peroxy-radicals [Fraga *et al.*, 2014]. It has been commonly used to analyze TAC in biological fluids [Człapka-Matyasik & Ast, 2014], and to measure the antioxidant potential of food products [Chitisankul *et al.*, 2022].

Another assay is the total radical-trapping antioxidant parameter (TRAP), conducted in aqueous solutions using 2,2'-azobis(2-methylpropionamide) dihydrochloride (AAPH) as a thermolabile stoichiometric and water-soluble azoradical generator. This method has been successfully applied to measure the antioxidant capacity in the plasma collected from patients with atherosclerosis and hepatitis [Niculescu *et al.*, 2001; Ozenirler *et al.*, 2011].

Cupric ion reducing antioxidant capacity (CUPRAC) was proposed in 2004 as a method developed to measure the antioxidant capacity of vitamin C and E, and polyphenols [Apak *et al.*, 2004]. The method involves mixing the analyzed sample with a copper(II) chloride solution, a neocuproine alcoholic solution,

and an ammonium acetate aqueous buffer at pH 7, followed by measuring absorbance at 450 nm after 30 min. This method has been applied to measure TAC in serum samples [Apak *et al.*, 2010] and is commonly used for the measurement of TAC in food products [Karadag *et al.*, 2020].

The photochemiluminescence (PCL) assay involves the synergistic combination of photochemically generated free radicals with sensitive detection through chemiluminescence [Pegg *et al.*, 2007]. It relies on the photo-induced autoxidation inhibition of luminol by antioxidants, mediated by the radical anion superoxide. This method is suitable for assessing the radical scavenging properties of individual antioxidants and more complex systems in the nanomolar range. Luminol serves as both a photosensitizer and an oxygen radical detection reagent. The PCL assay is performed separately for antioxidant capacity in water (ACW) and in lipids (ACL). ACW represents the TAC of water-soluble compounds, such as flavonoids and vitamin C, while ACL measures the activity of lipid-soluble compounds, including tocopherols and carotenoids. The PCL assay has been used to measure the TAC in biological fluids after strawberry consumption in animal study [Žary-Sikorska *et al.*, 2021] and to determine the TAC of fortified gluten-free products [Drabińska *et al.*, 2018; Krupa-Kozak *et al.*, 2021].

EFFECT OF KETOGENIC DIET ON THE OXIDATIVE STRESS

Mitochondria play a key role in determining cellular energy production through oxidative phosphorylation. In this process, the electron transport chain activity contributes to the synthesis of cellular adenosine triphosphate (ATP). Electrons traverse these complexes, establishing a transmembrane proton gradient linked to ATP synthesis through ATP synthase. In many advanced malignancies, there is an upregulation of glycolysis and glucose uptake, with a notable diversion of the glycolytic end product (pyruvate) away from the mitochondrial tricarboxylic acid cycle. Instead of entering the cycle, pyruvate is preferentially reduced to form lactate, concurrently generating nicotinamide adenine

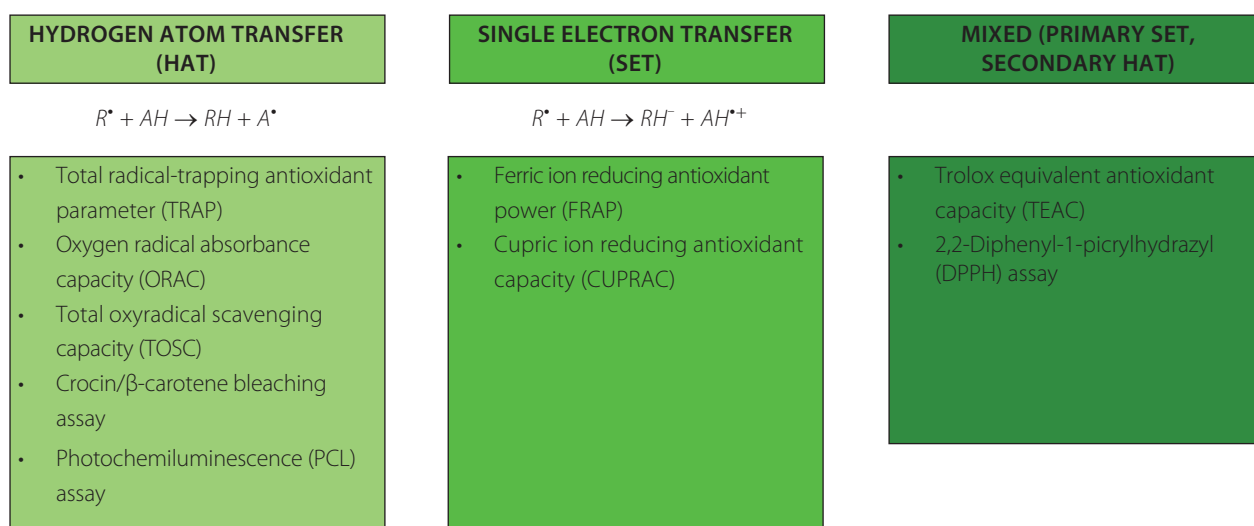


Figure 4. Classification of the methods used for the measurement of total antioxidant capacity (TAC) [Ialongo, 2017; Pegg *et al.*, 2007].

dinucleotide (NAD⁺). This metabolic adaptation allows glycolysis to persist even in the presence of normal oxygen levels (normoxia). Contrary, KD has been found to reduce the production of ROS by suppressing glycolysis [Milder & Patel, 2012]. For example, cancer cells, unlike healthy cells, exhibit elevated glucose metabolism and alterations in mitochondrial oxidative metabolism, believed to result from persistent metabolic OS [Alhamzah *et al.*, 2023]. It is theorized that the increased level of ROS is the primary reason for mitochondrial susceptibility to mutations. Ketone bodies are exclusively metabolized in the mitochondria; therefore, cells with damaged mitochondria, like cancer cells, are unable to utilize them to produce energy [Poff *et al.*, 2013]. Succinyl-CoA: 3-ketoacid CoA-transferase (SCOT) is not produced by cancer cells, preventing ketone body metabolism and potentially leading to cancer cell death [Sawai *et al.*, 2004]. Consequently, the inhibitory effect of KD on OS has spurred special interest in auxiliary cancer therapies [Alhamzah *et al.*, 2023]. This section presents a summary of findings obtained through *in vitro*, *in vivo* and clinical trials aimed to assess the effect of KD on OS and mitochondrial functions.

■ **In vitro studies**

In countering OS, β -hydroxybutyrate serves as a natural inhibitor of class I and class IIa histone deacetylases (HDACs) [Shimazu *et al.*, 2013]. To confirm that, human embryonic kidney 293 (HEK293) cells were incubated with varying levels of β -hydroxybutyrate for 8 h. The findings from this study revealed that inhibiting HDACs facilitates the transcription of detoxifying genes, including CAT, mitochondrial SOD, and metallothionein, providing protection against OS. Moreover, HDAC inhibition was associated with comprehensive alterations in transcription, involving genes responsible for oxidative stress resistance factors, such as *FOXO3A* and *MT2*. The exposure of cells to β -hydroxybutyrate led to enhanced histone acetylation at the promoters of forkhead box O3 (*Foxo3a*) and metallothionein-2 (*Mt2*), and the activation of both genes occurred with the selective depletion of HDAC1 and HDAC2. In line with heightened *FOXO3A* and *MT2* activity, mice treated with β -hydroxybutyrate exhibited significant protection against OS [Shimazu *et al.*, 2013].

Another cell line, *i.e.*, HT-22 cells of the hippocampus, was exposed to varying doses of β -hydroxybutyric acid to investigate its neurotropic effects, OS markers, mitochondrial function, and apoptosis [Majrashi *et al.*, 2021]. At a moderate dose (250 μ M), β -hydroxybutyric acid exhibited a substantial increase in the viability of hippocampal neurons. Moreover, β -hydroxybutyric acid demonstrated antioxidant effects by reducing prooxidant markers of OS, including ROS and nitrite content, while elevating glutathione content, resulting in decreased lipid peroxidation. Additionally, the study revealed that β -hydroxybutyric acid enhanced mitochondrial functions by increasing the activities of Complex-I and Complex-IV. Moreover, it significantly reduced caspase-1 and caspase-3 activities, indicating a potential protective effect against apoptosis [Majrashi *et al.*, 2021].

In a study with cortical primary cultures obtained from Wistar rat embryos treated with a physiological and a non-physiological

isomer of β -hydroxybutyrate, both isomers demonstrated the ability to reduce ROS production. However, only the physiological ketone body stimulated ATP production [Julio-Amilpas *et al.*, 2015]. Interestingly, in a dose-dependent evaluation, 10 mmol/L of β -hydroxybutyrate was found to elicit the highest neuroprotective effects. Another ketone body, *i.e.*, acetoacetate, was addressed in a study of Board *et al.* [2017]. The authors compared the utility of acetoacetate and glucose by mesenchymal stem cells and found that acetoacetate was oxidized 35 times faster than glucose. Moreover, the production of ROS during oxidation was 45 times lower in the case of acetoacetate than glucose.

The molecular mechanism behind glucose deficiency-induced cytotoxicity and the protective role of β -hydroxybutyrate using SH-SY5Y cells was reported by Lamichhane *et al.* [2017]. Cell viability significantly decreased under glucose deficiency, accompanied by elevated ROS production and reduced phosphorylation of extracellular signal-regulated kinase (ERK) and glycogen synthase 3 (*GSK3 β*). Inhibition of ROS reversed glucose deficiency-induced cytotoxicity and restored the diminished phosphorylation of ERK and *GSK3 β* . β -Hydroxybutyrate reversed cytotoxicity, ROS production, and the decrease in phosphorylation of ERK and *GSK3 β* induced by glucose deficiency. The authors have concluded that glucose deficiency-induced cytotoxicity involves ERK inhibition through ROS production and that this process is attenuated by β -hydroxybutyrate [Lamichhane *et al.*, 2017].

The impact of the VLCKD on ROS production and cell viability was assessed *in vitro* by exposing Hep-G2 cells to sera obtained from patients with obesity following VLCKD for 8 weeks [Valenzano *et al.*, 2019]. Significant effects on body weight, adiposity, and blood chemistry parameters were observed in the participants due to the dietary intervention, with a noticeable reduction in visceral adipose tissue. The viability of Hep-G2 cells remained unaffected after 24, 48, and 72 h of incubation with patients' sera, both before and after the VLCKD. Additionally, ROS production was not significantly affected by the dietary treatment, which demonstrated that the short-term mild dietary ketosis did not exhibit cytotoxic effects and had no effect on OS [Valenzano *et al.*, 2019].

■ **In vivo studies**

A KD has been found to elevate hippocampal glutathione biosynthesis in rats, enhancing mitochondrial antioxidant capacity [Jarrett *et al.*, 2008]. This effect has been linked to the activation of NF E2-related factor 2 (*Nrf2*), a transcription factor that responds to OS by upregulating genes associated with antioxidant pathways, including those related to GSH synthesis and conjugation. Following a 3-week diet, rats on the KD exhibited *Nrf2* nuclear accumulation and enhanced activity of its target NAD(P)H: quinone oxidoreductase (*NQO1*), in the hippocampus [Milder *et al.*, 2010].

In a mouse study, mitochondrial uncoupling protein (UCP) activity was measured to check whether KD can affect the ROS production through affecting UCP [Sullivan *et al.*, 2004]. The maximum rates of mitochondrial respiration were markedly higher

in animals administered a KD compared to those on a standard diet, suggesting an augmentation of UCP-mediated proton conductance capable of reducing ROS production. Western blots revealed significant or nearly significant increases in protein levels of UCP2, UCP4, and UCP5, with elevated immunoreactivity to these three UCP isoforms, particularly observed in the dentate gyrus of KD-fed mice. Furthermore, they observed a significant reduction in oligomycin-induced ROS production in KD-fed mice, which was not observed in the control group. The authors concluded that the mechanism of reduction of ROS production is associated with the activation of mitochondrial UCPs [Sullivan *et al.*, 2004].

The combination of KD with radiation was found to reduce tumour growth in mice with lung cancer [Allen *et al.*, 2013]. Notably, tumors of animals fed with KD exhibited elevated oxidative damage, predominantly through lipid peroxidation, confirmed by the presence of 4HNE-modified proteins. Additionally, there was a reduction in proliferation, as indicated by decreased immunoreactive proliferating cell nuclear antigen. It suggests that KD may enhance the efficacy of radiotherapy in cancer treatment [Allen *et al.*, 2013].

Significant increases in hippocampal NAD⁺/NADH ratio and blood ketone bodies were detected in rats fed with KD after 2 days and remained elevated at three weeks, indicating an early and persistent metabolic shift [Elamin *et al.*, 2017]. According to the authors, an increased NAD during ketolytic metabolism may be a primary mechanism of potential health-beneficial effects of KD.

The study by Julio-Amilpas *et al.* [2015] investigated the effect of β -hydroxybutyrate on the neuronal death induced by severe non-coma hypoglycemia in rats. A reduction in ROS production was noted in distinct cortical areas and subregions of the hippocampus, which resulted in the prevention of neuronal death in the cortex. The authors have concluded that the protective effects of ketone bodies stem not only from its metabolic actions but also from its ability to diminish ROS, positioning β -hydroxybutyrate as a promising candidate for addressing ischemic and traumatic injuries.

Another study analyzed the effect of KD on the OS in rat with traumatic brain injury [Greco *et al.*, 2016]. Following injury, OS significantly increased at 6 and 24 h, and this effect was mitigated by the KD. The KD also induced the expression of antioxidant proteins, including NQO1 and SOD. The authors have concluded that KD enhance cerebral metabolism post-traumatic brain injury by providing alternative substrates and exerting antioxidant effects, thereby preventing OS-mediated mitochondrial dysfunction [Greco *et al.*, 2016]. A study with a spinal cord injury showed similar effects [Wang *et al.*, 2017]. Two-week intervention with KD or other-day fasting resulted in the 31–43% inhibition of the spinal cord HDAC activity and the enhanced expressions of acetylated histone ACh3K9 and ACh3K14 and genes associated with anti-oxidative stress, such as *Foxo3a* and *Mt2*. Consequently, the content of SOD, *Foxo3a* and CAT proteins increased. Notably, a reduction in the MDA concentration was noted, which was suggested to contribute to the neuroprotection of the spinal

cord against oxidative damage [Wang *et al.*, 2017]. The positive effect of KD on the elevated OS caused by injury was also observed in a rat model of carotid artery balloon-injury [Xu *et al.*, 2023]. The KD suppressed OS caused by the injury. This was evident in the decreased levels of ROS, MDA, and MPO activity, with simultaneous increase in the SOD activity [Xu *et al.*, 2023].

A very comprehensive study, analyzing the short- and long-term effects of KD on the multi-organ OS and mitochondria functions in rats, was reported by Kephart *et al.* [2017]. Both KD and the standard diet supplemented with exogenous ketone bodies were followed for one week and eight months. The rats on a short-term KD diet had significantly higher levels of ketones in their blood, indicating that the diet itself (not ketone bodies supplementation) caused an increase in ketones. In short-term, the rats fed with KD and exogenous ketone bodies had higher liver antioxidant capacity. In the long term, the KD-fed rats showed higher liver antioxidant capacity and higher expression of *GPx* compared to standard diet, as well as the lowest level of liver protein carbonyls. Contrary, KD negatively affected skeletal muscle mitochondrial physiology with higher production of ROS in the mitochondria of the gastrocnemius muscle [Kephart *et al.*, 2017].

A recent study evaluated the effect of KD on OS in young rats with diet-induced obesity [Drabińska *et al.*, 2022]. In this study, rats were fed with a calorie-restrictive KD or a standard diet for four weeks. At the end of experiment, there was no difference in AGEs and MDA, while an increase in SOD activity was recorded in the KD-fed rats. The observed changes were inconclusive and do not allow to definitely claim about KD effect on OS [Drabińska *et al.*, 2022]. No effect on the OS was reported in another study with rats following KD or a standard diet throughout the lifespan [Parry *et al.*, 2018]. The length of life was longer in the rats fed with KD compared to the control animals (762 vs. 624 days), and the activity of citrate synthase, representing estimated volume of mitochondria, was higher in the KD-fed rats. However, no differences were detected in various OS markers, including SOD, CAT, *GPx*, 4-HNE and carbonyls [Parry *et al.*, 2018].

The composition of low-carbohydrate diets was evaluated in a study by Kaburagi *et al.* [2019]. Diets consisting of lard vs. MCT oil were compared in non-obese mice fed *ad libitum* for 13 weeks. Increased renal weight, glomerular hypertrophy, and enlargement of intraglomerular small vessels with wall thickening were observed in both groups. In the kidney, the level of N^ε-(carboxymethyl)lysine was significantly lower in the mice fed a lard-based diet. Contrary, the concentration of N^ε-(carboxyethyl)lysine was the lowest in the MCT-fed mice [Kaburagi *et al.*, 2019]. This study underlined the importance of diet composition, not only the ratio between fat and other nutrients.

A testicular OS was a focus of interest in a recent study conducted by Üstündağ *et al.* [2023]. These authors evaluated the effects of KD and intermittent fasting, separately and together, on testicular health. In the KD-fed rats, an increase in body and testis weight was observed, along with elevated testosterone and reduced oestradiol levels. KD alone as well as combined with intermittent fasting exhibited positive effects on OS by lowering

MDA and MPO levels, while increasing glutathione, CAT, and nitric oxide in testicular tissue, suggesting that KD may have a positive effect on the male reproductive system [Üstündağ *et al.*, 2023].

■ Clinical trials

The number of clinical trials evaluating the effect of KD on OS is much lower than of *in vitro* and *in vivo* investigations. In a study with healthy women, KD was applied for 14 days to evaluate their blood redox status [Nazarewicz *et al.*, 2007]. At the end of the study, although participants had the body mass index (BMI) within a normal range, weight loss was observed; however, without the differences in the fat mass. Moreover, an increase in TAC, uric acid, and sulfhydryl content was observed, while the activity of SOD and CAT as well as MDA content remained unmodified. The authors have concluded that even a short-term intervention with KD increased the TAC without increasing OS. It is particularly interesting, since the adaptation of ketosis has not been achieved in this study and it is surprising that so vivid changes were observed in healthy subjects.

Another study was performed in a group of 18 Taekwondo players following KD for three weeks [Rhyu *et al.*, 2014]. There was no notable difference observed in body composition, ROS, and SOD levels between the individuals following KD and the control group. However, the KD group exhibited an increased high-density lipoprotein (HDL) cholesterol level, while the control group demonstrated elevated lactate dehydrogenase and MDA levels after three weeks. The authors have implied that weight loss due to three weeks of calorie restriction and exercise may induce OS and that the KD could be beneficial in preventing it [Rhyu *et al.*, 2014]. However, it has to be kept in mind that the adaptation to ketosis takes at least 4 weeks; hence, it was also not achieved in this study.

KD is applied mainly as a therapy for the drug-resistant epilepsy. A recent study evaluated the effect of three-month KD on the OS and the seizure incidence in 40 pediatric patients with epilepsy [Poorshiri *et al.*, 2023]. Out of 40, 34 children completed the study, and among them, 21 had a 50% reduction in seizure frequency after KD. The serum levels of OS parameters, including MDA and 8-oxo-dG, were significantly reduced after KD implementation. The KD appears to decrease brain OS by elevating ketosis, which was negatively correlated with OS markers. The authors have suggested that the reduction of OS can be responsible for the potential anti-seizure mechanism of KD [Poorshiri *et al.*, 2023].

The analysis of the clinical trial database (clinicaltrials.gov) indicated that there are two ongoing studies evaluating the effect of KD on OS and mitochondrial functions in subjects with obesity. In the first study, the study protocol of which can be found in my previous work [Drabińska *et al.*, 2023], the OS markers, including MDA, uric acid, SOD, F₂-IsoPs and 8-oxo-dG, will be analyzed in samples collected from 80 women following KD for 8 weeks. The second study will measure mitochondrial functions and OS in 63 participants with obesity divided into four groups: (1) KD group; (2) calorie-restricted standard diet group; (3) intermittent fasting 16/8; and (4) usual diet [U.S.

National Institutes of Health, 2023]. The intervention will be followed for one month. Taking into account that the intervention part had been completed in both studies, we can expect the results in near future.

SUMMARY AND FUTURE PERSPECTIVES

The presented review discussed the significance of redox homeostasis and its intricate metabolic pathways. Despite the growth in knowledge over the last decades, OS remains not fully understood. Numerous studies, conducted *in vitro* and on animal models, have shown the potential of the KD in alleviating the adverse effects of OS, particularly in situations where OS is elevated, such as injuries. However, the clinical effects of KD and its impact on redox homeostasis are not yet fully elucidated. More long-term studies, conducted with larger groups and sufficient sample sizes, are needed. The adaptation to ketosis, which can last from 4 to 6 weeks, should be considered when planning such studies. Appropriate adaptation to ketosis may yield different results than those observed in short-term dietary interventions. Moreover, considering the multidimensionality of redox balance, studies focused on OS should analyze multiple markers simultaneously to observe all the by-products resulting from ROS-mediated modifications. This includes also measuring the activity of enzymes involved in ROS generation and antioxidant defense, as well as assessing the antioxidant potential of the organism itself. As the metabolic effects of KD are not fully understood, it is worthwhile to analyze different enzymes and by-products generated to determine which group of compounds is most susceptible to KD interventions. Finally, both the short-term and long-term effects of KD should be evaluated, especially in cases where KD is applied for weight reduction, as it is often followed for only a short period but it may result in the consequences in future.

RESEARCH FUNDING

This study was financially supported by the National Science Centre, Poland (Project No. 2021/41/B/NZ9/01278).

CONFLICT OF INTERESTS

The author declares no conflict of interest.

ORCID ID

N. Drabińska

<https://orcid.org/0000-0001-5324-5982>

REFERENCES

1. Afshinnia, F., Zeng, L., Byun, J., Gadegbeku, C.A., Magnone, M.C., Whatling, C., Valastro, B., Kretzler, M., Pennathur, S. (2017). Myeloperoxidase levels and its product 3-chlorotyrosine predict chronic kidney disease severity and associated coronary artery disease. *American Journal of Nephrology*, 46(1), 73–81. <https://doi.org/10.1159/000477766>
2. Alhamzah, S.A., Gatar, O.M., Alruwaili, N.W. (2023). Effects of ketogenic diet on oxidative stress and cancer: A literature review. *Advances in Cancer Biology - Metastasis*, 7, art. no.100093. <https://doi.org/10.1016/j.adcanc.2023.100093>
3. Allen, B.G., Bhatia, S.K., Buatti, J.M., Brandt, K.E., Lindholm, K.E., Button, A.M., Szweida, L.I., Smith, B.J., Spitz, D.R., Fath, M.A. (2013). Ketogenic diets enhance oxidative stress and radio-chemo-therapy responses in lung cancer xenografts. *Clinical Cancer Research*, 19(14), 3905–3913. <https://doi.org/10.1158/1078-0432.CCR-12-0287>
4. Apak, R., Güçlü, K., Özyürek, M., Bektaşoğlu, B., Bener, M. (2010). Cupric ion reducing antioxidant capacity assay for antioxidants in human serum and for

- hydroxyl radical scavengers. In: D. Armstrong (Ed). *Advanced Protocols in Oxidative Stress II*, Human Press, pp. 215–239.
https://doi.org/10.1007/978-1-60761-411-1_15
5. Apak, R., Güçlü, K., Özyürek, M., Karademir, S.E. (2004). Novel total antioxidant capacity index for dietary polyphenols and vitamins C and E, using their cupric ion reducing capability in the presence of neocuproine: CUPRAC method. *Journal of Agricultural and Food Chemistry*, 52(26), 7970–7981.
<https://doi.org/10.1021/jf048741x>
 6. Aratani, Y. (2018). Myeloperoxidase: Its role for host defense, inflammation, and neutrophil function. *Archives of Biochemistry and Biophysics*, 640, 47–52.
<https://doi.org/10.1016/j.abb.2018.01.004>
 7. Bafana, A., Dutt, S., Kumar, A., Kumar, S., Ahuja, P.S. (2011). The basic and applied aspects of superoxide dismutase. *Journal of Molecular Catalysis B: Enzymatic*, 68(2), 129–138.
<https://doi.org/10.1016/j.molcatb.2010.11.007>
 8. Barry, D., Ellul, S., Watters, L., Lee, D., Haluska, R., White, R. (2018). The ketogenic diet in disease and development. *International Journal of Developmental Neuroscience*, 68(1), 53–58.
<https://doi.org/10.1016/j.ijdevneu.2018.04.005>
 9. Bártíková, H., Boušová, I., Matoušková, P., Szotáková, B., Skálová, L. (2017). Effect of green tea extract-enriched diets on insulin and leptin levels, oxidative stress parameters and antioxidant enzymes activities in obese mice. *Polish Journal of Food and Nutrition Sciences*, 67(3), 233–240.
<https://doi.org/10.1515/pjfn-2017-0004>
 10. Bartoli, M.L., Novelli, F., Costa, F., Malagrino, L., Melosini, L., Bacci, E., Cianchetti, S., Dente, F.L., Di Franco, A., Vagaggini, B., Paggiaro, P.L. (2011). Malondialdehyde in exhaled breath condensate as a marker of oxidative stress in different pulmonary diseases. *Mediators of Inflammation*, 2011, art. no. 891752.
<https://doi.org/10.1155/2011/891752>
 11. Barzegar, M., Afghani, M., Tarmahi, V., Behtari, M., Rahimi Khamaneh, S., Raeisi, S. (2021). Ketogenic diet: overview, types, and possible anti-seizure mechanisms. *Nutritional Neuroscience*, 24(4), 307–316.
<https://doi.org/10.1080/1028415X.2019.1627769>
 12. Bedard, K., Krause, K.-H. (2007). The NOX family of ROS-generating NADPH oxidases: Physiology and pathophysiology. *Physiological Reviews*, 87(1), 245–313.
<https://doi.org/10.1152/physrev.00044.2005>
 13. Board, M., Lopez, C., van den Bos, C., Callaghan, R., Clarke, K., Carr, C. (2017). Acetoacetate is a more efficient energy-yielding substrate for human mesenchymal stem cells than glucose and generates fewer reactive oxygen species. *The International Journal of Biochemistry Cell Biology*, 88, 75–83.
<https://doi.org/10.1016/j.biocel.2017.05.007>
 14. Bostock, E.C.S., Kirkby, K.C., Taylor, B.V., Hawrelak, J.A. (2020). Consumer reports of “keto flu” associated with the ketogenic diet. *Frontiers in Nutrition*, 7, art. no. 20.
<https://doi.org/10.3389/fnut.2020.00020>
 15. Broedbaek, K., Siersma, V., Henriksen, T., Weimann, A., Petersen, M., Andersen, J.T., Jimenez-Solem, E., Stovgaard, E.S., Hansen, L.J., Henriksen, J.E., Bonnema, S.J., de Fine Olivarius, N., Poulsen, H.E. (2011). Urinary markers of nucleic acid oxidation and long-term mortality of newly diagnosed type 2 diabetic patients. *Diabetes Care*, 34(12), 2594–2596.
<https://doi.org/10.2337/dc11-1620>
 16. Chatuphonprasert, W., Sriset, Y., Jarukamjorn, K. (2019). Continuous consumption of reused palm oil induced hepatic injury, depletion of glutathione stores, and modulation of cytochrome P450 profiles in mice. *Polish Journal of Food and Nutrition Sciences*, 69(1), 53–61.
<https://doi.org/10.31883/pjfn-2019-0009>
 17. Chen, S., Chen, H., Du, Q., Shen, J. (2020). Targeting myeloperoxidase (MPO) mediated oxidative stress and inflammation for reducing brain ischemia injury: Potential Application of natural compounds. *Frontiers in Physiology*, 11, art. no. 433.
<https://doi.org/10.3389/fphys.2020.00433>
 18. Chitisankul, W., Shimada, K., Tsukamoto, C. (2022). Antioxidative capacity of soyfoods and soy active compounds. *Polish Journal of Food and Nutrition Sciences*, 72(1), 101–108.
<https://doi.org/10.31883/pjfn/146562>
 19. Cristani, M., Speciale, A., Saija, A., Gangemi, S., Minciullo, P., Cimino, F. (2016). Circulating advanced oxidation protein products as oxidative stress biomarkers and progression mediators in pathological conditions related to inflammation and immune dysregulation. *Current Medicinal Chemistry*, 23(34), 3862–3882.
<https://doi.org/10.2174/0929867323666160902154748>
 20. Crosby, L., Davis, B., Joshi, S., Jardine, M., Paul, J., Neola, M., Barnard, N.D. (2021). Ketogenic diets and chronic disease: Weighing the benefits against the risks. *Frontiers in Nutrition*, 8, art. no. 702802.
<https://doi.org/10.3389/fnut.2021.702802>
 21. Czapka-Matyasik, M., Ast, K. (2014). Total antioxidant capacity and its dietary sources and seasonal variability in diets of women with different physical activity levels. *Polish Journal of Food and Nutrition Sciences*, 64(4), 267–276.
<https://doi.org/10.2478/pjfn-2013-0026>
 22. Davies, M.J. (2016). Protein oxidation and peroxidation. *Biochemical Journal*, 473(7), 805–825.
<https://doi.org/10.1042/BJ20151227>
 23. Deponte, M. (2013). Glutathione catalysis and the reaction mechanisms of glutathione-dependent enzymes. *Biochimica et Biophysica Acta (BBA) - General Subjects*, 1830(5), 3217–3266.
<https://doi.org/10.1016/j.bbagen.2012.09.018>
 24. Dizdaroglu, M., Jaruga, P., Birincioglu, M., Rodriguez, H. (2002). Free radical-induced damage to DNA: Mechanisms and measurement. *Free Radical Biology and Medicine*, 32(11), 1102–1115.
[https://doi.org/10.1016/S0891-5849\(02\)00826-2](https://doi.org/10.1016/S0891-5849(02)00826-2)
 25. Drabińska, N., Ciska, E., Szmatowicz, B., Krupa-Kozak, U. (2018). Broccoli by-products improve the nutraceutical potential of gluten-free mini sponge cakes. *Food Chemistry*, 267, 170–177.
<https://doi.org/10.1016/j.foodchem.2017.08.119>
 26. Drabińska, N., Juśkiewicz, J., Wiczowski, W. (2022). The effect of the restrictive ketogenic diet on the body composition, haematological and biochemical parameters, oxidative stress and advanced glycation end-products in young Wistar rats with diet-induced obesity. *Nutrients*, 14(22), art. no. 4805.
<https://doi.org/10.3390/nu14224805>
 27. Drabińska, N., Romaszko, J., White, P. (2023). The effect of isocaloric, energy-restrictive, KETOgenic diet on metabolism, inflammation, nutrition deficiencies and oxidative stress in women with overweight and obesity (KETO-MINOX): Study protocol. *PLoS ONE*, 18(5), art. no. e0285283.
<https://doi.org/10.1371/journal.pone.0285283>
 28. Drabińska, N., Wiczowski, W., Piskula, M. K. (2021). Recent advances in the application of a ketogenic diet for obesity management. *Trends in Food Science and Technology*, 110, 28–38.
<https://doi.org/10.1016/j.tifs.2021.01.080>
 29. Dreiβigacker, U., Suchy, M.-T., Maassen, N., Tsikas, D. (2010). Human plasma concentrations of malondialdehyde (MDA) and the F2-isoprostane 15(S)-8-iso-PGF2a may be markedly compromised by hemolysis: Evidence by GC-MS/MS and potential analytical and biological ramifications. *Clinical Biochemistry*, 43(1–2), 159–167.
<https://doi.org/10.1016/j.clinbiochem.2009.10.002>
 30. Elamin, M., Ruskin, D.N., Masino, S.A., Sacchetti, P. (2017). Ketone-based metabolic therapy: Is increased NAD+ a primary mechanism? *Frontiers in Molecular Neuroscience*, 10, art. no. 377.
<https://doi.org/10.3389/fnmol.2017.00377>
 31. Fraga, C.G., Oteiza, P.I., Galleano, M. (2014). *In vitro* measurements and interpretation of total antioxidant capacity. *Biochimica et Biophysica Acta (BBA) - General Subjects*, 1840(2), 931–934.
<https://doi.org/10.1016/j.bbagen.2013.06.030>
 32. Frijhoff, J., Winyard, P.G., Zarkovic, N., Davies, S.S., Stocker, R., Cheng, D., Knight, A.R., Taylor, E.L., Oetrich, J., Ruskovska, T., Gasparovic, A. C., Cuadrado, A., Weber, D., Poulsen, H.E., Grune, T., Schmidt, H.H.H.W., Ghezzi, P. (2015). Clinical relevance of biomarkers of oxidative stress. *Antioxidants Redox Signaling*, 23(14), 1144–1170.
<https://doi.org/10.1089/ars.2015.6317>
 33. Greco, T., Glenn, T.C., Hovda, D.A., Prins, M.L. (2016). Ketogenic diet decreases oxidative stress and improves mitochondrial respiratory complex activity. *Journal of Cerebral Blood Flow and Metabolism*, 36(9), 1603–1613.
<https://doi.org/10.1177/0271678X15610584>
 34. Harvey, C.J.d.C., Schofield, G.M., Williden, M. (2018). The use of nutritional supplements to induce ketosis and reduce symptoms associated with keto-induction: A narrative review. *PeerJ*, 6, art. no. e4488.
<https://doi.org/10.7717/peerj.4488>
 35. Ho, E., Karimi Galougahi, K., Liu, C.-C., Bhindi, R., Figtree, G.A. (2013). Biological markers of oxidative stress: Applications to cardiovascular research and practice. *Redox Biology*, 1(1), 483–491.
<https://doi.org/10.1016/j.redox.2013.07.006>
 36. Ialongo, C. (2017). Preanalytic of total antioxidant capacity assays performed in serum, plasma, urine and saliva. *Clinical Biochemistry*, 50(6), 356–363.
<https://doi.org/10.1016/j.clinbiochem.2016.11.037>
 37. Ilyasova, D., Morrow, J.D., Ivanova, A., Wagenknecht, L.E. (2004). Epidemiological marker for oxidant status: comparison of the ELISA and the gas chromatography/mass spectrometry assay for urine 2,3-dinor-5,6-dihydro-15-F2t-isoprostane. *Annals of Epidemiology*, 14(10), 793–797.
<https://doi.org/10.1016/j.jannepidem.2004.03.003>
 38. Jarrett, S.G., Milder, J.B., Liang, L., Patel, M. (2008). The ketogenic diet increases mitochondrial glutathione levels. *Journal of Neurochemistry*, 106(3), 1044–1051.
<https://doi.org/10.1111/j.1471-4159.2008.05460.x>
 39. Johnston, B.C., Kanters, S., Bandayrel, K., Wu, P., Najif, F., Siemieniuk, R.A., Ball, G.D.C., Busse, J.W., Thorlund, K., Guyatt, G., Jansen, J.P., Mills, E.J. (2014). Comparison of weight loss among named diet programs in overweight and obese adults: A meta-analysis. *JAMA*, 312(9), 923–933.
<https://doi.org/10.1001/jama.2014.10397>

40. Jorgensen, A., Broedbaek, K., Fink-Jensen, A., Knorr, U., Greisen Soendergaard, M., Henriksen, T., Weimann, A., Jepsen, P., Lykkesfeldt, J., Enghusen Poulsen, H., Balslev Jorgensen, M. (2013). Increased systemic oxidatively generated DNA and RNA damage in schizophrenia. *Psychiatry Research*, 209(3), 417–423. <https://doi.org/10.1016/j.psychres.2013.01.033>
41. Jørs, A., Lund, M.A.V., Jespersen, T., Hansen, T., Poulsen, H.E., Holm, J.-C. (2020). Urinary markers of nucleic acid oxidation increase with age, obesity and insulin resistance in Danish children and adolescents. *Free Radical Biology and Medicine*, 155, 81–86. <https://doi.org/10.1016/j.freeradbiomed.2020.05.009>
42. Julio-Amilpas, A., Montiel, T., Soto-Tinoco, E., Gerónimo-Olvera, C., Massieu, L. (2015). Protection of hypoglycemia-induced neuronal death by β -hydroxybutyrate involves the preservation of energy levels and decreased production of reactive oxygen species. *Journal of Cerebral Blood Flow Metabolism*, 35(5), 851–860. <https://doi.org/10.1038/jcbfm.2015.1>
43. Kaburagi, T., Kanaki, K., Otsuka, Y., Hino, R. (2019). Low-carbohydrate diet inhibits different advanced glycation end products in kidney depending on lipid composition but causes adverse morphological changes in a non-obese model mice. *Nutrients*, 11(11), art. no. 2801. <https://doi.org/10.3390/nu11112801>
44. Karadag, A., Bozkurt, F., Bekiroglu, H., Sagdic, O. (2020). Use of principal component analysis and cluster analysis for differentiation of traditionally-manufactured vinegars based on phenolic and volatile profiles, and antioxidant activity. *Polish Journal of Food and Nutrition Sciences*, 70(4), 347–360. <https://doi.org/10.31883/pjfn/127399>
45. Karim, N., Jenduang, N., Tangpong, J. (2018). Anti-glycemic and anti-hepatotoxic effects of mangosteen vinegar rind from *Garcinia mangostana* against HFD/STZ-induced type II diabetes in mice. *Polish Journal of Food and Nutrition Sciences*, 68(2), 163–169. <https://doi.org/10.1515/pjfn-2017-0018>
46. Keene, D.L. (2006). A systematic review of the use of the ketogenic diet in childhood epilepsy. *Pediatric Neurology*, 35(1), 1–5. <https://doi.org/10.1016/j.pediatrneurol.2006.01.005>
47. Kehm, R., Baldensperger, T., Raupbach, J., Höhn, A. (2021). Protein oxidation – Formation mechanisms, detection and relevance as biomarkers in human diseases. *Redox Biology*, 42, art. no. 101901. <https://doi.org/10.1016/j.redox.2021.101901>
48. Kephart, W., Mumford, P., Mao, X., Romero, M., Hyatt, H., Zhang, Y., Mobley, C., Quindry, J., Young, K., Beck, D., Martin, J., McCullough, D., D'Agostino, D., Lowery, R., Wilson, J., Kavazis, A., Roberts, M. (2017). The 1-week and 8-month effects of a ketogenic diet or ketone salt supplementation on multi-organ markers of oxidative stress and mitochondrial function in rats. *Nutrients*, 9(9), art. no. 1019. <https://doi.org/10.3390/nu9091019>
49. Krupa-Kozak, U., Drabińska, N., Bączek, N., Śimková, K., Starowicz, M., Jeliński, T. (2021). Application of broccoli leaf powder in gluten-free bread: an innovative approach to improve its bioactive potential and technological quality. *Foods*, 10(4), art. no. 819. <https://doi.org/10.3390/foods10040819>
50. Lamichhane, S., Bastola, T., Pariyar, R., Lee, E.-S., Lee, H.-S., Lee, D., Seo, J. (2017). ROS production and ERK activity are involved in the effects of d- β -hydroxybutyrate and metformin in a glucose deficient condition. *International Journal of Molecular Sciences*, 18(3), art. no. 674. <https://doi.org/10.3390/ijms18030674>
51. Ligor, M., Ligor, T., Gadżala-Kopciuch, R., Buszewski, B. (2015). The chromatographic assay of 4-hydroxynonenal as a biomarker of diseases by means of MEPS and HPLC technique. *Biomedical Chromatography*, 29(4), 584–589. <https://doi.org/10.1002/bmc.3317>
52. Liśkiewicz, D., Liśkiewicz, A., Grabowski, M., Nowacka-Chmielewska, M.M., Jabłońska, K., Wojakowska, A., Marczak, Barski, J.J., Małecki, A. (2021). Upregulation of hepatic autophagy under nutritional ketosis. *The Journal of Nutritional Biochemistry*, 93, art. no. 108620. <https://doi.org/10.1016/j.jnutbio.2021.108620>
53. Magnani, F., Mattevi, A. (2019). Structure and mechanisms of ROS generation by NADPH oxidases. *Current Opinion in Structural Biology*, 59, 91–97. <https://doi.org/10.1016/j.sbi.2019.03.001>
54. Majrashi, M., Altukri, M., Ramesh, S., Govindarajulu, M., Schwartz, J., Almaghrabi, M., Smith, F., Thomas, T., Suppiramaniam, V., Moore, T., Reed, M., Dhanasekaran, M. (2021). β -Hydroxybutyric acid attenuates oxidative stress and improves markers of mitochondrial function in the HT-22 hippocampal cell line. *Journal of Integrative Neuroscience*, 20(2), 321–329. <https://doi.org/10.31083/jjin2002031>
55. Marocco, I., Altieri, F., Peluso, I. (2017). Measurement and clinical significance of biomarkers of oxidative stress in humans. *Oxidative Medicine and Cellular Longevity*, 2017, art. no. 6501046. <https://doi.org/10.1155/2017/6501046>
56. Martinon, F., Pétrilli, V., Mayor, A., Tardivel, A., Tschopp, J. (2006). Gout-associated uric acid crystals activate the NALP3 inflammasome. *Nature*, 440(7081), 237–241. <https://doi.org/10.1038/nature04516>
57. Milder, J.B., Liang, L.-P., Patel, M. (2010). Acute oxidative stress and systemic Nrf2 activation by the ketogenic diet. *Neurobiology of Disease*, 40(1), 238–244. <https://doi.org/10.1016/j.nbd.2010.05.030>
58. Milder, J., Patel, M. (2012). Modulation of oxidative stress and mitochondrial function by the ketogenic diet. *Epilepsy Research*, 100(3), 295–303. <https://doi.org/10.1016/j.eplepsyres.2011.09.021>
59. Moolwong, J., Klinthong, W., Chuacharoen, T. (2023). Physicochemical properties, antioxidant capacity, and consumer acceptability of ice cream incorporated with avocado (*Persea Americana* Mill.) pulp. *Polish Journal of Food and Nutrition Sciences*, 73(3), 289–296. <https://doi.org/10.31883/pjfn/170938>
60. Moreno, B., Crujeiras, A.B., Bellido, D., Sajoux, I., Casanueva, F.F. (2016). Obesity treatment by very low-calorie-ketogenic diet at two years: reduction in visceral fat and on the burden of disease. *Endocrine*, 54, 681–690. <https://doi.org/10.1007/s12020-016-1050-2>
61. Nathan, C., Cunningham-Bussell, A. (2013). Beyond oxidative stress: An immunologist's guide to reactive oxygen species. *Nature Reviews Immunology*, 13(5), 349–361. <https://doi.org/10.1038/nri3423>
62. Nazarewicz, R.R., Ziolkowski, W., Vaccaro, P.S., Ghafourifar, P. (2007). Effect of short-term ketogenic diet on redox status of human blood. *Rejuvenation Research*, 10(4), 435–440. <https://doi.org/10.1089/rej.2007.0540>
63. Nguyen, T.P.T., Tran, T.T.T., Ton, N.M.N., Le, V.V.M. (2023). Use of cashew apple pomace powder in pasta making: Effects of powder ratio on the product quality. *Polish Journal of Food and Nutrition Sciences*, 73(1), 50–58. <https://doi.org/10.31883/pjfn/159360>
64. Niculescu, L., Stancu, C., Sima, A., Toporan, D., Simionescu, M. (2001). The total peroxyl radical trapping potential in serum – an assay to define the stage of atherosclerosis. *Journal of Cellular and Molecular Medicine*, 5(3), 285–294. <https://doi.org/10.1111/j.1582-4934.2001.tb00162.x>
65. Nishino, T., Okamoto, K., Eger, B.T., Pai, E.F., Nishino, T. (2008). Mammalian xanthine oxidoreductase – mechanism of transition from xanthine dehydrogenase to xanthine oxidase. *The FEBS Journal*, 275(13), 3278–3289. <https://doi.org/10.1111/j.1742-4658.2008.06489.x>
66. Ota, M., Matsuo, J., Ishida, I., Takano, H., Yokoi, Y., Hori, H., Yoshida, S., Ashida, K., Nakamura, K., Takahashi, T., Kunugi, H. (2019). Effects of a medium-chain triglyceride-based ketogenic formula on cognitive function in patients with mild-to-moderate Alzheimer's disease. *Neuroscience Letters*, 690, 232–236. <https://doi.org/10.1016/j.neulet.2018.10.048>
67. Ozenirler, S., Erkan, G., Gulbahar, O., Bostankolu, O., Ozbas Demirel, O., Bilgihan, A., Akyol, G. (2011). Serum levels of advanced oxidation protein products, malonyldialdehyde, and total radical trapping antioxidant parameter in patients with chronic hepatitis C. *Turkish Journal of Gastroenterology*, 22(1), 47–53. <https://doi.org/10.4318/tjg.2011.0156>
68. Paoli, A. (2014). Ketogenic diet for obesity: Friend or foe? *International Journal of Environmental Research and Public Health*, 11(2), 2092–2107. <https://doi.org/10.3390/ijerph110202092>
69. Papierska, K., Ignatowicz, E., Jodynis-Liebert, J., Kujawska, M., Biegańska-Marecik, R. (2022). Effects of long-term dietary administration of kale (*Brassica oleracea*; L. var. *acephala* DC) leaves on the antioxidant status and blood biochemical markers in rats. *Polish Journal of Food and Nutrition Sciences*, 72(3), 239–247. <https://doi.org/10.31883/pjfn/152434>
70. Parry, H.A., Kephart, W.C., Mumford, P.W., Romero, M.A., Mobley, C.B., Zhang, Y., Roberts, M.D., Kavazis, A.N. (2018). Ketogenic diet increases mitochondria volume in the liver and skeletal muscle without altering oxidative stress markers in rats. *Heliyon*, 4(11), art. no. e00975. <https://doi.org/10.1016/j.heliyon.2018.e00975>
71. Pegg, R.B., Amarowicz, R., Naczek, M., Shahidi, F. (2007). PHOTOCHEM[®] for determination of antioxidant capacity of plant extracts. In F. Shahidi, C.T. Ho (Eds.), *Antioxidant Measurement and Applications*, ACS Symposium Series 956, Washington, USA, pp. 140–158. <https://doi.org/10.1021/bk-2007-0956.ch011>
72. Pelclova, D., Zdimal, V., Schwarz, J., Dvorackova, S., Komarc, M., Ondracek, J., Kostejn, M., Kacer, P., Vlckova, S., Fenclova, Z., Popov, A., Lischkova, L., Zakharov, S., Bello, D. (2018). Markers of oxidative stress in the exhaled breath condensate of workers handling nanocomposites. *Nanomaterials*, 8(8), art. no. 611. <https://doi.org/10.3390/nano8080611>
73. Pellegrini, N., Vitaglione, P., Granato, D., Fogliano, V. (2020). Twenty-five years of total antioxidant capacity measurement of foods and biological fluids: merits and limitations. *Journal of the Science of Food and Agriculture*, 100(14), 5064–5078. <https://doi.org/10.1002/jsfa.9550>
74. Phillips, M.C.L., Murtagh, D.K.J., Gilbertson, L.J., Asztely, F.J.S., Lynch, C.D.P. (2018). Low-fat versus ketogenic diet in Parkinson's disease: A pilot randomized controlled trial. *Movement Disorders*, 33(8), 1306–1314. <https://doi.org/10.1002/mds.27390>

75. Pilone, V., Tramontano, S., Renzulli, M., Romano, M., Cobellis, L., Berselli, T., Schiavo, L. (2018). Metabolic effects, safety, and acceptability of very low-calorie ketogenic dietetic scheme on candidates for bariatric surgery. *Surgery for Obesity and Related Diseases*, 14(7), 1013–1019. <https://doi.org/10.1016/j.soard.2018.03.018>
76. Poff, A.M., Ari, C., Seyfried, T.N., D'Agostino, D.P. (2013). The ketogenic diet and hyperbaric oxygen therapy prolong survival in mice with systemic metastatic cancer. *PLoS ONE*, 8(6), art. no. e65522. <https://doi.org/10.1371/journal.pone.0065522>
77. Poorshiri, B., Barzegar, M., Afghan, M., Shiva, S., Shahabi, P., Golchinfar, Z., Yousefi Nohed, H.R., Raeisi, S. (2023). The effects of ketogenic diet on beta-hydroxybutyrate, arachidonic acid, and oxidative stress in pediatric epilepsy. *Epilepsy Behavior*, 140, art. no. 109106. <https://doi.org/10.1016/j.yebeh.2023.109106>
78. Qu, C., Keijer, J., Adjobo-Hermans, M.J.W., van de Wal, M., Schirris, T., van Karnebeek, C., Pan, Y., Koopman, W.J.H. (2021). The ketogenic diet as a therapeutic intervention strategy in mitochondrial disease. *The International Journal of Biochemistry Cell Biology*, 138, art. no. 106050. <https://doi.org/10.1016/j.biocel.2021.106050>
79. Ratcliffe, N., Wiczorek, T., Drabińska, N., Gould, O., Osborne, A., De Lacy Costello, B. (2020). A mechanistic study and review of volatile products from peroxidation of unsaturated fatty acids: An aid to understanding the origins of volatile organic compounds from the human body. *Journal of Breath Research*, 14(3), art. no. 034001. <https://doi.org/10.1088/1752-7163/ab7f9d>
80. Rhyu, H., Cho, S.-Y., Roh, H.-T. (2014). The effects of ketogenic diet on oxidative stress and antioxidative capacity markers of Taekwondo athletes. *Journal of Exercise Rehabilitation*, 10(6), 362–366. <https://doi.org/10.12965/jer.140178>
81. Sawai, M., Yashiro, M., Nishiguchi, Y., Ohira, M., Hirakawa, K. (2004). Growth-inhibitory effects of the ketone body, monoacetoacetin, on human gastric cancer cells with succinyl-CoA: 3-oxoacid CoA-transferase (SCOT) deficiency. *Anticancer Research*, 24(4), art. no. 2213–2218. <http://ar.iiarjournals.org/content/24/4/2213.abstract>
82. Sepasi Tehrani, H., Moosavi-Movahedi, A.A. (2018). Catalase and its mysteries. *Progress in Biophysics and Molecular Biology*, 140, 5–12. <https://doi.org/10.1016/j.pbiomolbio.2018.03.001>
83. Shimazu, T., Hirschey, M.D., Newman, J., He, W., Shirakawa, K., Le Moan, N., Grueter, C.A., Lim, H., Saunders, L.R., Stevens, R.D., Newgard, C.B., Farese, R.V., de Cabo, R., Ulrich, S., Akassoglou, K., Verdin, E. (2013). Suppression of oxidative stress by β -hydroxybutyrate, an endogenous histone deacetylase inhibitor. *Science*, 339(6116), 211–214. <https://doi.org/10.1126/science.1227166>
84. Sies, H., Berndt, C., Jones, D.P. (2017). Oxidative stress. *Annual Review of Biochemistry*, 86(1), 715–748. <https://doi.org/10.1146/annurev-biochem-061516-045037>
85. Sullivan, P.G., Rippey, N.A., Dorenbos, K., Concepcion, R.C., Agarwal, A.K., Rho, J.M. (2004). The ketogenic diet increases mitochondrial uncoupling protein levels and activity. *Annals of Neurology*, 55(4), 576–580. <https://doi.org/10.1002/ana.20062>
86. Ta, T.M.N., Hoang, C.H., Nguyen, T.M., Tran, T.T.T., Ton, N.M.N., Van Viet Man, L. (2023). Effects of mulberry pomace addition and transglutaminase treatment on the quality of pasta enriched with antioxidants and dietary fiber. *Polish Journal of Food and Nutrition Sciences*, 73(4), 301–310. <https://doi.org/10.31883/pjfn/172244>
87. Taylor, E.L., Armstrong, K.R., Perrett, D., Hattersley, A.T., Winyard, P.G. (2015). Optimisation of an advanced oxidation protein products assay: Its application to studies of oxidative stress in diabetes mellitus. *Oxidative Medicine and Cellular Longevity*, 2015, art. no. 496271. <https://doi.org/10.1155/2015/496271>
88. Ułamek-Kozioł, M., Czuczwar, S.J., Januszewski, S., Pluta, R. (2019). Ketogenic diet and epilepsy. *Nutrients*, 11(10), art. no. 2510. <https://doi.org/10.3390/nu11102510>
89. U.S. National Institutes of Health. (2023). ClinicalTrials.gov. In *U.S. National Institutes of Health* (p. ClinicalTrials.gov Identifier: NCT05200468). <http://clinicaltrials.gov/>
90. Üstündağ, H., Doğanay, S., Öztürk, B., Köse, F., Kurt, N., Aydemir Celep, N., Huyut, M.T., Özgeriş, F.B. (2023). Exploring the impact of ketogenic diet and intermittent fasting on male rats' testicular health: an analysis of hormonal regulation, oxidative stress, and spermatogenesis. *Journal of Food Biochemistry*, 2023, art. no. 5562120. <https://doi.org/10.1155/2023/5562120>
91. Valenzano, A., Polito, R., Trimigno, V., Di Palma, A., Moscatelli, F., Corso, G., Sessa, F., Salerno, M., Montana, A., Di Nunno, N., Astuto, M., Daniele, A., Carotenuto, M., Messina, G., Cibelli, G., Monda, V. (2019). Effects of very low calorie ketogenic diet on the orexinergic system, visceral adipose tissue, and ROS production. *Antioxidants*, 8(12), art. no. 643. <https://doi.org/10.3390/antiox8120643>
92. Wang, X., Wu, X., Liu, Q., Kong, G., Zhou, J., Jiang, J., Wu, X., Huang, Z., Su, W., Zhu, Q. (2017). Ketogenic metabolism inhibits histone deacetylase (HDAC) and reduces oxidative stress after spinal cord injury in rats. *Neuroscience*, 366, 36–43. <https://doi.org/10.1016/j.neuroscience.2017.09.056>
93. Watanabe, M., Tuccinardi, D., Ernesti, I., Basciani, S., Mariani, S., Genco, A., Manfrini, S., Lubrano, C., Gnassi, L. (2020). Scientific evidence underlying contraindications to the ketogenic diet: An update. *Obesity Reviews*, 21(10), art. no. e13053. <https://doi.org/10.1111/obr.13053>
94. WHO. (2016). Obesity and overweight: Fact sheet. In *WHO Media Centre*.
95. WHO. (2023). *World Health Statistics 2023 - A visual summary*. <https://www.who.int/data/stories/world-health-statistics-2023-a-visual-summary/>
96. Wiczorek, M.N., Kowalczewski, P.Ł., Drabińska, N., Różańska, M.B., Jeleń, H.H. (2022). Effect of cricket powder incorporation on the profile of volatile organic compounds, free amino acids and sensory properties of gluten-free bread. *Polish Journal of Food and Nutrition Sciences*, 72(4), 431–442. <https://doi.org/10.31883/pjfn/156404>
97. Xu, X., Xie, L., Chai, L., Wang, X., Dong, J., Wang, J., Yang, P. (2023). Ketogenic diet inhibits neointimal hyperplasia by suppressing oxidative stress and inflammation. *Clinical and Experimental Hypertension*, 45(1), art. no. 2229538. <https://doi.org/10.1080/10641963.2023.2229538>
98. Yapca, O.E., Borekci, B., Suleyman, H. (2013). Ischemia-reperfusion damage. *The Eurasian Journal of Medicine*, 45(2), 126–127. <https://doi.org/10.5152/eajm.2013.24>
99. Żary-Sikorska, E., Fotschki, B., Kosmala, M., Milala, J., Matusevicius, P., Rawicka, A., Juśkiewicz, J. (2021). Strawberry polyphenol-rich fractions can mitigate disorders in gastrointestinal tract and liver functions caused by a high-fructose diet in experimental rats. *Polish Journal of Food and Nutrition Sciences*, 71(4), 423–440. <https://doi.org/10.31883/pjfn/143057>
100. Zhang, Q., Wu, C., Sun, Y., Li, T., Fan, G. (2019). Cytoprotective effect of *Morchella esculenta* protein hydrolysate and its derivative against H₂O₂-induced oxidative stress. *Polish Journal of Food and Nutrition Sciences*, 69(3), 255–265. <https://doi.org/10.31883/pjfn/110134>
101. Zhao, Z., Lange, D.J., Voustantiouk, A., MacGrogan, D., Ho, L., Suh, J., Humala, N., Thiyagarajan, M., Wang, J., Pasinetti, G.M. (2006). A ketogenic diet as a potential novel therapeutic intervention in amyotrophic lateral sclerosis. *BMC Neuroscience*, 7, art. no. 29. <https://doi.org/10.1186/1471-2202-7-29>
102. Zielonka, J., Hardy, M., Michalski, R., Sikora, A., Zielonka, M., Cheng, G., Ouari, O., Podsiadly, R., Kalyanaraman, B. (2017). Recent developments in the probes and assays for measurement of the activity of NADPH oxidases. *Cell Biochemistry and Biophysics*, 75(3–4), 335–349. <https://doi.org/10.1007/s12013-017-0813-6>
103. Zilberter, T., Zilberter, Y. (2018). Ketogenic ratio determines metabolic effects of macronutrients and prevents interpretive bias. *Frontiers in Nutrition*, 5, art. no. 75. <https://doi.org/10.3389/fnut.2018.00075>

73 VOLUME'S REVIEWERS

The Editors gratefully thank the following reviewers for their valuable help in reviewing manuscripts published in this volume and other papers reviewed between 1st January 2023 and 31st December 2023.

Aidi Wannas W., Laboratory of Medicinal and Aromatic Plants, Hammam-Lif, Tunisia

Almoselhy R., Food Technology Research Institute – Agricultural Research Center, Egypt

Amarowicz R., Department of Physical and Chemical Properties of Food, Institute of Animal Reproduction and Food Research of the Polish Academy of Sciences, Olsztyn, Poland

Arason S., Faculty of Food Science and Nutrition, University of Iceland and Matís – Icelandic Food and Biotech R&D, Iceland

Arribas C., INIA-CSIC Food Technology Department, Spain

Borda D., Faculty of Food Science and Engineering, Dunarea de Jos University of Galati, Romania

Bou R., Institut de Recerca i Tecnologia Agroalimentàries (IRTA), Spain

Chen K., Zhejiang Gongshang University, China

Chen X., State Key Laboratory of Food Science and Technology, Nanchang University, Nanchang, Jiangxi, China

Chuacharoen Th., Faculty of Science and Technology, Suan Sunandha Rajabhat University, Thailand

Cygan-Szczegieliński D., UTP University of Science and Technology, Bydgoszcz, Poland

Djuričić I.D., University of Belgrade, Serbia

Drabińska N., Institute of Animal Reproduction and Food Research of Polish Academy of Sciences, Poland

du Plessis H., Agricultural Research Council, ARC Infruitec-Niet-voorbij, Stellenbosch, South Africa

Florek M., Department of Quality Assessment and Processing of Animal Products, University of Life Sciences in Lublin, Poland

Fotschki B., Department of Biological Functions of Food, Institute of Animal Reproduction and Food Research of the Polish Academy of Sciences, Olsztyn, Poland

Gai F., Institute of Sciences of Food Production, Italian National Research Council, Grugliasco, Italy

Gençelep H., University of Ondokuz Mayıs, Turkey

Gerschenson L., Buenos Aires University, Buenos Aires, Argentina

Giuggioli N.R., Department of Agricultural Forest and Food Science-DISAFI, University of Turin, Grugliasco, Italy

Gomes da Cruz A., Science and Technology of Rio de Janeiro (IFRJ), Department of Food, Federal Institute of Education, Rio de Janeiro, Brazil

González-Estrada R.R., División de Estudios de Posgrado e Investigación, Tecnológico Nacional de México/Instituto Tecnológico de Tepic, Mexico

Grembecka M., Department of Bromatology, Medical University of Gdansk, Poland

Habschied K., Faculty of Food Technology Osijek, Josip Juraj Strossmayer University of Osijek, Croatia

Hernandez-Aguilar C., Instituto Politecnico Nacional, Mexico

Hou Ch., Institute of Food Science and Technology, Chinese Academy of Agricultural Sciences, China

Jakobek L., Department of Applied Chemistry and Ecology, Josip Juraj Strossmayer University of Osijek, Croatia

Janiak M.A., Department of Physical and Chemical Properties of Food, Institute of Animal Reproduction and Food Research of the Polish Academy of Sciences, Olsztyn, Poland

Jaroslawska J., Department of Biological Functions of Food, Institute of Animal Reproduction and Food Research of the Polish Academy of Sciences, Olsztyn, Poland

Jurgoński A., Department of Biological Functions of Food, Institute of Animal Reproduction and Food Research of the Polish Academy of Sciences, Olsztyn, Poland

Karamać M., Department of Chemical and Physical Properties of Food, Institute of Animal Reproduction and Food Research of the Polish Academy of Sciences, Poland

Kelebek H., Science and Technology University, Adana, Turkey

Kopcewicz M., Department of Biological Functions of Food, Institute of Animal Reproduction and Food Research of the Polish Academy of Sciences, Olsztyn, Poland

Kozłowska M., Department of Chemistry, Institute of Food Science, Warsaw University of Life Sciences-SGGW, Poland



- Lopez-Martinez L., Coordinación de Tecnología de Alimentos de Origen Vegetal, CONACYT-CIAD, Mexico
- Machcińska-Zielińska S., Department of Biological Functions of Food, Institute of Animal Reproduction and Food Research of the Polish Academy of Sciences, Olsztyn, Poland
- Mańko-Jurkowska D., Department of Chemistry, Warsaw University of Life Sciences, Poland
- Martinez-Flores H., Facultad de Químico Farmacobiología, Universidad Michoacana de San Nicolás de Hidalgo, Mexico
- Marzouk B., Faculté des Sciences de Tunis, Campus Universitaire, Tunis, Tunisia
- Mascheroni R., Universidad Nacional de la Plata, La Plata, Argentina
- Matusevicius P., Lithuanian University of Health Sciences, Veterinary Academy, Kaunas, Lithuania
- Micić D.M., University of Belgrade, Serbia
- Nguyen M., Nha Trang University, Viet Nam
- Ningrum A., Department of Food and Agricultural Product Technology, Universitas Gadjah Mada, Yogyakarta, Indonesia
- Papierska K., Department of Pharmaceutical Biochemistry, Poznan University of Medical Sciences, Poland
- Pedreschi R., Pontificia Universidad Católica de Valparaíso, Chile
- Pelvan E., TUBITAK Marmara Research Center (MAM), Gebze, Turkey
- Ramirez Ascheri J.L., Brazilian Agricultural Research Corporation (EMBRAPA), Brasília, Brazil
- Rezaei K., Department of Food Science, Engineering and Technology, University of Tehran, Karaj, Iran
- Rodríguez-Miranda J., Tecnológico Nacional de México/Instituto Tecnológico de Tuxtepec, Tuxtepec, Oaxaca, Mexico
- Rutkowska J., Warsaw University of Life Sciences, Poland
- Rybicka I., Department of Technology and Instrumental Analysis, Poznań University of Economics and Business, Poland
- Serrano M., Universidad Miguel Hernández, Spain
- Stajic S., University of Belgrade, Serbia
- Srivastava A., President/Principal Consultant, Anya Baking Lab, United States
- Staroszczyk H., Gdańsk University of Technology, Poland
- Starowicz M., Department of Chemistry and Biodynamics of Food, Institute of Animal Reproduction and Food Research of the Polish Academy of Sciences, Olsztyn, Poland
- Szumny A., Wrocław University of Environmental and Life Sciences, Wrocław, Poland
- Szymczak M., Department of Toxicology, Dairy Technology and Food Storage, West Pomeranian University of Technology, Szczecin, Poland
- Topalovic A., Agrochemical Laboratory, University of Montenegro, Biotechnical Faculty, Montenegro
- Tran T., Can Tho University, Viet Nam
- Turabi Yolaçaner E., Food Engineering, Hacettepe University, Turkey
- Walendzik K., Department of Biological Functions of Food, Institute of Animal Reproduction and Food Research of the Polish Academy of Sciences, Olsztyn, Poland
- Wang Sh., Biological and Food Engineering Institute, Anhui Polytechnic University, China
- Wang Y., College of Agriculture and Forestry, Longdong University, China
- Wang Z., China
- Wiczowski W., Department of Chemistry and Biodynamics of Food, Institute of Animal Reproduction and Food Research of the Polish Academy of Sciences, Olsztyn, Poland
- Wiśniewska J., Laboratory of Cell and Tissue Analysis and Imaging, Institute of Animal Reproduction and Food Research of the Polish Academy of Sciences, Olsztyn, Poland
- Wronkowska M., Department of Chemistry and Biodynamics of Food, Institute of Animal Reproduction and Food Research of the Polish Academy of Sciences, Olsztyn, Poland
- Yang Ch., School of Design, Jiangnan University, Taiwan
- Zimoch-Korzycka A., Department of Functional Food Products Development, Wrocław University of Environmental and Life Sciences, Poland

INSTRUCTIONS FOR AUTHORS

SUBMISSION. Original contributions relevant to food and nutrition sciences are accepted on the understanding that the material has not been, nor is being, considered for publication elsewhere. All papers should be submitted and will be processed electronically via Editorial Manager system (available from PJFNS web site: <http://journal.pan.olsztyn.pl>). On submission, a corresponding author will be asked to provide: Cover letter; Files with Manuscripts, Tables, Figures/Photos; and Names of two potential reviewers (one from the author's homeland – but outside author's Institution, and the other from abroad). All papers which have been qualified as relevant with the scope of our Journal are reviewed. All contributions, except the invited reviews are charged. Proofs will be sent to the corresponding author and should be returned within one week since receipt. No new material may be inserted in the text at proof stage. It is the author's duty to proofread proofs for errors.

Authors should very carefully consider the preparation of papers to ensure that they communicate efficiently, because it permits the reader to gain the greatest return for the time invested in reading. Thus, we are more likely to accept those that are carefully designed and conform the instruction. Otherwise, papers will be rejected and removed from the online submission system.

SCOPE. The Polish Journal of Food and Nutrition Sciences publishes original, basic and applied papers, and reviews on fundamental and applied food research, preferably these based on a research hypothesis, in the following Sections:

Food Technology:

- Innovative technology of food development including biotechnological and microbiological aspects
- Effects of processing on food composition and nutritional value

Food Chemistry:

- Bioactive constituents of foods
- Chemistry relating to major and minor components of food
- Analytical methods

Food Quality and Functionality:

- Sensory methodologies
- Functional properties of food
- Food physics
- Quality, storage and safety of food

Nutritional Research:

- Nutritional studies relating to major and minor components of food (excluding works related to questionnaire surveys)

"News" section:

- Announcements of congresses
- Miscellanea

OUT OF THE SCOPE OF THE JOURNAL ARE:

- Works which do not have a substantial impact on food and nutrition sciences
- Works which are of only local significance i.e. concern indigenous foods, without wider applicability or exceptional nutritional or health related properties
- Works which comprise merely data collections, based on the use of routine analytical or bacteriological methods (i.e. standard methods, determination of mineral content or proximate analysis)
- Works concerning biological activities of foods but not providing the chemical characteristics of compounds responsible for these properties
- Nutritional questionnaire surveys
- Works related to the characteristics of foods purchased at local markets
- Works related to food law
- Works emphasizing effects of farming / agricultural conditions / weather conditions on the quality of food constituents
- Works which address plants for non-food uses (i.e. plants exhibiting therapeutic and/or medicinal effects)

TYPES OF CONTRIBUTIONS. *Reviews:* (at least: 30 pages and 70 references) these are critical and conclusive accounts on trends in food and nutrition sciences; *Original papers:* (maximally: 30 pages and 40 references) these are reports of substantial research; *Reports on post and forthcoming scientific events, and letters to the Editor* (all up to three pages) are also invited (free of charge).



REVIEW PROCESS. All scientific contributions will be peer-reviewed on the criteria of originality and quality. Submitted manuscripts will be preevaluated by Editor-in-Chief and Statistical Editor (except for review articles), and when meeting PJFNS' scope and formal requirements, they will be sent to a Section Editor who upon positive preevaluation will assign at least two reviewers from Advisory Board Members, reviewers suggested by the author or other experts in the field. Based on the reviews achieved, Section Editor and Editor-in-Chief will make a decision on whether a manuscript will be accepted for publication, sent back to the corresponding author for revision, or rejected. Once a manuscript is sent back to the corresponding author for revision, all points of the reviews should be answered or rebuttal should be provided in the Explanation letter. The revised manuscripts will be checked by Section Editor and by the original reviewers (if necessary), and a final decision will be made on acceptance or rejection by both Section Editor and Editor-in-Chief.

Polish Journal of Food and Nutrition Sciences uses CrossCheck's iThenticate software to detect instances of similarity in submitted manuscripts. In publishing only original research, PJFNS is committed to deterring plagiarism, including self-plagiarism.

COPYRIGHT LICENSE AGREEMENT referring to Authorship Responsibility and Acknowledgement, Conflict of Interest and Financial Disclosure, Copyright Transfer, are required for all authors, i.e. *Authorship Responsibility and Acknowledgement*: Everyone who has made substantial intellectual contributions to the study on which the article is based (for example, to the research question, design, analysis, interpretation, and written description) should be an author. It is dishonest to omit mention of someone who has participated in writing the manuscript ("ghost authorship") and unfair to omit investigator who have had important engagement with other aspects of the work. All contributors who do not meet the criteria for authorship should be listed in an Acknowledgments section. Examples of those who might be acknowledged include a person who provided purely technical help, writing assistance, or a department chairperson who provided only general support. Any financial and material support should also be acknowledged. *Conflict of Interest and Financial Disclosure*: Authors are responsible for disclosing financial support from the industry or other conflicts of interest that might bias the interpretation of results. *Copyright License Agreement*: Authors agree to follow the Creative Commons Attribution-Non-Commercial-NoDerivs 4.0 License.

A manuscript will not be published once the signed form has not been submitted to the Editor with the manuscript revised after positive reviews.

CHANGES TO AUTHORSHIP. Authors are expected to consider carefully the list and order of authors before submitting their manuscript and provide the definitive list of authors at the time of the original submission. Any addition, deletion or rearrangement of author names in the authorship list should be made only before the manuscript has been accepted and only if approved by the journal Editor. To request such a change, the Editor must receive the following from the corresponding author: (a) the reason for the change in author list and (b) written confirmation (e-mail, letter) from all authors that they agree with the addition, removal or rearrangement. In the case of addition or removal of authors, this includes confirmation from the author being added or removed.

ETHICAL APPROVAL OF STUDIES AND INFORMED CONSENT. For all manuscripts reporting data from studies involving human participants or animals, formal approval by an appropriate institutional review board or ethics committee is required and should be described in the Methods section. For those investigators who do not have formal approval from ethics review committees, the principles outlined in the Declaration of Helsinki should be followed. For investigations of humans, state in the Methods section the manner in which informed consent was obtained from the study participants (i.e., oral or written). Editors may request that authors provide documentation of the formal review and recommendation from the institutional review board or ethics committee responsible for oversight of the study.

UNAUTHORIZED USE. Unauthorized use of the PJFNS name, logo, or any content for commercial purposes or to promote commercial goods and services (in any format, including print, video, audio, and digital) is not permitted by IAR&FR PAS.

MANUSCRIPTS. A manuscript in English must be singesided, preferably in Times New Roman (12) with 1.5-point spacing, without numbers of lines. The Editor reserves the right to make literary corrections and to make suggestions to improve brevity. English is the official language. The English version of the paper will be checked by Language Editor. Unclear and unintelligible version will be returned for correction.

Every paper should be divided under the following headings in this order: a **Title** (possibly below 150 spaces); the **Name(s)** of the author(s) in full. In paper with more than one author, the asterisk indicates the name of the author to whom correspondence and inquiries should be addressed, otherwise the first author is considered for the correspondence. Current full postal address of the indicated corresponding author or the first author must be given in a footnote on the title page; the **Place(s)** where the work was done including the institution name, city, country if not Poland. In papers originated from several institutions the names of the authors should be marked with respective superscripts; the **Key words** (up to 6 words or phrases) for the main topics of the paper; an **Abstract** (up to 250 words for regular papers and reviews) summarizing briefly main results of the paper, no literature references; an **Introduction** giving essential background by saying why the research is important, how it relates to previous works and stating clearly the objectives at the end; **Materials and Methods** with sufficient experimental details permitting to repeat or extend the experiments. Literature references to the methods, sources of material, company names and location (city, country) for specific instruments must be given. Describe how the data were evaluated, including selection criteria used; **Results and Discussion** presented together (in one chapter). Results should be presented concisely and organized to supplement, but not repeat, data in tables and figures. Do not display the data in both tabular and graphic form. Use narrative form to present the data for which tables or figures are unnecessary. Discussion should cover the implications and consequences, not merely recapitulating the results, and it must be accomplished with concise **Conclusions**; **Acknowledgements** should be made to persons who do not fill the authorship criteria (see: Authorship forms); **Research funding** should include financial and material support; **Conflict of Interests**: Authors should reveal any conflicts of interest that might bias the interpretation of results; and **References** as shown below.

REFERENCES each must be listed alphabetically at the end of the paper (each should have an Arabic number in the list) in the form as follows: **Periodicals** – names and initials of all the authors, year of publication, title of the paper, journal title as in Chemical Abstracts, year of publication, volume, issue, inclusive page numbers, or article id.; **Books** – names and initials of all the authors, names of editors, chapter title, year of publication, publishing company, place of publication, inclusive page numbers; **Patents** – the name of the application, the title, the country, patent number or application number, the year of publication.

For papers published in language other than English, manuscript title should be provided in English, whereas a note on the original language and English abstract should be given in parentheses at the end.

The reference list should only include peer-reviewed full-text works that have been published or accepted for publication. Citations of MSc/PhD theses and works unavailable to international Editors, Reviewers, and Readers should be limited as much as possible.

References in the text must be cited by name and year in square parentheses (e.g.: one author – [Tokarz, 1994]; two authors – [Słoniński & Campbell, 1987]; more than two authors – [Amarowicz *et al.*, 1994]). If more than one paper is published in the same year by the same author or group of authors use [Tokarz, 1994a, b]. Unpublished work must only be cited where necessary and only in the text by giving the person's name.

Examples:

Article in a journal:

Słoniński, B.A., Campbell, L.D., Batista, E., Howard B. (2008). Gas chromatographic determination of indole glucosinolates. *Journal of Science and Food Agriculture*, 40(5), 131–143.

Asher, A., Tintle, N.L., Myers, M., Lockshon, L., Bacareza, H., Harris, W.S. (2021). Blood omega-3 fatty acids and death from COVID-19: A pilot study. *Prostaglandins, Leukotrienes and Essential Fatty Acids*, 166, art. no. 102250.

Book:

Weber, W., Ashton, L., Milton, C. (2012). *Antioxidants – Friends or Foes?* 2nd edition. PBD Publishing, Birmingham, UK. pp. 218–223.

Chapter in a book:

Uden, C., Gambino, A., Lamar, K. (2016). Gas chromatography. In M. Queresi, W. Bolton (Eds.), *CRC Handbook of Chromatography*, CRC Press Inc., Boca Raton, Florida, USA, pp. 44–46.

ABBREVIATIONS AND UNITS. Abbreviations should only be used when long or unwieldy names occur frequently, and never in the title; they should be given at the first mention of the name. Metric SI units should be used. The capital letter L should be used for liters. Avoid the use of percentages (% g/g, % w/w; Mol%; vol%), ppm, ppb. Instead, the expression such as g/kg, g/L, mg/kg, mg/mL should be used. A space must be left between a number and a symbol (e.g. 50 mL not 50mL). A small x must be used as multiplication sign between numeric values (e.g. 5 × 10² g/mL). Statistics and measurements should be given in figures, except when the number begins a sentence. Chemical formulae and solutions must specify the form used. Chemical abbreviations, unless they are internationally known, Greek symbols and unusual symbols for the first time should be defined by name. Common species names should be followed by the Latin at the first mention, with contracting it to a single letter or word for subsequent use.

FIGURES should be submitted in separate files. Each must have an Arabic number and a caption. Captions of all Figures should be provided on a separate page "Figure Captions". Figures should be comprehensible without reference to the text. Self-explanatory legend to all figures should be provided under the heading "Legends to figures"; all abbreviations appearing on figures should be explained in figure footnotes. Three-dimensional graphs should only be used to illustrate real 3D relationships. Start the scale of axes and bars or columns at zero, do not interrupt them or omit missing data on them. Figures must be cited in Arabic numbers in the text.

TABLES should be submitted in separate files. They should be as few in number and as simple as possible (like figures, they are expensive and space consuming), and include only essential data with appropriate statistical values. Each must have an Arabic number and a caption. Captions of all Tables should be provided on a separate page "Table Captions". Tables should be self-explanatory; all abbreviations appearing in tables should be explained in table footnotes. Tables must be cited in Arabic numbers in the text.

PAGE CHARGES. A standard publication fee has been established at the rate of 450 EUR + tax (if applicable, e.g. for private persons) irrespective of the number of pages and tables/figures. For Polish Authors an equivalent fee was set at 1950 PLN + VAT. Payment instructions will be sent to Authors via e-mail with acceptance letter.

Information on publishing and subscription is available from:

Ms. Joanna Molga

Editorial Office of Pol. J. Food Nutr. Sci.

Institute of Animal Reproduction and Food Research Tuwima 10 Str., 10–748 Olsztyn 5, Poland

phone (48 89) 523–46–70, fax (48 89) 523–46–70;

e-mail: pjfns@pan.olsztyn.pl; <http://journal.pan.olsztyn.pl>

Nutrition

